



**U.S. Army Corps of Engineers
Portland District**

Hydroacoustic Evaluation of Fish Passage at The Dalles Dam in 2001

FINAL REPORT

Prepared by

R. A. Moursund

K.D. Ham

P.S. Titzler

R. P. Mueller

G.E. Johnson

Pacific Northwest National Laboratory, Richland, Washington

J. Hedgepeth

Tenera Inc., San Francisco, California

J.R. Skalski

University of Washington, Seattle, Washington

June 2002

Contract DACW57-00-D-0008

Task Order 04

Battelle's Pacific Northwest Division

P.O. Box 999

Richland, Washington 99352

Executive Summary

At The Dalles Dam in 2001, turbine intake occlusion plates with J-extensions (hereafter called “J-occlusions”) were installed to decrease turbine passage rates of downstream migrant salmon and steelhead. The premise behind the J-occlusions was that they would cause water to be drawn into the turbines from deeper in the water column than without them, thereby reducing entrainment of surface-oriented smolts. The main objective of this fixed-location hydroacoustic research on fish passage was to evaluate the performance of the partial powerhouse prototype J-occlusions placed at Main Units 1-5. Secondary objectives were to (a) estimate overall fish passage metrics, such as project-wide fish passage efficiency, spill efficiency, and sluiceway efficiency, (b) estimate passage rates between the gaps between adjacent J-occlusions, and (c) compare smolt movement patterns in the nearfield of Sluice 1-2 with and without J-occlusions.

The study period was April 24 to July 15, 2001. Based on species composition data from the Smolt Monitoring Program at John Day Dam, the cut-off between spring and summer seasons was designated as June 13. Because 2001 was such a low-water year (flows 45% of the 10-year average), spill was limited, occurring only from May 16 to June 17. The sluiceway was operated 24 h/d during the study, discharging about 4,750 cfs from the sluice entrances above Main Units 1-1, 1-2, and 1-3. Hydroacoustic transducers were deployed to estimate passage rates at all possible routes for downstream migrants (turbines, spillway, and sluiceway).

The original randomized-block experimental design called for consistent turbine operations across 6-day blocks, with each 3-day treatment of J-occlusions IN or OUT randomly assigned. This design was not met for a number of reasons. Mechanical difficulties lead to one or more J-occlusions being stuck and not in the treatment configuration for some or all of a treatment. Dam operations at Main Units 1-5 were variable across treatments. Thus, the planned treatment analysis was not relevant and had to be abandoned. Accordingly, a focused analysis of the treatment region using graphical presentations was performed.

Regarding the main objective, more than one factor appeared to influence fish passage at the J-occlusion units. Spill appeared to strongly influence turbine passage during unoccluded treatments, suggesting that spill had the greatest influence on fish that would have passed via the unoccluded route. Occlusions decreased turbine passage in the absence of spill, but not during spill. Sluice passage and efficiency increased during occlusion treatments at night, but not during the day. Spill also influenced sluice passage more during the unoccluded treatment. The evidence suggests that occlusion plates are most effective at night and in the absence of spill.

Results from the secondary objectives were informative. Overall, FPE was 83% in spring and 14% in summer. Sluiceway efficiency relative to the powerhouse was 53% in spring and 6% in summer. Relative to the entire project, sluiceway efficiency was 18% and 5% in spring and summer, respectively. Spillway efficiency was 65% in spring and 9% in summer. Gap loss was about 17 fish per hour, although expanded estimates represent a small proportion of passage. Effects of the J-occlusions on smolt movements were evident as noticeable, distinct differences in movement patterns between the IN and

OUT conditions. Mean fish velocities, movement proportions, and fate probabilities all demonstrated differences between J-occlusions IN and OUT. Generally, the J-occlusions appeared to cause fish in the nearfield of Sluice 1-2 to decrease westward movement, decrease movement toward the dam, and increase upward movement in the water column.

In conclusion, fish passage at the turbine units of the partial powerhouse J-occlusion prototype was influenced by multiple factors. Factors, arranged in rank order of apparent influence are: spill, occlusion, diel effects, and adjacent unit configuration. In addition, the data indicated that the J-occlusions only affected smolt movement and passage in a region relatively close to the occluded intakes. To minimize the influence of extraneous factors, future studies should include provisions for block-loading the turbine units associated with the J-occlusions and for addressing spill flow variability.

Acknowledgments

We sincerely acknowledge the cooperation, assistance, and hard work of the following: Blaine Ebberts, Rock Peters, and Mike Langeslay of the U.S. Army Corps of Engineers, Portland District, for oversight. Don Hibbs district dive coordinator and Larry Lawrence for dive coordination. Bob Cordie and Miro Zyndol for fisheries research coordination with The Dalles Dam project. Dick Harrison and the operators, riggers, mechanics, and electricians of The Dalles Dam project for their support and for making it happen. Rich Vaughn for drawings and advice regarding the J-occlusions. Bill Nagy and Gene Ploskey for their hydroacoustic expertise. Joanne Duncan for autotracker calibration. Traci Degerman for acoustic camera data and presentation graphics. Susan Thorsten for data management and server maintenance. Peter Johnson for staff hiring and Mevatec subcontract administration. Shon Zimmerman, Charlie Escher, and Mike Hanks from Mevatec for hydroacoustic equipment support. Zack Strankman, Jennifer Fortin, and Mark Vucelick, Associated Western Universities fellows for acoustic camera support at the dam and post-processing. Honald Crane for the mobile crane and operator support. Gayle Dirkes and Terrie Bear for administrative assistance. Kathy Lavender and Kristi Brinkerhoff for project finance administration, and Al Garcia for contracts. Cliff Pereira for helpful comments on the draft manuscript.

Contents

Executive Summary	iii
Acknowledgments.....	v
1.0 Introduction.....	1
1.1 Background.....	1
1.2 Study Goals and Objectives.....	2
1.2.1 General Fish Passage.....	2
1.2.2 Focused Analysis of MU1-5.....	2
1.2.3 Acoustic Camera Evaluation of J-Gap Passage.....	2
1.2.4 Smolt Movements Near Sluice 1-2.....	3
1.3 Study Site Description.....	3
1.3.1 Forebay Bathymetry	3
1.3.2 The Dalles Dam.....	4
1.3.3 J-occlusions	4
1.4 Report Organization	6
2.0 Study Conditions.....	7
2.1 River Discharge and Temperature.....	7
2.2 Species Composition	7
2.3 Dam Operations.....	8
2.3.1 Overall.....	8
2.3.2 Main Units 1-5.....	9
2.3.3 J-Gap Evaluation	11
2.4 Realized Treatment Schedule	11
2.5 Study Analysis Matrix.....	12
3.0 General Fish Passage Estimates.....	15
3.1 Objectives	15
3.2 Methods	15
3.2.1 Turbine	16
3.2.2 Sluiceway	17

3.2.3	Spillway.....	18
3.2.4	Autotracking and Detectability.....	19
3.3	Results	20
3.3.1	Passage Metrics	20
3.3.2	Diel Plots.....	25
3.3.3	Horizontal Distributions.....	26
3.4	Discussion.....	29
4.0	Focused Analysis of Main Units 1-5.....	31
4.1	Objectives	31
4.2	Methods	31
4.3	Results	32
4.3.1	Hydraulic Environment	32
4.3.2	Treatment Schedule.....	34
4.3.3	Treatment Differences: Intended Configuration (FU1 - MU5).....	35
4.3.4	Treatment Differences: Movable (MU1-4)	36
4.3.5	Treatment Differences: Stationary Occlusions (FU1-2, MU5)	38
4.3.6	Influence of Adjacent Units: Main Unit 2.....	42
4.3.7	Treatment Differences: Sluice.....	44
4.4	Discussion.....	47
5.0	Acoustic Camera Evaluation of J-Gap Passage	49
5.1	Objectives	49
5.2	Methods	49
5.2.1	Dual-Frequency Identification Sonar (DIDSON)	49
5.2.2	Field Deployment.....	50
5.2.3	Data Analysis	51
5.3	Results	52
5.3.1	Images	52
5.3.2	Fish Behavior, Trajectory, and Fate	53
5.3.3	J-Gaps as a Passage Route.....	54
5.4	Discussion.....	55
6.0	Smolt Movements Near Sluice 1-2	57
6.1	Objectives	57

6.2 Methods	57
6.3 Results	61
6.3.1 Track Description	61
6.3.2 Mean Fish Velocity	62
6.3.3 Direction of Movement Proportions	63
6.3.4 Movement Fate Probabilities	64
6.4 Discussion	72
7.0 References	73

- Appendix A: Equipment Diagrams
- Appendix B: System Calibrations
- Appendix C: Autotracker Parameters
- Appendix D: Hydraulic Environment
- Appendix E: Effective Beam Widths
- Appendix F: Post Tracking Filters
- Appendix G: Hydroacoustic Error Sensitivity Analysis
- Appendix H: Statistical Synopsis
- Appendix I: Sonar Tracker Analysis Methods

Figures

Figure 1. Aerial photograph of The Dalles Dam. Flow is from right to left.	1
Figure 2. Location of The Dalles Dam in relation to other mainstem hydroelectric facilities in the Columbia River Basin.	3
Figure 3. Plan view of The Dalles Dam showing forebay and tailrace bathymetry.	4
Figure 4. Plan view of The Dalles Dam and shoreline (left). Three quarter view of the J-occlusions as deployed (right).	5
Figure 5. Computation fluid dynamics (CFD) simulation of flows into an unoccluded main unit (left), and an occluded main unit (right).	6
Figure 6. 2001 and 10-yr average outflow, spill, and temperature. Data are from DART.	7
Figure 7. Spring species composition data from the John Day Dam smolt monitoring facility.	8
Figure 8. Summer species composition data from the John Day Dam smolt monitoring facility.	8
Figure 9. Hourly dam operations at The Dalles Dam in the spring of 2001. The vertical line divides spring and summer on Julian day 164 at 0500 h.	9
Figure 10. Operations of MU3 and MU4 operations during the acoustic camera J-gap evaluation.	11
Figure 11. Powerhouse, sluiceway, and spillway transducer locations at The Dalles Dam, 2001.	16
Figure 12. Turbine passage transducer deployments: a) occluded, and b) unoccluded. FU1-2 and MU5 were occluded for the duration of the study.	17
Figure 13. Sluiceway transducer deployments: a) occluded, and b) unoccluded.	18
Figure 14. Cross sectional view of a spillway transducer deployment.	19
Figure 15. FPE during day night and spring summer.	20
Figure 16. Sluice passage rates (#/hr) during day night and spring summer.	21
Figure 17. Sluice effectiveness during day night and spring summer.	21
Figure 18. Sluice efficiency in relation to MU1-5 during day night and spring summer.	22
Figure 19. Sluice efficiency in relation to the powerhouse during day night and spring summer.	22

Figure 20. Sluice efficiency in relation to the project during day night and spring summer.	23
Figure 21. Spill passage during day night and spring summer.....	23
Figure 22. Spill effectiveness during day night and spring summer.	24
Figure 23. Spill efficiency during day night and spring summer.	24
Figure 24. Diel passage per flow of the turbine, sluice, and spillway during spring. Error bars are 95% confidence intervals.	25
Figure 25. Diel passage per flow of the turbine, sluice, and spillway during summer. Error bars are 95% confidence intervals.	25
Figure 26. Spring horizontal distribution of fish passage at the spillway, turbine intakes, and the sluiceway above MU1 by day and night.....	26
Figure 27. Spring horizontal distribution of fish passage per flow at the spillway, turbine intakes, and the sluiceway above MU1 by day and night.....	27
Figure 28. Summer horizontal distribution of fish passage at the spillway, turbine intakes, and the sluiceway above MU1 by day and night.....	28
Figure 29. Summer horizontal distribution of fish passage per flow at the spillway, turbine intakes, and the sluiceway above MU1 by day and night.....	29
Figure 30. Transducer deployment for sampling fish passage at main units during the unoccluded treatments. EDmag is velocity in feet per second as measured in the plane shown in the figure.	32
Figure 31. Transducer deployment for sampling fish passage at main units during the occluded treatments. EDmag is velocity in feet per second as measured in the plane shown in the figure.....	33
Figure 32. Transducer deployment for sampling fish passage at fish units. EDmag is velocity in feet per second as measured in the plane shown in the figure.	33
Figure 33. Dam operations. Colored cells indicate the unit was on or the condition was true during an hour. Empty vertical spaces indicate discarded hours where the occlusions were in a transitional state.	34
Figure 34. Daily mean passage per hour through Fish Units 1and 2 and Main Units 1 through 5 during the day. Blue circles indicate Occluded treatment, red squares indicate Unoccluded.....	35
Figure 35. Daily mean passage per hour through Fish Units 1and 2 and Main Units 1 through 5 at night. Blue circles indicate Occluded treatment, red squares indicate Unoccluded.....	36

Figure 36. Daily mean passage per hour through Main Units 1 through 4 during the day. Blue circles indicate Occluded treatment, red squares indicate Unoccluded.....	37
Figure 37. Daily mean passage per hour through Main Units 1 through 4 during the night. Blue circles indicate Occluded treatment, red squares indicate Unoccluded.....	37
Figure 38. Daily mean passage per hour through Fish Unit 1 during the day. Blue circles indicate Occluded treatment, red squares indicate Unoccluded.	38
Figure 39. Daily mean passage per hour through Fish Unit 1 during the night. Blue circles indicate Occluded treatment, red squares indicate Unoccluded.	39
Figure 40. Daily mean passage per hour through Fish Unit 2 during the day. Blue circles indicate Occluded treatment, red squares indicate Unoccluded.	39
Figure 41. Daily mean passage per hour through Fish Unit 2 during the night. Blue circles indicate Occluded treatment, red squares indicate Unoccluded.	40
Figure 42. Daily mean passage per hour through Main Unit 5 during the day. Blue circles indicate Occluded treatment, red squares indicate Unoccluded.	41
Figure 43. Daily mean passage per hour through Main Unit 5 during the night. Blue circles indicate Occluded treatment, red squares indicate Unoccluded.	41
Figure 44. Hourly passage rates through Main Unit 2 during the Occluded treatment during the day. Black circles indicate that the adjacent unit is OFF, green squares indicate the adjacent unit is ON. .	42
Figure 45. Hourly passage rates through Main Unit 2 during the Occluded treatment during the night. Black circles indicate that the adjacent unit is OFF, green squares indicate the adjacent unit is ON.....	43
Figure 46. Hourly passage rates through Main Unit 2 during the Unoccluded treatment during the day. Black circles indicate that the adjacent unit is OFF, green squares indicate the adjacent unit is ON.....	43
Figure 47. Hourly passage rates through Main Unit 2 during the Unoccluded treatment during the night. Black circles indicate that the adjacent unit is OFF, green squares indicate the adjacent unit is ON.....	44
Figure 48. Daily mean passage per hour through the Sluice during the day. Blue circles indicate Occluded treatment, red squares indicate Unoccluded.....	45
Figure 49. Daily mean passage per hour through the Sluice during the night. Blue circles indicate Occluded treatment, red squares indicate Unoccluded.	45

Figure 50. Daily sluice efficiency relative to fish unit 1 through main unit 5 during the day. Blue circles indicate Occluded treatment, red squares indicate Unoccluded.....	46
Figure 51. Daily sluice efficiency relative to fish unit 1 through main unit 5 during the night. Blue circles indicate Occluded treatment, red squares indicate Unoccluded.....	47
Figure 52. Screen capture from DIDSON display showing two fish in foreground and I-beam along the center portion of view (the sonar is located at bottom of figure).....	50
Figure 53. DIDSON mounted to 3-axis rotator, trolley, and I-beam near the forebay deck (left). Front view of occlusion plates, elevation of the DIDSON, and approximate area of coverage (right).	51
Figure 54. Acoustic images of adults (2 left image) and smolts (2 right images) above J-gap.	52
Figure 55. Acoustic image series of an adult sized fish swimming across a J-gap.....	53
Figure 56. Acoustic image of a school of shad near the surface. The sonar is looking out into the forebay.	53
Figure 57. J-gap zone of influence in relation to flows.....	54
Figure 58. Photograph of the active fish tracking sonar.	58
Figure 59. Schematic showing an AFTS, with tracker and split-beam components, and data flow via network (CAT 5) cable from the equipment shed at MU 1 2 to an office trailer at the dam. Two of these systems were deployed.....	59
Figure 60. Side and front views of sample volumes for conditions with (left figures) and without (right figures) J occlusions.....	60
Figure 61. Isometric view of example tracks with (left figure) and without (right figure) J occlusions. Data are from the first 250 tracks collected on April 28 and May 2 for J occlusions IN and OUT, respectively.....	61
Figure 62. Mean observed fish velocity data by period (defined in Table 1) for day and night separately. Shaded areas are data for J occlusions OUT. Positive X is to the east, positive Y is away from the dam, and positive Z is upward in the water column. Periods 1-4 had no spill; periods 5-7 had spill.....	63
Figure 63. Sluice fate probabilities.	66
Figure 64. Bottom fate probabilities.	67
Figure 65. West fate probabilities.....	68

Figure 66. Mean fate probabilities from the Markov-Chain analysis for J-occlusions IN vs. OUT for day and night separately, no spill. (A similar plot for data collected during spill is not available because there were not enough data for the condition with J-occlusions OUT to run the Markov-Chain analysis.)..... 70

Figure 67. Volumetric analyses of sluice, west, and turbot fate probabilities during no spill for day and night separately. The data are the total volume of cells in the Markov sample volume with sluice fate probabilities greater than 0.7, 0.8, and 0.9..... 71

Tables

Table 1. MU1-5 operations pattern frequency. The counts on the right are the number of hours of data collected in that configuration. Dates included are April 25 (Julian day 114) at 1300 h to June 4 (Julian day 155) at 0800 h.....	10
Table 2. Approximate daily realized treatment schedule. An asterisk refers to times in which mechanical problems prevented full deployment of the J-occlusions.....	12
Table 3. Analysis matrix. “nd” means data not available. “n/a” means analysis not applicable.	13
Table 4. The turbine unit combinations used in analyses of adjacent unit effects.....	35
Table 5. Dates and deployment location of data collection.	49
Table 6. Table of fates of fish detected through the sampling range.	54
Table 7. Boundaries of the actual sample volumes by dimension for J occlusions IN/OUT and spill/no spill. (Too few data were available to include the condition of J occlusions OUT and spill.) The data (in meters) are referenced to “dam coordinates” with the origin at the Intake 1 2 centerline at the plane of the pier noses at the water surface (elevation 158 ft). Positive X is to the east, positive Y is away from the dam, and positive Z is upward in the water column	59
Table 8. Descriptive track statistics separately for J occlusions IN and OUT.....	62
Table 9. Summary mean proportions with 95% confidence levels for direction of movement separately for each dimension (X, Y, Z) for J-occlusions IN, OUT, day, night, no spill, and spill. Movement directions obtained from signs of regression coefficients for each dimension of each fish track (regression of position on time).	64

1.0 Introduction

1.1 Background

Development of long-term protection measures for juvenile salmon at The Dalles Dam (Figure 1) is a high priority in the endeavor to increase smolt survival through the Federal Columbia River Power System (National Marine Fisheries Service 2001). At The Dalles Dam, development has entailed use of spill, the design and testing of a prototype extended submerged bar screen (ESBS) and juvenile bypass system (JBS), and testing of intake occlusions and surface collection. The decision to construct the JBS has been delayed until the potential of surface collection and other options have been explored. Currently, the only non-turbine passage routes for downstream migrants are the sluiceway and spillway, which are both used to protect smolts while other fish protection options are being evaluated. Estimates of project-wide fish passage efficiency (FPE) range from 80 to 90%, depending on the percentage of spill, among other factors (Ploskey et al. 2001a,b). Thus, there is a need to improve FPE at this critical passage point in the Columbia River.

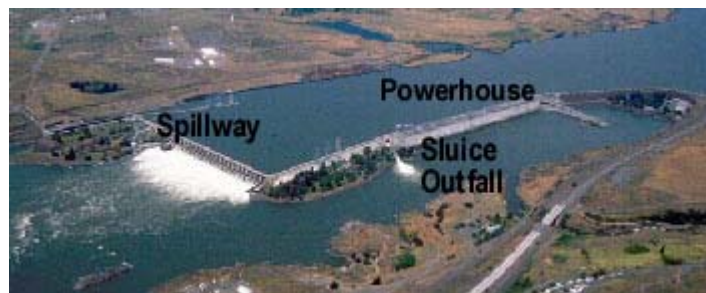


Figure 1. Aerial photograph of The Dalles Dam. Flow is from right to left.

Prior to 2001, turbine intake occlusions were tested at The Dalles, Bonneville, Wanapum, and Lower Granite dams with mixed results. In 1995, occlusion plates were first tested at The Dalles Dam, however, no significant differences in sluiceway efficiency with and without occlusion plates were observed (Nagy and Shuttles 1995). In 1996, occlusion plates were evaluated again at The Dalles Dam, but the results were inconclusive, mainly because of difficulty estimating turbine passage behind the blockages (BioSonics 1996). The 1995 and 1996 tests involved only occlusion plates over the upper portion of the turbine intakes at Main Units 1-5. J-extensions were added for the 2001 test to deepen the turbine flow net. At Bonneville Dam First Powerhouse (B1) in 1996, the upper half of the turbine intakes at Units 3 and 5 were occluded and sluiceway gates at 3B and 5B were opened. The stated purpose of the occlusion at B1 was to intensify and deepen the “zone of separation” between turbine and sluiceway flow nets in an attempt to decrease turbine passage and increase sluiceway fish passage. However, the differences in passage between conditions with and without occlusions were not statistically significant because daily passage was highly variable (Ploskey et al. 2001c). Based on the results of occlusion plate tests at B1 in 1996, reviewers recommended that turbine intake occlusion be investigated further at dams where

enhancing sluiceway passage is a priority (Johnson and Giorgi 1999). At Wanapum Dam, the surface attraction channel that was installed on the forebay side of the powerhouse essentially occluded the upper 20% of the turbine intakes. The apparent effect was to reduce turbine entrainment rates at intakes below the channel (Kumagai et al. 1996). At Lower Granite Dam in 1998, a Simulated Wells Intake (SWI) was retrofit on the existing surface bypass and collector structure. The SWI occluded the upper 20% of the intakes at Units 4-6. A fish budget analysis of juvenile passage from hydroacoustic data indicated that the SWI reduced turbine entrainment when the fish budget coefficients were compared to previous studies without the SWI (Dauble et al. 1999). Thus, the collective results of occlusion plate tests were promising enough that, in conjunction with deepening of the turbine flow net from the new J-extensions, research on the J-occlusions at TDA was a high priority in 2001.

1.2 Study Goals and Objectives

The goal of this study was to evaluate the effects of the J-occlusions on fish passage at The Dalles Dam. Fish passage data from the sluice, spill, and turbine routes provide the means to evaluate and potentially to optimize fish passage survival at this facility. This research provides critical information for the Corp's surface bypass and spill passage programs. The study period was April 24 to July 15, 2001.

1.2.1 General Fish Passage

The objectives of this portion of the study was to enumerate downstream migrant passage through various routes at the dam using fixed-location hydroacoustic techniques. We estimated proportions of the numbers and density (fish per unit flow) of juvenile salmon passing the dam through each route. The effect of the J-occlusion treatments was the objective addressed in the following section. Split-beam transducer at each type of passage route were used to estimate the average backscattering cross section of fish for detectability modeling and the direction of fish travel through sampling volumes to assess the assumptions of the acoustic screen model.

1.2.2 Focused Analysis of MU1-5

The objective of this component of the study was to provide an in-depth analysis of fish passage through Main Units 1-5 and the sluiceway to evaluate localized effects of J-occlusions.

1.2.3 Acoustic Camera Evaluation of J-Gap Passage

As part of the overall performance evaluation of the J-occlusions, the purpose of this portion of the study was to elucidate the extent to which J-gap losses may influence fish passage. Presumably, fish lost through the gaps would otherwise have been available for passage through another route (e.g., the ice and trash sluiceway or the spillway). This was the first application of sonar imaging or acoustic camera

technology. The specific objectives were to determine whether or not smolts were being entrained through gaps and to estimate the rate of entrainment. We also noted the occurrence of predators in the vicinity of the J-sections.

1.2.4 Smolt Movements Near Sluice 1-2

Smolt movements were quantified with a sonar tracker in order to describe movement patterns in terms of observed fish velocities and movement fates. Movement patterns with and without J-occlusions in place were compared. We also assessed specific hypotheses about smolt movement patterns in relation to the presence or absence of J-occlusions.

1.3 Study Site Description

The Dalles Dam, located at Columbia River mile 192, is comprised of a navigation lock, a spillway perpendicular to the main river channel, and a powerhouse parallel to the main river channel with non-overflow dams on each side. Situated between Bonneville and John Day Dams, it is the second dam upstream of the mouth of the Columbia River (Figure 2).

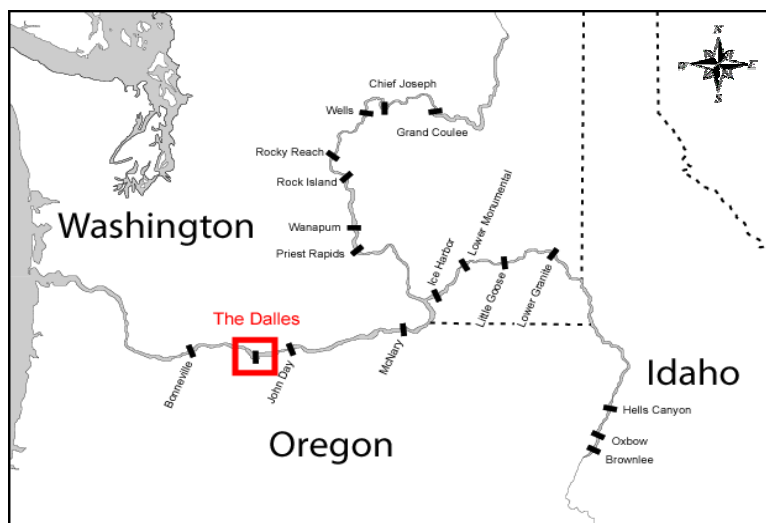


Figure 2. Location of The Dalles Dam in relation to other mainstem hydroelectric facilities in the Columbia River Basin.

1.3.1 Forebay Bathymetry

The historical river channel, or thalweg, passes the east end of the powerhouse. A bathymetric map of the forebay shows the main channel of the river along the south shore and deep areas in front of the powerhouse (Figure 3). Much of the forebay, however, is relatively shallow (< 20 m deep). The majority of flow in the reservoir above the dam is through the thalweg. This may influence fish passage patterns,

with the bulk of migrants following the bathymetric contours (Johnson and Dauble 1995). The forebay environment is one factor that makes fish passage patterns unique at each hydroelectric facility.

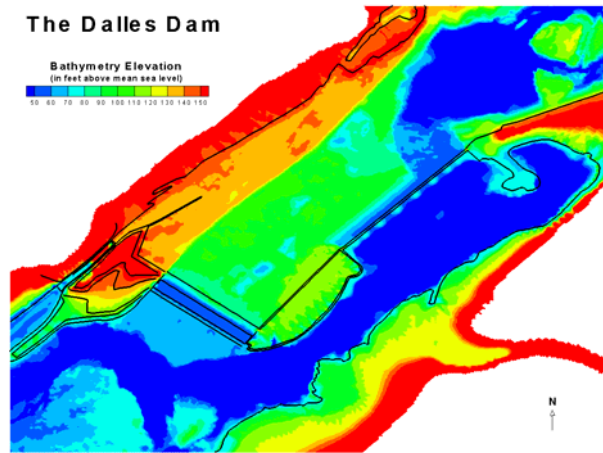


Figure 3. Plan view of The Dalles Dam showing forebay and tailrace bathymetry.

1.3.2 The Dalles Dam

The powerhouse spans 2089 ft and has 22 main units (MU), numbered from the west (downstream) end. Each unit has three intakes, numbered again from west to east. Reference to a specific turbine intake is expressed as the turbine unit and intake number, e.g., 2-3 for the east intake of MU2 and 1-2 for the center intake of MU1. Two fish units are located just west of MU1 and have only two intakes each. Total hydraulic capacity of the 22 unit powerhouse is about 375 kcfs. The face of the dam is at an 11.3° angle off vertical. The spillway spans 1380 ft and has 23 bays, numbered from the Washington shore.

An ice and trash sluiceway extends the entire length of the powerhouse. Skimmer gates may be opened above each turbine intake and discharged into the sluiceway. During the fish passage season (April through November), the three gates above MU1 are typically opened. This operation is based on previous research (e.g., Nichols and Ransom 1980). Maximum discharge of the ice and trash sluiceway through all three gates of one turbine unit is approximately 4750 cfs with the forebay at elevation 160 ft. The capacity of the sluiceway is limited hydraulically because of a constriction in the downstream end of the channel near where it exits the powerhouse. The sill at each sluiceway entrance is at elevation 151 ft. Actual discharge fluctuates with forebay elevation and is a relatively small proportion of total project discharge (~1-5%).

1.3.3 J-occlusions

At The Dalles Dam in 2001, prototype turbine intake occlusion plates with J-extensions were evaluated as a new means of protecting migrating juvenile salmon. The intake occlusions were formed by a sheet of steel that rested against the upstream side of the trashracks. The occlusion plates covered the

upper half of the intakes at Fish Units 1-2 and Main Units 1-5 and prevented flow from entering the turbine intake above an elevation of 100 ft. At the lower edge of the occlusion, another steel sheet extended 20 ft into the forebay, perpendicular to the trashracks. Then, at the upstream edge of this horizontal, there was a 5 ft high vertical piece. Thus, the entire occlusion assembly had the shape of the capital letter “J” when viewed from the side (Figure 4).

The premise behind the J-occlusions is that deepening the turbine flow net will decrease fish entrainment into turbines because juvenile migrants are naturally oriented toward the surface (Figure 5). The J-occlusions at MU1-4 were raised and lowered via dedicated hydraulic winches. Thus, J-occlusions at main units 1-4 may be raised or lowered depending upon the desired operation. At FU1-2 and MU5, the J-occlusions were left in the occluded position for the entire season. Gaps were present between each horizontal panel in the J because of turbine intake piers between adjacent vertical occlusions. These gaps were the width of each piernose. The gaps between units were wider than the gaps between adjacent intakes of a single unit.

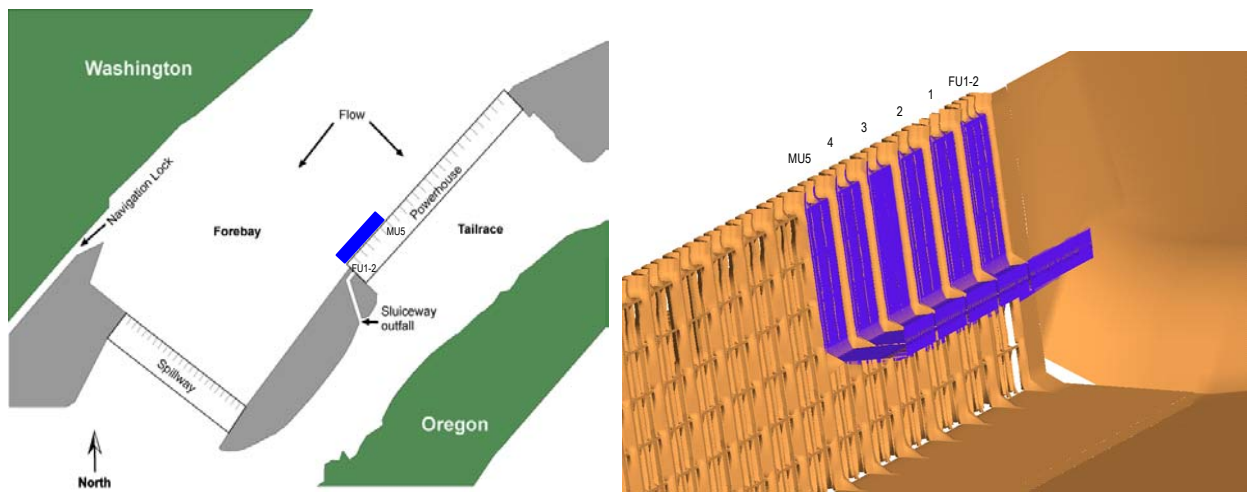


Figure 4. Plan view of The Dalles Dam and shoreline (left). Three quarter view of the J-occlusions as deployed (right).

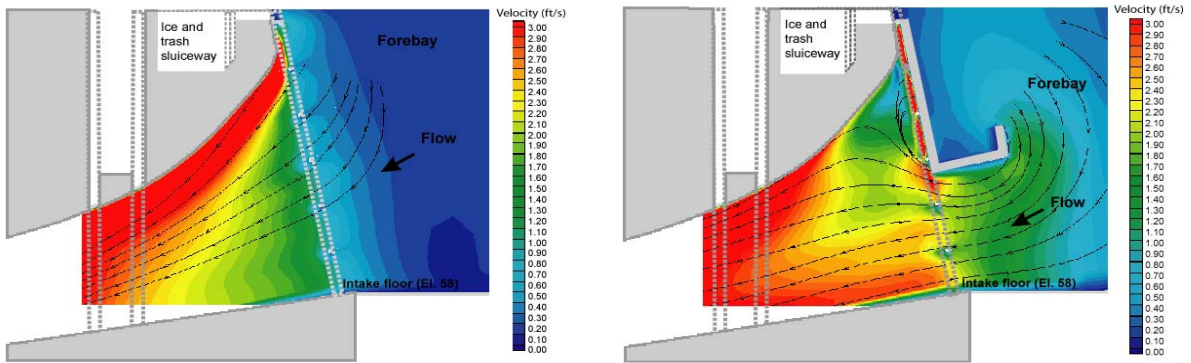


Figure 5. Computation fluid dynamics (CFD) simulation of flows into an unoccluded main unit (left), and an occluded main unit (right).

1.4 Report Organization

This report has several sections. The study and explanation of the research are put into context in the Introduction. The Study Conditions section describes the environmental and operational characteristics of during the 2001 study. The General Fish Passage section reports on fish passage efficiency and other project-wide fish passage metrics. Turbine passage at MU1-5 is examined in detail in relation to the realized J-occlusion treatments in the section called Focused Analysis of MU1-5. The Acoustic Camera Evaluation of J-Gap Passage section examines fish passage through the main unit gaps using a new sonar technology. Smolt Movements Near Sluice 1-2 describes smolt movement patterns as evaluated using a sonar tracker. All References and Appendices entail the final two sections.

2.0 Study Conditions

2.1 River Discharge and Temperature

Outflow during the 2001 study period (April 24 to July 15, 2001) was 45.5% of the 10-year average. Spill was only 13% of the 10-yr average. Spill occurred from May 16 to June 15. River temperature was slightly elevated at 106% of the 10-yr average (Figure 6).

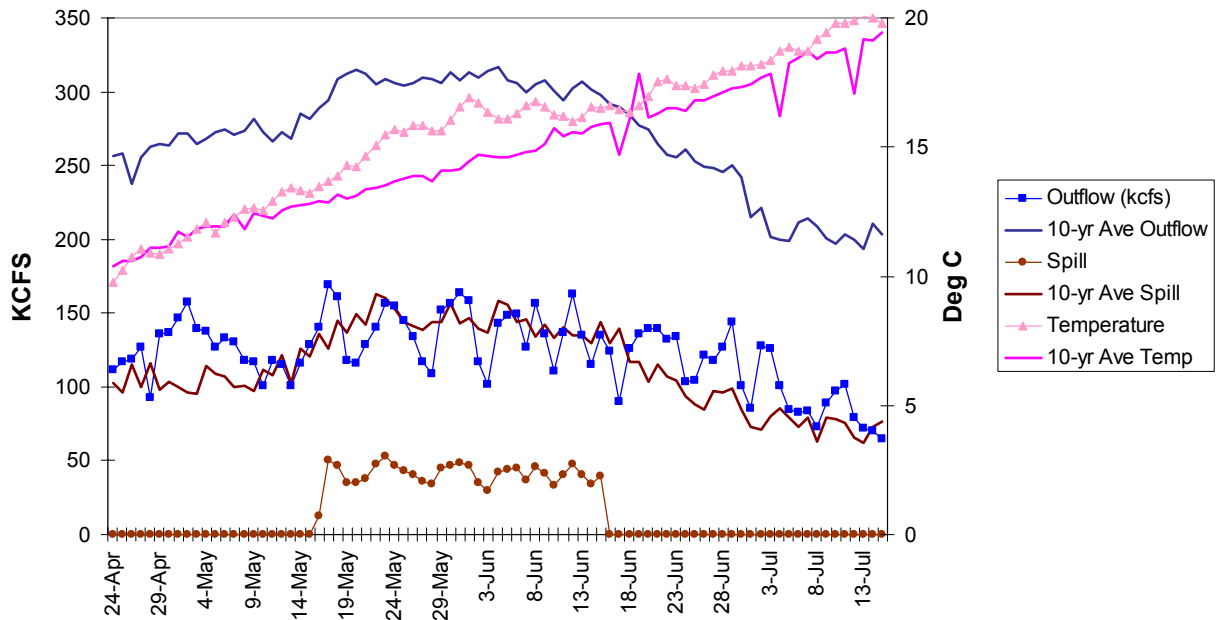


Figure 6. 2001 and 10-yr average outflow, spill, and temperature. Data are from DART.

2.2 Species Composition

During spring, 70% of the downstream migrants were yearling chinook, and 24% were juvenile steelhead as indicated by smolt monitoring data from the sampling site at John Day Dam. The remainder of the run consisted of coho, sockeye, and sub-yearling chinook smolts (Figure 7). The spring-summer cutoff was June 13 at 0500h, based on the shift in dominance from yearling chinook to subyearling chinook.

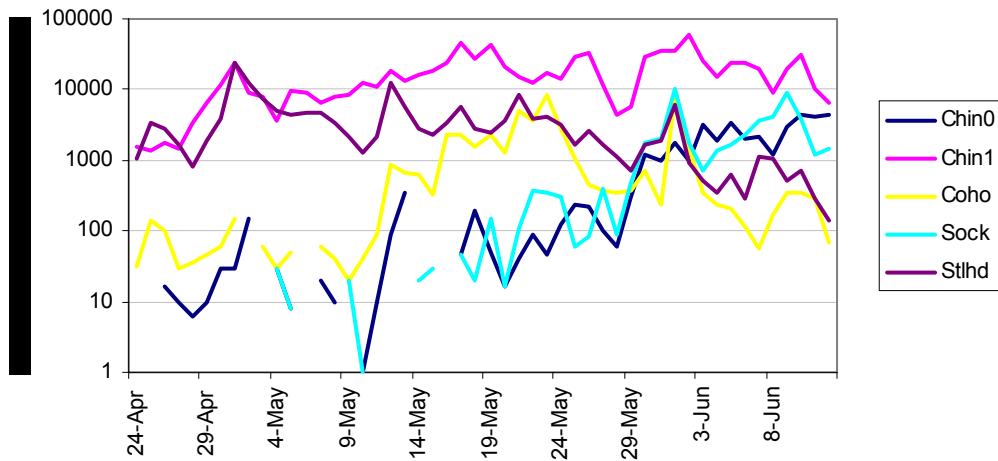


Figure 7. Spring species composition data from the John Day Dam smolt monitoring facility.

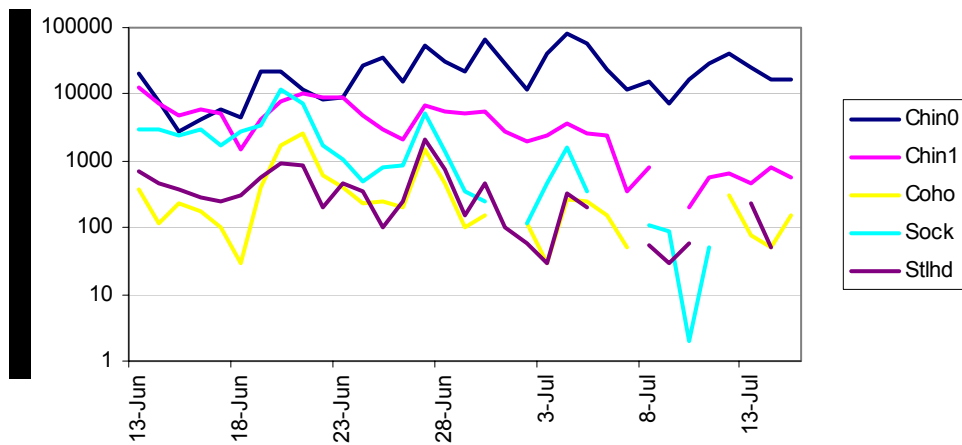


Figure 8. Summer species composition data from the John Day Dam smolt monitoring facility.

2.3 Dam Operations

2.3.1 Overall

Spill was limited and did not occur for part of spring and nearly all of summer. The hourly dam operations data for spring and summer (Figure 9) show considerable variability in powerhouse and spillway discharges. Sluice operations, however, were nearly constant.

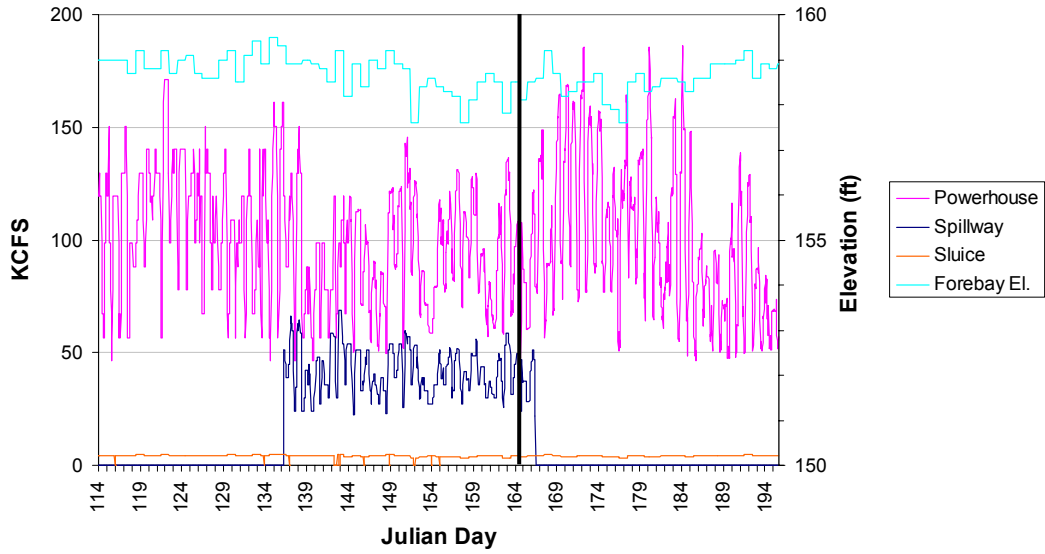


Figure 9. Hourly dam operations at The Dalles Dam in the spring of 2001. The vertical line divides spring and summer on Julian day 164 at 0500 h.

2.3.2 Main Units 1-5

Main units 1-5, which were critical to evaluating the J-occlusions, were not operated consistently. We observed nearly every conceivable combination of operating turbines. Table 1 shows the unit pattern and frequency of data available for evaluating J-occlusion treatments.

Table 1. MU1-5 operations pattern frequency. The counts on the right are the number of hours of data collected in that configuration. Dates included are April 25 (Julian day 114) at 1300 h to June 4 (Julian day 155) at 0800 h.

FU1	FU2	MU1	MU2	MU3	MU4	MU5
OFF						
ON	OFF	OFF	OFF	OFF	OFF	OFF
ON	ON	OFF	OFF	OFF	OFF	OFF
ON	ON	ON	OFF	OFF	OFF	OFF
ON	ON	OFF	ON	OFF	OFF	OFF
ON	ON	ON	ON	OFF	OFF	OFF
ON	ON	ON	OFF	ON	OFF	OFF
ON	ON	ON	ON	ON	OFF	OFF
ON	ON	ON	OFF	OFF	ON	OFF
ON	ON	OFF	ON	OFF	ON	OFF
ON	ON	ON	ON	OFF	ON	OFF
ON	ON	ON	OFF	ON	ON	OFF
ON	ON	OFF	ON	ON	ON	OFF
ON	ON	ON	ON	ON	ON	OFF
ON	ON	OFF	OFF	OFF	OFF	ON
ON	ON	ON	OFF	OFF	OFF	ON
ON	ON	OFF	ON	OFF	OFF	ON
ON	ON	ON	ON	OFF	OFF	ON
ON	ON	OFF	OFF	ON	OFF	ON
ON	ON	ON	OFF	ON	OFF	ON
ON	ON	OFF	ON	ON	OFF	ON
ON	ON	ON	ON	ON	OFF	ON
ON	ON	OFF	OFF	OFF	ON	ON
ON	ON	ON	OFF	OFF	ON	ON
ON	ON	OFF	ON	OFF	ON	ON
ON	ON	ON	ON	OFF	ON	ON
ON	ON	ON	OFF	ON	ON	ON
ON	ON	OFF	ON	ON	ON	ON
ON						

Occluded Night	Occluded Day	Unoccluded Night	Unoccluded Day	Discarded
				3
				51
				6
	1			
		3		
6			3	
	4			
	6		9	
	3			1
3	5			
				2
			7	
		1		
6	1	17	1	13
	4			
6	3			1
26	18	13	8	
8	26	26	17	3
		1		
13		7		
	6	1		
16	4	5	4	7
3	6	4	2	
	47	1	45	
49	14	56	31	
24	49	16	71	6
11	5	17	9	
	1		6	
27	11	45	19	25

2.3.3 J-Gap Evaluation

Project flows were variable through the J-gap evaluation and ranged from 110 to 162 kcfs. The average spill was 40.3 kcfs and the sluice was drew 4.3 kcfs through the ice and trash sluiceway. At the 3-4 gap, unit 3 was on for only about half the time (Figure 10). The acoustic camera data were collected during an occluded treatment, however the MU4-3 occlusion was not deployed due to a mechanical failure.

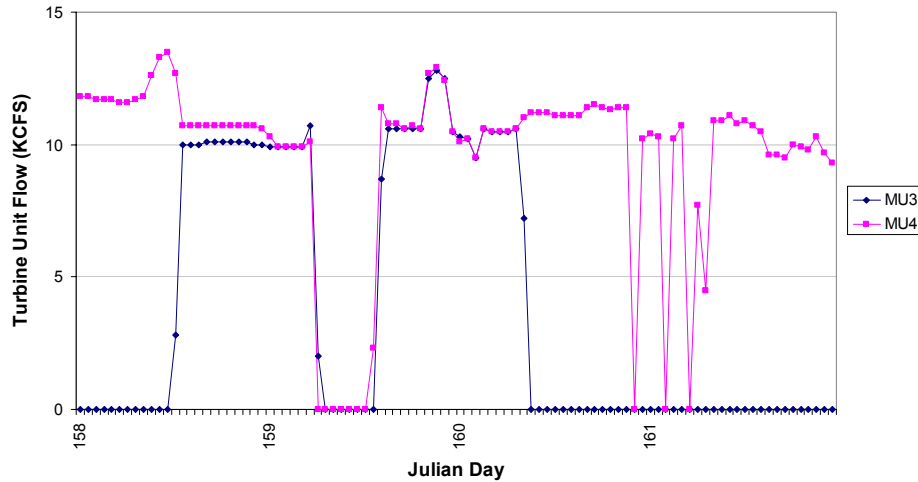


Figure 10. Operations of MU3 and MU4 operations during the acoustic camera J-gap evaluation.

2.4 Realized Treatment Schedule

The original experimental design called for 6 day blocks, with each 3-day treatment randomly assigned to either the first or last half of each block. This design was not met for a number of reasons. The transition times (the amount of time it took to change the configuration to either occluded or unoccluded) varied up to 12 hours, causing many blocks to be truncated. Mechanical difficulties occasionally lead to one or more J-occlusions being stuck and not in the planned treatment configuration for some or all of a treatment (Table 2). The absence of some patterns in specific diel and treatment combinations means that comparisons of the original treatment blocks would be subject to the influence of spatial and temporal influences unrelated to the question of interest. Due to this, the planned treatment analysis was not relevant and had to be abandoned.

Table 2. Approximate daily-realized treatment schedule. An asterisk refers to times in which mechanical problems prevented full deployment of the J-occlusions.

Date	Treatment	Spill	Date	Treatment	Spill	Date	Treatment	Spill
24-Apr	Transition	No	22-May	Unoccluded	Spill	19-Jun	Occluded*	No
25-Apr	Occluded	No	23-May	Transition	Spill	20-Jun	Occluded*	No
26-Apr	Occluded	No	24-May	Occluded	Spill	21-Jun	Occluded*	No
27-Apr	Occluded	No	25-May	Occluded	Spill	22-Jun	Occluded*	No
28-Apr	Occluded	No	26-May	Transition	Spill	23-Jun	Occluded*	No
29-Apr	Occluded	No	27-May	Unoccluded	Spill	24-Jun	Occluded*	No
30-Apr	Transition	No	28-May	Unoccluded	Spill	25-Jun	Occluded*	No
1-May	Unoccluded	No	29-May	Transition	Spill	26-Jun	Occluded*	No
2-May	Unoccluded	No	30-May	Occluded	Spill	27-Jun	Occluded*	No
3-May	Unoccluded	No	31-May	Occluded	Spill	28-Jun	Occluded*	No
4-May	Unoccluded	No	1-Jun	Transition	Spill	29-Jun	Occluded*	No
5-May	Transition	No	2-Jun	Unoccluded	Spill	30-Jun	Occluded*	No
6-May	Occluded	No	3-Jun	Unoccluded	Spill	1-Jul	Occluded*	No
7-May	Occluded	No	4-Jun	Transition	Spill	2-Jul	Occluded*	No
8-May	Occluded	No	5-Jun	Occluded*	Spill	3-Jul	Occluded*	No
9-May	Occluded	No	6-Jun	Occluded*	Spill	4-Jul	Occluded*	No
10-May	Occluded	No	7-Jun	Occluded*	Spill	5-Jul	Occluded*	No
11-May	Transition	No	8-Jun	Occluded*	Spill	6-Jul	Occluded*	No
12-May	Unoccluded	No	9-Jun	Occluded*	Spill	7-Jul	Occluded*	No
13-May	Unoccluded	No	10-Jun	Transition	Spill	8-Jul	Occluded*	No
14-May	Transition	No	11-Jun	Transition	Spill	9-Jul	Occluded*	No
15-May	Occluded*	No	12-Jun	Transition	Spill	10-Jul	Occluded*	No
16-May	Occluded*	Spill	13-Jun	Transition	Spill	11-Jul	Occluded*	No
17-May	Transition	Spill	14-Jun	Transition	Spill	12-Jul	Occluded*	No
18-May	Unoccluded	Spill	15-Jun	Transition	Spill	13-Jul	Occluded*	No
19-May	Unoccluded	Spill	16-Jun	Occluded*	No	14-Jul	Occluded*	No
20-May	Unoccluded	Spill	17-Jun	Occluded*	No	15-Jul	Occluded*	No
21-May	Unoccluded	Spill	18-Jun	Occluded*	No			

2.5 Study Analysis Matrix

Due to the dam and J-occlusion operations described above, analyses were limited. Table 3 describes the available analyses included in this report. Limited statistical tests were possible based on treatment. The seasonal fish passage metrics reported include all data, regardless of J-occlusion state.

Table 3. Analysis matrix. “nd” means data not available. “n/a” means analysis not applicable.

Objective	Parameter		Spring									Summer		
			In			Out			All			In/All		
			D	N	C	D	N	C	D	N	C	D	N	C
Passage (Apr 24–Jun 13) (Jun 14–Jul 15)	MU 1	#/hr	●	●	●	●	●	●	n/a	n/a	n/a	n/a	n/a	n/a
	MU 2	#/hr	●	●	●	●	●	●	n/a	n/a	n/a	n/a	n/a	n/a
	MU 3	#/hr	nd	nd	nd	nd	nd	nd	n/a	n/a	n/a	n/a	n/a	n/a
	MU 4	#/hr	●	●	●	●	●	●	n/a	n/a	n/a	n/a	n/a	n/a
	MU 5	#/hr	●	●	●	●	●	●	n/a	n/a	n/a	n/a	n/a	n/a
	MU 1-4	#/hr	▲	▲	●	▲	▲	●	n/a	n/a	n/a	n/a	n/a	n/a
	MU 1-5	#/hr	▲	▲	●	▲	▲	●	n/a	n/a	n/a	n/a	n/a	n/a
	MU 1-22	#/flow	n/a	n/a	n/a	n/a	n/a	n/a	●	●	●	●	●	●
	SL	#/hr	▲	▲	●	▲	▲	●	●	●	●	●	●	●
	SLY 1-5	sl/1-5	▲	▲	●	▲	▲	●	●	●	●	●	●	●
	SLY powerhouse	sl/ph	n/a	n/a	n/a	n/a	n/a	n/a	●	●	●	●	●	●
	SLY project	sl/proj	n/a	n/a	n/a	n/a	n/a	n/a	●	●	●	●	●	●
	SLE		n/a	n/a	n/a	n/a	n/a	n/a	●	●	●	●	●	●
	SP	#/hr	nd	nd	nd	nd	nd	nd	●	●	●	nd	nd	nd
SPE	#/flow	nd	nd	nd	nd	nd	nd	●	●	●	nd	nd	nd	
SPY	ratio	nd	nd	nd	nd	nd	nd	●	●	●	nd	nd	nd	
FPE	ratio	nd	nd	nd	nd	nd	nd	●	●	●	nd	nd	nd	
Gap Loss (June 7–10)	Gap passage	rate	●	●	●	nd	nd	nd						
Nearfield Movements (Apr 24–Jun 1)	Mean Velocity		●	●	●	●	●	●	●	●	●	nd	nd	nd
	Proportion		●	●	●	●	●	●	●	●	●	nd	nd	nd
	Fates		●	●	●	●	●	●	Nd	nd	nd	nd	nd	nd

3.0 General Fish Passage Estimates

3.1 Objectives

The objectives of this portion of the study were to utilize fixed-location hydroacoustic techniques to enumerate downstream migrant passage through various routes at the dam. Specifically, we estimated the proportion of juvenile salmon passing the dam through each route, and passage as a proportion of discharge.

Spill was not manipulated for the purposes of this study, and only the juvenile—or nighttime—spill pattern was used. The juvenile spill pattern initiates spill at the north side of the spillway, and typically has spill at bays 1-14. Fixed-location hydroacoustic techniques were used to sample passage at the spillway, sluiceway, and turbine intakes. Passage estimates for each route, for each hour, were made by the expansion of sampling time and volume. Fish passage was monitored 24 hours/day, 7 days/week. Passage through unmonitored routes was estimated by interpolation. Spring data collection occurred from April 24 through June 13, 2000. Summer data collection occurred from June 14 through July 15. Nighttime extended from 1900 through 0559 hours.

3.2 Methods

A combination of 6° single-beam and 6° split-beam transducers were deployed to estimate fish passage rates and distributions. This approach uses the acoustic screen model to determine passage rates. Split-beam transducers provided data to determine weighting factors, assess assumptions of the model, and determine the magnitude of any biases. Split-beam transducer deployments at each type of passage route were used to estimate the average backscattering cross section of fish for detectability modeling and the direction of fish travel through sampling volumes to assess the assumptions of the acoustic screen model. Single and split-beam transducers were deployed to sample fish passage at the spillway, ice and trash sluiceway, and turbines (Figure 11). Transducer sampling volumes were strategically aimed to minimize ambiguity in ultimate fish passage routes and the potential for multiple detections.

Single-beam data collection employed five PAS single-beam multiplexed systems. Split-beam data collection included three PAS split-beam systems, with two systems being multiplexed. All of these systems operated at 420 kHz. The single-beam data collection system consisted of Harp-1B Single-Beam Data Acquisition/Signal Processing Software installed on a personal computer controlling a PAS-103 Multi-Mode Scientific Sounder. The PAS-103 Sounder then operated a PAS 420 kHz single-beam transducer deployed in a main turbine unit, fish unit, or spill bay. Appendix A describes the equipment layout in detail. Appendix B describes the calibration for each system.

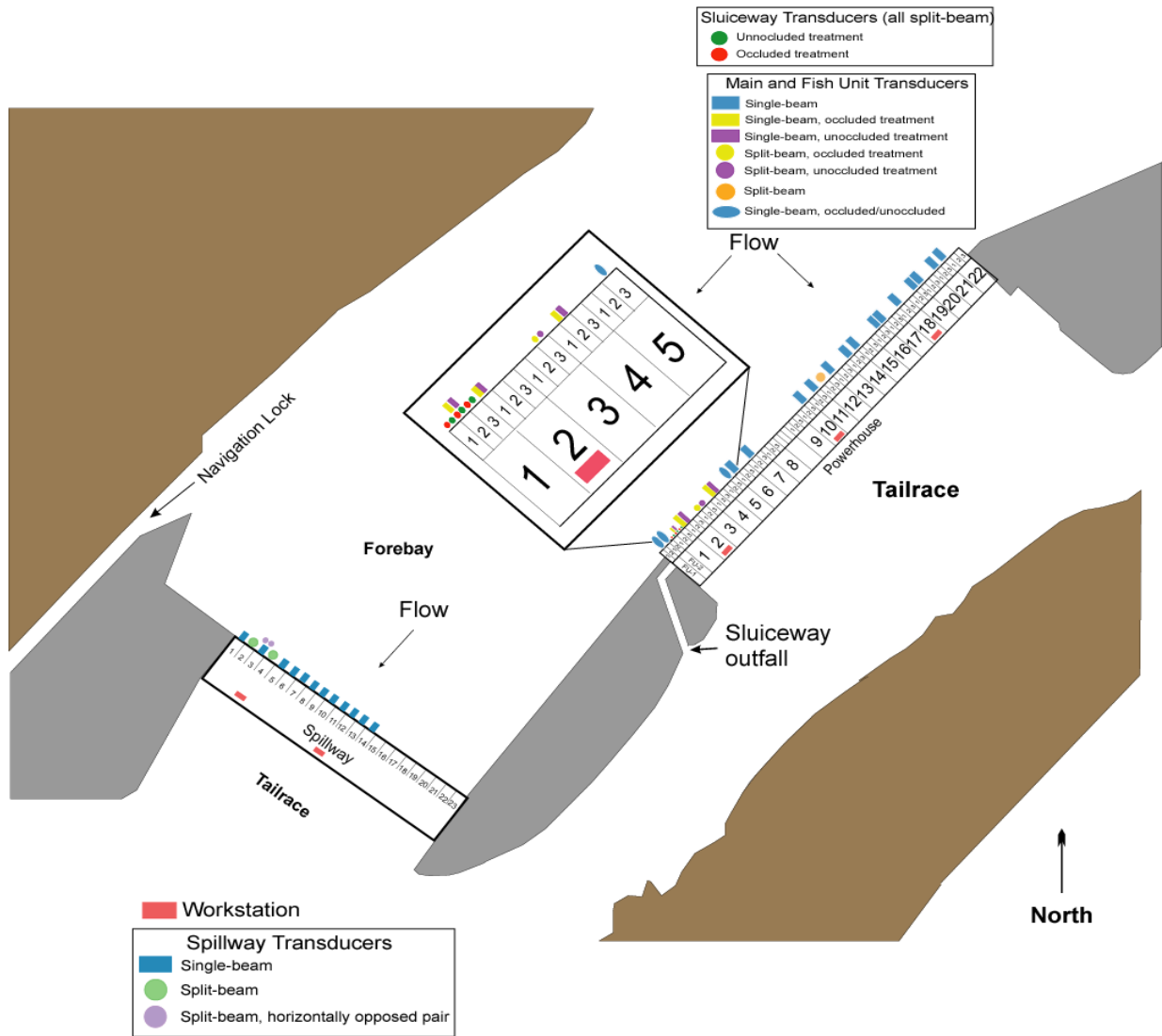


Figure 11. Powerhouse, sluiceway, and spillway transducer locations at The Dalles Dam, 2001.

3.2.1 Turbine

Single-beam System C with 9 transducers and split-beam System W with 8 transducers were both used to monitor Main Units 1-5, Fish Units 1-2, and the sluiceway openings at MU 1 during both occluded and unoccluded treatments. Occluded transducers were all looking down and attached to the inside of the trash rack at an elevation of 135 feet, aimed downstream at a 15° angle to the plane of the trash rack looking towards the bottom (Figure 12a). Unoccluded transducers were all looking up and attached to the inside of the trash rack at an elevation of 75 feet, aimed downstream at a 31° angle to the plane of the trash rack looking towards the intake ceiling (Figure 12b). Both systems sampled at a rate of 15 pings per second, running 1 transducer at 1-minute time intervals, 10 times per hour.

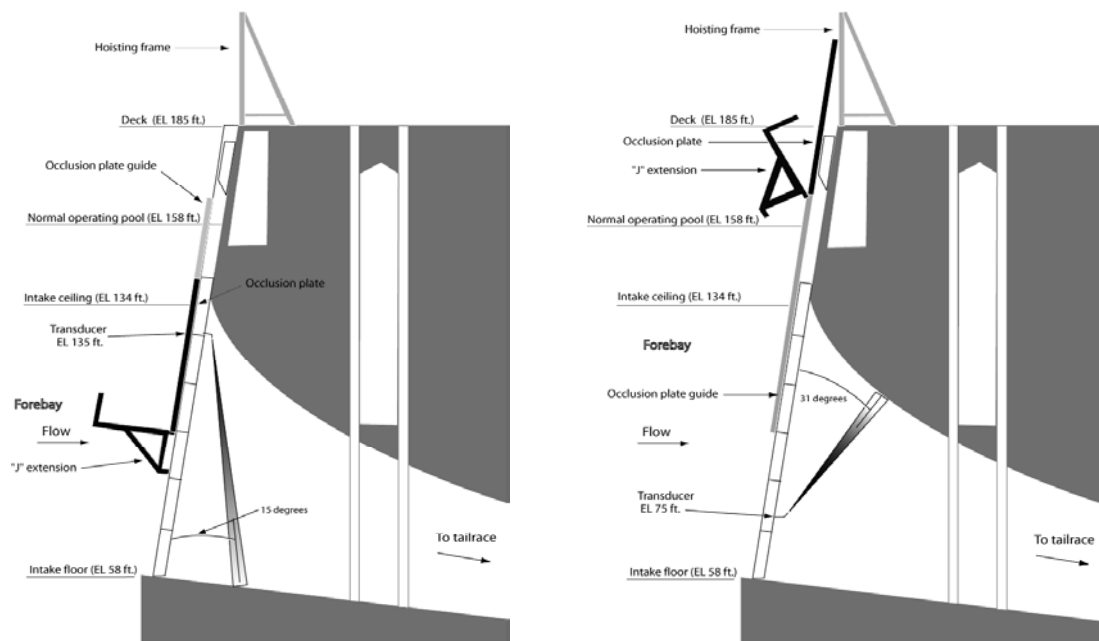


Figure 12. Turbine passage transducer deployments: a) occluded, and b) unoccluded. FU1-2 and MU5 were occluded for the duration of the study.

3.2.2 Sluiceway

Monitoring the sluiceway openings at MU 1 entailed the use of 6 split-beam transducers from System W. In order to monitor both occluded and unoccluded treatments, there were 2 transducers in each of main units 1-1m, 1-2m, and 1-3m. For the occluded treatments, the second transducer was attached to the upstream side of the occlusion plate at an elevation of 110 feet, aimed upstream at a 5° angle to the plane of the trash rack looking up toward the forebay water surface (Figure 13a). For the unoccluded treatments, one transducer was attached to the outside of the trash rack at an elevation of 95 feet, aimed upstream at a 5° angle to the plane of the trash rack looking up toward the intake ceiling (Figure 13b). System W at the sluiceway opening sampled at a rate of 15 pings per second, running 1 transducer at 1 minute time intervals, 15 times per hour.

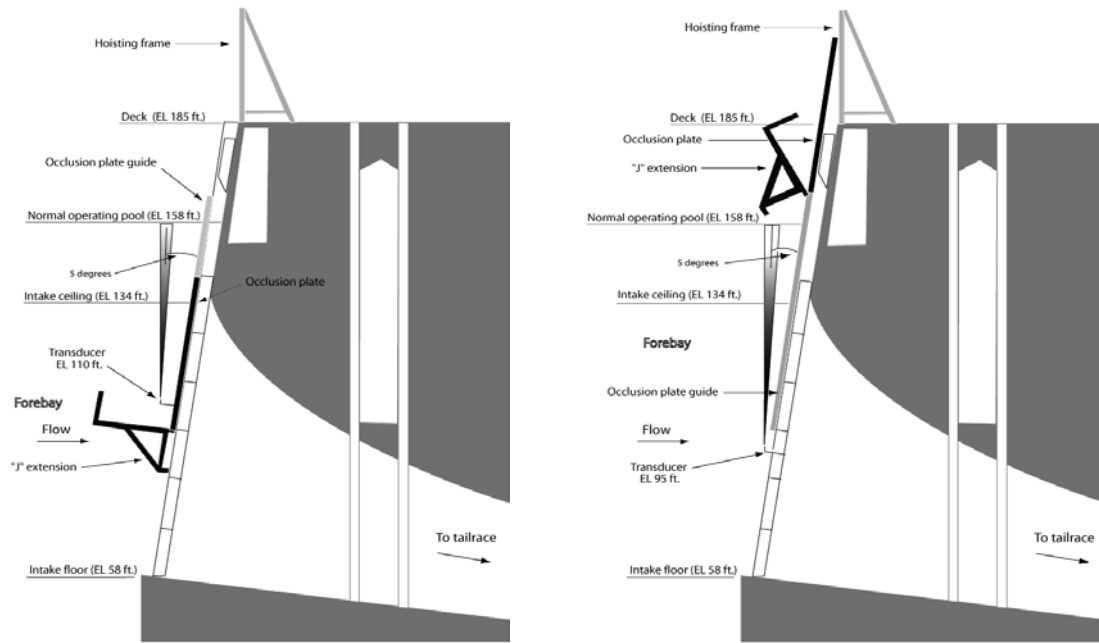


Figure 13. Sluiceway transducer deployments: a) occluded, and b) unoccluded.

3.2.3 Spillway

At spill bays 1-14, we deployed 10° single-beam and 12° split-beam transducers. Pole mounts were used for all transducer deployments (Figure 14). In addition, each pole-mounted transducer was placed randomly in either a north (n), middle (m), or south (s) location in an attempt for non-uniform horizontal distribution through the spill bays. Spill bay sampling locations (bay-position) were: 1n, 2m, 3m, 4s, 5n, 6m, 7s, 8m, 9s, 10n, 11n, 12s, 13m, and 14n. Single-beam deployment was split into two systems. System G sampled spill bays 1, 3, and 5-8 and System F sampled bays 9-14. System Q was a split-beam system deployed to sample bays 2, 3, and 4. Each transducer was deployed in the forebay at an elevation of 155 ft. They were aimed downstream toward the tainter gate opening at an 8° angle from vertical. System G and system F transducers sampled at a rate of 27 pings per second, running 1 transducer at 1-minute time intervals, 10 times per hour.

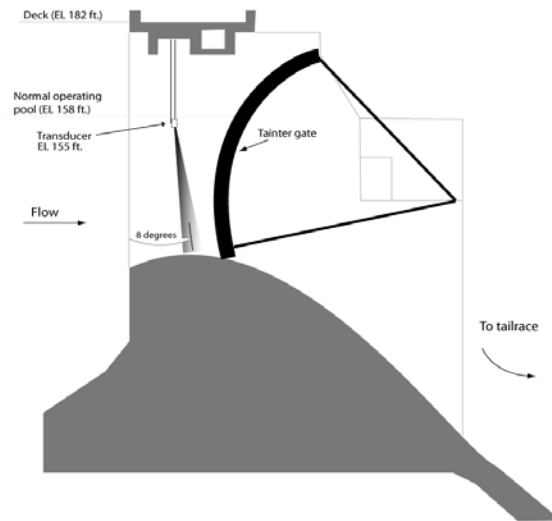


Figure 14. Cross sectional view of a spillway transducer deployment.

3.2.4 Autotracking and Detectability

The data produced by both single- and split-beam transducers were processed with autotracking software. The parameters used are described in Appendix C. Split-beam data of smolt movements through the beam were then used as an input into the detectability model. For regions that contained either zero or too few fish to comprise a reasonable statistical sample, hydraulic model data was used to aid in missing value estimation. These data from a computational fluid dynamics model are shown in Appendix D.

Under the acoustic screen model, the number of tracks within the beam is expanded spatially and temporally to represent total passage through a single passage route. Effective beam widths are used to correct the spatial expansion factors involved in estimates of fish passage. Appendix E shows the effective beam widths used under each operational condition of this study.

Post-tracking filters were developed to eliminate traces having trace statistics inconsistent with a smolt-sized fish committed to passing the dam by the monitored route. These filters were based upon fields contained in the track statistics output by the autotracker and are described in detail in Appendix F. Finally, an error sensitivity analysis of hydroacoustic passage estimates is presented as Appendix G.

3.3 Results

3.3.1 Passage Metrics

The following figures contain graphic and tabular data on fish passage rates (#/hr), fish passage per unit flow, fish passage efficiency, sluiceway efficiency, and spillway efficiency. Recall, spring was defined as the period from April 24 to June 13 and summer was June 14 to July 15. Some important points from these data include the following:

- Overall, FPE was 83% in spring and 14% in summer.
- Sluiceway efficiency relative to the powerhouse was 53% in spring and 6% in summer. Relative to the entire project, sluiceway efficiency was 18% and 5% in spring and summer, respectively.
- Spillway efficiency was 65% in spring and 9% in summer.

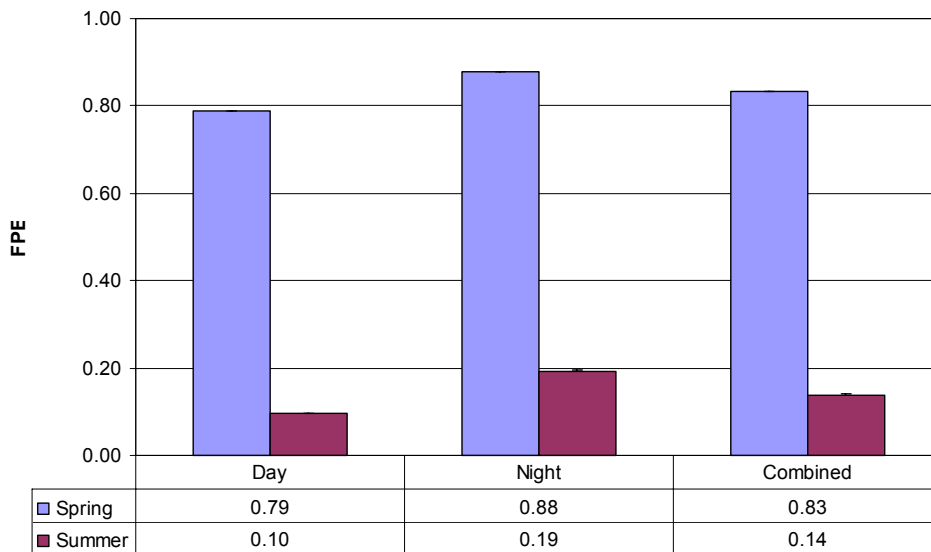


Figure 15. FPE during day|night and spring|summer.

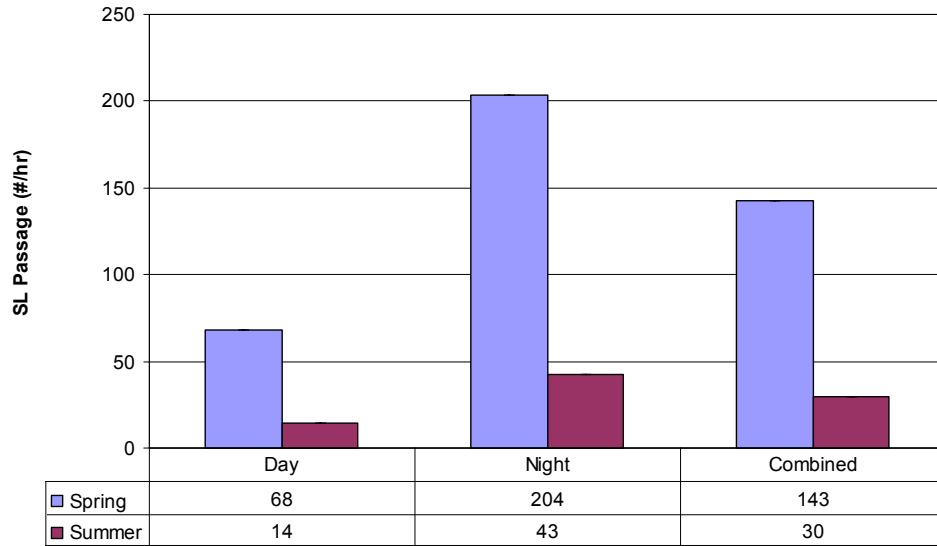


Figure 16. Sluice passage rates (#/hr) during day|night and spring|summer.

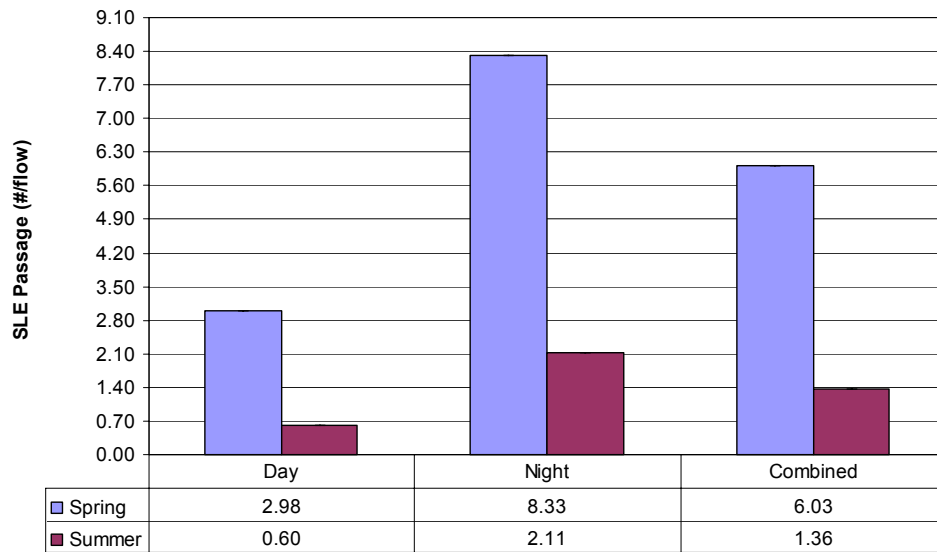


Figure 17. Sluice effectiveness during day|night and spring|summer.

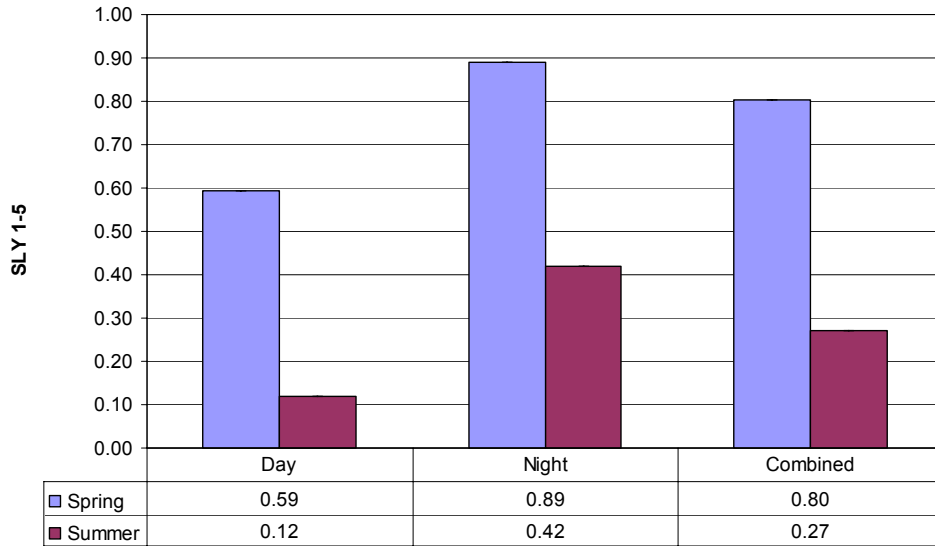


Figure 18. Sluice efficiency in relation to MU1-5 during day|night and spring|summer.

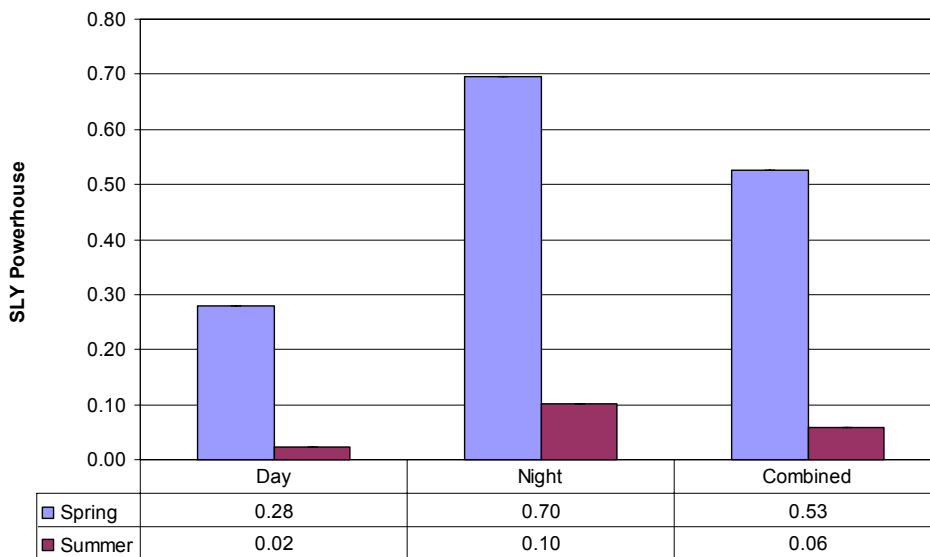


Figure 19. Sluice efficiency in relation to the powerhouse during day|night and spring|summer.

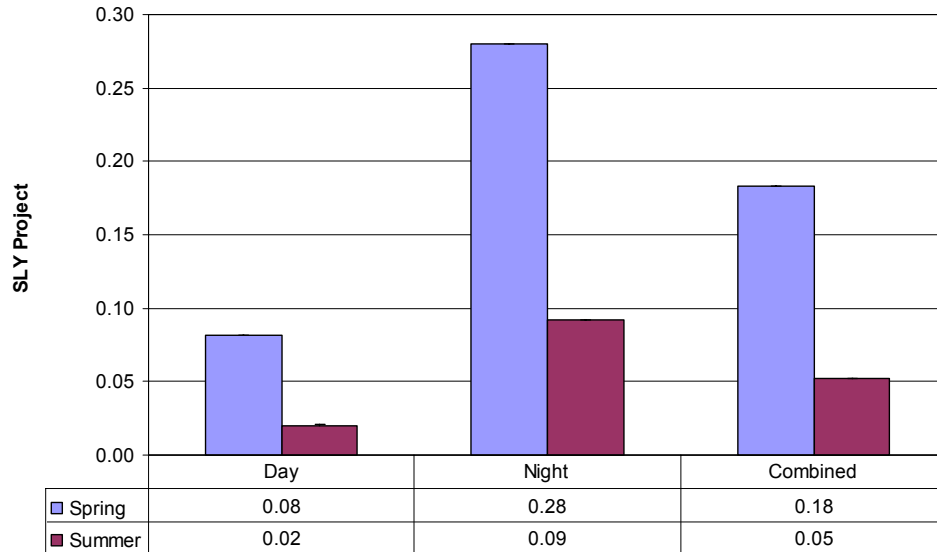


Figure 20. Sluice efficiency in relation to the project during day|night and spring|summer.

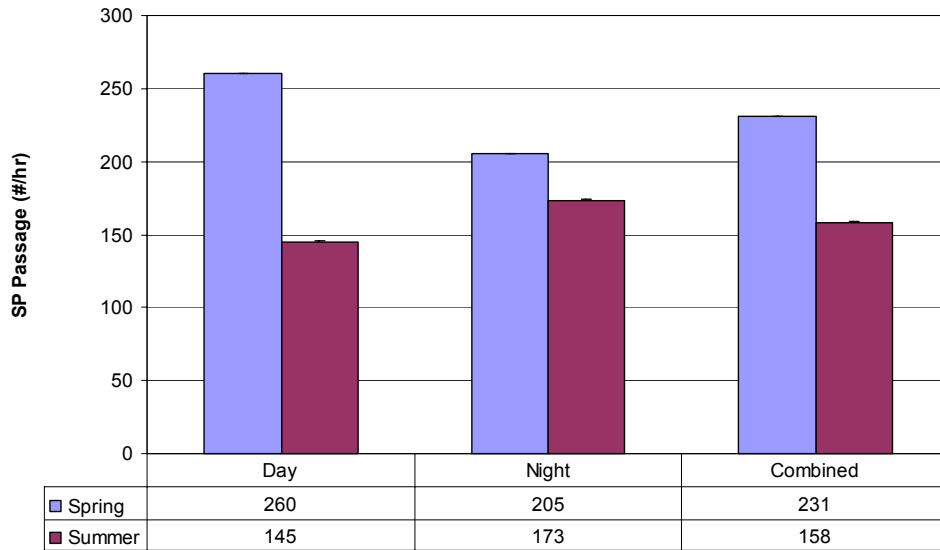


Figure 21. Spill passage during day|night and spring|summer.

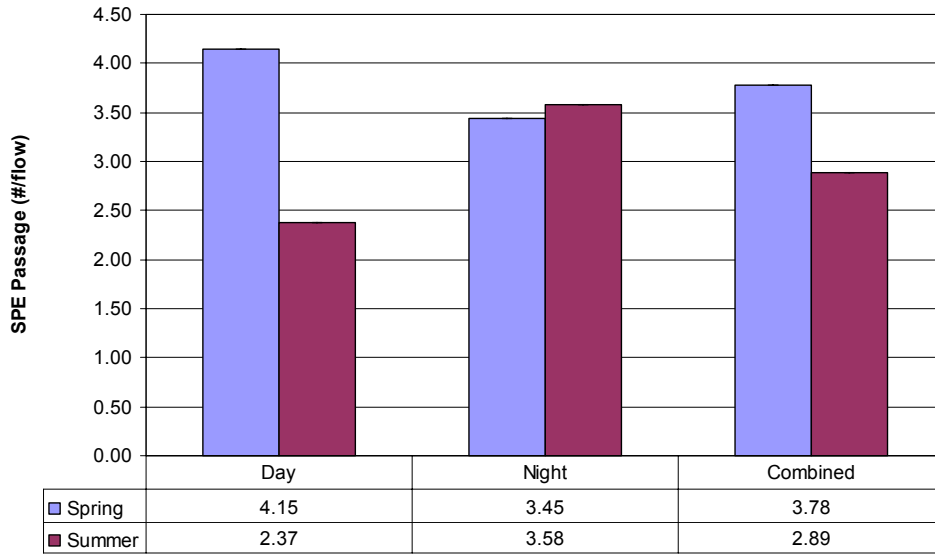


Figure 22. Spill effectiveness during day|night and spring|summer.

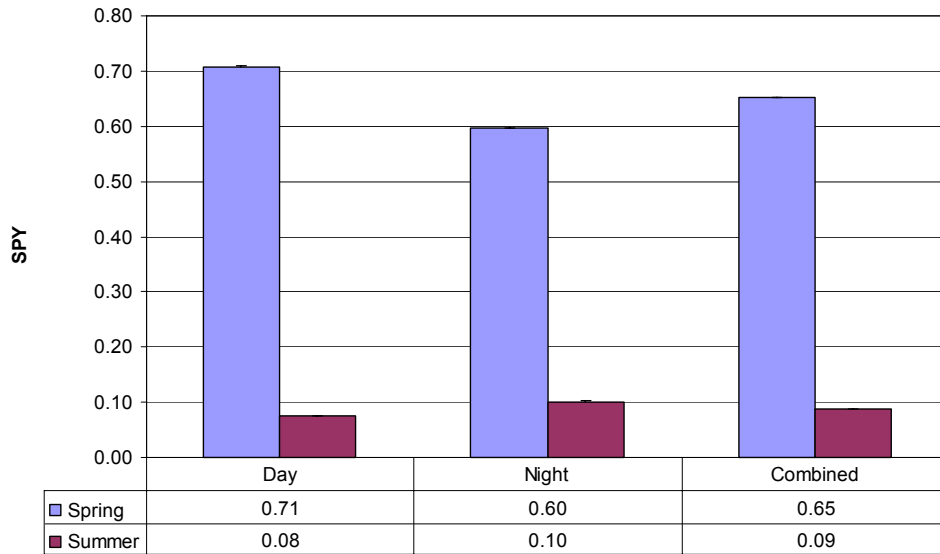


Figure 23. Spill efficiency during day|night and spring|summer.

3.3.2 Diel Plots

The following figures contain diel passage data. Passage rates at the sluiceway were higher during night than day. But, passage at the spillway and turbines was fairly uniform on a diel basis.

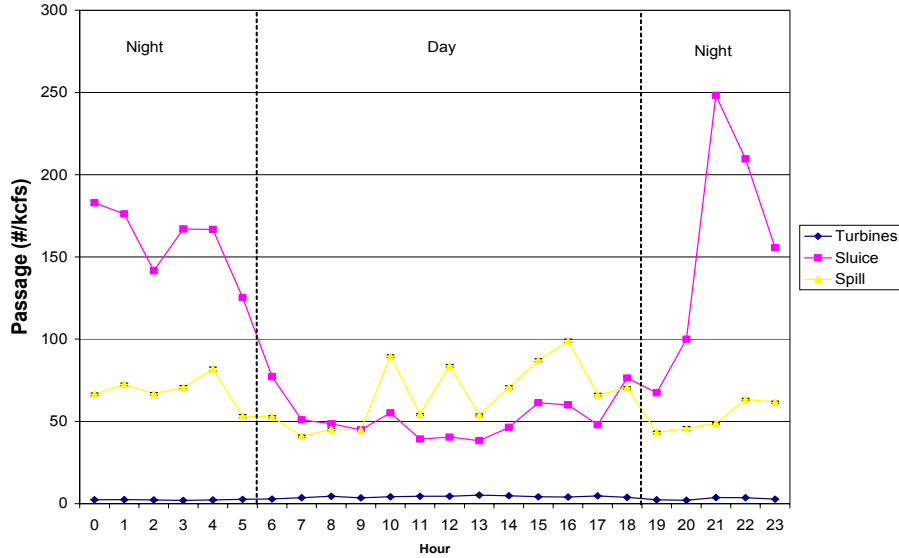


Figure 24. Diel passage per flow of the turbine, sluice, and spillway during spring. Error bars are 95% confidence intervals.

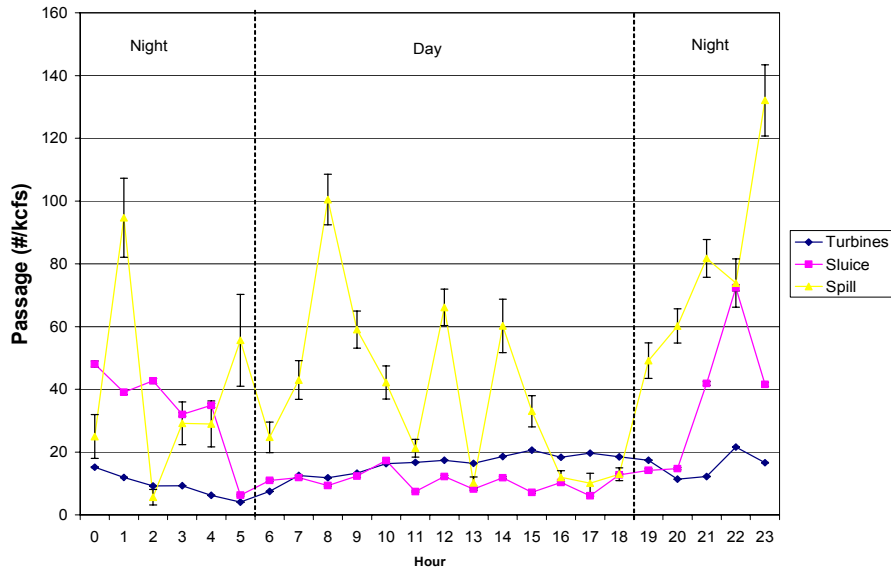


Figure 25. Diel passage per flow of the turbine, sluice, and spillway during summer. Error bars are 95% confidence intervals.

3.3.3 Horizontal Distributions

The following figures show the horizontal distribution of passage both normalized by flow and not normalized. At the the powerhouse turbines, highest passage rates per unit flow occurred at the east end of the dam. At the sluiceway, highest passage rates were observed at sluice 1-2. At the spillway, highest passage rates were toward the center of the spillway. The seasonal trend, consistent with previous studies, of summer migrants passing via the upstream side of the powerhouse is evident.

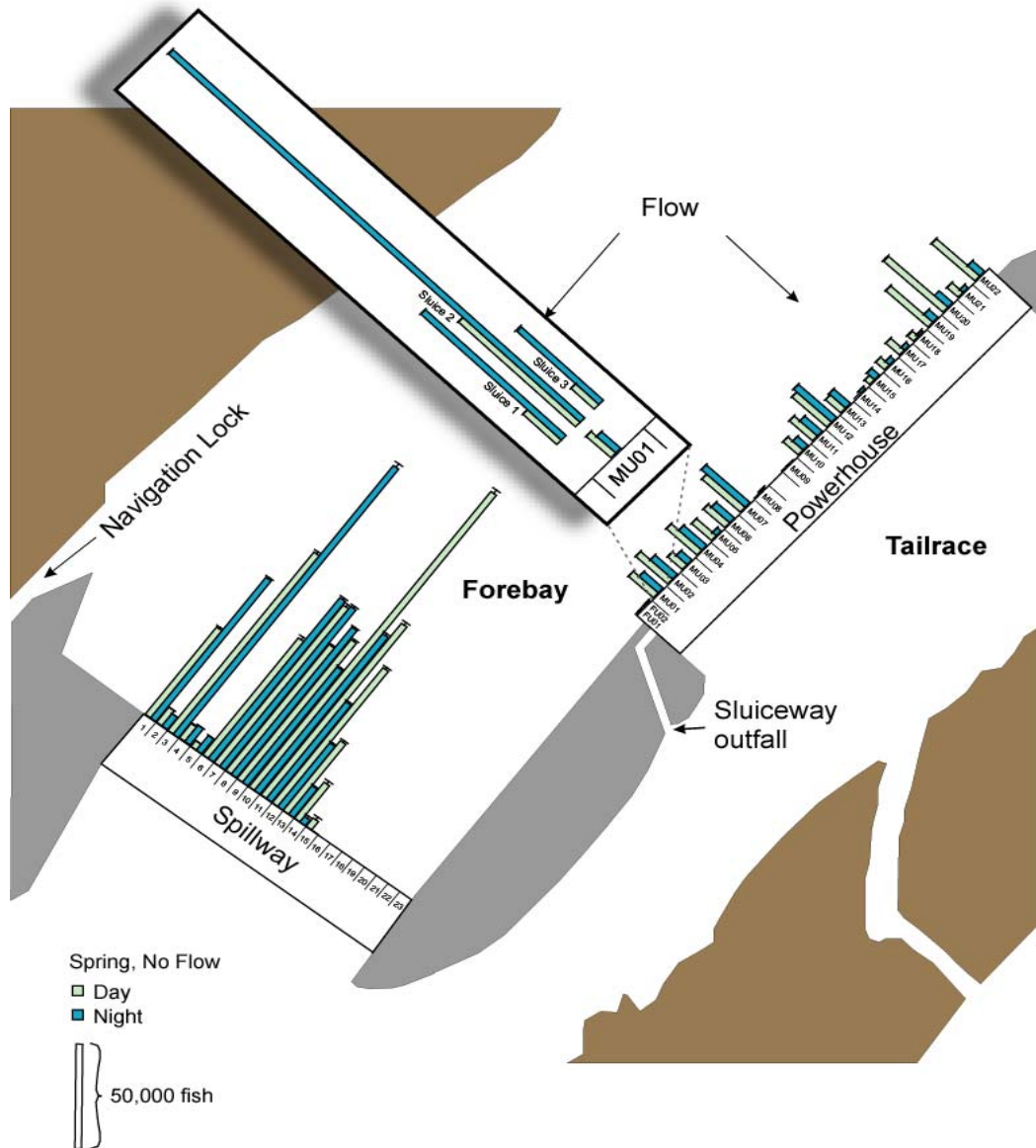


Figure 26. Spring horizontal distribution of fish passage at the spillway, turbine intakes, and the sluiceway above MU1 by day and night.

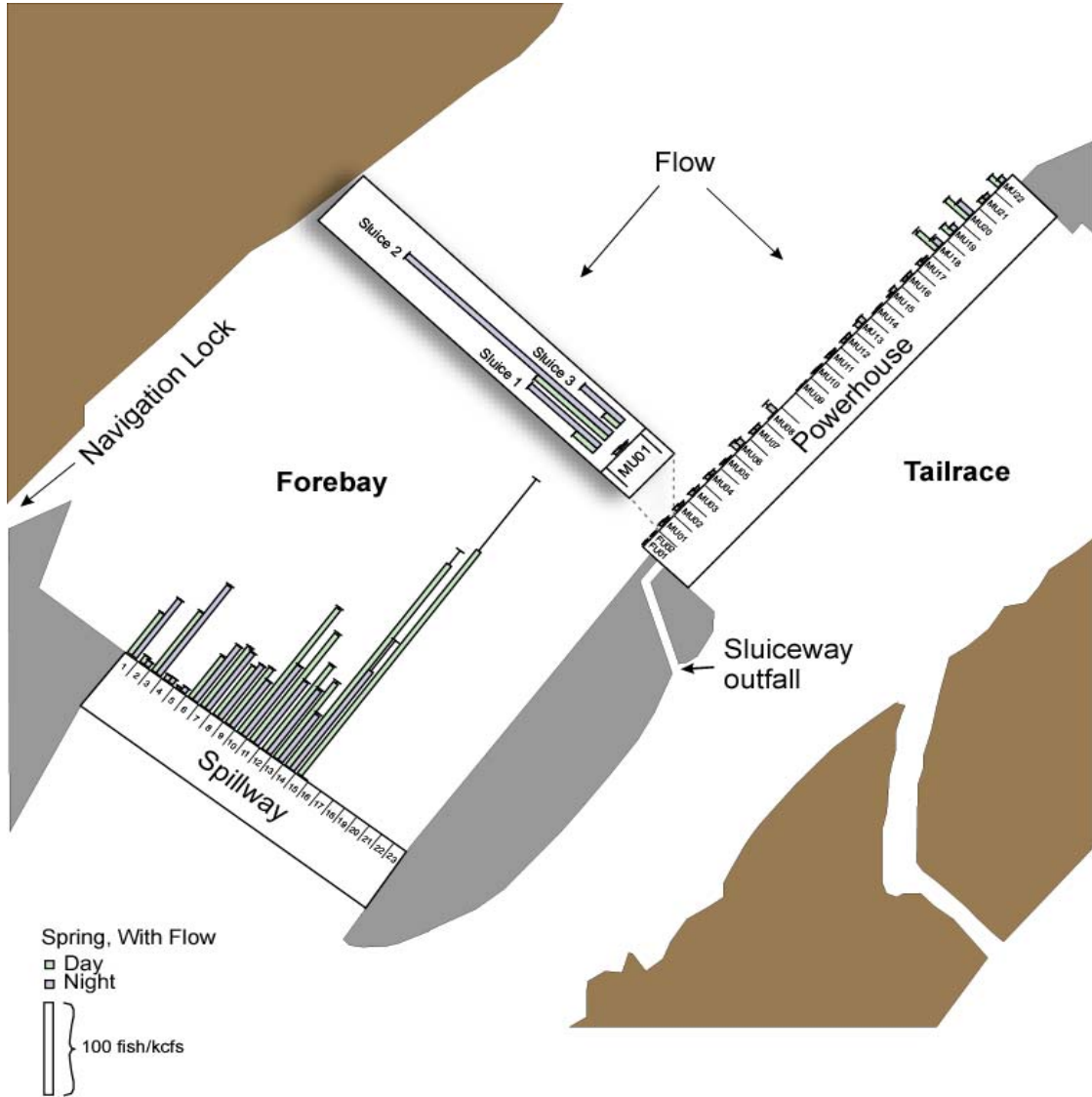


Figure 27. Spring horizontal distribution of fish passage per flow at the spillway, turbine intakes, and the sluiceway above MU1 by day and night.

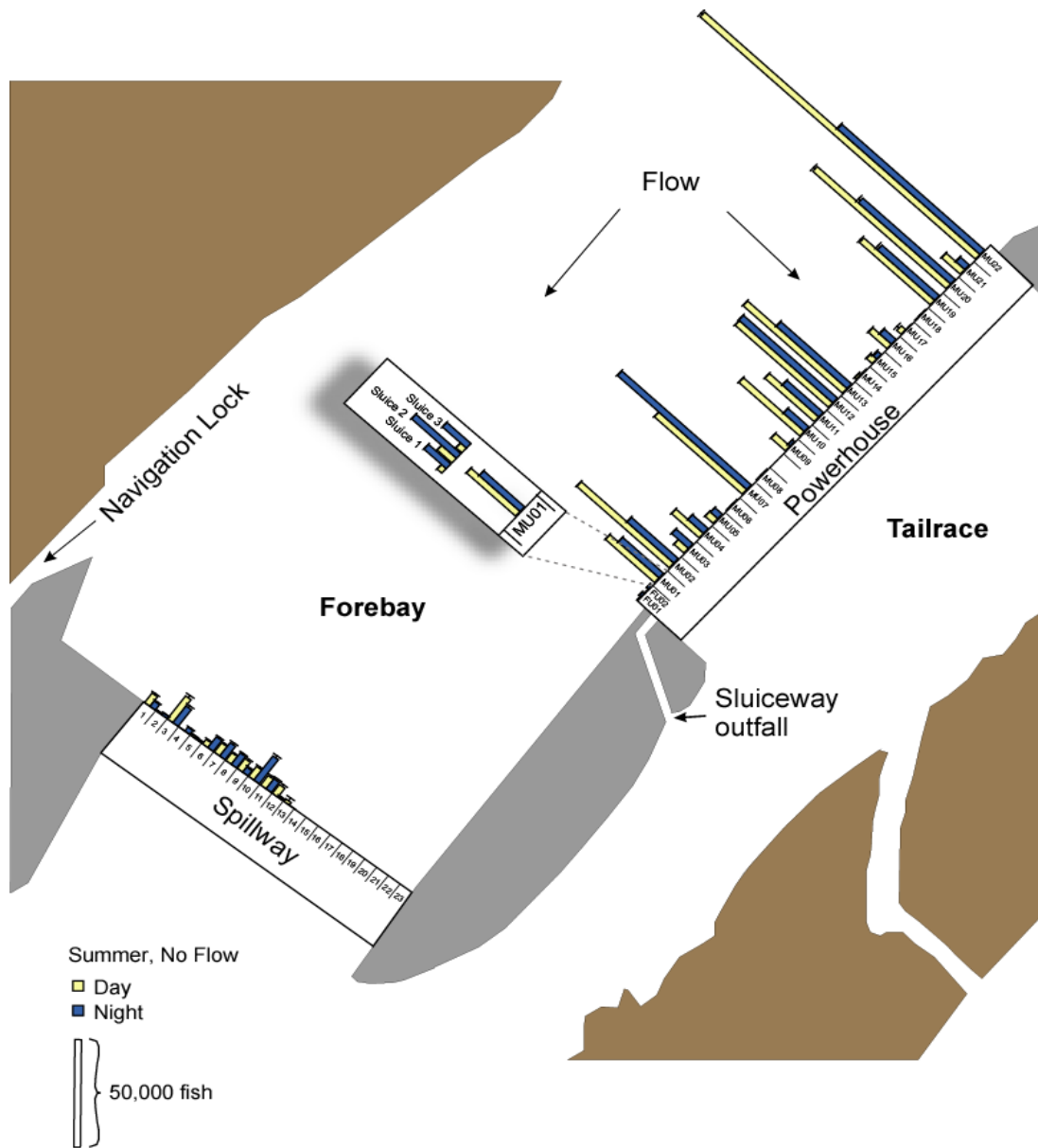


Figure 28. Summer horizontal distribution of fish passage at the spillway, turbine intakes, and the sluiceway above MU1 by day and night.

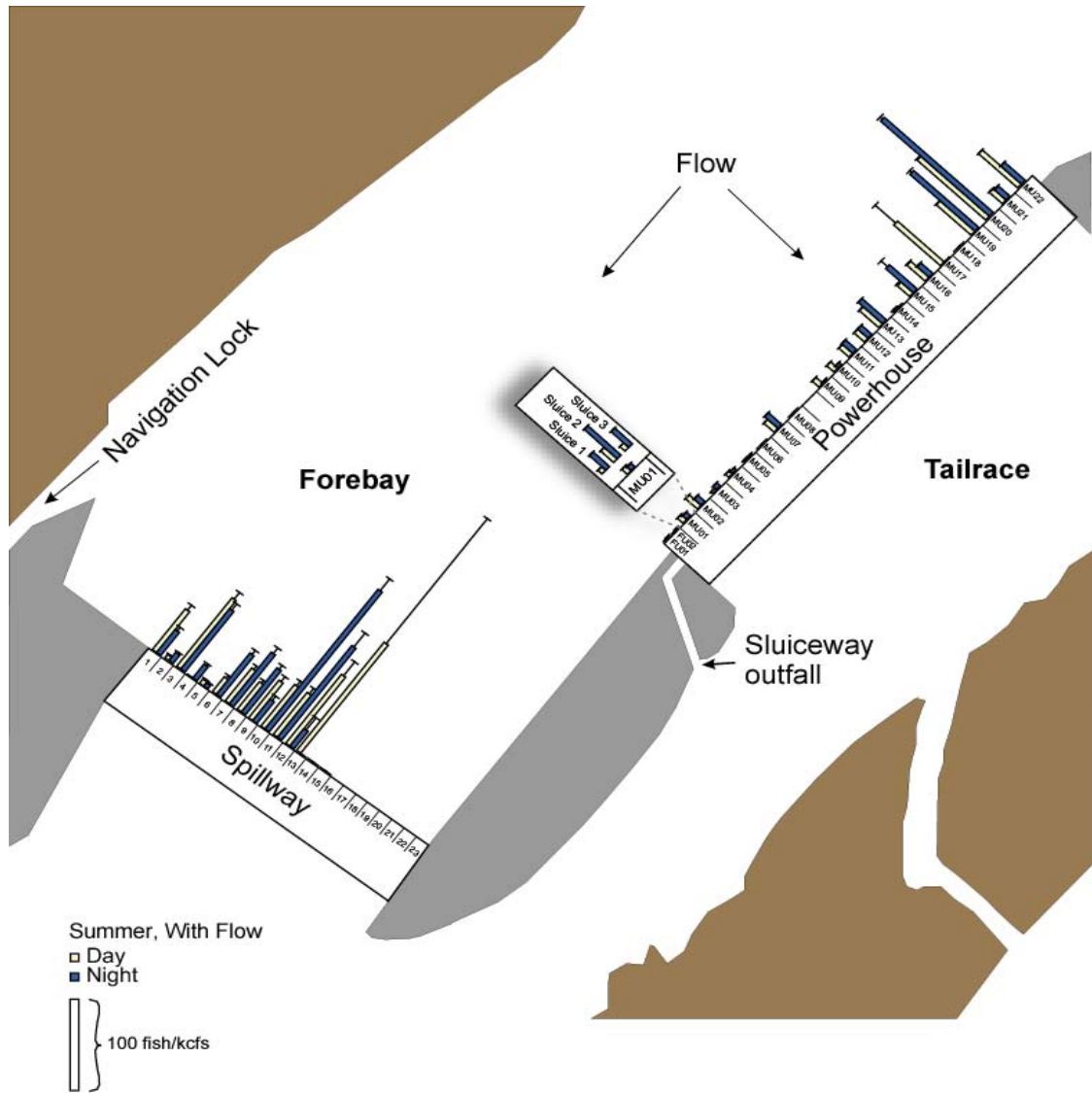


Figure 29. Summer horizontal distribution of fish passage per flow at the spillway, turbine intakes, and the sluiceway above MU1 by day and night.

3.4 Discussion

Dam operations, specifically spill, greatly influenced FPE. A combined day/night spill efficiency during the spring of 0.65 versus 0.09 for summer was due to the times spill occurred. A combined sluice efficiency (SLY1-5) of 0.8 shows that most of the fish in the area of MU1-5 passed via the sluice in the spring. In the summer, that proportion dropped considerably, as fish passed via the east end of the powerhouse, and did not have the opportunity to utilize the sluice. Both the sluice and spillway continued to be very effective at passing fish per unit flow.

Fish used the sluice predominately at night (from 2100 to 0500h). This trend was consistent in both spring and summer, but differs from observations in previous studies. Turbine intake passage did not show any diel trends. Low sample sizes in the summer increased the variability of the spill diel.

The horizontal distribution at the powerhouse showed fish pass predominately through the intakes on the east end of the powerhouse during summer, while more fish pass through the west end of the powerhouse in spring. The horizontal distribution of passage at the powerhouse in spring and summer is consistent with observations in previous studies. Sluice passage was highest in the middle slot with most of them going over at night and in the spring.

The spillway horizontal distribution was highest along the bays on the north side of the spillway in spring for the bays that spilled water, but it was skewed toward bays 12-14 in summer. Although different in spring and summer, the end bays of those that passed water were the most effective.

4.0 Focused Analysis of Main Units 1-5

4.1 Objectives

This chapter provides an analysis of passage through Main Units 1-5 in the context of limited J-occlusion tests performed in 2001. A stratified random block design was planned to test the effect of the J-occlusions. Temporal changes in unit loading confounded the effects of flow with the effects of the occlusions, leading us to abandon the planned experimental design. Graphical presentations will be used to illustrate the effects of J-occlusions in the context of treatment and operational factors. This includes analysis of passage rates at MU1-5 as a group and by treating removable and stationary occlusions separately. The possible influence of flow at adjacent turbine units on passage rates at a single turbine unit is also addressed.

4.2 Methods

As mentioned above, the planned treatment analysis of a stratified random block design was abandoned due to treatment problems and the actual turbine operations of MU1-5 encountered in 2001. In addition, mechanical and safety issues eventually lead to the decision to cease movement of the J-occlusions, and they remained occluded after 04 June 2001. These issues prevent the data from being subdivided into comparable replicates, so formal statistical testing is not appropriate. To extract the available information on treatment effects within the context of these operational issues, we used a graphical approach that allows the complex temporal changes in treatment and operational factors to be visualized along with the passage rate estimates. The influence of treatment and other factors can be evaluated graphically. Because the graphical presentations explicitly contain the passage of time, planned treatment blocks will be ignored.

Our analysis in this section begins by looking for overall treatment effects by comparing combined passage for FU1-MU5. We then compare passage among treatments for 3 types of routes: the removable occlusion section (MU1-4), and two stationary sections (FU1-2, MU5). MU2 is examined for possible insight into adjacency effects by comparing passage among treatments with an adjacent unit on or off. For the analysis of the influence of adjacent unit flows, the two most common patterns of unit operation were selected for analysis. Finally, times in which the J-occlusions were only partially deployed due to transition between treatments or mechanical difficulties were discarded from the analysis. The resulting subset of data represents the best opportunity to evaluate treatment differences.

4.3 Results

4.3.1 Hydraulic Environment

This section shows data from a static computational fluid dynamic model of The Dalles Dam forebay. These data were used in the detectability modeling. Of particular interest are the hydraulic differences shown between the unoccluded (Figure 30) and occluded intakes (Figure 31). The fish units were occluded for these tests (Figure 32).

The hydraulic environment of the turbine intake was radically altered when the occlusion was in place. While a change in flow patterns was predicted, this static model shows only some of the differences our instrumentation encountered. Our sensors also recorded changes in the acoustic noise environment and in the fish trace characteristics when the J-occlusions were deployed. Each of these differences must be dealt with correctly to provide a meaningful comparison between treatments. These issues are not unique to this study and standardized methods are in place to account for each. To reconcile issues related to the changes in the intake environment and fish passage measured within them, we combined data from the computational fluid dynamics model, split-beam deployments, and the split-beam trace patterns. These inputs were entered into detectability models. In addition, autotracking calibration occurred separately for each configuration to account for differences in fish movement patterns. Brief noisy periods were removed and interpolated, while samples obscured by noise were discarded.

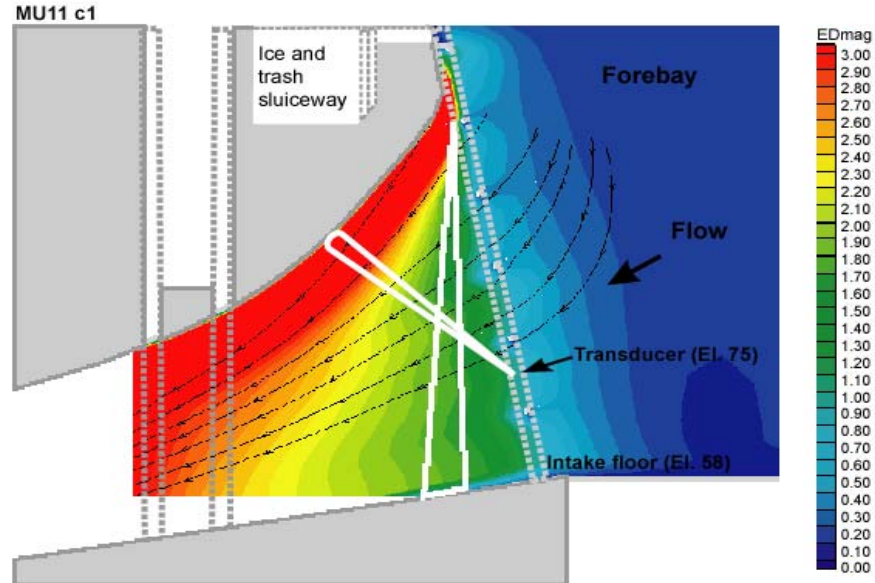


Figure 30. Transducer deployment for sampling fish passage at main units during the unoccluded treatments. EDmag is velocity in feet per second as measured in the plane shown in the figure.

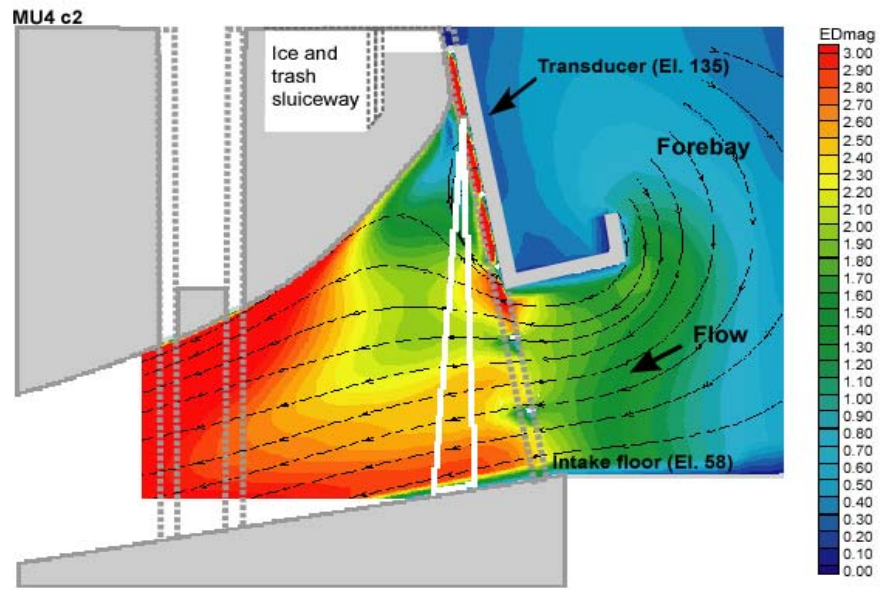


Figure 31. Transducer deployment for sampling fish passage at main units during the occluded treatments. EDmag is velocity in feet per second as measured in the plane shown in the figure.

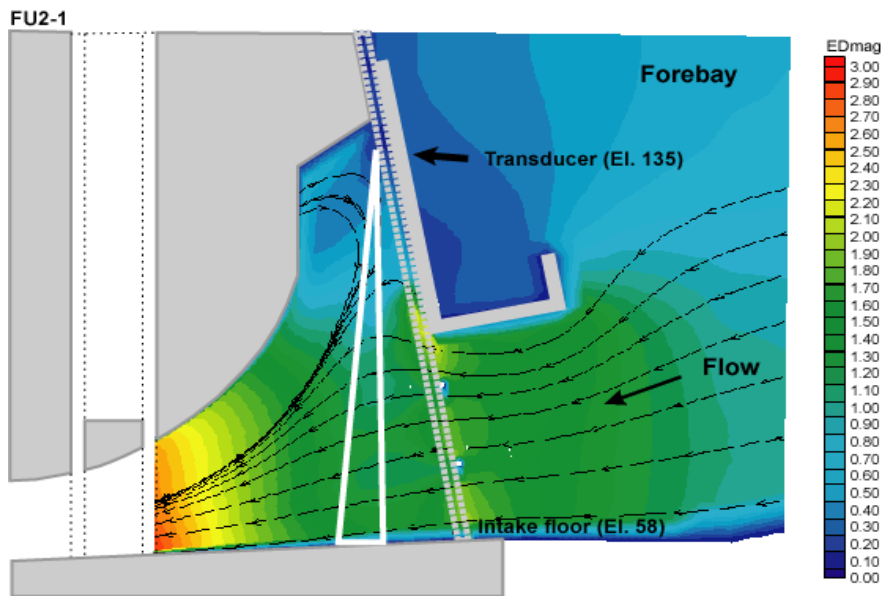


Figure 32. Transducer deployment for sampling fish passage at fish units. EDmag is velocity in feet per second as measured in the plane shown in the figure.

4.3.2 Treatment Schedule

The patterns of turbine unit operational combinations and their frequency of occurrence were illustrated in Table 1 above. Figure 35 illustrates the operational, treatment, and diel change for each unit by hour. Blank hours are those that were discarded because the j-occlusions were in a transitional state. This figure illustrates the confounding of occlusion treatment effects with unit flows and the occurrence of spill. This complex diagram provides the context within which passage must be interpreted.

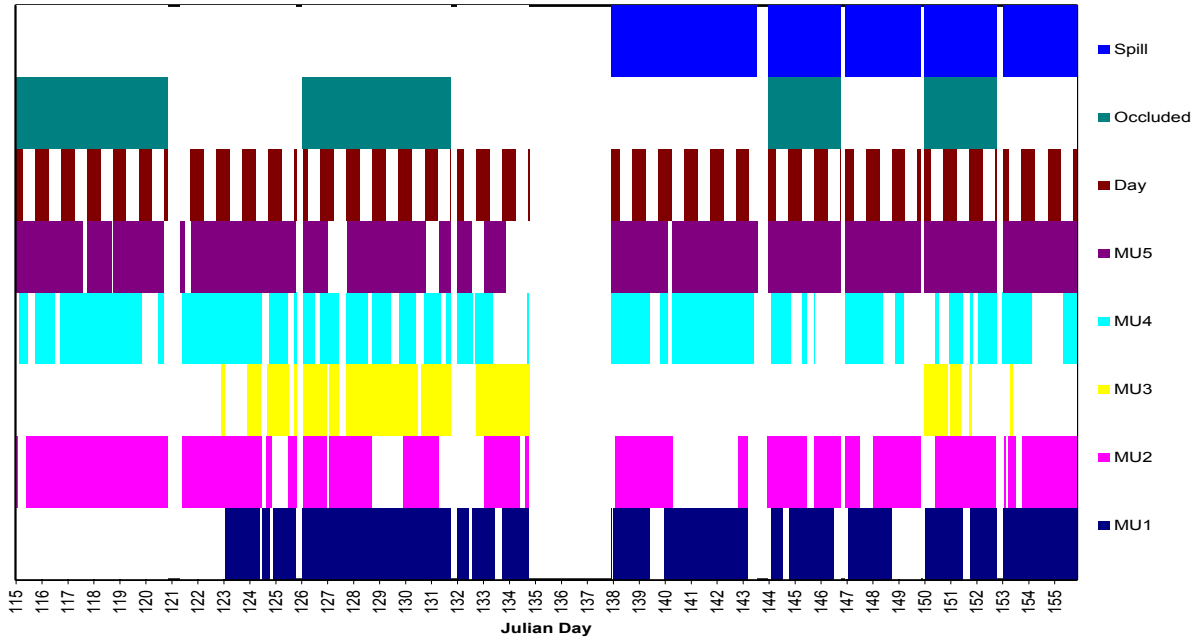


Figure 33. Dam operations. Colored cells indicate the unit was on or the condition was true during an hour. Empty vertical spaces indicate discarded hours where the occlusions were in a transitional state.

In an effort to resolve the influence of adjacent unit flow on passage rates, a set of hours were sought with consistent operations in each diel and treatment combination. MU3 was not on for most of this period, so we excluded those patterns of operation where MU3 was on from further analyses. Times where MU3 was unoccluded when it was supposed to be occluded were removed (they are listed in the Discarded column of Table 1). The two most common turbine unit configurations, and the ones selected for further analysis, are shown in Table 4. The turbine unit combinations used in analyses of adjacent unit effects. Pattern 1 was a one of the most common patterns of operation. Because Pattern 2 varied by only one turbine unit (MU1) and MU3 was off during both patterns, we were able to investigate effects of MU1 operations on MU2 intake passage.

Table 4. The turbine unit combinations used in analyses of adjacent unit effects.

	FU1	FU2	MU1	MU2	MU3	MU4	MU5
Pattern 1	On	On	Off	On	Off	On	On
Pattern 2	On	On	On	On	Off	On	On

4.3.3 Treatment Differences: Intended Configuration (FU1 - MU5)

Figure 34 and Figure 35 illustrate how daily mean passage changed through time. The influence of the occlusion treatment is difficult to interpret because it differs markedly from the first half of the period to the last. Referring to Figure 33, it is evident that spill differs between those two periods, with no spill in the first period. The latter period is characterized by lower passage rates for the unoccluded condition. Overall passage at the entire dam has not gone down during that period, which begins about mid May (Figure 9). Less obvious than the apparent influence of spill is the influence of the J-occlusions. In the absence of spill, the occlusions appear to reduce passage at these units perhaps slightly, but during spill the opposite is true. Passage rates within a treatment do not appear to differ much due to diel differences. These pieces of evidence suggest that J-occlusions reduce turbine passage in the absence of spill, but have the opposite effect during spill. From this result it is clear that the influence of spill must be considered in any evaluation of the effect of occlusion plates on fish passage.

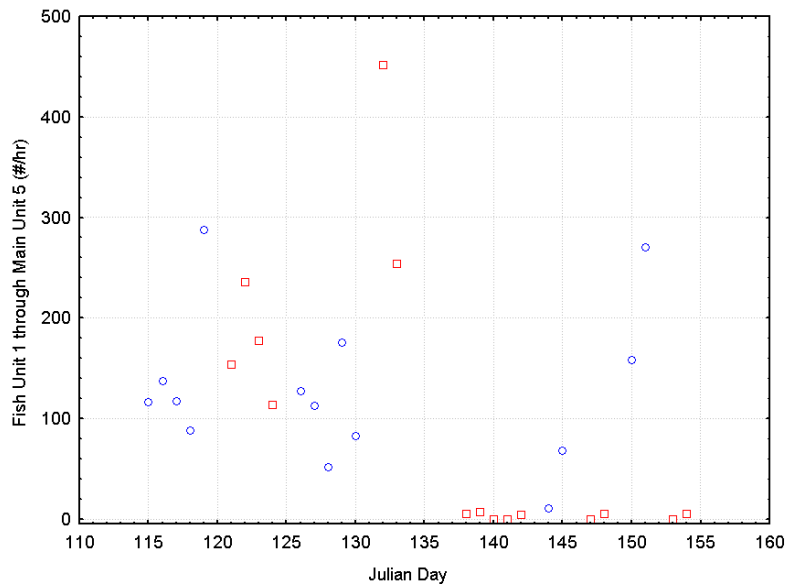


Figure 34. Daily mean passage per hour through Fish Units 1 and 2 and Main Units 1 through 5 during the day. Blue circles indicate Occluded treatment, red squares indicate Unoccluded.

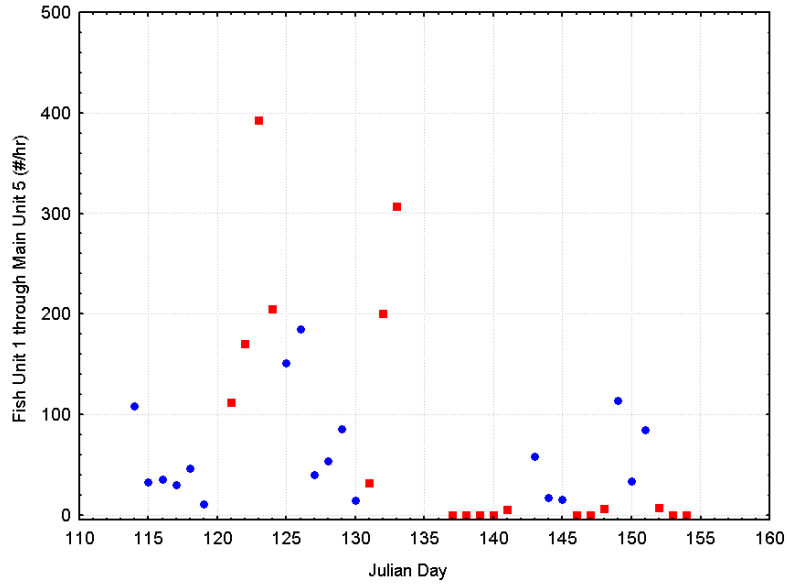


Figure 35. Daily mean passage per hour through Fish Units 1 and 2 and Main Units 1 through 5 at night. Blue circles indicate Occluded treatment, red squares indicate Unoccluded.

4.3.4 Treatment Differences: Movable (MU1-4)

We split out the movable (MU1-4) sections of the J-occlusion area for a more in-depth examination of possible treatment effects, since the fish units and main unit 5 remained occluded in both treatments. Figure 36 and Figure 37 illustrate the trends in passage at main units 1 through 4. Trends are very similar to those found in the previous section, suggesting that those trends are not dependent on the stationary units. Spill and treatment both appear to have an influence, and there is an interaction between them. There is no obvious effect of diel differences.

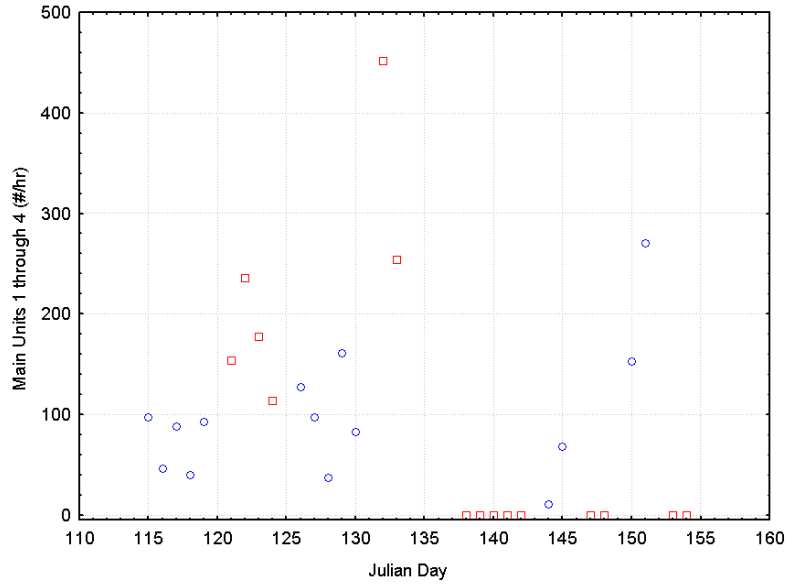


Figure 36. Daily mean passage per hour through Main Units 1 through 4 during the day. Blue circles indicate Occluded treatment, red squares indicate Unoccluded

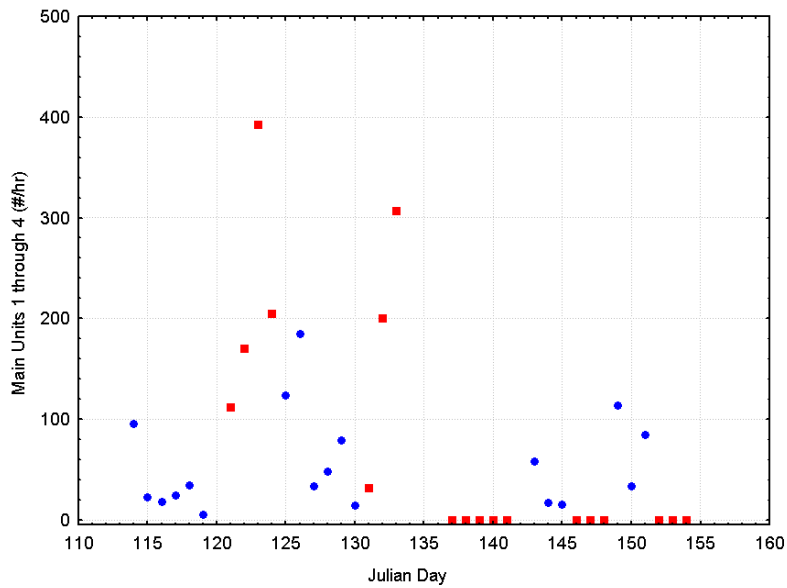


Figure 37. Daily mean passage per hour through Main Units 1 through 4 during the night. Blue circles indicate Occluded treatment, red squares indicate Unoccluded.

4.3.5 Treatment Differences: Stationary Occlusions (FU1-2, MU5)

Occlusion plates at the fish units and main unit 5 remained in place during both treatments for the entire season. Changes in passage at these units may be influenced by the presence or absence of occlusions at the nearby units. By examining passage at these nearby units, we might glean information on alternate routes for fish that are influenced by the occlusion plates.

Figure 38 through Figure 41 indicate that passage at the fish units is very low under all conditions. Differences illustrated in these figures would have little influence on passage metrics including other units. Trends are not obvious, but fish unit passage does appear to increase somewhat during the latter part of the sample period. That period is associated with higher spill, but also with greater frequency of main unit 1 operation. Since main unit 1 is adjacent to fish unit 2, we assume it is likely to influence passage there. There is no obvious relationship among passage and diel changes. Overall, the numbers of fish that passed at the fish units are so low that they can be ignored without changing the interpretation of any results about the occlusion plates.

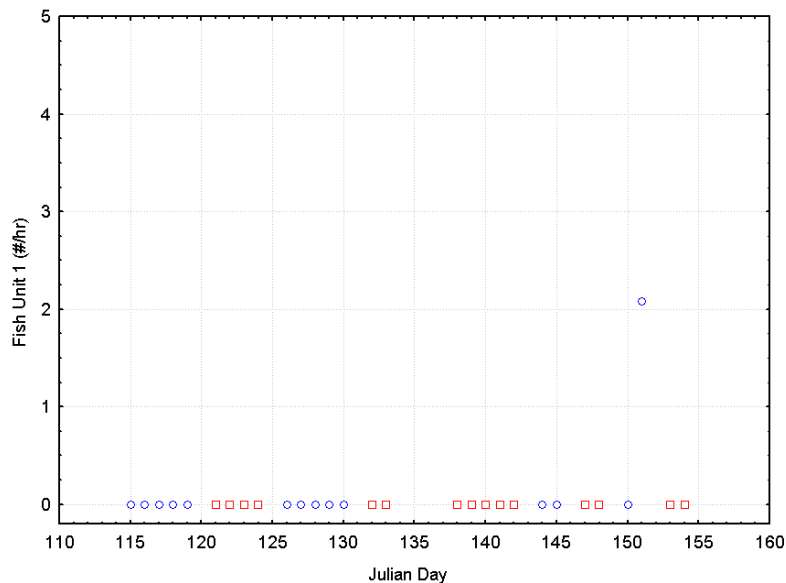


Figure 38. Daily mean passage per hour through Fish Unit 1 during the day. Blue circles indicate Occluded treatment, red squares indicate Unoccluded.

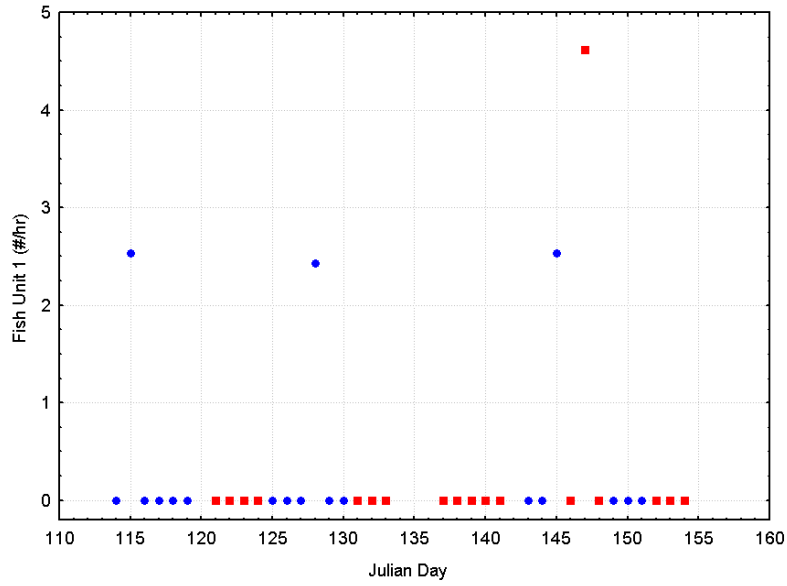


Figure 39. Daily mean passage per hour through Fish Unit 1 during the night. Blue circles indicate Occluded treatment, red squares indicate Unoccluded.

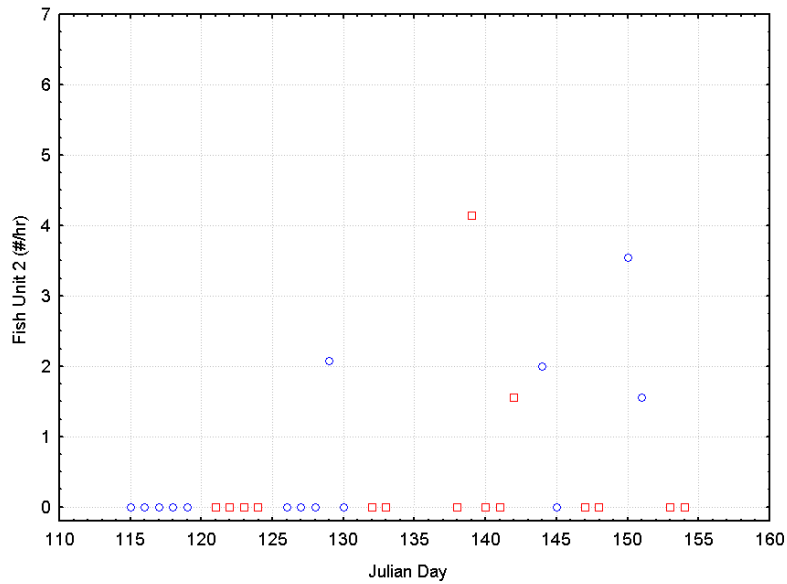


Figure 40. Daily mean passage per hour through Fish Unit 2 during the day. Blue circles indicate Occluded treatment, red squares indicate Unoccluded.

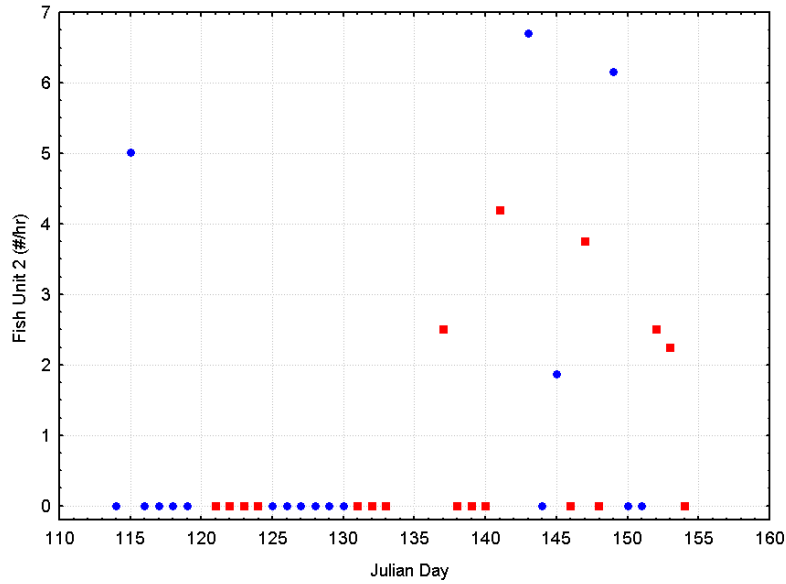


Figure 41. Daily mean passage per hour through Fish Unit 2 during the night. Blue circles indicate Ocluded treatment, red squares indicate Unoccluded.

Main unit 5 was always occluded, but unlike the fish units it is of similar size and depth as the other main units. Figure 42 and Figure 43 illustrate the trends in passage at main unit 5. It is obvious that very few fish passed MU5 (which is always occluded) when MU1-4 were unoccluded. During the early part of the sample period, relatively more fish passed through MU5 during the occluded treatment, but the trend does not extend into the latter part of the sample period where the influence of spill appears most important. The early period also shows an apparent difference between day and night during the occluded treatment.

If we summarize the trends for removable and stationary occlusions, it appears that the great majority of fish passed via MU1-4 when they were unoccluded, rather than under the stationary occlusions. When the occlusions were in place, passage at main unit 5 increased in the early half of the sample period. The latter half of the sample period appears to differ greatly from the first, possibly due to the influence of spill. Unfortunately spill is confounded with other temporal changes, so we cannot be sure whether the influence is the result of spill or another variable.

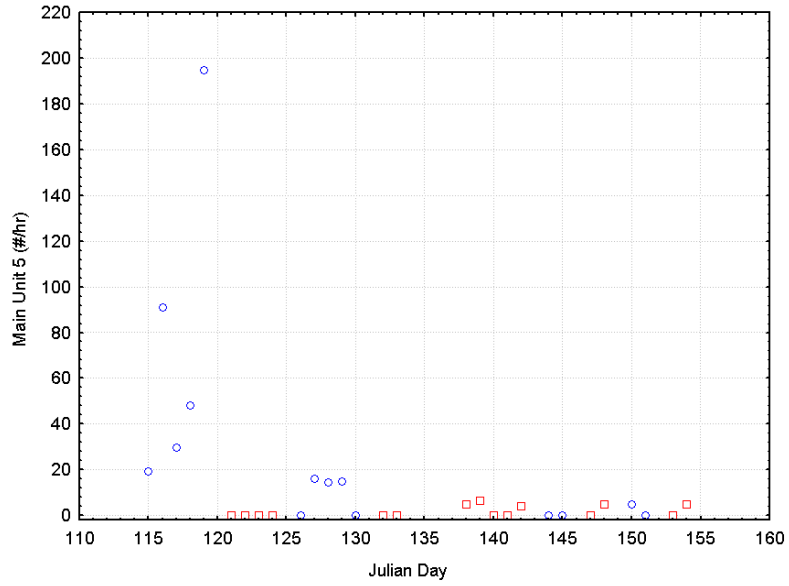


Figure 42. Daily mean passage per hour through Main Unit 5 during the day. Blue circles indicate Occluded treatment, red squares indicate Unoccluded.

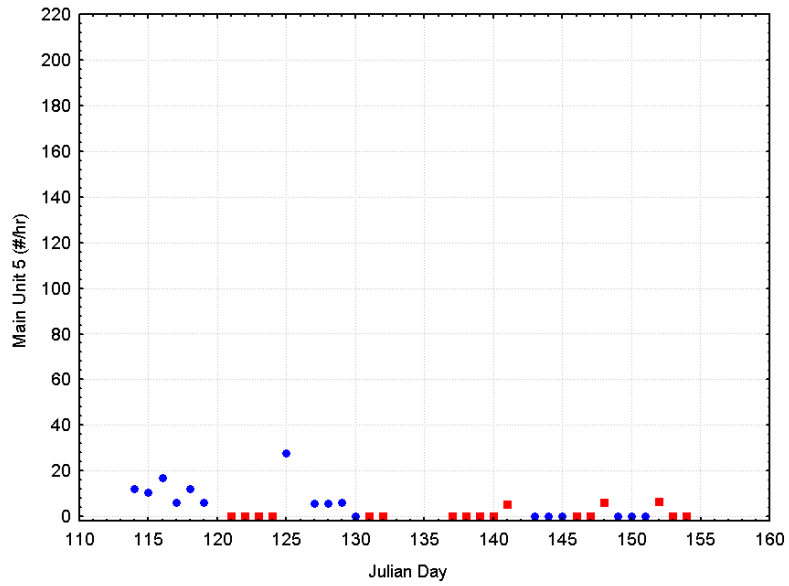
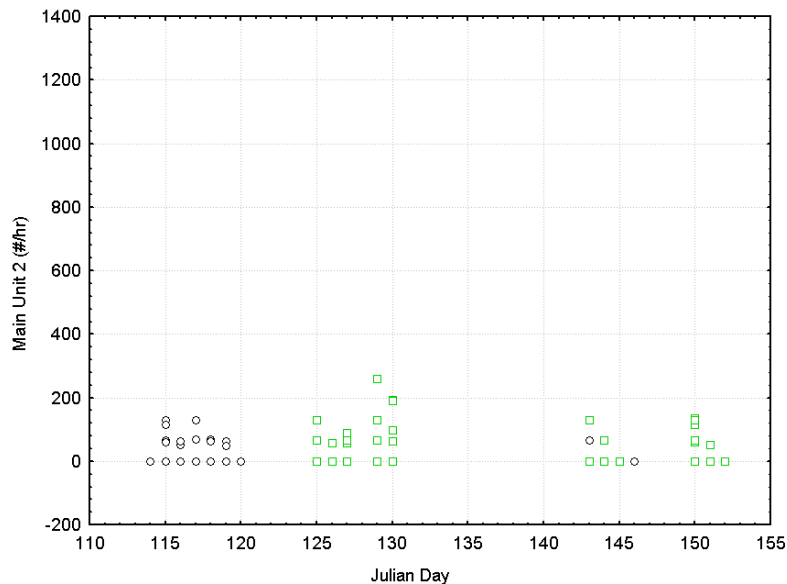


Figure 43. Daily mean passage per hour through Main Unit 5 during the night. Blue circles indicate Occluded treatment, red squares indicate Unoccluded.

4.3.6 Influence of Adjacent Units: Main Unit 2

To gather some insight into the effects of adjacent turbine unit operations on passage at a single unit of interest, fish passage at MU2 was compared between operational Patterns 1 and 2. These are the two most frequent combinations of turbine operations and also vary only by the turbine unit, MU1. The comparable pattern with both adjacent units on occurred too infrequently to be included in this analysis. The comparison of greatest interest here is whether treatment effects differed when an adjacent unit was on. We refer to changes in passage at the unit of interest relative to changes in operations at nearby units as adjacency effects. Since MU3 was off for both these patterns, then the adjacent unit referred to is MU1.

The trends in Figure 44 through Figure 47 do not suggest that the adjacent unit operations have much of an influence on passage. The available data are not ideally suited to evaluate the influence of adjacent unit operations, and there is not enough evidence to speculate on how adjacent unit operations influence passage. The operational patterns chosen do not control for spill differences, and the influence of spill is evident during the unoccluded treatments. The effect is much less obvious during occluded treatments.



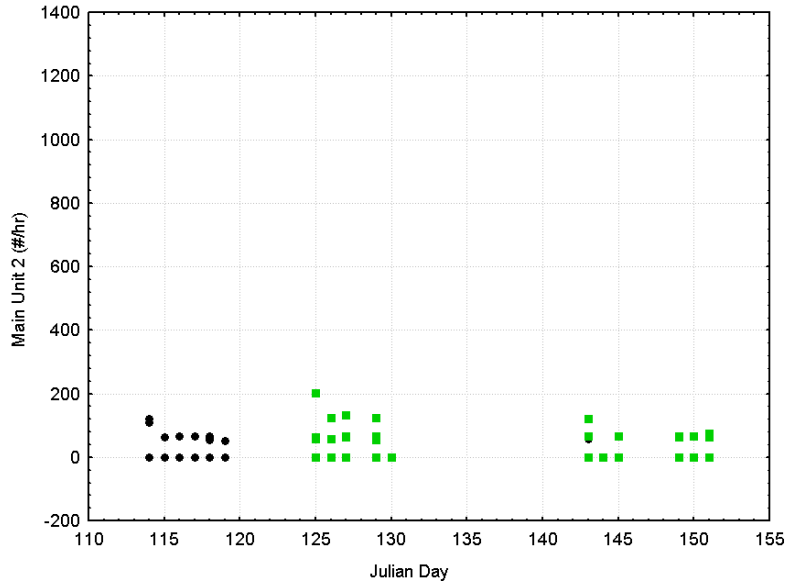


Figure 45. Hourly passage rates through Main Unit 2 during the Occluded treatment during the night. Black circles indicate that the adjacent unit is OFF, green squares indicate the adjacent unit is ON.

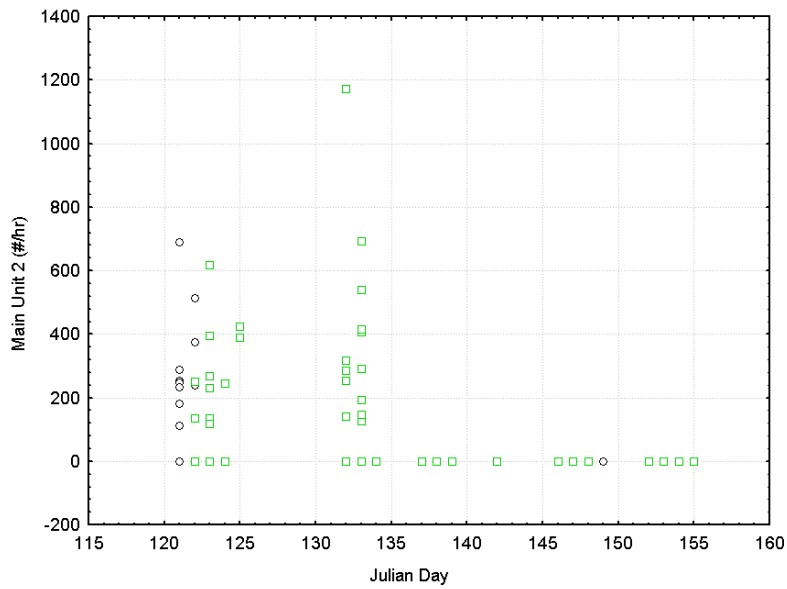


Figure 46. Hourly passage rates through Main Unit 2 during the Unoccluded treatment during the day. Black circles indicate that the adjacent unit is OFF, green squares indicate the adjacent unit is ON.

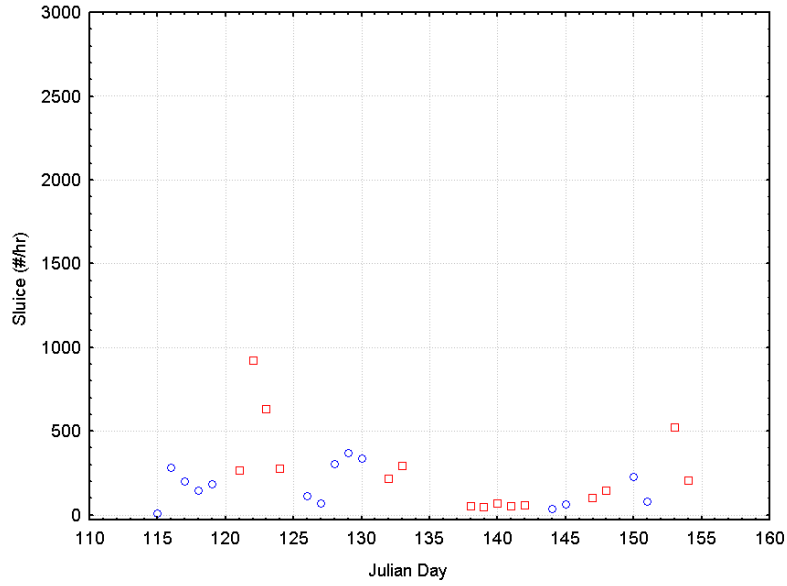


Figure 48. Daily mean passage per hour through the Sluice during the day. Blue circles indicate Occluded treatment, red squares indicate Unoccluded.

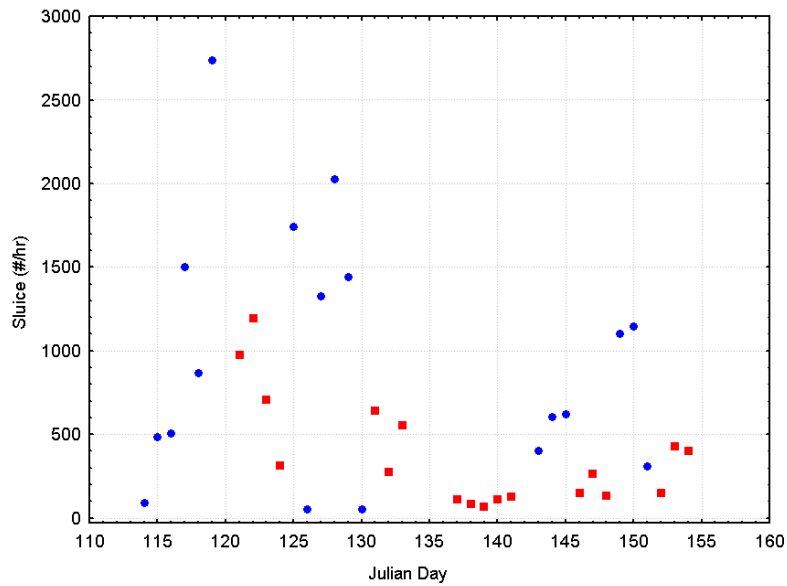


Figure 49. Daily mean passage per hour through the Sluice during the night. Blue circles indicate Occluded treatment, red squares indicate Unoccluded.

Similar trends are evident in sluice efficiency (Figure 50 and Figure 51). Sluice efficiency is higher at night. Efficiency increases during the latter part of the sample period, suggesting a possible influence

of spill. More specifically, it suggests that spill reduces turbine passage more than it reduces sluice passage. During the early part of the sample period, occlusions appear to have a greater influence on passage at night than during the day, with efficiency being highest during the occluded period.

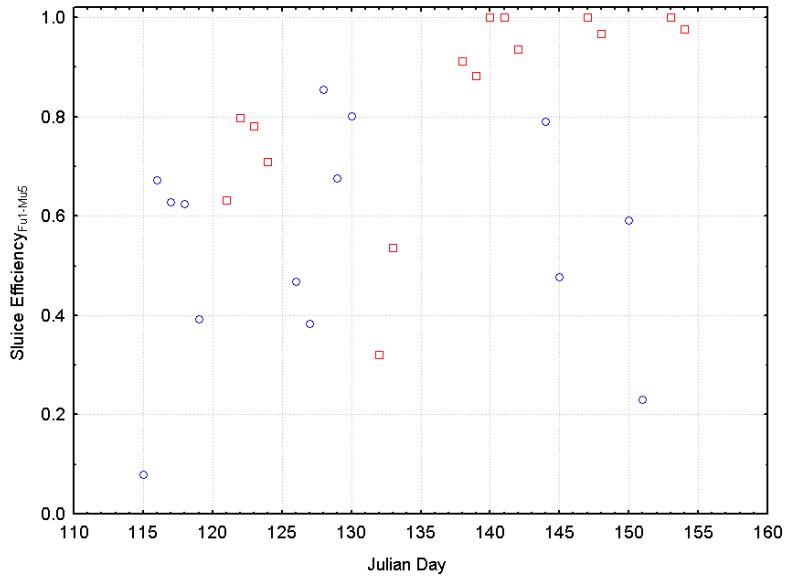


Figure 50. Daily sluice efficiency relative to fish unit 1 through main unit 5 during the day. Blue circles indicate Occluded treatment, red squares indicate Unoccluded.

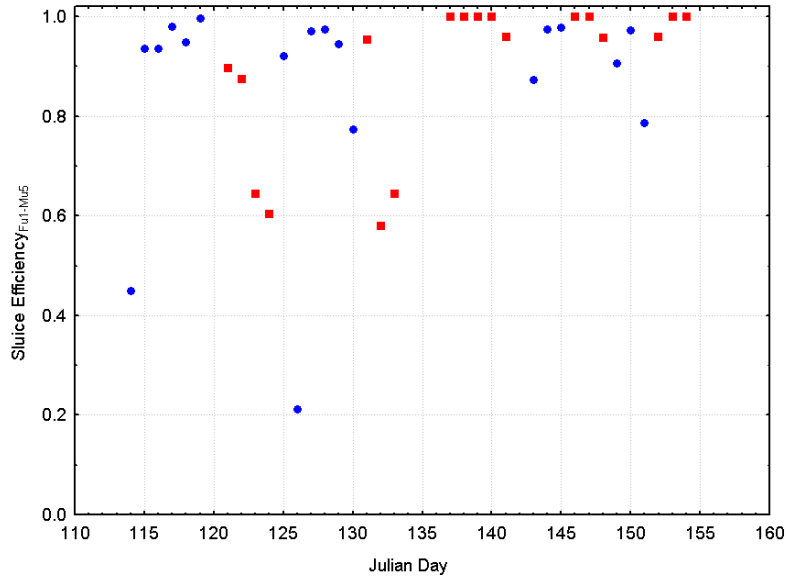


Figure 51. Daily sluice efficiency relative to fish unit 1 through main unit 5 during the night. Blue circles indicate Occluded treatment, red squares indicate Unoccluded.

4.4 Discussion

The realized dam and J-occlusion operations in 2001 prevented the planned statistical analyses of treatment effects because no comparable replicates exist. To resolve treatment effects in spite of variable operations and mechanical problems, we abandoned the stratified random block experimental design and used graphical presentations. These presentations illustrate the effects of J-occlusions in the context of temporally complex treatment and operational factors. To evaluate the effects of adjacent units we analyzed the J-occlusion section relative to a limited set of operational conditions that occurred in both treatments. We restricted the turbine operations to two specific patterns. The two patterns together account for 31% of sample time from April 25 at 1300 h to June 4 at 0800 h, though they are not distributed evenly throughout that period. The caveat that should accompany this analysis is that the results based upon this limited subset of data may not be representative of future years. Any inferences for summer runs of fish are particularly tenuous.

Combined passage rates for fish unit 1 through main unit 5 differed greatly from the first half of the sample period to the last half. Spill did not occur during the first half and was nearly constant during the last half. Other influences have not been ruled out, so it is speculative to attribute those differences to the occurrence of spill. In the absence of spill, occlusions appear to reduce combined passage through these units, but the opposite is true during spill. Combined passage did not differ between day and night. Combined passage at only those units with removable occlusions (MU1-4) showed the same trends.

The fish units and main unit 5 remained occluded during all treatments, but passage through main unit 5 was greater when units 1-4 were occluded. This effect was evident only in the first half of the sample

period, which suggests that spill reduced passage at main unit 5. Fish unit passage was negligible, and any trends would have little effect on a larger scale assessment of passage. The influence of main unit 1 operation on passage at main unit 2 was not evident. The limited available data prevents us from drawing any conclusions about the influence of adjacent unit operations.

Sluice passage and efficiency relative to FU1-MU5 differed greatly between the first and last half of the sample period, which suggest that spill is influencing passage at the sluice. Sluice passage increased at night, especially during the occluded treatment. This effect was evident throughout the sample period. Treatment effects are less straightforward. During the day, unoccluded passage is slightly higher, but at night the reverse is true.

More than one factor appears to influence fish passage at the J-occlusion units. Spill appears to strongly influence turbine passage during unoccluded treatments, suggesting that spill has the greatest influence on fish that would have passed by the unoccluded route. Occlusions decrease turbine passage in the absence of spill, but not during spill. Sluice passage and efficiency increase during occlusion treatments at night, but not during the day. Spill also influenced sluice passage more during unoccluded treatment. The evidence suggests that during the unoccluded treatments fish are more influenced by spill and that occlusion plates are most effective at night and in the absence of spill.

5.0 Acoustic Camera Evaluation of J-Gap Passage

5.1 Objectives

Gaps in the "J" portion of the occlusion exist between adjacent intakes. The acoustic camera, a Dual-Frequency Identification Sonar (DIDSON), was used to record the behavior of fish above J-occlusion plates and gaps between adjacent J-occlusion plates at The Dalles Dam. As part of the overall performance evaluation of the J-occlusions, the objective here was to elucidate the extent to which J-gap losses may influence fish passage. Presumably, fish lost through the gaps would otherwise have been available for passage through another route (e.g., the ice and trash sluiceway or the spillway). The specific objectives of this research were to:

1. Determine whether or not smolts were being entrained into this area.
2. If so, estimate the number of smolts entrained into the gap
3. Note the occurrence of predators in the vicinity of the J sections

Data was collected from 1700h to midnight on June 7-10 and June 12-13, above the J-occlusion gaps between Main Units 1-2 and 3-4. Sampling occurred primarily at the MU3-4 gap to minimize the influence of the edges of the J-blocks and the ice and trash sluiceway (Table 5). Thus, data from the MU3-4 gap were intended to be representative of a generic gap. Because the gaps exist only when the J-occlusion plates were deployed, data were collected only during the occluded treatment period. The small gaps, between intakes of the same unit, were not sampled. Further, because the MU1-2 gap was only partially occluded, the data from June 12-13 was excluded from the analysis.

Table 5. Dates and deployment location of data collection.

Dates	Location	Water Depth	Duration	Gap Configuration
June 7	PH 3-4	128 ft	16:37 – 20:00	Full deployment
June 8	PH 3-4	143 and 128 ft	0:00 – 24:00	Full deployment
June 9	PH 3-4	128 ft	17:31 – 24:00	Full deployment
June 10	PH 3-4	128 ft	18:26 – 24:00	Full deployment
June 12	PH 1-2	140 ft	17:17 – 24:00	Plate 2-1 was up
June 13	PH 1-2	140 ft	0:00 – 18:40	Plate 2-1 was up

5.2 Methods

5.2.1 Dual-Frequency Identification Sonar (DIDSON)

The Dual-Frequency Identification Sonar (DIDSON) was developed by the Applied Physics Laboratory (APL) at the University of Washington for the Space and Naval Warfare Systems Center harbor surveillance program (Belcher et al. 1999). It can detect objects out to 48 meters and provide near

video-quality images to identify objects out to 8 meters. DIDSON was designed to bridge the gap between existing sonar, which can detect acoustic targets at long ranges but cannot record the shapes or sizes of targets and optical systems, which can videotape fish in clear water but are limited at low light levels or when turbidity is high. It has a high resolution and fast frame rate designed to allow it to substitute for optical systems in turbid or dark water. The 7×12×8-in. unit weighs only 15 lbs in air.

A near photographic image clarity is possible because the field of view is composed of 96 different 0.33×8.5 -degree beams operating at 1.8 MHz and 48 different 0.6×8.5 -degree beams operating at 1 MHz with a 29-degree field of view. The multiple beams allow image processing that produces a near-field image similar to that of a CCD video camera. Unlike single and split-beam hydroacoustic transducers, the acoustic camera has multiple narrow beams that allow it to be aimed oblique to a flat surface and still record fish swimming very near the water's surface or a solid surface (Figure 52).

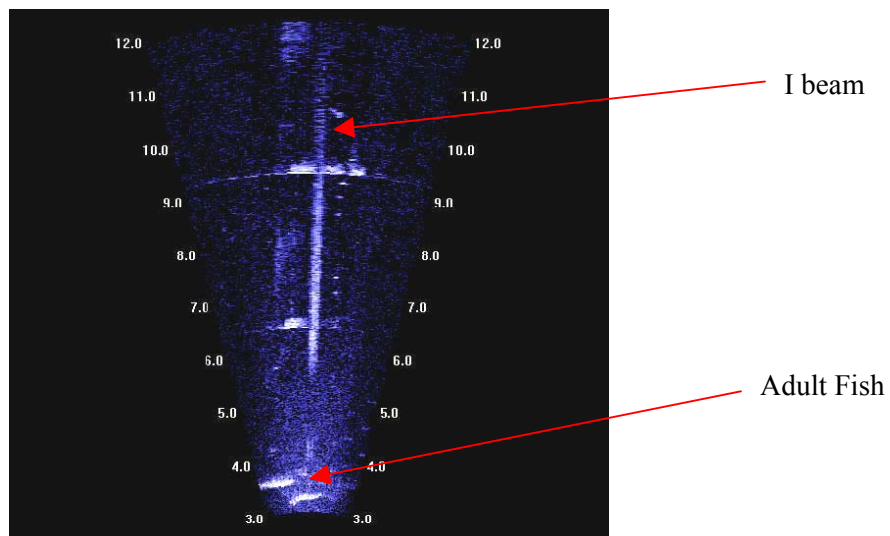


Figure 52. Screen capture from DIDSON display showing two fish in foreground and I-beam along the center portion of view (the sonar is located at bottom of figure).

5.2.2 Field Deployment

The DIDSON was deployed from the forebay deck (EL 185 ft) using sections of steel I-beam and trolley system in conjunction with an underwater 3-axis rotator so that both the depth and aiming angle of the instrument were adjustable. The DIDSON was deployed at two locations at The Dalles Dam powerhouse between main pier-nose 1-2 and 3-4. In order to know aiming angle of the array we used a R.J. Electronics 3-axis rotator (PTE-200 and R-200) with positive feedback on all 3 axes. This instrument allowed us to position the DIDSON array with relatively high accuracy ($\pm 1^\circ$) on the pan, tilt, and rotate axes. The rotator was bolted to a custom-made aluminum trolley that was lowered down along a length of 4" steel I-beam (Figure 3). The total coverage area at the floor at a 9 m range formed a $6.2 \text{ ft} \times 15.3 \text{ ft}$ square at the floor, or 94.8 sq ft. DIDSON was used in the high frequency mode and the frame rate was 5

frames/sec. Data files were saved to an external hard drive connected to a notebook computer. Separate files were generated sequentially at 5-minute intervals.

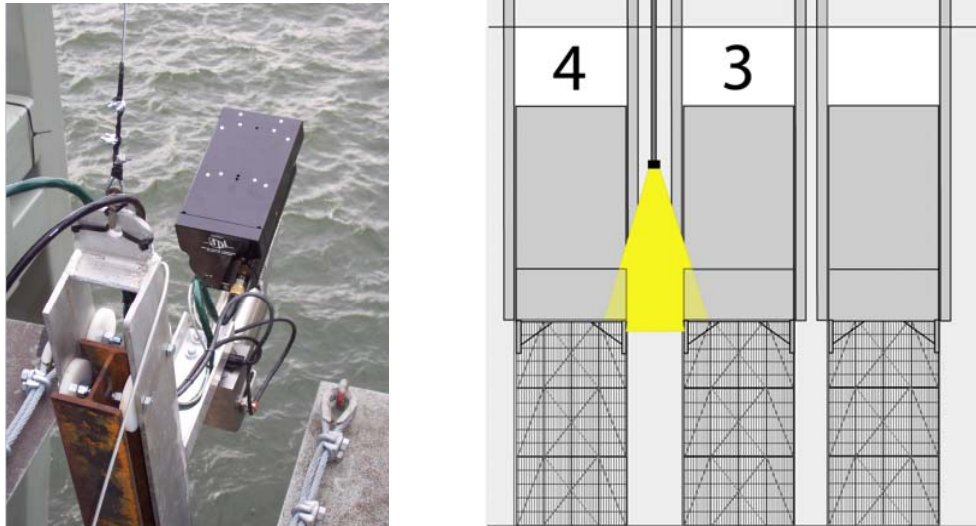


Figure 53. DIDSON mounted to 3-axis rotator, trolley, and I-beam near the forebay deck (left). Front view of occlusion plates, elevation of the DIDSON, and approximate area of coverage (right).

5.2.3 Data Analysis

All data was reviewed and manually assigned to categories. Fish counts were adjusted for beam spreading. Assuming that at 9 m range (the range from the transducer head to the floor), and the nominal beam width is 29°, the beam is 4.66 m wide at the gap. The vertical distribution of counts was adjusted according to the following formula:

$$W = \frac{I}{2R \tan\left(\frac{\theta}{2}\right)}$$

where,

- W = the weighted fish
- I = width of the intake in meters
- R = range of the fish in meters
- θ = nominal beam width in degrees

5.3 Results

5.3.1 Images

Acoustic movies, at 5 frames/sec, were recorded by the sonar. For reporting purposes, still images of the acoustic video clips are shown. The gap itself is visible simultaneous with fish observations and both adults and smolts are clearly distinguishable based on size (Figure 54). Footage of an adult crossing the gap (Figure 55) demonstrated the non-entrainment flows for larger fish. The multiple fish target resolution of the sonar exceeded expectations. Figure 56 shows more than 50 fish in a school resolved simultaneously. These images are the direct real-time output of the DIDSON sonar. They are unaltered screen snapshots.

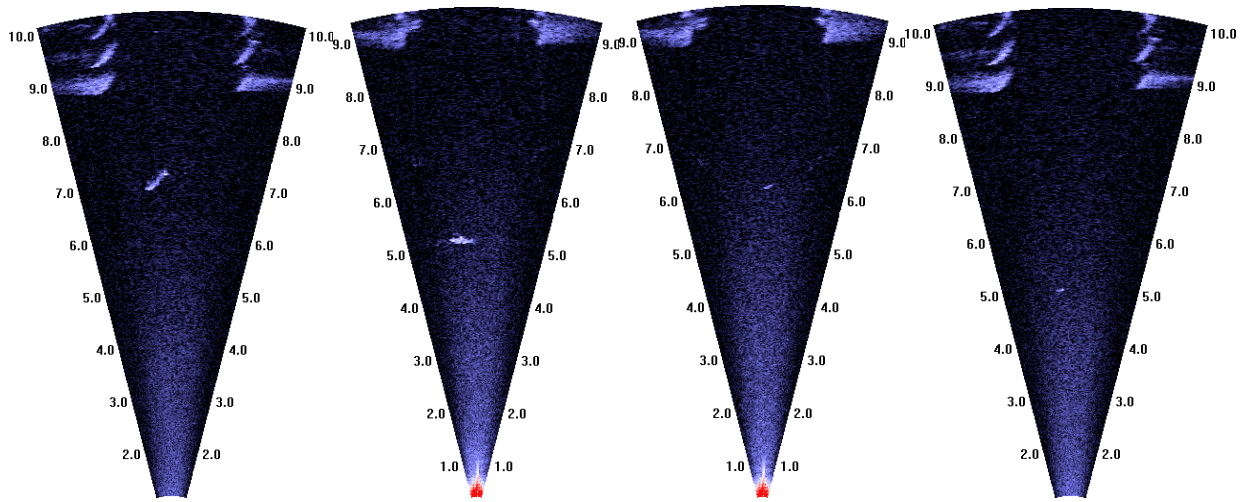


Figure 54. Acoustic images of adults (2 left image) and smolts (2 right images) above J-gap.

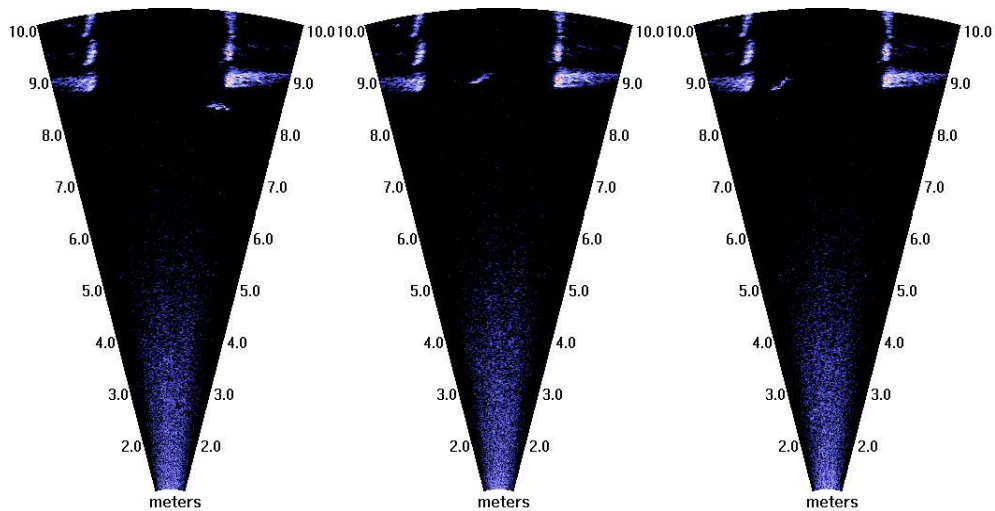


Figure 55. Acoustic image series of an adult sized fish swimming across a J-gap.

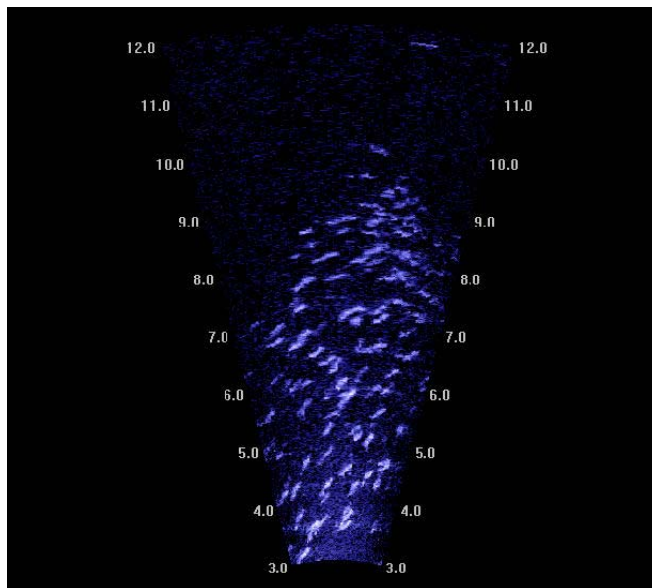


Figure 56. Acoustic image of a school of shad near the surface. The sonar is looking out into the forebay.

5.3.2 Fish Behavior, Trajectory, and Fate

During the 4 days sampled at MU3-4, 196 smolts and 83 adults were detected and their behavior was categorized. Smolt-sized fish were observed going through the gap (the gap itself is in view at the same time). Our results indicate the zone of influence of the gap is relatively small, on the order of 2-3m. Overall, 15% of smolt detections (adjusted for beam spreading) moved through the gap, 23% of smolts were headed east (upstream), 30% were headed west (downstream), and 31% moved off-axis prior to reaching the edges of the beam. To highlight this zone of influence, 48% of smolt-sized fish within 3m of

the gap went through the gap while only 2% of smolt-sized fish from 3-8m above the gap passed through the gap.

Adult-sized fish behaved differently in the gap region. Only 14% of adult-sized fish within 3m of the gap went through the gap while 1% of adults above 3 m of the gap passed through the gap. Overall, with 14% of detections moving through the gap, 49% of adults were headed east, 31% were headed west, and 12% moved off-axis prior to reaching the edges of the beam. After making adjustment for beam expansion, adult-sized targets were detected consistently higher in the water column with 72% of the detections occurring 5 m above the gap or higher.

Table 6. Table of fates of fish detected through the sampling range.

Fish Size	Below 3 m & passed through gap	Above 3 m & passed through gap
Smolt	48% (w = 151)	2% (w = 130)
Adult	13% (w = 40)	4% (w = 102)

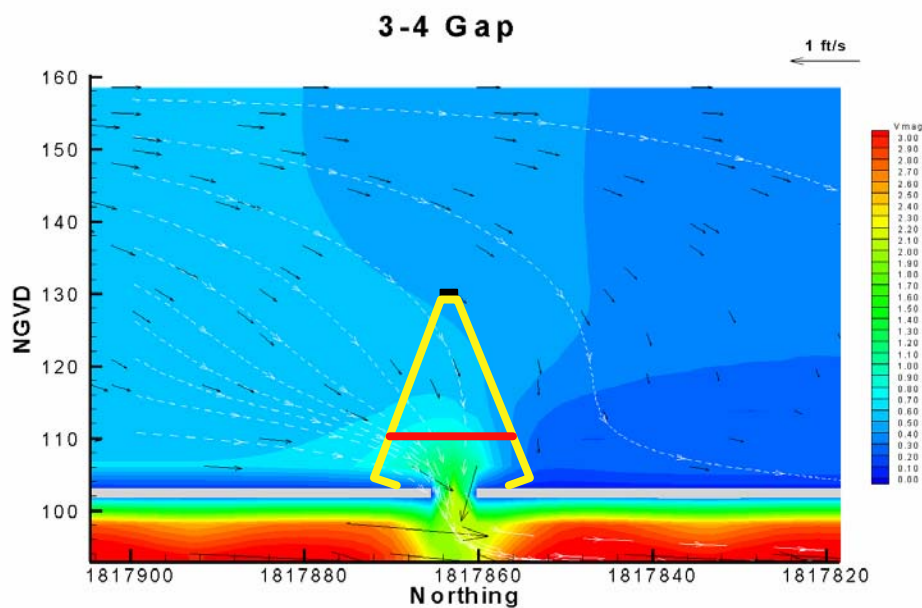


Figure 57. J-gap zone of influence in relation to flows.

5.3.3 J-Gaps as a Passage Route

The smolts observed entering the gap over the sample period may also be enumerated as another passage route. Using these techniques for expansion an estimation of the rate of smolts passing through the gap can be calculated. In the 39.5 hrs sampled at the 3-4 gap, 76 smolts were detected headed downward through the gap after adjusting for the beam expansion. At 9 m range, the beam is 6.2 ft wide

(on the axis perpendicular to the powerhouse). Multiplying by 3.2 expands to a full 20 ft J-extension and multiplying again by 4 main unit gaps expands to the MU1-5 J-occlusions. Lastly, since we have sampled at the peak passage times, we can adjust by .70 to reach a combined day/night estimate (based on sluice abundance). We estimate that 17 smolts per hour passed through the gaps during the sampling period. Passage through the small gaps between same-turbine intakes was assumed to be 0. An average of 1192 fish/hr passed the project according to the smolt monitoring program on June 7-10. A rate of 17 fish/hr is 1.4% of the run.

5.4 Discussion

The DIDSON sonar was able to document smolts that were entrained into the gaps present where the occlusion plates were deployed. The DIDSON's ability to track fish close to structure was beneficial in the determination of smolt entrainment under the occlusion floor structure. We were also able to document a zone of influence in which fish are more susceptible to being entrained below the floor. That zone is relatively small (on the order of 3 m) for smolts and nonexistent for adults. It is assumed that once smolts pass below the floor of the J-extension that they pass through the turbine unit, although this may not necessarily be true.

Adult sized fish were also observed throughout the sampling range. Although the species of these fish was not determined, in at least one instance a school of smolt sized fish was seen moving rapidly upstream and shortly after an adult sized fish appeared along a similar track. Specific predators were not observed, though we believe that the sonar's aiming aspect was poor for identification.

For future studies, we propose sampling in both spring and summer with attention paid to comparative locations. The I-beam and trolley deployment worked well. While the top down view of the gaps granted a good field of view, a side aspect would provide a better signal strength and identification of species-specific characteristics.

6.0 Smolt Movements Near Sluice 1-2

6.1 Objectives

We collected data on smolt movements in the nearfield (within 10 m) of Sluice 1-2 from April 24 to June 1, 2001. These data were useful to interpret and explain the J-occlusion performance data, the “bottom-line” for decisions about the J-occlusions. The objectives of the smolt movement research were to:

1. Describe smolt movements patterns in terms of observed fish velocities and movement fates. (Fates are probabilities on which side a tracked fish will exit the sample volume.)
2. Compare smolt movement patterns with and without J-occlusions in place.
3. Assess specific hypotheses about smolt movements relative to J-occlusions, including:
 - the zone of influence of the sluiceway as determined by fate probabilities will be larger with J-occlusions than without;
 - the overall probability of passage toward the west will be higher with J-occlusions than without;
 - the overall probability of passage toward the turbines will be lower with J-occlusions than without.

6.2 Methods

We used an active fish tracking sonar (AFTS), commonly called a sonar tracker, to intensively sample smolt movements in the region immediately upstream of a sluiceway entrance at TDA. AFTS as applied at a dam was first described by Hedgepeth and Condiotty (1995), and later published in BioSonics (1996), Hedgepeth et al. (1999) and Hedgepeth et al. (2000). AFTS was also a key element in the Behavioral Acoustic Tracking System that is used to track acoustic-tagged fish (Johnson et al. 1998). MacLennan and Simmonds (1992) explain split-beam hydroacoustics, a main component of AFTS.

The AFTS systems (BioSonics 1998) (Figure 58) included a 208 kHz BioSonics DT4000 digital split-beam echo sounder, a 7° split-beam transducer, two high-speed stepper motors for dual axis rotation, a controller unit, a laptop computer, a desktop computer, and cables (Figure 59). See Johnson et al. (2001) for an error analysis of AFTS.

AFTS is based on the principle of tracking radar. Once a fish was detected after the transducer was randomly aimed into the sample volume, two high-speed stepper motors aligned the axis of the digital split-beam transducer on the target. As the fish moved from ping to ping, deviation of the target from the beam axis was calculated and a predictive tracking algorithm was applied to re-aim the transducer, thereby tracking the target. The predictive tracking algorithm was a discounted least-squares fit (Brookner 1998), where the most recent velocity estimate (magnitude and direction) was weighted by unity, the next most recent by one-half, the next by one fourth, the next by one-eighth, and so on. If no target was detected after 30 sec of pinging at a given position, the aiming angles were changed to another

random position. The ping rate was approximately 10 pps. The echo sounder threshold was set at -60 dB on-axis. For each ping the target was tracked, data on fish X, Y, Z position relative to the transducer and target strength were recorded to disk. Fish position resolution can be inferred from the angular resolution ($\pm 0.35^\circ$). At 10 m from the transducer, this would amount to ± 6 cm, and at 1 m the error would be ± 0.6 cm.



Figure 58. Photograph of the active fish tracking sonar.

Two AFTS systems were deployed at Main Unit 1-2 to sample in the primary area of interest, a region 10 m wide, 15 m from the dam, and 10 m deep immediately in front of Sluice 1-2. One tracker was mounted on the tip of the J-extension to sample fish movements when the J-occlusions were in place. The sample volume for this tracker incorporated the region in front of Sluice 1-2 from the surface to the J-section and out about 18 m into the forebay (Figure 60; Table 7). The other tracker was mounted about 20 m deep on a trashrack to sample fish movements when the J-occlusions were out of the water. The sample volume for this tracker incorporated the region in front of Sluice 1-2 from the surface to the transducer and out about 16 m into the forebay (Figure 60; Table 7). The sample volumes were not identical between J-occlusion treatments because of differences in tracker location (IN tracker on J-tip and OUT tracker on trashrack). In the analyses comparing smolt movement between J-occlusions IN and OUT, it was necessary to use only the region where the two sampling volumes overlapped.

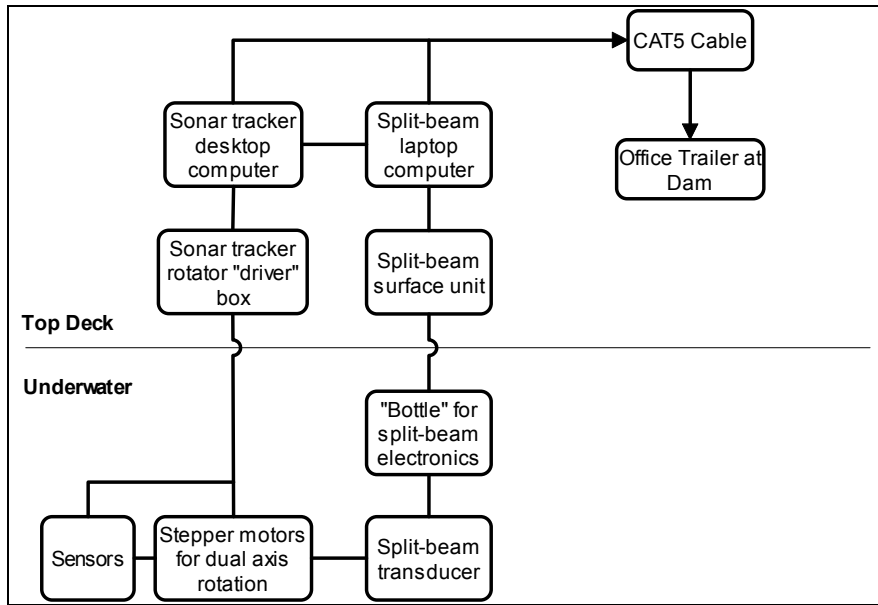


Figure 59. Schematic showing an AFTS, with tracker and split-beam components, and data flow via network (CAT 5) cable from the equipment shed at MU 1 2 to an office trailer at the dam. Two of these systems were deployed.

Table 7. Boundaries of the actual sample volumes by dimension for J occlusions IN/OUT and spill/no spill. (Too few data were available to include the condition of J occlusions OUT and spill.) The data (in meters) are referenced to “dam coordinates” with the origin at the Intake 1 2 centerline at the plane of the pier noses at the water surface (elevation 158 ft). Positive X is to the east, positive Y is away from the dam, and positive Z is upward in the water column

J-OCCLUSIONS	SPILL	X	Y	Z
IN	No	-4 to +4 m	+3 to +18 m	-0.5 to -8 m
IN	Yes	-4 to +3 m	+4 to +14 m	-0.5 to -5 m
OUT	No	-2 to +6 m	+4 to +16 m	-0.5 to -8 m

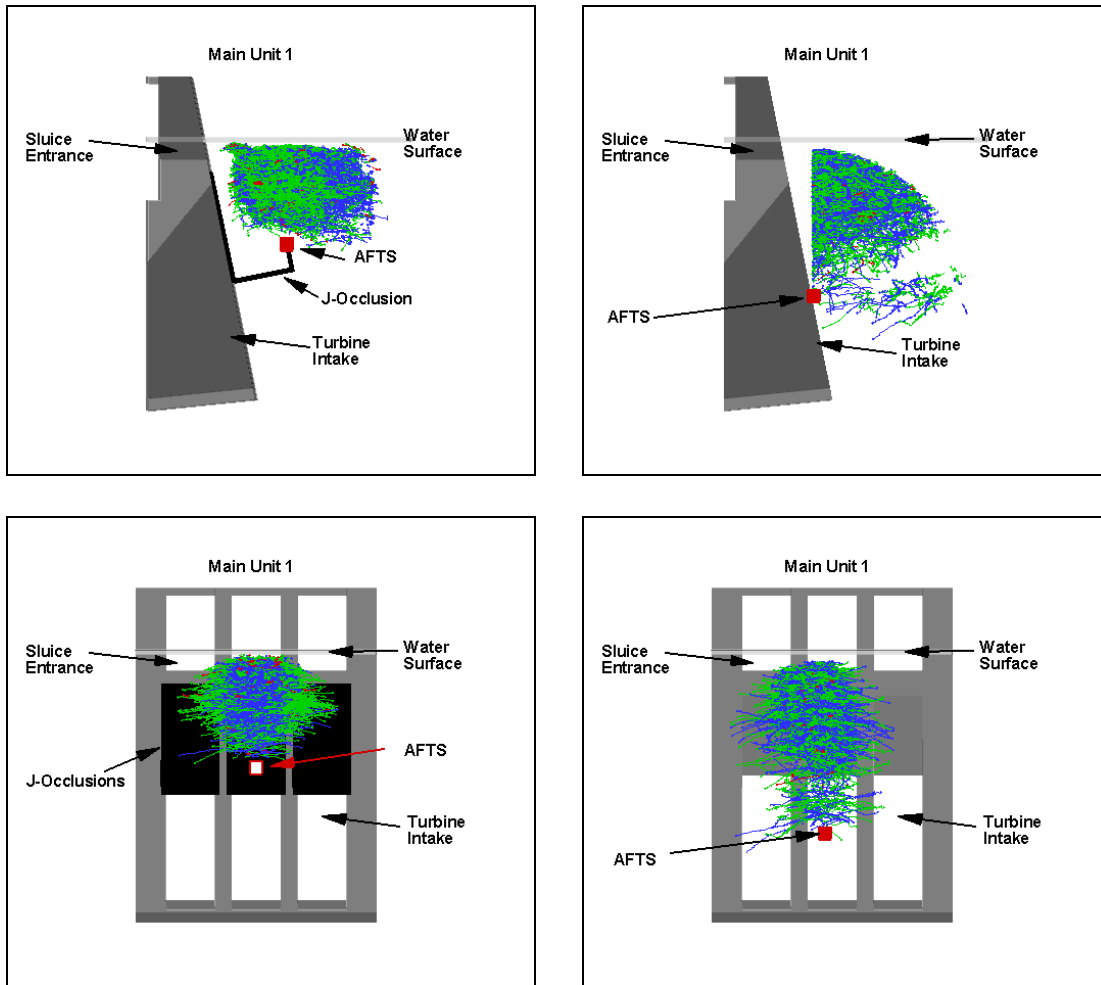


Figure 60. Side and front views of sample volumes for conditions with (left figures) and without (right figures) J occlusions.

Overall, smolt movement data were collected on 32 of 39 possible days in spring 2001 at The Dalles Dam. We tracked about five times as many fish in the IN condition as in the OUT condition. The total of ~38,000 tracked fish was less than half the total number tracked in the 2000 study. However, statistical analysis in the context of a formal experimental design were not appropriate for these data because the replication necessary for statistical testing was not realized. Thus, quantitative statistical tests were not conducted. We did have observational “periods” under different test conditions, e.g., J-occlusions IN, nighttime, no spill. We analyzed the smolt movement data in the context of three analysis factors: J-occlusions IN/OUT; Day/Night; and Spill/No Spill. Data reduction and analysis steps are described in detail in Appendix I.

6.3 Results

The 2001 study results include track description, mean smolt velocities, direction of movement proportions, movement fates, comparison of J-occlusions in and out, and evaluation of hypotheses about J-occlusion effects. The results are typically presented separately for the various combinations of treatment conditions, e.g., J-occlusions IN/day/spill.

6.3.1 Track Description

Fish tracks from AFTS were described using example tracks, track length, and average number of pings per track. Example tracks with the J-occlusions IN and OUT show similar patterns (Figure 61). Tracked fish generally were moving toward the dam and upward in the water column (diamonds in Figure 61 depict the end of each track). Track length varied with short (~1 m) tracks interspersed with long (~5 m) tracks, as shown in the scaled Figure 61. The number of pings per track was higher for the deployment with J-occlusions IN (99 pings/track) than with them OUT (32 pings/track) (Table 8). The number of pings per track was higher during night than day (Table 8).

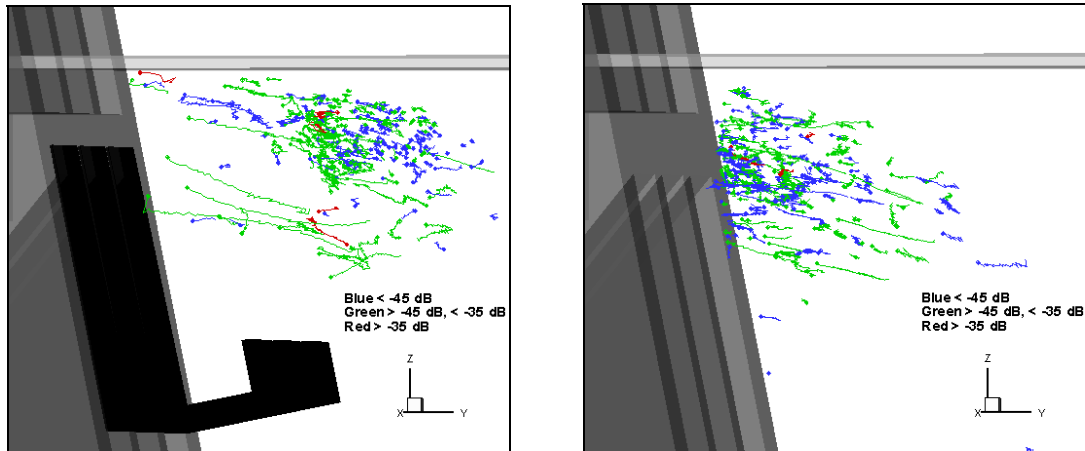


Figure 61. Isometric view of example tracks with (left figure) and without (right figure) J occlusions. Data are from the first 250 tracks collected on April 28 and May 2 for J occlusions IN and OUT, respectively.

Table 8. Descriptive track statistics separately for J occlusions IN and OUT.

		IN	OUT
Day	Pings	1,156,492	144,389
	Tracks	16,343	4,947
	Pings/track	71	29
Night	Pings	1,859,700	90,252
	Tracks	14,101	2,439
	Pings/track	132	37
Combined	Pings	3,016,192	234,641
	Tracks	30,444	7,386
	Pings/track	99	32

6.3.2 Mean Fish Velocity

Mean fish velocities in the three dimensions were stronger to the west (X), toward the dam (Y), and upward (Z) with J occlusions IN than OUT for periods with the same spill condition (Figure 62). Differences in mean fish velocity between treatments were not large, ranging from 0.02 to 0.11 m/s, but they clearly showed a trend. Patterns between day and night were similar, except during spill velocity magnitude was greater for day than night. A dramatic shift in velocity toward the west occurred between periods 4 and 5 when spill changed from off to on; mean velocity in the X-dimension went from ~0.0 to ~0.2 m/s during day and night. Thus, these descriptive fish velocity data indicated that the J-occlusions affected fish movements.

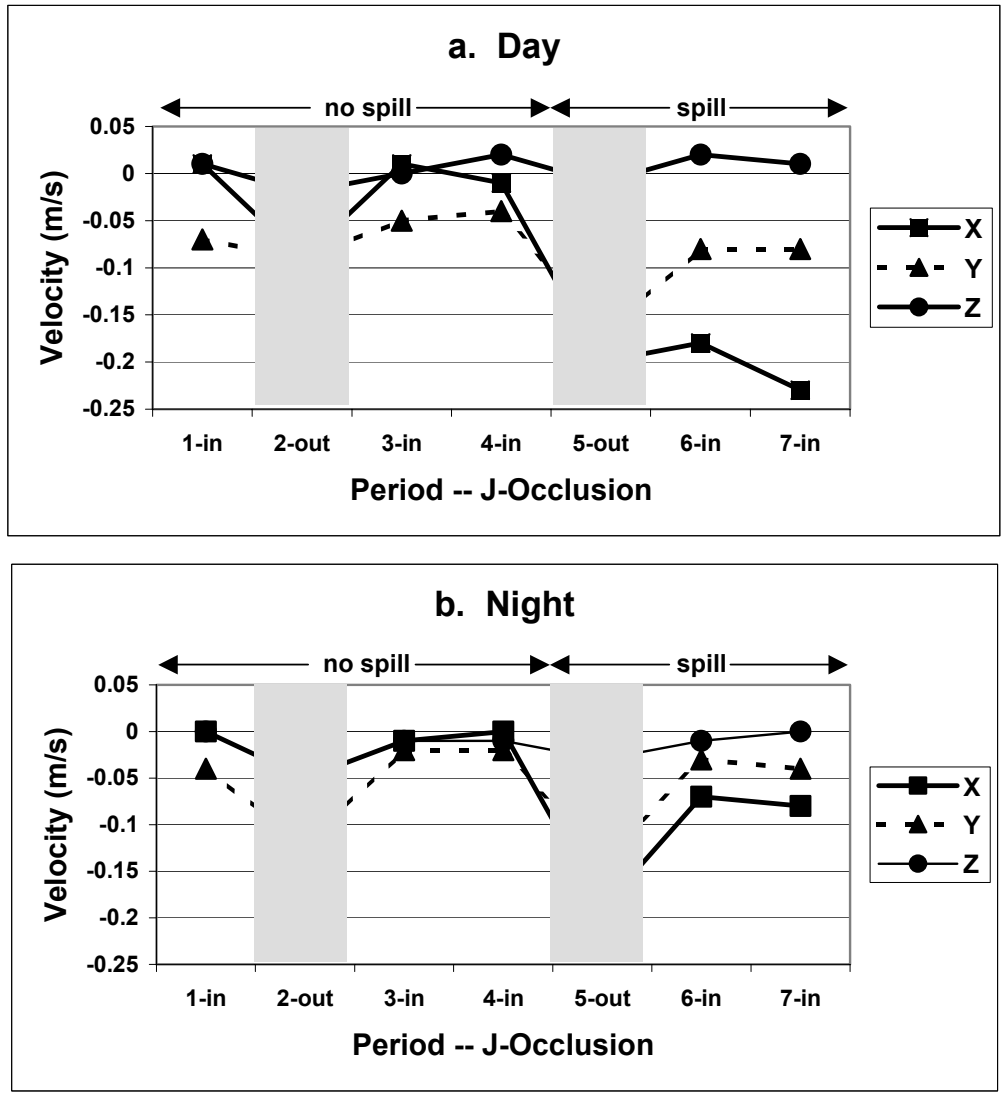


Figure 62. Mean observed fish velocity data by period (defined in Table 1) for day and night separately. Shaded areas are data for J occlusions OUT. Positive X is to the east, positive Y is away from the dam, and positive Z is upward in the water column. Periods 1-4 had no spill; periods 5-7 had spill.

6.3.3 Direction of Movement Proportions

Smolt track directionality relative to the presence of J-occlusions can be summarized using proportions of movement based on individual track regressions in each of the three dimensions (Table 9). The proportion of fish moving westward toward the spillway (out of the total west plus east; the X-dimension) was 0.11 higher with J-occlusions IN than OUT. The proportion of fish moving toward the dam (out of the total toward plus away; the Y-dimension) was also 0.11 higher during IN than OUT.

And, the proportion of fish moving upward (out of the total up plus down; the Z-dimension) was 0.12 higher with J-occlusions IN than OUT. In general, movement proportions toward the dam and upward were 0.03-0.04 stronger during day than night. When water was spilled, the proportion of fish moving westward toward the spillway was 0.12 higher than during no spill. In conclusion, the direction of movement proportions indicated that with the J-occlusions IN resulted in less movement to the west, less movement toward the dam, and less movement downward in the water column than with them OUT.

Table 9. Summary mean proportions with 95% confidence levels for direction of movement separately for each dimension (X, Y, Z) for J-occlusions IN, OUT, day, night, no spill, and spill. Movement directions obtained from signs of regression coefficients for each dimension of each fish track (regression of position on time).

	X		Y		Z	
	EAST (+)	WEST (-)	AWAY (+)	TOWARD (-)	UP (+)	DOWN (-)
IN	0.48 ±0.01	0.52 ±0.01	0.41 ±0.01	0.59 ±0.01	0.50 ±0.01	0.50 ±0.01
OUT	0.37 ±0.01	0.63 ±0.01	0.30 ±0.01	0.70 ±0.01	0.38 ±0.005	0.62 ±0.005
Day	0.46 ±0.04	0.54 ±0.04	0.37 ±0.03	0.63 ±0.03	0.50 ±0.03	0.50 ±0.03
Night	0.47 ±0.02	0.53 ±0.02	0.42 ±0.02	0.58 ±0.02	0.47 ±0.02	0.53 ±0.02
Spill	0.36 ±0.04	0.64 ±0.04	0.38 ±0.03	0.62 ±0.03	0.52 ±0.02	0.48 ±0.02
No Spill	0.48 ±0.02	0.52 ±0.02	0.40 ±0.02	0.60 ±0.02	0.48 ±0.02	0.52 ±0.02

6.3.4 Movement Fate Probabilities

The Markov-Chain analysis of fish movements resulted in estimates of the probability of passage out of particular sides of the sample volume. We call these “movement fates.” For example, exit out the sluiceway side of the sample volume from the surface to 4 m deep corresponded to the “Sluice” fate. Possible fates were Sluice, Turbine, Bottom, East, West, Reservoir, and Not Moving. The data set included the region in front of the Sluice 1-2 entrance, 3.5-14.5 m upstream, and 6.0 m deep. The three-dimensional contour plot of the fate probabilities in Figures 19, 20, and 21 show 0.5 m slices +/- 3.5 on the centerline of Sluice 1-2 (X), 3.5-14.5 m from the dam (Y), and 1.0-6.0 m deep (Z). We present data for the sluice, west, and bottom fates because they are the most pertinent to this study.

The probability that fish exited the upper 4 m of the side of the Markov sample volume facing the dam (the “sluice fate” probability) is instructive because it denotes passage toward the entrance of Sluice 1-2. (Recall, the “Markov” sample volume was a subset of the total sample volumes for the two trackers and was identical for each J-occlusion condition.) Based on visual inspection, the sluice fate probability was clearly higher and more prevalent with J-occlusions IN than OUT (Figure 63a-d). The extent of noticeable sluice probabilities (> 0.2) was greater with the J-occlusions IN than OUT, extending out 10-12 m from the dam as opposed to 5-7 m (Figure 63a-d). At night with J-occlusions OUT, the sluice fate was minimal (Figure 63d). Sluice probabilities were conspicuously lower during spill than no spill (Figure 63e,f). Overall, the sluice probability contour plots showed that differences between J-occlusions IN and OUT were noticeable and that spill negatively affected sluice fate probabilities.

The probability that fish exited the bottom of the Markov sample volume (6 m deep; “bottom fate” probability) is useful, because we would expect movement in that direction (presumably toward the turbine intakes) could be affected by the presence of the J-occlusions, which were located over the upper half of turbine intakes and formed a vertical barrier 7.6 m wide about 18 m deep. The bottom fate probabilities were higher with J-occlusions OUT than IN (Figure 64).

The probability fish exited the west side of the Markov sample volume (“west fate” probability) is important because movement westward toward the spillway due to the J-occlusions would be a positive effect if the fish otherwise would have passed into turbines. We observed a great difference in the west fate between J-occlusions IN and OUT (Figure 65a-d). However, west fates for day and night were similar (Figure 65a-d). As expected from previous results, however, there was strong westward movement out of the sample volume during spill compared to no spill, especially during day.

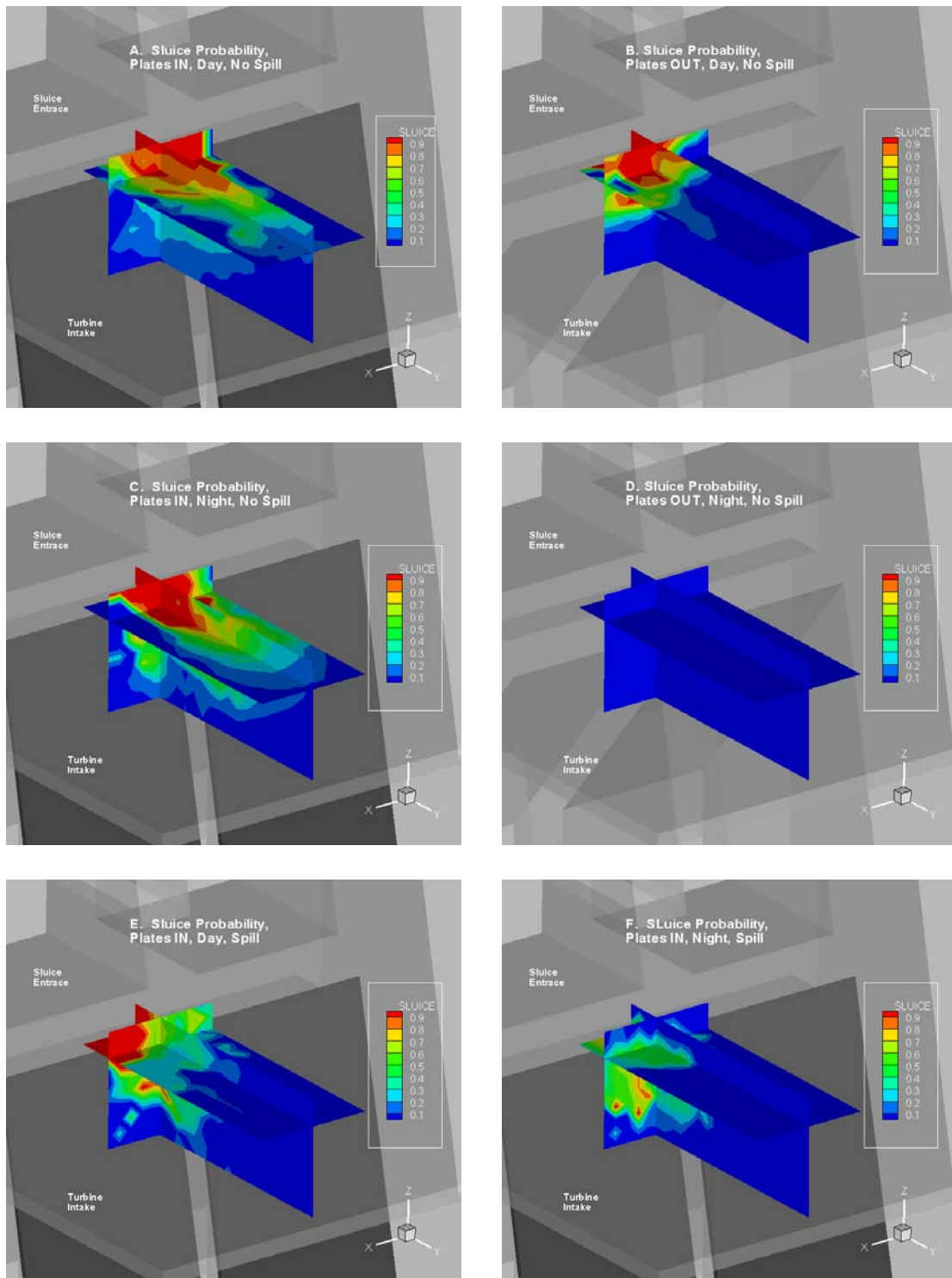


Figure 63. Sludge fate probabilities.

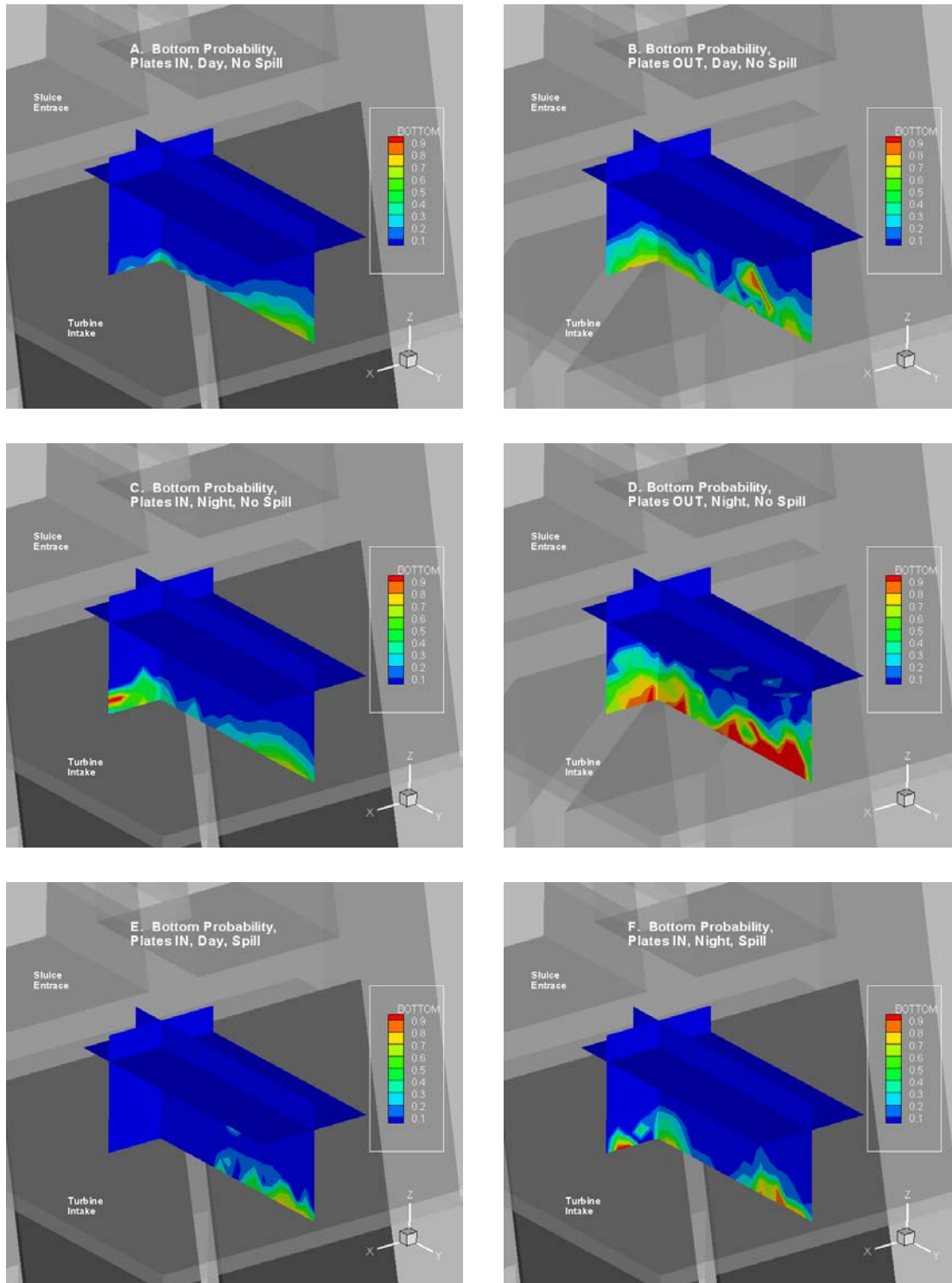


Figure 64. Bottom fate probabilities.

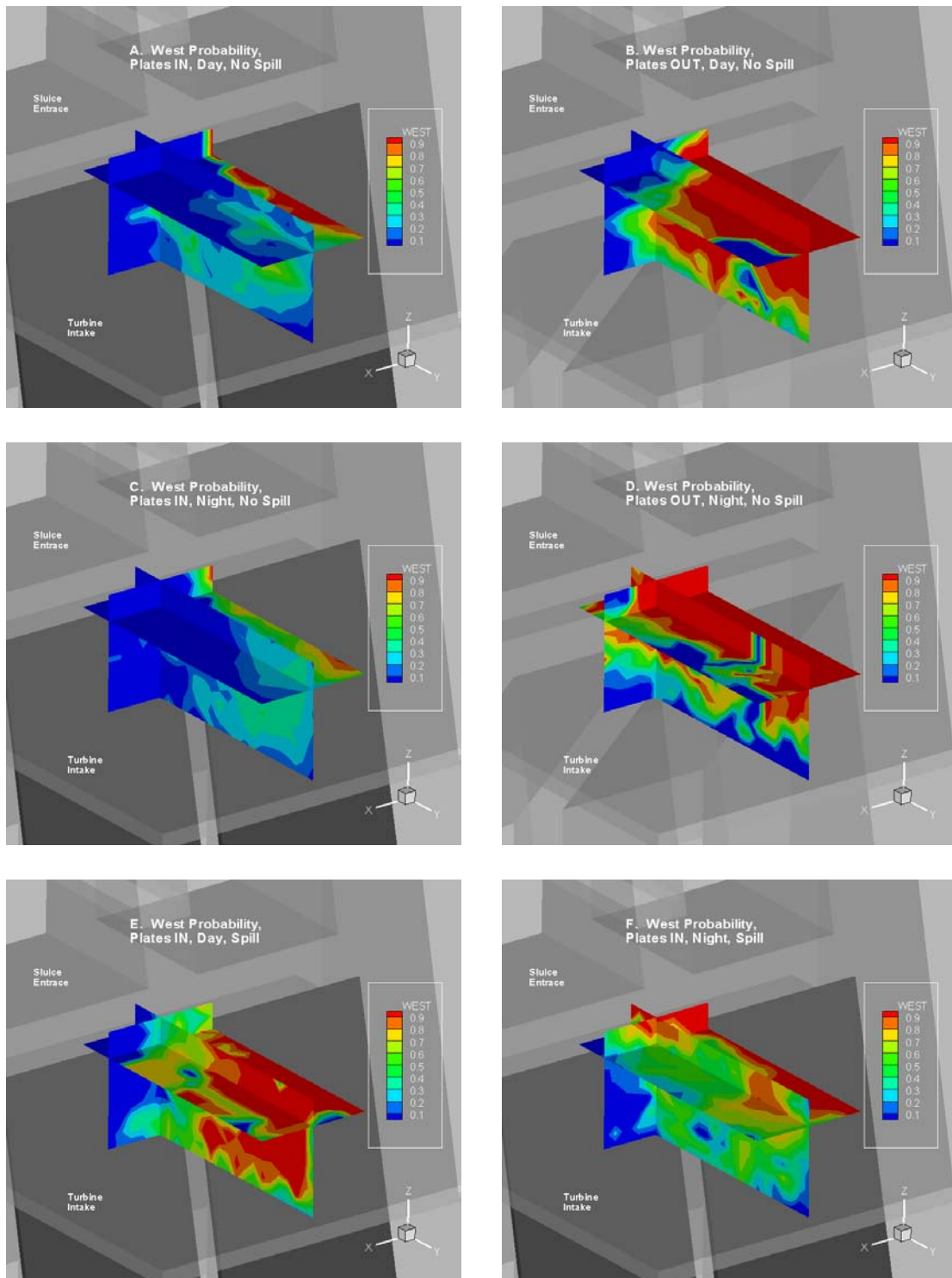


Figure 65. West fate probabilities.

We summarized the fate probabilities by averaging the cell-by-cell probabilities over the same sample volume for J-occlusions IN vs. OUT. We only used fish tracked during no spillway discharge. For the purpose of this analysis, turbine and bottom fates were combined into a fate called “Turbot” to represent all fish entrained or moving toward the turbine intakes. The fate summary data are presented in Figure 66.

Prominent differences were observed between J-occlusions IN and OUT. West fate probability was 0.37 (absolute difference 37%) higher during day and 0.34 higher during night with plates IN than OUT. East fate was 0.24-0.24 higher IN than OUT. Sluice fate was 0.12 higher IN than OUT during day and, during night, sluice fate was negligible with plates OUT. Turbot fate was 0.12 higher IN than OUT during night; no differences during day. West fate with J-occlusions OUT was the largest (0.59-0.66), followed by east (0.34-0.35) and sluice (0.22-0.25) with plates IN. The reservoir fate was the smallest (0.02-0.04).

Assessment of Hypotheses about J-Occlusion Effects

In this section, we assess a priori hypotheses about the effects of the J occlusions on smolt movements in the nearfield of Sluice 1-2. This assessment relied on volumetric analyses of fate probability data. It was qualitative, however, as there were no statistical comparisons.

Hypothesis -- The zone of influence for the sluiceway entrance at Sluice 1-2 will be larger with J-occlusions IN than OUT (as determined by fate probabilities).

Explanation – The flow net for the sluiceway, and hence its zone of influence, could be enhanced, or perceived to be such by smolts, due to less competing flow moving down toward the turbine intakes with J-occlusions in place.

Assessment – This hypothesis was supported by the sluice fate volumetric data. Defining the zone of influence (ZOI) of the sluiceway as the region where sluice fate probabilities are 0.9 or greater, then the sluice ZOI was larger with J-occlusions IN (18 m³ day and 25 m³ night) than OUT (14 m³ day and 0 m³ night) (Figure 66).

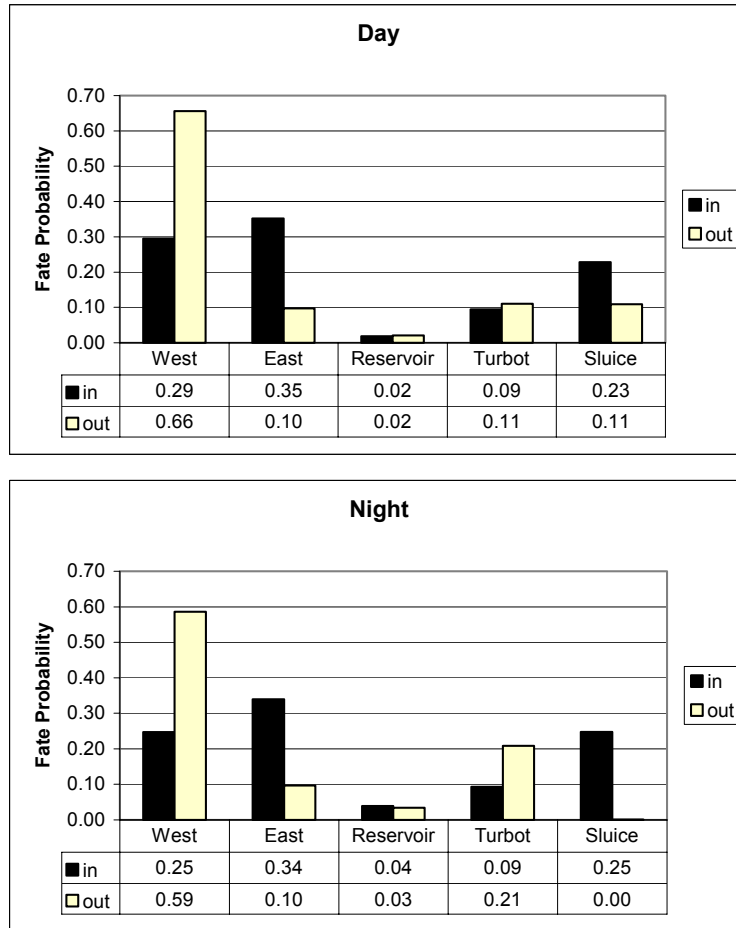


Figure 66. Mean fate probabilities from the Markov-Chain analysis for J-occlusions IN vs. OUT for day and night separately, no spill. (A similar plot for data collected during spill is not available because there were not enough data for the condition with J-occlusions OUT to run the Markov-Chain analysis.)

Hypothesis -- The overall probability of passage to the west toward the spillway will be higher with J occlusions IN than OUT.

Explanation – The J-occlusions could serve to guide fish along the face of the dam to the west, fish that might otherwise pass into turbines.

Assessment – This hypothesis was not supported by the fate probability data, as the opposite effect was observed. The volume of west fate probability was an order of magnitude greater with J-occlusions OUT than IN (Figure 67).

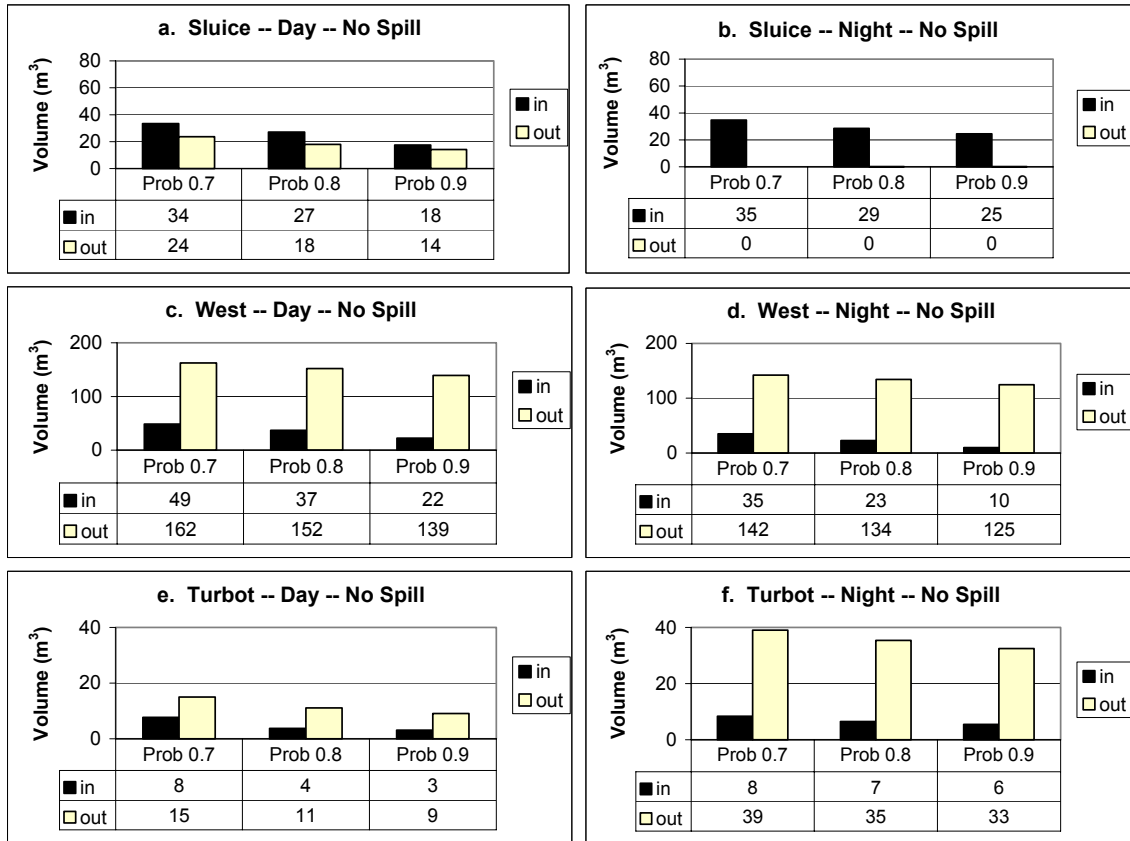


Figure 67. Volumetric analyses of sluice, west, and turbot fate probabilities during no spill for day and night separately. The data are the total volume of cells in the Markov sample volume with sluice fate probabilities greater than 0.7, 0.8, and 0.9.

Hypothesis -- The overall probability of passage out the turbine/bottom sides of the sample volume toward the turbine intake will be lower with J-occlusions IN than OUT.

Explanation – Passage out the turbine/bottom sides of the sample volume should be less because the J-occlusions should decrease the downward flow toward turbines from the surface waters in the nearfield of Sluice 1-2.

Assessment – This hypothesis was supported by the turbot fate volumetric data for day and night (Figure 67e,f). For turbot fate probabilities greater than 0.9 during day, the volume was 3 m³ with J-occlusions IN and 9 m³ with them OUT. However, during night, the differences were even greater between J-occlusions IN and OUT (Figure 24) (6 vs. 33 m³). In addition, the proportion of fish moving down in the water column (based on regression analysis) was greater with J-occlusions OUT than IN (50 vs. 62%, respectively) (Table 9).

6.4 Discussion

This aspect of the evaluation was designed to assess smolt movements in the nearfield (< 10 m) of the entrance to Sluice 1-2 and its associated turbine intake. The sample volume included the surface 6-8 m. It covered the 2-m region in front of the sluice sill as well as the top 2-4 m of the turbine intake below where the J-occlusions were installed/removed. Thus, the sample volume was directly applicable to study of J-occlusion effects on fish movements in front of Sluice 1-2 and the upper portion of Turbine Intake 1-2.

Effects of the J-occlusions on smolt movements were evident as noticeable, distinct differences in movement patterns between the IN and OUT conditions. Mean fish velocities, movement proportions, and fate probabilities all demonstrated differences between J-occlusions IN and OUT. Generally, the J-occlusions appeared to cause fish in the nearfield of Sluice 1-2 to decrease westward movement, decrease movement toward the dam, and increase upward movement in the water column. If these patterns translate to passage, then we would expect the J-occlusions to result in decreased turbine and increased sluiceway passage rates.

In addition, effects on fish movement patterns due to spill were noticeable. There was strong westward movement in the sample volume when water was spilled. This observation comports with previous data showing that sluice passage efficiency and effectiveness decrease as the proportion of spill increases (Ploskey et al. 2001). Fish apparently guided along the face of the powerhouse and non-overflow section, following bulk flow toward the spillway. Thus, spill likely passed some fish that would otherwise have gone through the sluiceway. The important question is whether the J-occlusions prevented some fish from passing into turbines and, hence, indirectly or directly guided them to the spillway or sluiceway.

7.0 References

- Belcher E.O., H.Q. Dinh, D.C. Lynn, and T.J. Laughlin. 1999. Beamforming and imaging with acoustic lenses in small, high-frequency sonars. Proceedings of Oceans 1999 Conference, September 13-16, Seattle, Washington.
- Belcher E., B. Matsuyama, and G. Trimble. 2001. Object identification with acoustic lenses. Proceedings of Oceans 2001 Conference, November 5-8, Honolulu, Hawaii.
- BioSonics, Inc. 1996. Hydroacoustic evaluation and studies at The Dalles Dam, spring/summer 1996. Volume 2 - Smolt behavior. Draft final report submitted to Portland District, U.S. Army Corps of Engineers by BioSonics, Inc. Seattle, WA. November 15, 1996.
- BioSonics, Inc. 1998. DT/DE Series User's Manual Version 4.02. BioSonics, Inc., Seattle WA, 57 pp.
- Brookner, E. 1998. Tracking and Kalman Filtering Made Easy. John Wiley and Sons, New York. 477 pp.
- Dauble, D. D., S. M. Anglea, and G. E. Johnson. 1999. Surface flow bypass development in the Columbia and Snake Rivers and implications to Lower Granite Dam. Final Report submitted to Walla Walla District, U.S. Army Corps of Engineers by Battelle. Richland, WA. July 21, 1999.
- ENSR, 2001. Three-Dimensional Computational Fluid Dynamics (CFD) Modeling of the Forebay of The Dalles Dam, Oregon. Final Report. June 2001. Document Number 3697-006-320. ENSR International, INCA Engineers. 206 pp.
- Hedgepeth, J.B. and J. Condiotty. 1995. Radar tracking principles applied for acoustic fish detection. Poster Presentation, ICES International Symposium on Fisheries and Plankton Acoustics, Aberdeen Scotland, 12-16 June 1995, Book of Abstracts page 10.
- Hedgepeth, J., D. Fuhriman and W. Acker. 1999. Fish behavior measured by a tracking radar-type acoustic transducer near hydroelectric dams. Pages 155-171 in M. Odeh, editor. Innovations in Fish Passage Technology. American Fisheries Society, Bethesda MD.
- Hedgepeth, J.B., D. Fuhriman, G.M.W. Cronkite, Y. Xie and T.J. Mulligan. 2000. A tracking transducer for following fish at close range. *Aquat. Living Resour.* 13(5): 305-311.
- Johnson, G.E. 2000. Assessment of the acoustic screen model to estimate smolt passage rates at dams: case study at The Dalles Dam in 1999. Prepared for the U.S. Army Corps of Engineers, Waterways Experiment Station, Vicksburg, Mississippi.
- Johnson G.E., and D.D. Dauble. 1995. Synthesis of existing physical and biological information relative to development of a prototype surface flow bypass system at Lower Granite Dam. Prepared for the U.S. Army Corps of Engineers, Walla Walla District, Walla Walla, Washington.

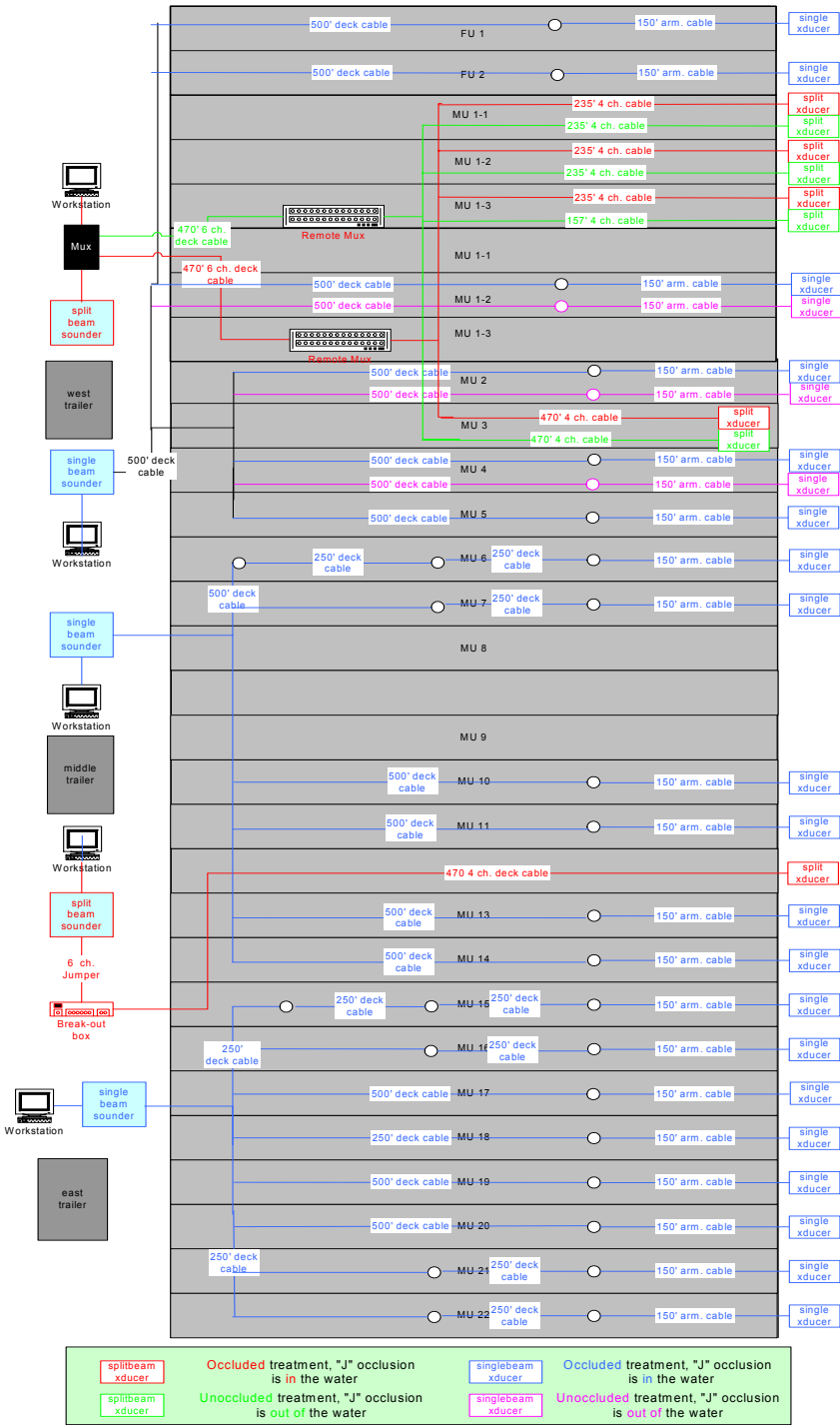
- Johnson, G. E. and A. E. Giorgi. 1999. Development of surface flow bypasses at Bonneville dam: a synthesis of data from 1995 to 1998 and a draft M&E plan for 2000. Final report ed. 1999 Oct 8.
- Johnson, G. E. J.B. Hedgepeth, A. E. Giorgi and J.R. Skalski. 2001. Evaluation of smolt movements using an active fish tracking sonar at the sluiceway surface bypass, The Dalles Dam, 2000. Final report. September 30, 2001.
- Johnson, R. L., D. R. Geist, R. P. Mueller, R. A. Moursund, J. Hedgepeth, D. Fuhriman, and A. Wirtz. 1998. Behavioral acoustic tracking system (BATS). Final report submitted to Walla Walla District, U.S. Army Corps of Engineers by Battelle. Richland, WA. January 1998.
- Kumagai, K. K., Ransom, B. H., and Sloan, H. A. Effectiveness of a prototype surface flow attraction channel for passing juvenile salmon and steelhead trout at Wanapum Dam during summer 1996. Final report. Seattle, Washington: Hydroacoustic Technology, Inc. 1996.
- MacLennan, D. N. and E. J. Simmonds. 1992. Fisheries Acoustics. Chapman and Hall. London, England. 325 pp.
- Nagy, W. T. and M. K. Shuttles. 1995. Hydroacoustic evaluation of surface collector prototypes at The Dalles Dam, 1995. Draft report by the Report by the Fisheries Field Unit, Portland District, U.S. Army Corps of Engineers. Cascade Locks, Oregon. 37 pages.
- National Marine Fisheries Service. 2000. Biological Opinion: Reinitiation of consultation on operation of the Federal Columbia River Power System, including the juvenile fish transportation program, and 19 Bureau of Reclamation projects in the Columbia Basin. National Marine Fisheries Service, Northwest Region: Seattle, Washington.
- Nichols, D.W. and B.H. Ransom. 1980. Development of The Dalles Dam trash sluiceway as a downstream migrant bypass system for juvenile salmonids. Oregon Department of Fish and Wildlife. Report to U.S. Army Corps of Engineers, Portland, Oregon. Contract No. DACW57 78 C 0058. 36pp. + app.
- Ploskey, G., T. Poe, A. Giorgi, and G. Johnson. 2001a. Synthesis of radio telemetry, hydroacoustic, and survival studies of juvenile salmon at The Dalles Dam (1982-2000). Final Report ed.; 2001 Sep.
- Ploskey, G., B. Nagy, L. Lawrence, M. Hanks, C. Schilt, P. Johnson, G. Johnson, D. Patterson, and J. Skalski. 2001b. Hydroacoustic evaluation of juvenile salmon passage at The Dalles Dam: 1999. Final report. ERDC/EL TR 01 11. Vicksburg, MS.
- Ploskey, G., W. Nagy, L. Lawrence, D. Patterson, C. Schilt, P. Johnson, and J. Skalski. 2001c. Hydroacoustic evaluation of juvenile salmonid passage through experimental routes at Bonneville Dam in 1998. Final report. ERDC/EL TR-01-2. Vicksburg, MS.
- Sokal, R.R and F.J. Rohlf. 1981. Biometry. The Principles and Practice of Statistics in Biological Research, 2 ed. W.H. Freeman and Company, San Francisco.

Taylor, H. and S. Karlin. 1998. *An Introduction to Stochastic Modeling*. 3rd ed. Academic Press. San Diego, CA. 631 pp.

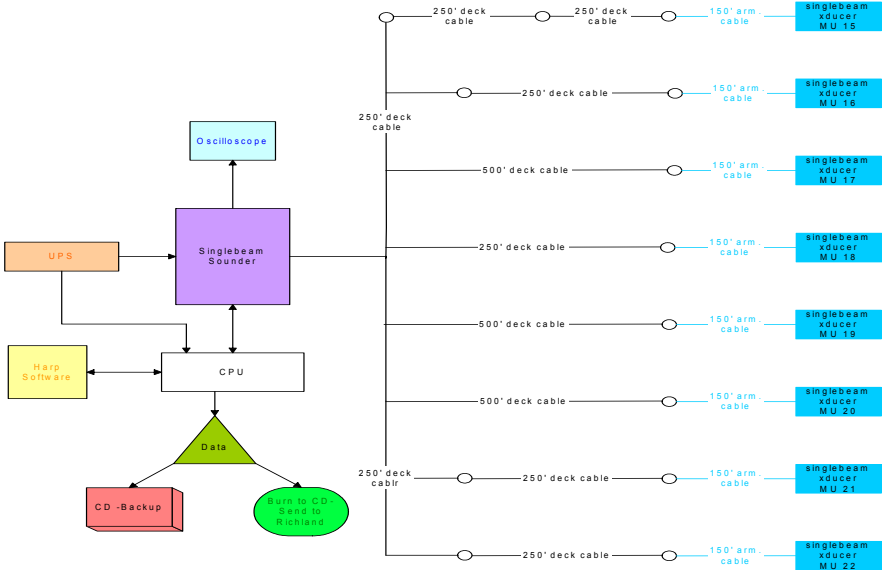
Appendix A

Equipment Diagrams

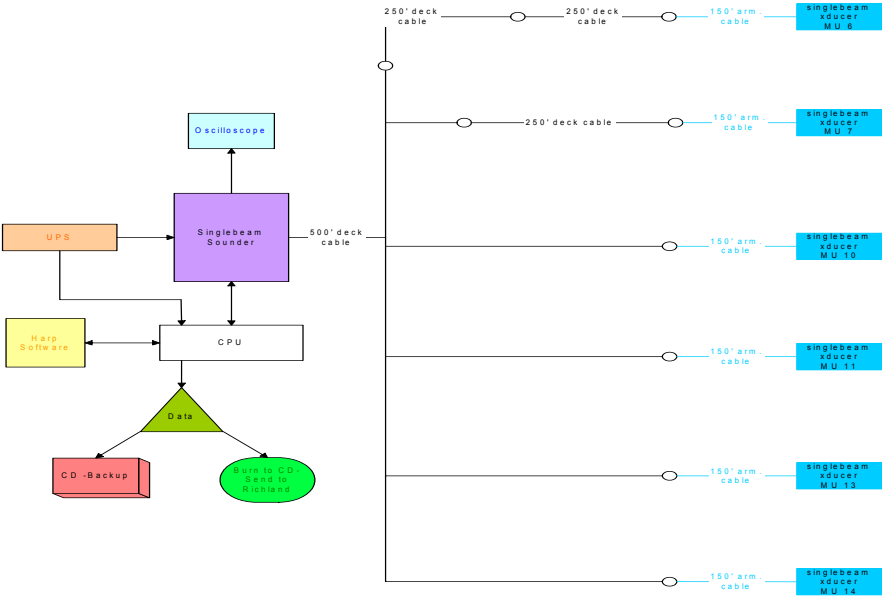
The Dalles Dam Powerhouse FU 1- MU 22
2001 Hydroacoustic System Setup



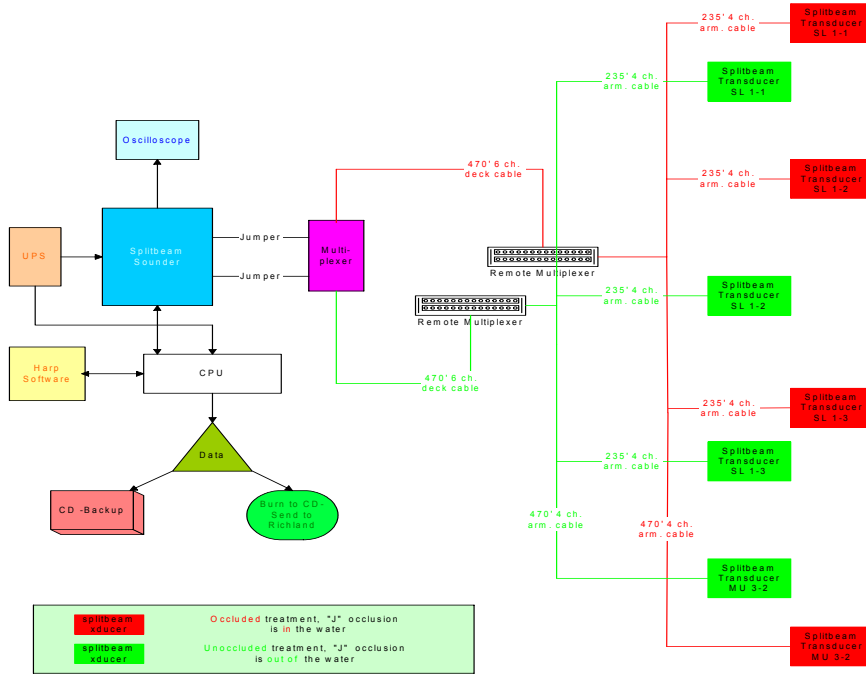
**The Dalles Dam Powerhouse
West End Singlebeam System "E" at MU 15 - MU 22**



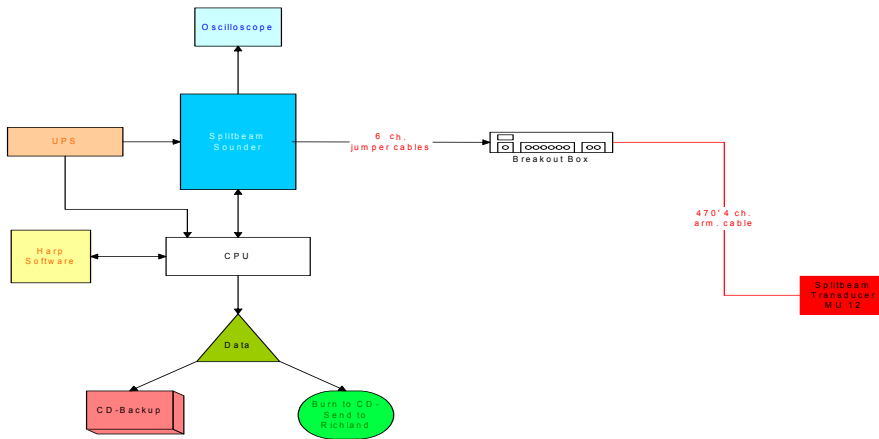
**The Dalles Dam Powerhouse
Middle Singlebeam System "D" at MU 6 - MU 14**



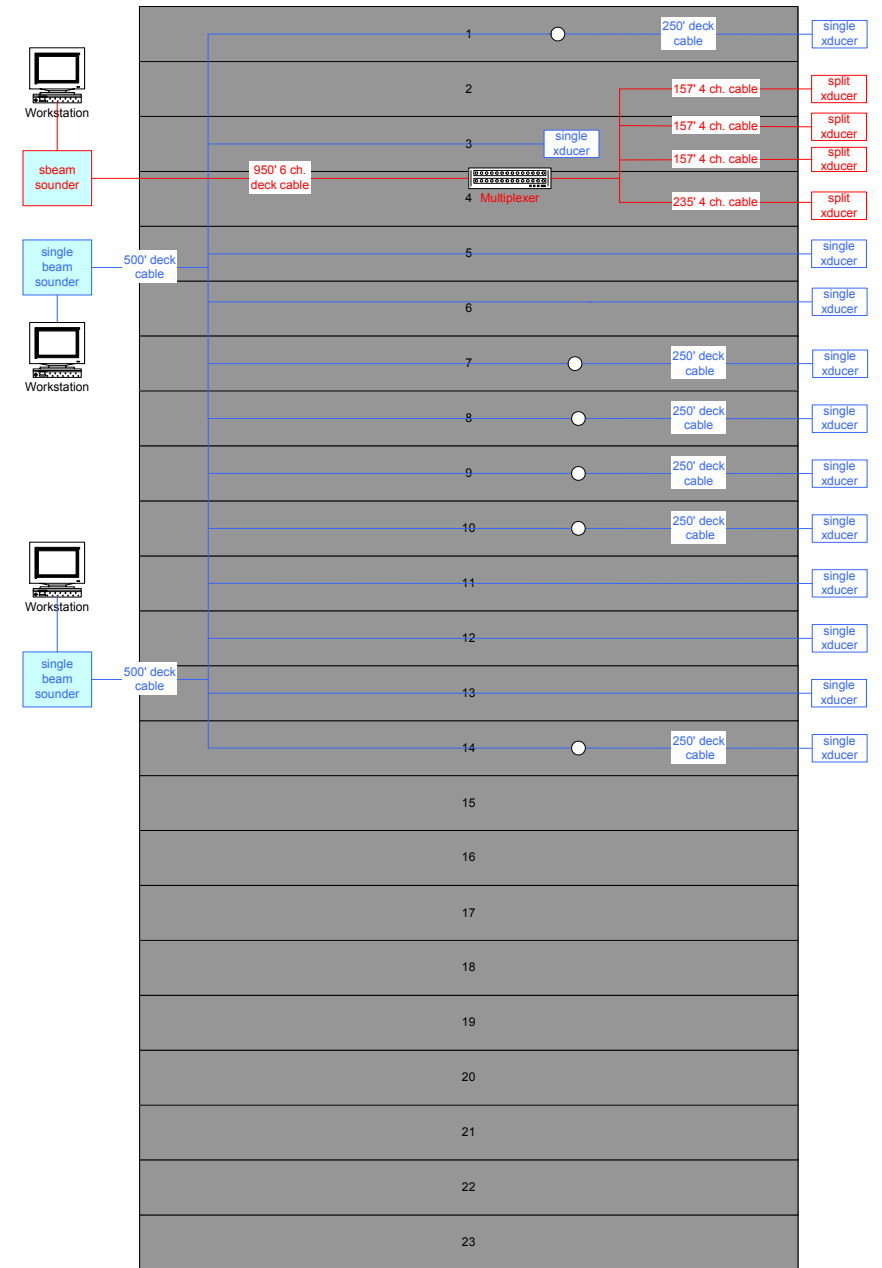
The Dalles Dam Powerhouse
Splitbeam System "W" at Sluiceway Unit 1 (slots 1-3) and Main Unit 3



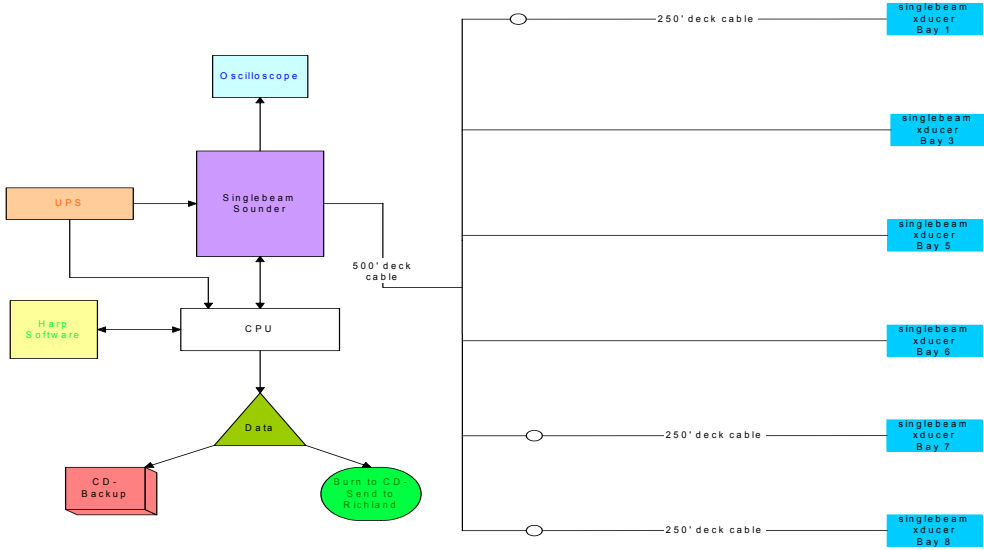
The Dalles Dam Powerhouse
Splitbeam System "V" at Main Unit 12



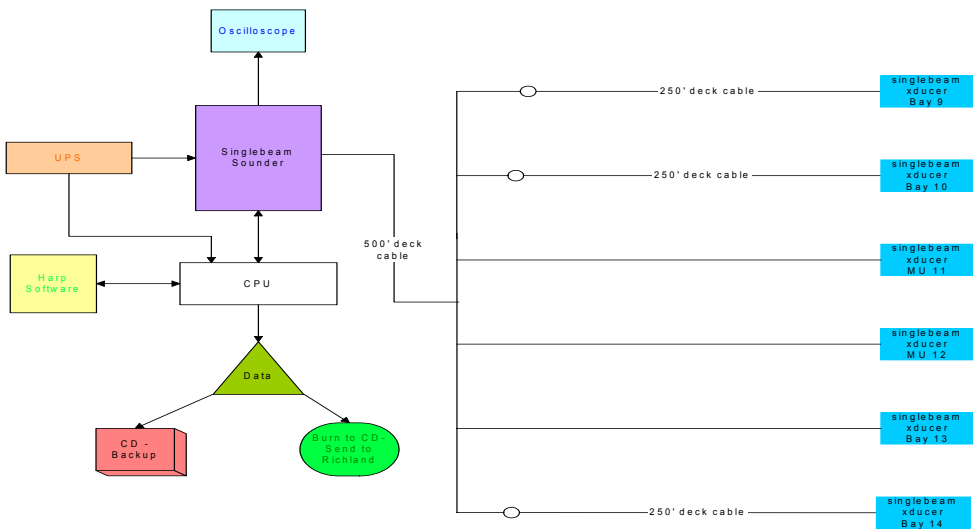
The Dalles Dam Spillway
2001 Hydroacoustic System Setup



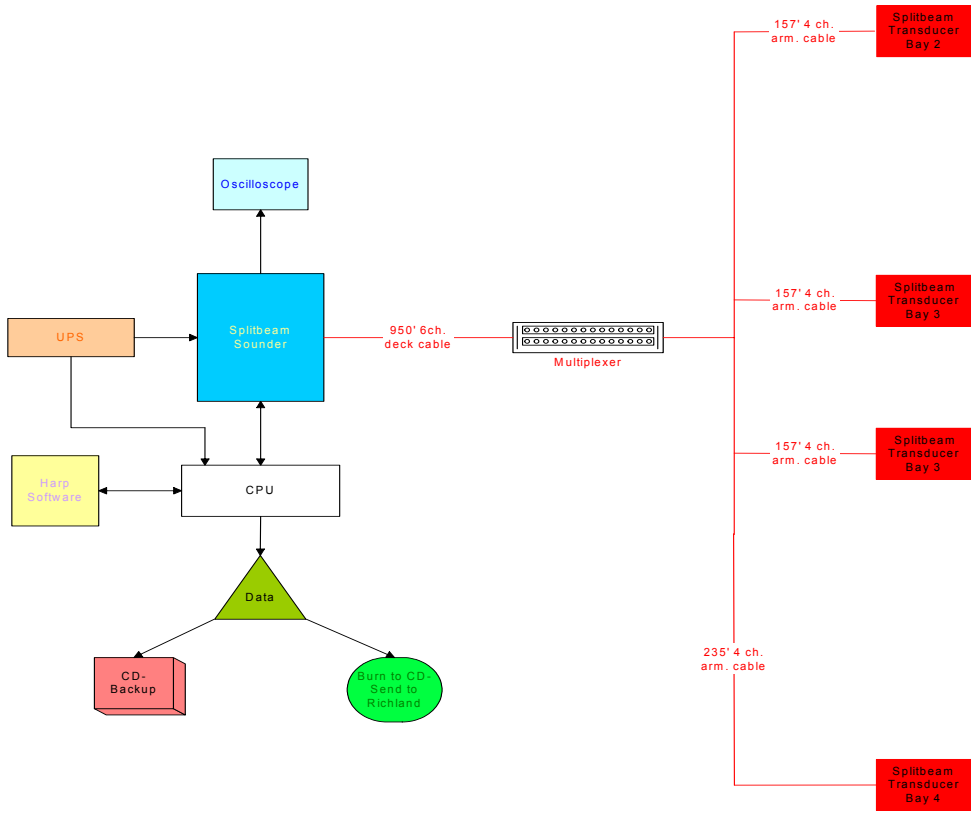
**The Dalles Dam Spillway
Singlebeam System "F" at Spillbay 1-8**



**The Dalles Dam Spillway
Singlebeam System "G" at Spillbay 9-14**



The Dalles Dam Spillway
Splitbeam System "Q" at Spillbays 2, 3, and 4



Appendix B

System Calibrations

2001 Deployment Location and Sampling Rates

Location Summary

System channel (on monitor)	Unit	Mounting	Treatment	Elevation	Aiming Angle	Xducer type	System	Mux channel	Ping Rate (pps)	Max. Range (m)	# of 1-min Samples Per Hr
1	FU02-1U	intake downlocker	Occluded	135	15° from plane of trashrack	single	C		15	24	10
2	FU01-2M	intake downlocker	Occluded	135	15° from plane of trashrack	single	C		15	24	10
3	MU02-1U	intake downlocker	Occluded	95	15° from plane of trashrack	single	C		15	24	10
4	MU01-2M	intake downlocker	Occluded	135	15° from plane of trashrack	single	C		15	19	10
5	MU05-3u	intake downlocker	Occluded	135	15° from plane of trashrack	single	C		15	24	10
6	MU04-2D	intake downlocker	Occluded	135	15° from plane of trashrack	single	C		15	24	10
1	FU01-2M	intake downlocker	Unoccluded	135	15° from plane of trashrack	single	C		15	24	10
2	FU02-1U	intake downlocker	Unoccluded	135	15° from plane of trashrack	single	C		15	24	10
3	MU05-3u	intake downlocker	Unoccluded	134	15° from plane of trashrack	single	C		15	24	10
4	MU04-2D	intake uplocker	Unoccluded	75	31° from plane of trashrack	single	C		15	19	10
5	MU02-1U	intake uplocker	Unoccluded	95	31° from plane of trashrack	single	C		15	19	10
6	MU01-2M	intake uplocker	Unoccluded	75	31° from plane of trashrack	single	C		15	24	10
1	MU13-1M	intake uplocker	NA	75	31° from plane of trashrack	single	D		15	19	20
2	MU11-3U	intake uplocker	NA	75	31° from plane of trashrack	single	D		15	19	20
3	MU14-2U	intake uplocker	NA	75	31° from plane of trashrack	single	D		15	19	20
4	MU10-3D	intake uplocker	NA	75	31° from plane of trashrack	single	D		15	19	20
5	MU06-1D	intake uplocker	NA	75	31° from plane of trashrack	single	D		15	19	20
6	MU07-2M	intake uplocker	NA	75	31° from plane of trashrack	single	D		15	19	20
1	MU17-1U	intake uplocker	NA	75	31° from plane of trashrack	single	E		15	19	15
2	MU18-2M	intake uplocker	NA	75	31° from plane of trashrack	single	E		15	19	15
3	MU19-3D	intake uplocker	NA	75	31° from plane of trashrack	single	E		15	19	15
4	MU20-1M	intake uplocker	NA	75	31° from plane of trashrack	single	E		15	19	15
5	MU21-2U	intake uplocker	NA	75	31° from plane of trashrack	single	E		15	19	15
6	MU22-1D	intake uplocker	NA	75	31° from plane of trashrack	single	E		15	19	15
7	MU15-1D	intake uplocker	NA	75	31° from plane of trashrack	single	E		15	19	15
8	MU16-3U	intake uplocker	NA	75	31° from plane of trashrack	single	E		15	19	15
1	SP-01n	polemount	NA	154	8° downstream of vertical	single	F		27		10
2	SP-03m	polemount	NA	154	8° downstream of vertical	single	F		27		10
3	SP-05n	polemount	NA	154	8° downstream of vertical	single	F		27		10
4	SP-06m	polemount	NA	154	8° downstream of vertical	single	F		27		10
5	SP-07s	polemount	NA	154	8° downstream of vertical	single	F		27		10
6	SP-08m	polemount	NA	154	8° downstream of vertical	single	F		27		10
1	SP-09s	polemount	NA	154	8° downstream of vertical	single	G		27		10
2	SP-10n	polemount	NA	154	8° downstream of vertical	single	G		27		10
3	SP-11n	polemount	NA	154	8° downstream of vertical	single	G		27		10
4	SP-12s	polemount	NA	154	8° downstream of vertical	single	G		27		10
5	SP-13m	polemount	NA	154	8° downstream of vertical	single	G		27		10
6	SP-14n	polemount	NA	154	8° downstream of vertical	single	G		27		10
1	MU12-2M	intake uplocker	NA	75	31° from plane of trashrack	split	V		15		15
10	MU03-3M	intake downlocker	Occluded	135	15° from plane of trashrack	split	W	10	15	19	15
11	MU01-3M	sluice uplocker on "J"	Occluded	110	5° from plane of trashrack	split	W	11	15	24	15
21	MU01-1M	sluice uplocker on "J"	Occluded	110	5° from plane of trashrack	split	W	12	15	24	15
31	MU01-2M	sluice uplocker on "J"	Occluded	110	5° from plane of trashrack	split	W	13	15	24	15
1	MU03-3M	intake uplocker	Unoccluded	75	31° from plane of trashrack	split	W	00	15	19	15
2	MU01-3M	sluice uplocker	Unoccluded	95	5° from plane of trashrack	split	W	01	15	19	15
3	MU01-2M	sluice uplocker	Unoccluded	95	5° from plane of trashrack	split	W	02	15	19	15
4	MU01-1M	sluice uplocker	Unoccluded	95	31° from plane of trashrack	split	W	03	15	19	15
1	SP-04s	polemount	NA	154	8° downstream of vertical	split	Y	0	20	11	15
2	SP-02m	polemount	NA	154	8° downstream of vertical	split	Y	1	20	11	15
3	SP-03south	horizontally opposed	NA	151.6	⊥ to flow & 20° down from horz	split	Y	2	20	11	15
4	SP-03north	horizontally opposed	NA	151.6	⊥ to flow & 20° down from horz	split	Y	3	20	11	15

2001 Receiver Calibrations

Calib System Letter	Location	Location	Installed System	Echo-sounder Number	Transducer Number and Phase (if split beams)	Calibrated Cable Length (ft)	Source Level (dB) - 6 dB Static Transmit	Maximum Output Voltage (dB)	40 logR Receiver Sensitivity (dB)	Target Strength of largest on-axis target of interest (db)	Calculated Receiver gain (dB)	Installed Cable Length (ft)	Difference in Cable Length Between Calibrated Cable and Installed Cable (ft)	Receiver Gain Adjusted for Difference in Cable Length (dB)	Source Level Adjusted for Difference in Cable Length (dB)	Receiver Sensitivity Adjusted for Difference in Cable Length (dB)	Target Strength On-axis Target (dB)
C	2-1U dn		C	31	82	650	215.29	90	-99.01	-36	9.72	650	0	9.72	215.29	-99.01	-56
C	FU-1-2U dn	FU-1-2U dn	C	31	84	650	215.99	90	-96.71	-36	6.72	626	24	6.57	216.11	-96.68	-56
C	FU-2-1U dn	FU-2-1U dn	C	31	85	650	215.82	90	-98.45	-36	8.63	652	-2	8.64	215.81	-98.45	-56
C	1-2M dn		C	31	86	650	216.07	90	-98.21	-36	8.14	626	24	7.99	216.19	-98.18	-56
D	5-3U down	5-3U down	C	30	80	900	214.06	90	-98.25	-36	10.19	647	253	8.57	215.35	-97.92	-56
D	4-2D down		C	30	81	900	213.97	90	-98.37	-36	10.40	650	250	8.80	215.25	-98.05	-56
D		4-2D up	C	30	72	900	214.64	90	-97.69	-36	9.05	650	250	7.45	215.92	-97.37	-56
D		2-1U up	C	30	78	650	215.39	90	-97.95	-36	8.56	650	0	8.56	215.39	-97.95	-56
D		1-2M up	C	30	79	650	215.50	90	-97.83	-36	8.33	650	0	8.33	215.50	-97.83	-56
C	13-1M		D	31	87	650	215.71	90	-98.35	-36	8.64	650	0	8.64	215.71	-98.35	-56
C	11-?		D	31	88	650	215.89	90	-98.43	-36	8.54	650	0	8.54	215.89	-98.43	-56
C	14-2U		D	31	89	650	215.81	90	-98.55	-36	8.74	650	0	8.74	215.81	-98.55	-56
D	10-3D		D	30	76	650	215.62	90	-97.71	-36	8.09	650	0	8.09	215.62	-97.71	-56
E	6-1D		D	5	70	750	213.37	90	-98.61	-36	11.24	1150	-400	13.80	211.33	-99.13	-56
E	7-2M		D	5	71	750	214.45	90	-97.39	-36	8.94	900	-150	9.90	213.69	-97.59	-56
D	9-2M		D	30	75	650	215.61	90	-97.97	-36	8.36	650	0	8.36	215.61	-97.97	-56
C	17-1U		E	31	93	900	214.70	70	-113.48	-36	4.78	650	250	2.55	215.66	-112.21	-56
E	18-2M		E	5	14	900	212.77	70	-114.35	-36	7.58	400	500	3.11	214.69	-111.80	-56
E	19-3D		E	5	15	650	214.48	70	-113.17	-36	4.69	650	0	4.69	214.48	-113.17	-56
E	20-1M		E	5	16	650	214.81	70	-112.83	-36	4.02	650	0	4.02	214.81	-112.83	-56
E	21-2U		E	5	30	650	214.76	70	-113.03	-36	4.27	650	0	4.27	214.76	-113.03	-56
E	22-1D		E	5	31	400	214.83	70	-111.69	-36	2.86	650	-250	5.09	213.87	-112.97	-56
E	Spare		E	5	32	650	214.57	70	-113.53	-36	4.96	650	0	4.96	214.57	-113.53	-56
C	15-1D		E	31	91	650	215.97	70	-113.12	-36	3.15	900	-250	5.39	215.01	-114.40	-56
C	16-3U		E	31	92	900	214.71	70	-113.52	-36	4.81	650	250	2.57	215.67	-112.25	-56
	Spill Bay 1		F	32	500	750	211.90	70	-108.13	-36	2.23	750	0	2.23	211.90	-108.13	-56
	3		F	32	501	500	211.08	70	-106.21	-36	1.13	500	0	1.13	211.08	-106.21	-56
	5		F	32	502	500	210.90	70	-106.29	-36	1.39	500	0	1.39	210.90	-106.29	-56
	6		F	32	503	500	210.39	70	-106.45	-36	2.06	500	0	2.06	210.39	-106.45	-56
	7		F	32	504	750	211.69	70	-108.55	-36	2.86	750	0	2.86	211.69	-108.55	-56
	8		F	32	505	750	212.21	70	-107.79	-36	1.58	750	0	1.58	212.21	-107.79	-56
	Spare		F	32	512	500	210.32	70	-106.57	-36	2.25	500	0	2.25	210.32	-106.57	-56
	Spare		F	32	513	750	212.03	70	-108.11	-36	2.08	750	0	2.08	212.03	-108.11	-56
	Spill Bay 9		G	33	506	750	211.61	70	-108.21	-36	2.60	750	0	2.60	211.61	-108.21	-56
	10		G	33	509	750	211.63	70	-107.91	-36	2.28	750	0	2.28	211.63	-107.91	-56
	11		G	33	516	500	210.98	70	-105.63	-36	0.65	500	0	0.65	210.98	-105.63	-56
	12		G	33	511	500	210.69	70	-105.79	-36	1.10	500	0	1.10	210.69	-105.79	-56
	13		G	33	514	500	210.47	70	-106.05	-36	1.58	500	0	1.58	210.47	-106.05	-56
	14		G	33	515	750	211.79	70	-107.79	-36	2.00	750	0	2.00	211.79	-107.79	-56
	Spare		G	33	516	500	210.98	70	-105.63	-36	0.65	500	0	0.65	210.98	-105.63	-56
	Opened		G	33	516	750	211.78	70	-107.63	-36	1.85	750	0	1.85	211.78	-107.63	-56
Occluded treatment - 10 rounds of 6 1-min samples at 15 pings / sec and 24 m max range																	
Unoccluded treatment - 10 rounds of 6 1-min samples at 15 pings / sec and 19 m max range																	
20 rounds of 3 pairs of transducers sampling at 15 pings / sec for 1 min per pair (19 m max range)																	
15 rounds of 4 pairs of transducers at 15 pings / sec for 1 min per pair (19 m max range)																	
10 rounds of 6 1-min samples at 27 pings per second																	
10 rounds of 6 1-min samples at 27 pings per second																	

		Remote Mux	Static Transmit Power	Echo-sounder Number	Transducer Number and Phase (if split beams)	Calibrated Cable Length (ft)	Source Level (dB)	Maximum Output Voltage (dB)	40 logR Receiver Sensitivity (dB)	Target Strength of largest on-axis target of interest (db)	Calculated Receiver gain (dB)	Installed Cable Length (ft)	Difference in Cable Length Between Calibrated Cable and Installed Cable (ft)	Receiver Gain Adjusted for Difference in Cable Length (dB)	Source Level Adjusted for Difference in Cable Length (dB)	Receiver Sensitivity Adjusted for Difference in Cable Length (dB)	
3-3M up	Local Mux	Port 0	RU-005 0	-5	23	405 (x)	940	214.03	80	-107.99	-36	9.96	940	0	9.96	214.03	-107.99
					23	405 (y)	940	213.99	80	-108.03	-36	10.04	940	0	10.04	213.99	-108.03
					23	405	940	214.01	80	-108.01	-36	10.00	940	0	10.00	214.01	-108.01
1-3M sluice		RU-005 1	-5	23	408 (x)	705	216.09	80	-108.13	-36	8.04	705	0	8.04	216.09	-108.13	
				23	408 (y)	705	216.10	80	-108.13	-36	8.03	705	0	8.03	216.10	-108.13	
				23	408	705	216.10	80	-108.13	-36	8.04	705	0	8.04	216.10	-108.13	
1-2M sluice		RU-005 2	-5	23	409 (x)	705	216.06	80	-108.33	-36	8.27	705	0	8.27	216.06	-108.33	
				23	409 (y)	705	216.09	80	-108.35	-36	8.26	705	0	8.26	216.09	-108.35	
				23	409	705	216.08	80	-108.34	-36	8.26	705	0	8.26	216.08	-108.34	
1-1M sluice		RU-006 3	-5	23	410 (x)	705	216.08	80	-108.37	-36	8.29	705	0	8.29	216.08	-108.37	
				23	410 (y)	705	216.08	80	-108.37	-36	8.29	705	0	8.29	216.08	-108.37	
				23	410	705	216.08	80	-108.37	-36	8.29	705	0	8.29	216.08	-108.37	
3-3M dn sluice	Port 1	RU-005 0	-5	23	407 (x)	940	213.95	80	-108.13	-36	10.18	940	0	10.18	213.95	-108.13	
				23	407 (y)	940	213.96	80	-108.15	-36	10.19	940	0	10.19	213.96	-108.15	
				23	407	940	213.96	80	-108.14	-36	10.19	940	0	10.19	213.96	-108.14	
1-3M J sluice		RU-006 1	-5	23	411 (x)	705	215.99	80	-108.59	-36	8.60	705	0	8.60	215.99	-108.59	
				23	411 (y)	705	215.97	80	-108.59	-36	8.62	705	0	8.62	215.97	-108.59	
				23	411	705	215.98	80	-108.59	-36	8.61	705	0	8.61	215.98	-108.59	
1-1M J sluice		RU-006 2	-5	23	423 (x)	705	215.84	80	-108.57	-36	8.73	705	0	8.73	215.84	-108.57	
				23	423 (y)	705	215.83	80	-108.57	-36	8.74	705	0	8.74	215.83	-108.57	
				23	423	705	215.84	80	-108.57	-36	8.73	705	0	8.73	215.84	-108.57	
1-2M J sluice		RU-006 3	-5	23	424 (x)	705	215.90	80	-108.57	-36	8.67	705	0	8.67	215.90	-108.57	
				23	424 (y)	705	215.87	80	-108.59	-36	8.72	705	0	8.72	215.87	-108.59	
				23	424	705	215.89	80	-108.58	-36	8.69	705	0	8.69	215.89	-108.58	
MU 12	None	None	-5	22	404 (x)	470	216.06	80	-105.29	-36	5.23	470	0	5.23	216.06	-105.29	
				22	404 (y)	470	216.06	80	-105.35	-36	5.29	470	0	5.29	216.06	-105.35	
				22	404	470	216.06	80	-105.32	-36	5.26	470	0	5.26	216.06	-105.32	
SB-4		RU-009 0		25	128 (x)	1185	210.96	80	-106.92	-36	11.96	1185	0	11.96	210.96	-106.92	
				25	128 (y)	1185	210.86	80	-107.04	-36	12.18	1185	0	12.18	210.86	-107.04	
				25	128	1185	210.91	80	-106.98	-36	12.07	1185	0	12.07	210.91	-106.98	
SB-2		RU-009 1	-3	25	125 (x)	1185	211.53	80	-106.08	-36	10.55	1185	0	10.55	211.53	-106.08	
				25	125 (y)	1185	211.53	80	-106.04	-36	10.51	1185	0	10.51	211.53	-106.04	
				25	125	1185	211.53	80	-106.06	-36	10.53	1185	0	10.53	211.53	-106.06	
SB 3 S.		RU-009 2	-3	25	127 (x)	1185	210.94	80	-106.54	-36	11.60	1185	0	11.60	210.94	-106.54	
				25	127 (y)	1185	210.91	80	-106.58	-36	11.67	1185	0	11.67	210.91	-106.58	
				25	127	1185	210.93	80	-106.56	-36	11.64	1185	0	11.64	210.93	-106.56	
SB 3 N.		RU-009 3	-3	25	129 (x)	1185	211.36	80	-106.42	-36	11.06	1185	0	11.06	211.36	-106.42	
				25	129 (y)	1185	211.21	80	-106.42	-36	11.21	1185	0	11.21	211.21	-106.42	
				25	129	1185	211.29	80	-106.42	-36	11.14	1185	0	11.14	211.29	-106.42	

Unoccluded sluice and 1 intake - slow mux 15 rounds of 4 1min samples; max range = 19 m

Occluded sluice - 15 rounds of 4 1-min samples; max range = 24 m (Ping rate=10 / sec on sluice and 15 / sec on MU3

MU 12 20 1-min samples per hour (every third min) at 15 pings / sec

Slow mux at 30 pings per second 15 rounds of 4 1-min samples with 11 m max range

2001 Hydroacoustic System Map for Powerhouse and Spillway, The Dalles Dam 2001

Powerhouse														
Unit	Mounting	system	xducer sn	Armored cable sn	Armored cable lengths	Mux	At Armored Deck cable sn/Length	Middle Deck cable sn/Length	At Sounder Deck cable sn/Length	Jumper cable sn	Sounder sn	Sounder Port Number		
1	MU2-1U	intake downlooker	C	single	82	43	150'	n/a	449/500		525	31	1	
2	FU1-2M	intake downlooker	C	single	84	6	126'	n/a	430/500		523	31	2	
3	FU2-1U	intake downlooker	C	single	85	22	152'	n/a	436/500		520	31	3	
4	MU1-2M	intake downlooker	C	single	86	58	126'	n/a	427/500		533	31	4	
5	MU5-3u	intake downlooker	C	single	80	47	147'	n/a	452/500		521	31	5	
6	MU4-2D	intake downlooker	C	single	81	191	150'	n/a	440/500		522	31	6	
2	FU1-2M	intake downlooker	C	single	84	6	126'	n/a	430/500		523	31	2	
3	FU2-1U	intake downlooker	C	single	85	22	152'	n/a	436/500		520	31	3	
5	MU5-3u	intake downlooker	C	single	80	47	147'	n/a	452/500		521	31	5	
7	MU4-2D	intake uplooker	C	single	72	202	150'	n/a	418/500		534	31	7	
8	MU2-1U	intake uplooker	C	single	78	206	150'	n/a	458/500		526	31	8	
9	MU1-2M	intake uplooker	C	single	79	201	150'	n/a	404/500		524	31	9	
1	MU3-3M	intake uplooker	W	split	405	81	470'	RU-005		59/470'		23	1/0	
2	MU1-3M	sluice uplooker	W	split	408	73	235'	RU-005		59/470'		23	1/1	
3	MU1-2M	sluice uplooker	W	split	409	74	235'	RU-005		59/470'		23	1/2	
4	MU1-1M	sluice uplooker	W	split	410	75	235'	RU-005		59/470'		23	1/3	
1	MU3-3M	intake downlooker	W	split	407	82	470'	RU-006		72/470'		23	0/0	
11	MU1-3M	sluice uplooker on "J"	W	split	411	76	235'	RU-006		72/470'		23	0/1	
21	MU1-1M	sluice uplooker on "J"	W	split	423	77	235'	RU-006		72/470'		23	0/2	
31	MU1-2M	sluice uplooker on "J"	W	split	424	78	235'	RU-006		72/470'		23	0/3	
18	MU12-2M	intake uplooker	V	split	404	71	470'	Breakout box		71/470'		22		
1	MU13-1M	intake uplooker	D	single	87	210	150'	n/a	415/500	-	535	30	1	
2	MU11-3U	intake uplooker	D	single	88	200	150'	n/a	437/500	-	537	30	2	
3	MU10-3D	intake uplooker	D	single	76	204	150'	n/a	450/500	-	536	30	3	
4	MU14-2U	intake uplooker	D	single	89	214	150'	n/a	461/500	-	532	30	4	
5	MU6-1D	intake uplooker	D	single	70	203	150'	n/a	483/250	468/250	434/500	531	30	5
6	MU7-2M	intake uplooker	D	single	71	207	150'	n/a	472/250	-	424/500	539	30	6
26	MU15-1D	intake uplooker	E	single	91	217	150'	n/a	474/250	476/250	475/250	507	5	7
27	MU16-3U	intake uplooker	E	single	92	215	150'	n/a	469/250	-	490/250	506	5	8
28	MU17-1U	intake uplooker	E	single	93	211	150'	n/a	431/500	-	-	505	5	1
29	MU18-2M	intake uplooker	E	single	14	218	150'	n/a	486/250	-	-	509	5	2
30	MU19-3D	intake uplooker	E	single	15	208	150'	n/a	438/500	-	-	530	5	3
31	MU20-1M	intake uplooker	E	single	16	212	150'	n/a	460/500	-	-	503	5	4
32	MU21-2U	intake uplooker	E	single	30	216	150'	n/a	480/250	-	471/250	504	5	5
33	MU22-1D	intake uplooker	E	single	31	213	150'	n/a	489/250	-	477/250	508	5	6

Spillway														
Unit	Mounting	system	xducer sn	Armored cable sn	Armored cable lengths	Mux	At Armored Deck cable sn/Length	Middle Deck cable sn/Length	At Sounder Deck cable sn/Length	Jumper cable sn	Sounder sn	Sounder Port Number		
Spillway														
1	SP-1N	Downlooker	F	single	500	N/A	N/A	n/a	459/500		478/250	544	32	1
2	SP-3M	Downlooker	F	single	501	N/A	N/A	n/a	406/500			542	32	2
3	SP-5N	Downlooker	F	single	502	N/A	N/A	n/a	414/500			543	32	3
4	SP-6M	Downlooker	F	single	503	N/A	N/A	n/a	421/500			545	32	4
5	SP-7S	Downlooker	F	single	504	N/A	N/A	n/a	446/500		842/250	546	32	5
6	SP-8M	Downlooker	F	single	505	N/A	N/A	n/a	419/500		491/250	547	32	6
7	SP-9S	Downlooker	G	single	506	N/A	N/A	n/a	462/500		487/250	513	33	1
8	SP-10N	Downlooker	G	single	509	N/A	N/A	n/a	410/500		484/250	515	33	2
9	SP-11N	Downlooker	G	single	516	N/A	N/A	n/a	433/500			510	33	3
10	SP-12S	Downlooker	G	single	511	N/A	N/A	n/a	457/500			518	33	4
11	SP-13M	Downlooker	G	single	514	N/A	N/A	n/a	453/500			511	33	5
12	SP-14N	Downlooker	G	single	515	N/A	N/A	n/a	425/500		485/250	512	33	6
13	SP-4s	Downlooker	Q	split	128	48	235'	RU-009		6D-950-44/950'	n/a	25	1	
14	SP-2m	Downlooker	Q	split	125	46	157'	RU-009		6D-950-44/950'	n/a	25	2	
15	SP-3m	Horizontal opposing	Q	split	127	47	157'	RU-009		6D-950-44/950'	n/a	25	3	
16	SP-3m	Horizontal opposing	Q	split	129	45	157'	RU-009		6D-950-44/950'	n/a	25	4	

Stratified Random Treatment Schedule

Spring Date	Julian Day	Day of Week	Treatment	Study Day	Summer Date	Julian Day	Day of the Week	Treatment	Study Day
20-Apr	110	Fri	Transition	1	1-Jun	152	Fri	Transition	43
21-Apr	111	Sat	Transition	2	2-Jun	153	Sat	Unoccluded	44
22-Apr	112	Sun	Transition	3	3-Jun	154	Sun	Unoccluded	45
23-Apr	113	Mon	Transition	4	4-Jun	155	Mon	Transition	46
24-Apr	114	Tue	Transition	5	5-Jun	156	Tue	Occluded	47
25-Apr	115	Wed	Occluded	6	6-Jun	157	Wed	Occluded	48
26-Apr	116	Thu	Occluded	7	7-Jun	158	Thu	Occluded	49
27-Apr	117	Fri	Occluded	8	8-Jun	159	Fri	Occluded	50
28-Apr	118	Sat	Occluded	9	9-Jun	160	Sat	Occluded	51
29-Apr	119	Sun	Unoccluded	10	10-Jun	161	Sun	Transition	52
30-Apr	120	Mon	Transition	11	11-Jun	162	Mon	Transition	53
1-May	121	Tue	Unoccluded	12	12-Jun	163	Tue	Transition	54
2-May	122	Wed	Unoccluded	13	13-Jun	164	Wed	Transition	55
3-May	123	Thu	Unoccluded	14	14-Jun	165	Thu	Transition	56
4-May	124	Fri	Unoccluded	15	15-Jun	166	Fri	Occluded	57
5-May	125	Sat	Transition	16	16-Jun	167	Sat	Occluded	58
6-May	126	Sun	Occluded	17	17-Jun	168	Sun	Occluded	59
7-May	127	Mon	Occluded	18	18-Jun	169	Mon	Occluded	60
8-May	128	Tue	Occluded	19	19-Jun	170	Tue	Occluded	61
9-May	129	Wed	Occluded	20	20-Jun	171	Wed	Occluded	62
10-May	130	Thu	Occluded	21	21-Jun	172	Thu	Occluded	63
11-May	131	Fri	Transition	22	22-Jun	173	Fri	Occluded	64
12-May	132	Sat	Unoccluded	23	23-Jun	174	Sat	Occluded	65
13-May	133	Sun	Unoccluded	24	24-Jun	175	Sun	Occluded	66
14-May	134	Mon	Transition	25	25-Jun	176	Mon	Occluded	67
15-May	135	Tue	Occluded	26	26-Jun	177	Tue	Occluded	68
16-May	136	Wed	Occluded	27	27-Jun	178	Wed	Occluded	69
17-May	137	Thu	Transition	28	28-Jun	179	Thu	Occluded	70
18-May	138	Fri	Unoccluded	29	29-Jun	180	Fri	Occluded	71
19-May	139	Sat	Unoccluded	30	30-Jun	181	Sat	Occluded	72
20-May	140	Sun	Unoccluded	31	1-Jul	182	Sun	Occluded	73
21-May	141	Mon	Unoccluded	32	2-Jul	183	Mon	Occluded	74
22-May	142	Tue	Unoccluded	33	3-Jul	184	Tue	Occluded	75
23-May	143	Wed	Transition	34	4-Jul	185	Wed	Occluded	76
24-May	144	Thu	Occluded	35	5-Jul	186	Thu	Occluded	77
25-May	145	Fri	Occluded	36	6-Jul	187	Fri	Occluded	78
26-May	146	Sat	Transition	37	7-Jul	188	Sat	Occluded	79
27-May	147	Sun	Unoccluded	38	8-Jul	189	Sun	Occluded	80
28-May	148	Mon	Unoccluded	39	9-Jul	190	Mon	Occluded	81
29-May	149	Tue	Transition	40	10-Jul	191	Tue	Occluded	82
30-May	150	Wed	Occluded	41	11-Jul	192	Wed	Occluded	83
31-May	151	Thu	Occluded	42	12-Jul	193	Thu	Occluded	84

Appendix C

Appendix C: Autotracker Parameters

By Kenneth D. Ham

Setup information is needed to process raw sonar data files into appropriate samples. The parameter file contains information about the setup of the sounder and the sampling scheme. These parameters allow the raw files to be processed into a usable echogram. The parameters of Blocksize, MaxRange, MinRange, MaxEchoStrength and MinEchoStrength are parameters that allow the raw files to be translated into blocks of echos that represent a sample period (Table 1).

The parameter Structurethreshold, BottomStartRange, BottomCtThold, BottomAmplThold, and Noise are used to identify structure, the bottom (or surface), and noisy areas of the echogram before identifying traces.

The autotracker can identify traces in the echogram files. It must be calibrated for each deployment type to effectively identify traces whose characteristics are a function of the fish, the flow environment, and angle of view. RangeNoise, Gatesize, DKMax, and Alpha control how trace segments are constructed. LinkGate and LinkDKMax determine which segments will be connected into a single trace.

The location indicates the general sampling location, such as a dam or river mile. It does not affect the operation of the autotracker, but is useful for differentiating among data sets.

Table 1. Processing parameters and definitions

Parameter	Definition
Name	The channel Name. 1st character is the system letter. The 2nd and 3rd characters are the Mux_Channel
BlockSize	The max number of pings processed for a channel within 1 sample. Generally greater than or equal to the ping rate/ second * 60 seconds.
MaxRange:	The maximum range (in meters) for echo processing.
MinRange	The minimum range (in meters) for echo processing.
StructureThreshold	The proportion of a range that must be occupied by echoes to be marked as structure. (0 –1)
RangeNoise	The amount of fuzziness used in assigning echoes to range bins to find linear features in decimeters.
GateSize	The maximum range difference the autotracker will check to find the next ping in a track segment
DKMax	The max ping difference the autotracker will check to find the next ping in a track segment
Alpha	The alpha value for the alpha- beta tracking algorithm, beta is computed
LinkGate	The max range difference the autotracker will check to link segments into a track
LinkDKMax	The maximum ping difference the autotracker will span to link segments into a track
MaxEchoStrength	The maximum echo strength (in decibels) that will be processed.
MinEchoStrength	The minimum echo strength (in decibels) that will be processed.
NOISE	The number of dilates and erodes used to identify noise regions (greater than 0)(-1 means do not do noise for a channel)
BottomStartRange	The range (in centimeters) to begin the routine to identify the surface or bottom range (should be between min and max range) (if bottom identification is not needed, set value greater than max range)
BottomCtThold	The proportion of a range that must be occupied by echoes > than the bottom amplitude threshold to be marked as bottom. (0 – 1)
BottomAmplThold	The minimum echo strength (in decibels) above which echoes will be tallied as bottom or surface echoes
Location	Text describing the general sampling area

Table 2 reports the values of parameters that were constant across all deployments. Table 3 reports the values that varied by deployment type. Table 4 reports the values of parameters that varied among individual transducers.

Table 2. Parameter values held constant across all deployments

Parameter	Value
RangeNoise	0.1
Noise	5
LinkGate	0.2
BottomAmplThold	-30
MinRange	1
StructureThreshold	0.075
Location	The Dalles

Table 3. Parameter values held constant within each deployment type.

Deployment Type	Gate Open	Block Size	Gate Size	DKMax	Alpha	Max Echo Strength	Min Echo Strength	Bottom Start Range	Bottom Ct Thold	Link DKMax
Fish Unit	n/a	901	0.15	3	0.32	-30	-56	36	0.3	12
Intake Downlooker	n/a	901	0.15	3	0.32	-30	-56	36	0.3	12
Intake Uplooker	n/a	901	0.15	3	0.32	-30	-56	36	0.3	13
Sluice Occluded	n/a	901	0.15	3	0.32	-20	-56	13	0.1	20
Sluice Unoccluded	n/a	901	0.15	3	0.32	-20	-56	17.5	0.2	20
Spill (single beam)	1 & 2 ft	1637	0.11	3	0.32	-30	-56	36	0.3	12
Spill (split beam)	1 ft	1201	0.11	3	0.60	-30	-56	36	0.3	12
Spill (split beam)	2 ft	1201	0.11	3	0.32	-30	-56	36	0.3	12
Spill	3,4,5 ft	1637	0.11	2	0.60	-30	-56	36	0.3	12

Table 4. Parameter values specific to individual transducers

Unit	Deployment Type	Name	BlockSize	MaxRange	MinRange
FU01	Fish Unit	C02	901	24.56	1
FU02	Fish Unit	C03	901	24.72	1
MU01	Intake Downlooker	C04	901	23.39	1
MU01	Intake Uplooker	C09	901	14.93	1
MU02	Intake Downlooker	C01	901	24.26	1
MU02	Intake Uplooker	C08	901	15.76	1
MU03	Intake Downlooker	W10	901	19.42	1
MU03	Intake Uplooker	W00	901	16.01	1
MU04	Intake Downlooker	C06	901	24.25	1
MU04	Intake Uplooker	C07	901	15.4	1
MU05	Intake Downlooker	C05	901	24.35	1
MU06	Intake Uplooker	D05	901	15.21	1
MU07	Intake Uplooker	D06	901	14.93	1
MU10	Intake Uplooker	D04	901	15.54	1
MU11	Intake Uplooker	D02	901	16.9	1
MU12	Intake Uplooker	V00	901	15.21	1
MU13	Intake Uplooker	D01	901	16.04	1
MU14	Intake Uplooker	D03	901	15.34	1
MU15	Intake Uplooker	E07	901	15.5	1
MU16	Intake Uplooker	E08	901	15.35	1
MU17	Intake Uplooker	E01	901	15.38	1
MU18	Intake Uplooker	E02	901	15.54	1
MU19	Intake Uplooker	E03	901	15.51	1
MU20	Intake Uplooker	E04	901	15.57	1
MU21	Intake Uplooker	E05	901	15.51	1
MU22	Intake Uplooker	E06	901	15.51	1
SLUICE1	Sluice Occluded	W12	901	18.00	1
SLUICE1	Sluice Unoccluded	W03	901	25.00	1
SLUICE2	Sluice Occluded	W13	901	18.00	1
SLUICE2	Sluice Unoccluded	W02	901	25.00	1
SLUICE3	Sluice Occluded	W11	901	18.00	1
SLUICE3	Sluice Unoccluded	W01	901	25.00	1
SP01	Spill	F01	1637	9.55	1
SP02	Spill	Q01	1201	9.56	1
SP03	Spill	F02	1637	9.47	1
SP04	Spill	Q00	1201	9.66	1
SP05	Spill	F03	1637	9.52	1
SP06	Spill	F04	1637	9.55	1
SP07	Spill	F05	1637	9.43	1
SP08	Spill	F06	1637	9.43	1
SP09	Spill	G01	1637	9.47	1
SP10	Spill	G02	1637	9.58	1
SP11	Spill	G03	1637	9.56	1
SP12	Spill	G04	1637	9.39	1
SP13	Spill	G05	1637	9.44	1
SP14	Spill	G06	1637	9.49	1

Appendix D

Hydraulic Environment

The powerhouse data is based on a static computational fluid dynamics model (StarCD™). The model runs were completed by PNNL, the original geometry was supplied by the CENWP.

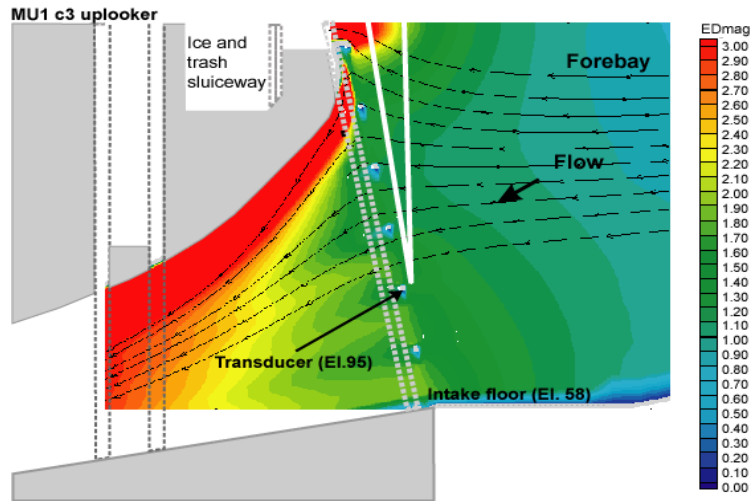


Figure 1. Unoccluded sluice passage transducer deployment and flow through the sample volume.

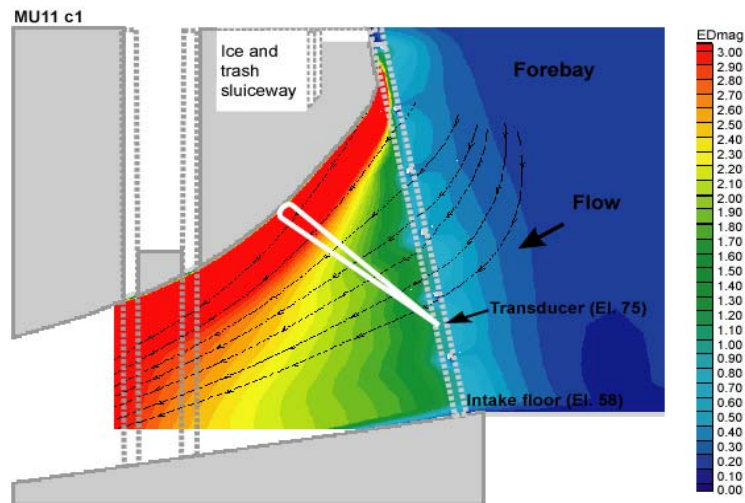


Figure 2. Unoccluded intake passage transducer deployment and flow through the sample volume.

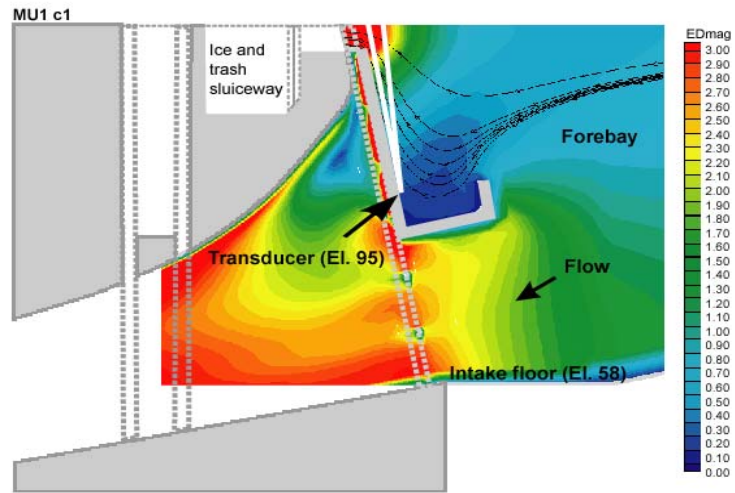


Figure 3. Occluded sluice passage transducer deployment and flow through the sample volume.

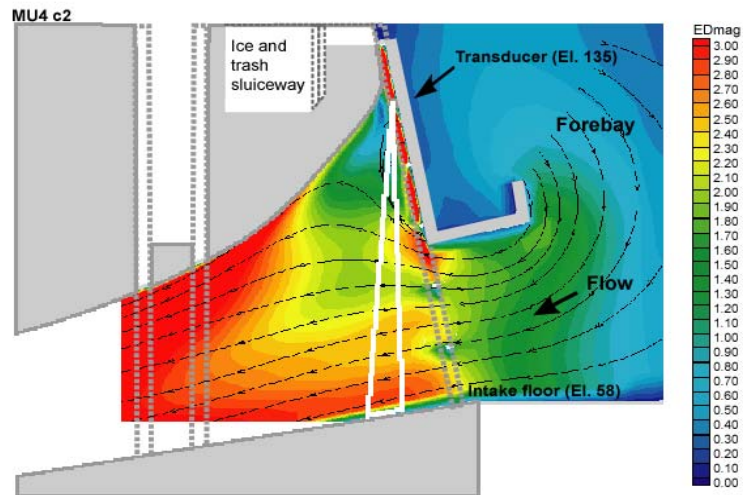


Figure 4. Occluded turbine intake passage transducer and flow through the sample volume.

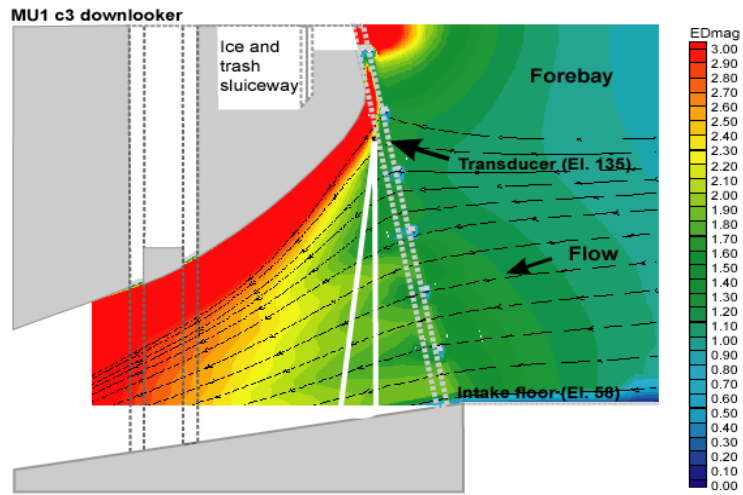


Figure 5. Unoccluded downlooker and flow through the sample volume.

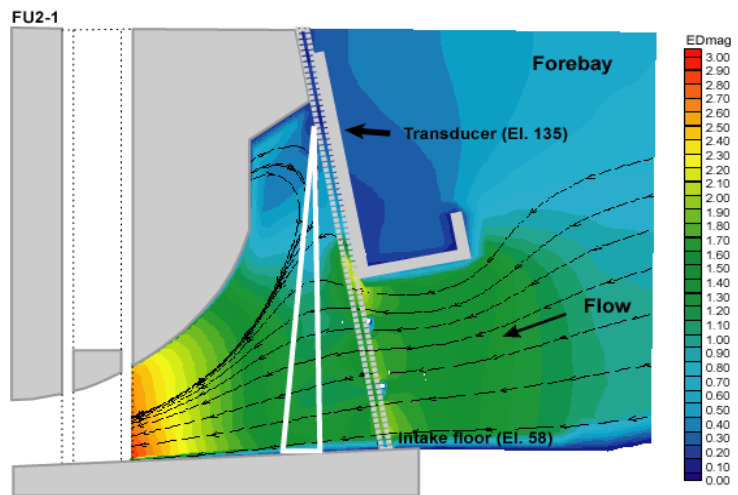


Figure 6. Fish Unit passage transducer deployment and flow through the sample volume.

The spillway data is based on models developed at PNNL for CENWP. (Flow3D™). The gate opening measurement is based on the vertical distance between the spillway crest and the tip of the gate. This comports with methods used by The Dalles/John Day/Willow Creek project.

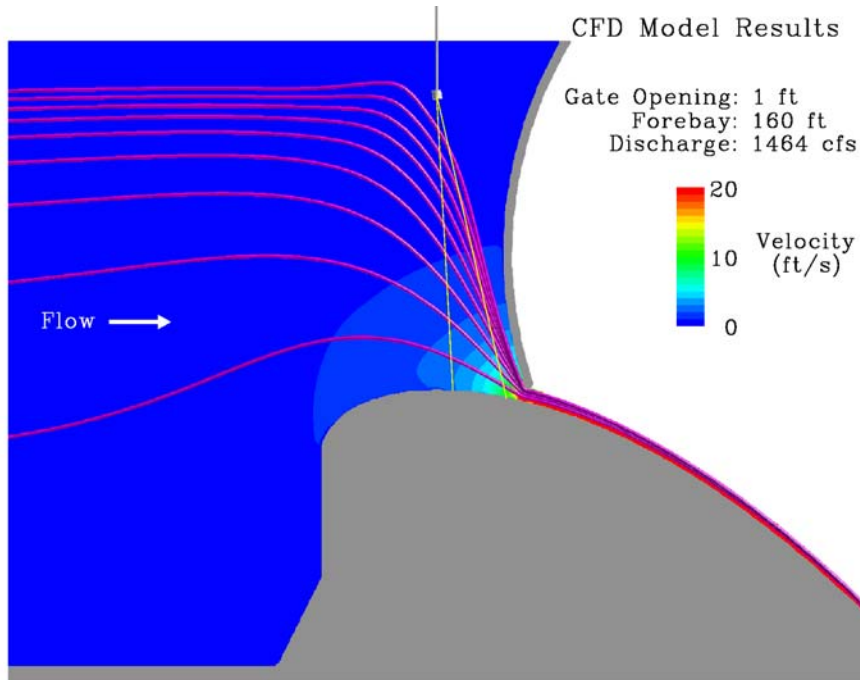


Figure 7. Flows at a 1 ft spill gate opening.

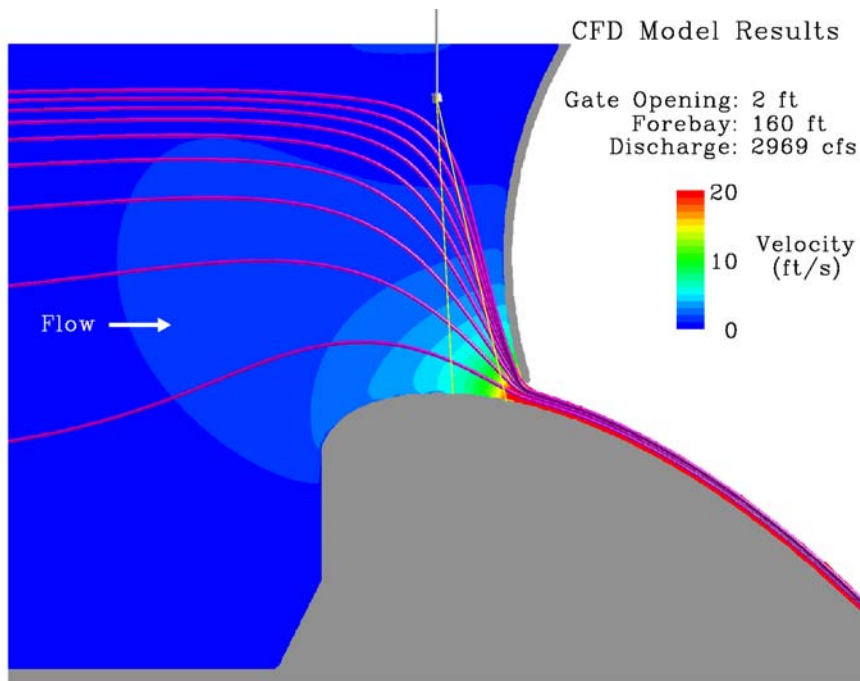


Figure 8. Flows at a 2 ft gate opening.

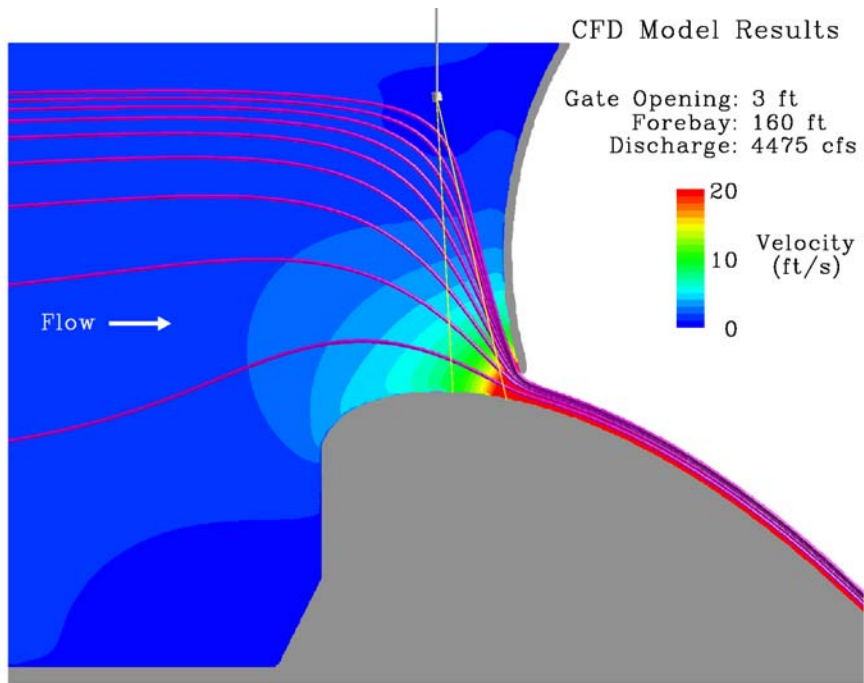


Figure 9. Flows at a 3 ft gate opening.

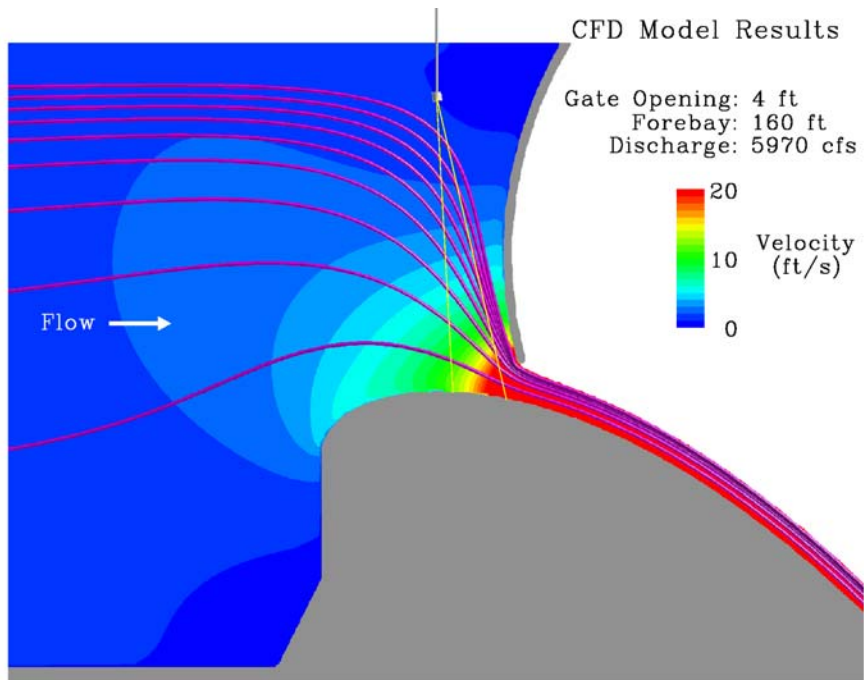


Figure 10. Flows at a 4 ft gate opening.

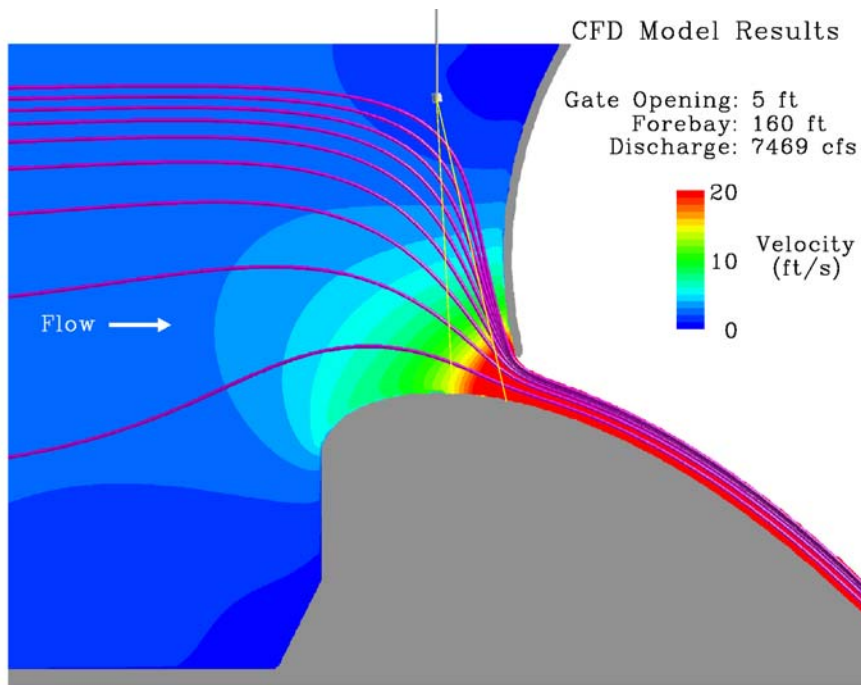


Figure 11. Flows at a 5 ft gate opening.

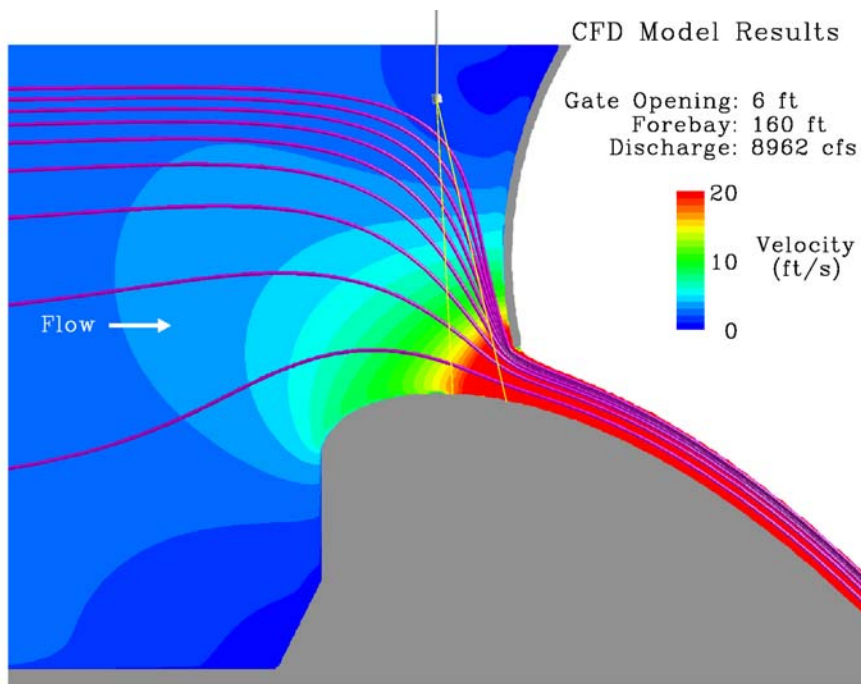
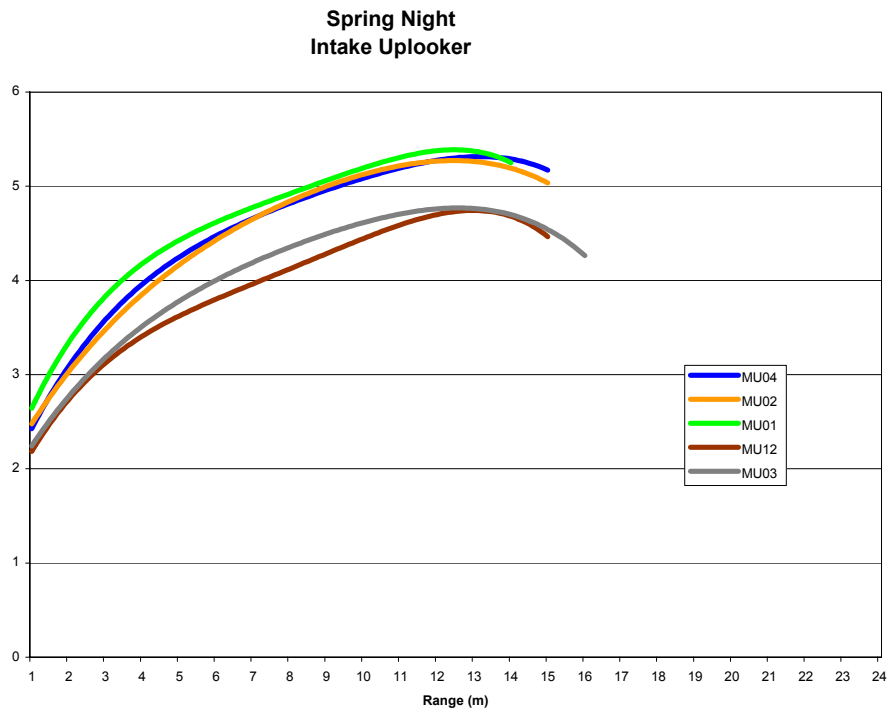
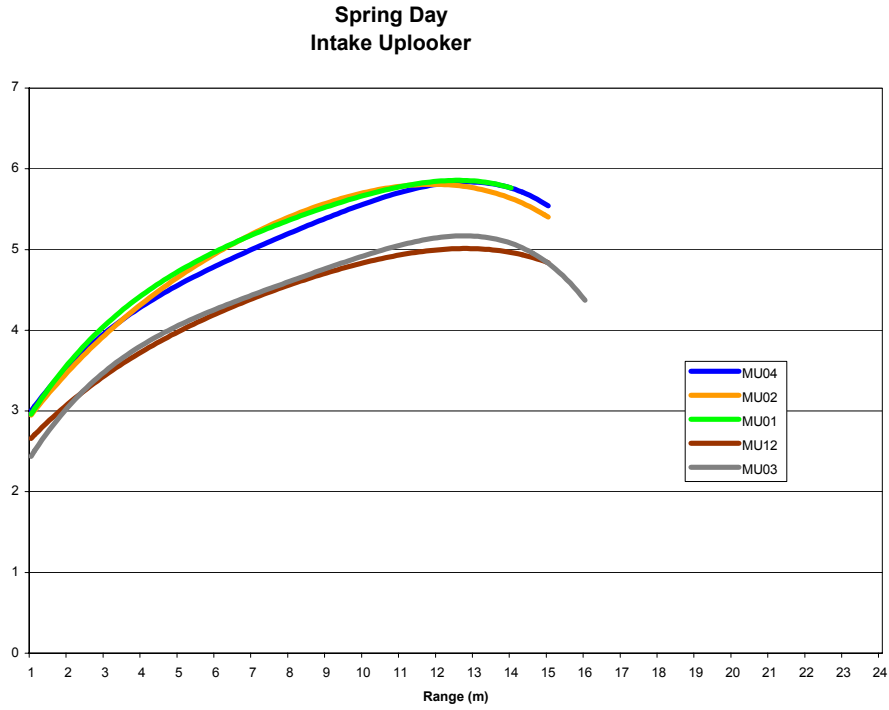


Figure 12. Flows at a 6 ft gate opening.

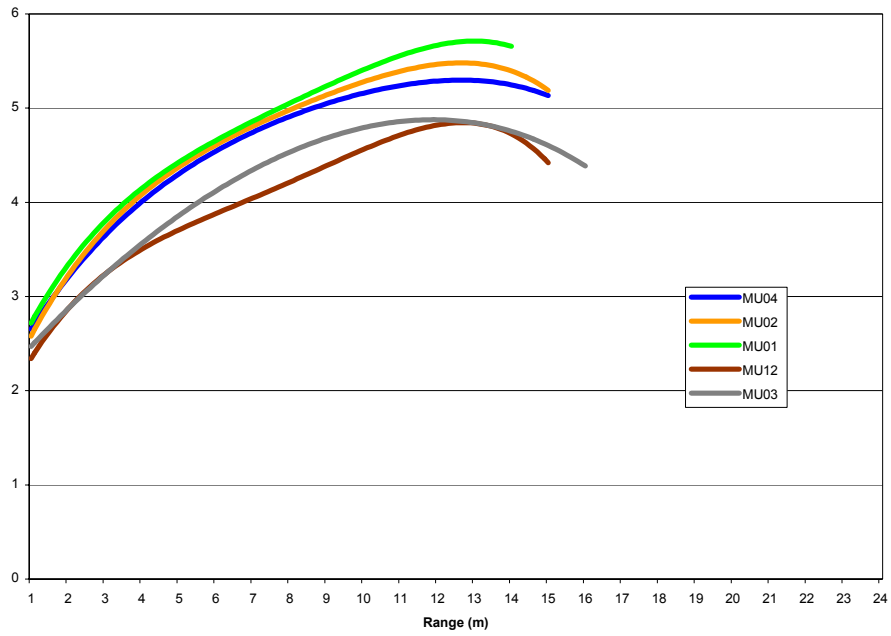
Appendix E

Effective Beam Widths

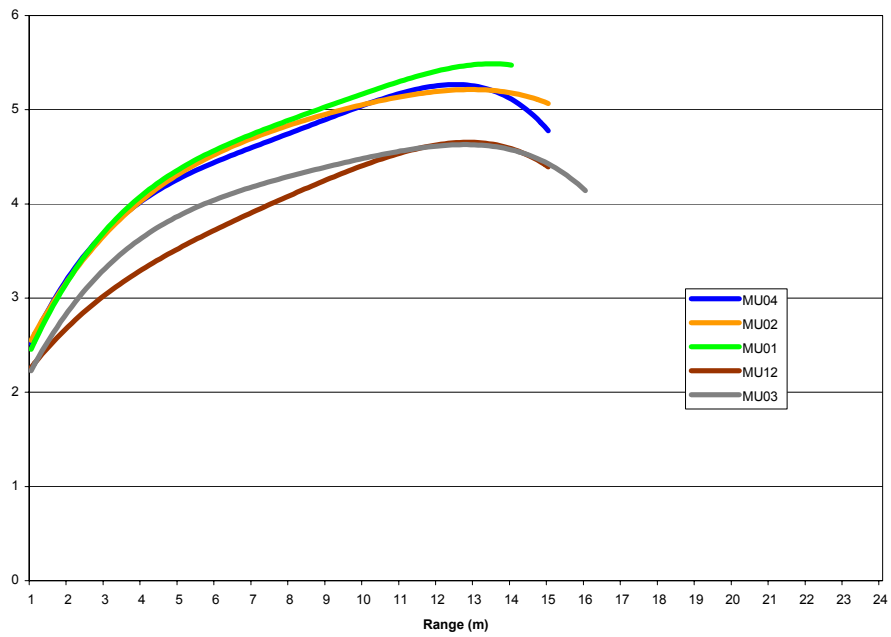
Note: the y-axis on the following graphs is the effective beam width in degrees.



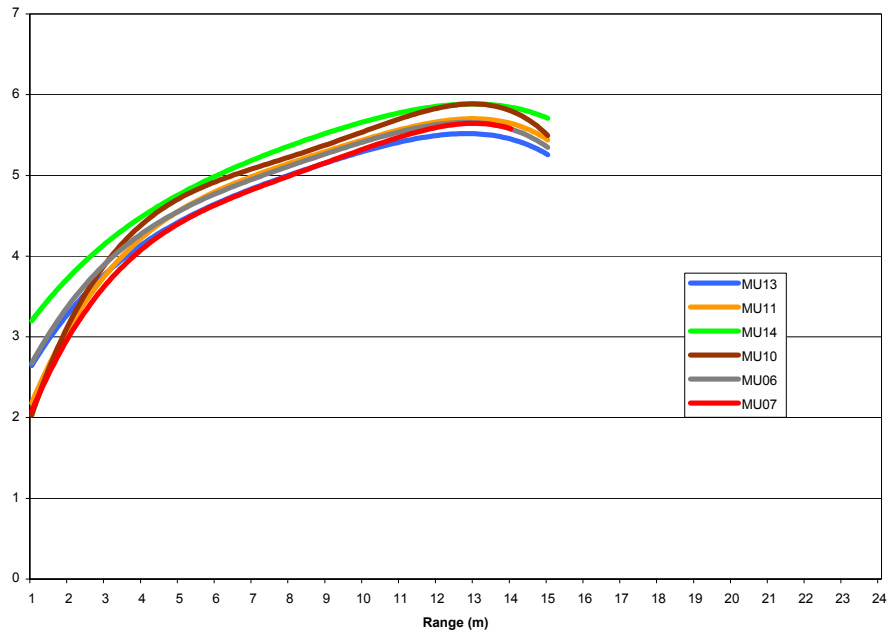
Summer Day Intake Uplooker



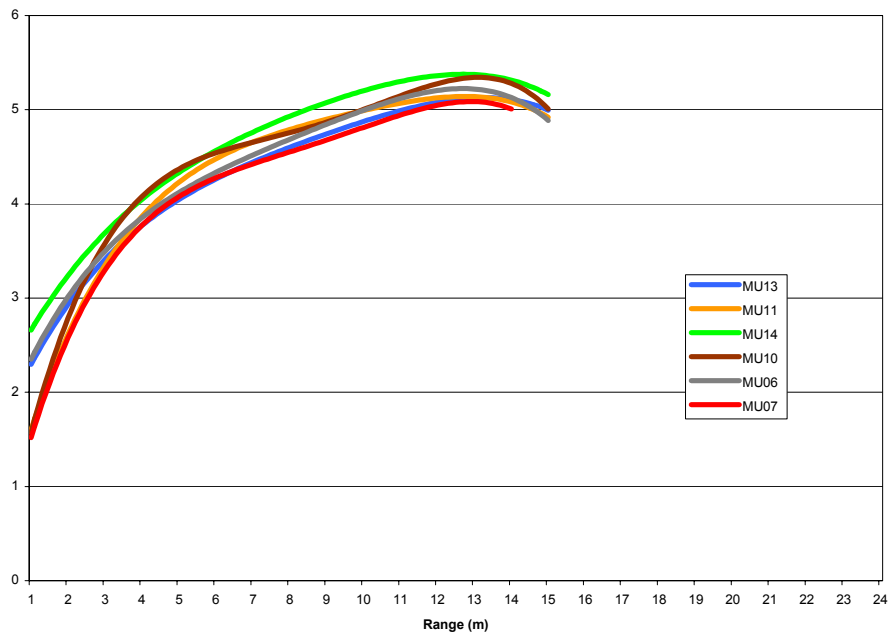
Summer Night Intake Uplooker



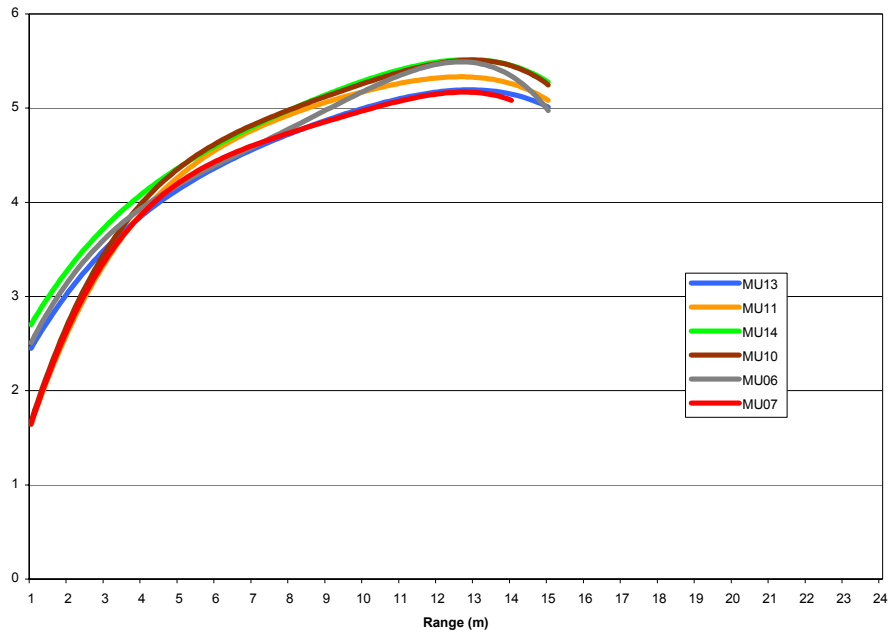
Spring Day Intake Uplooker



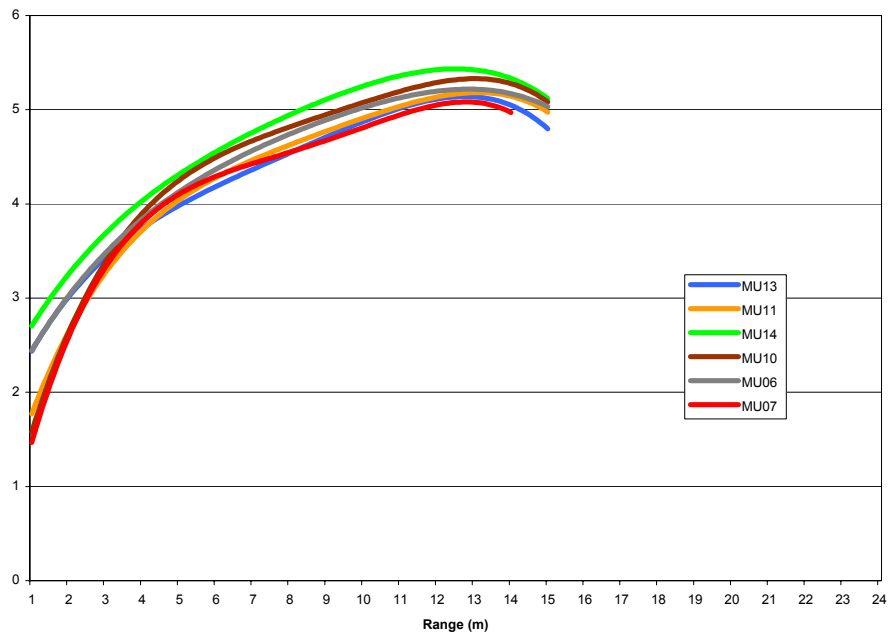
Spring Night Intake Uplooker



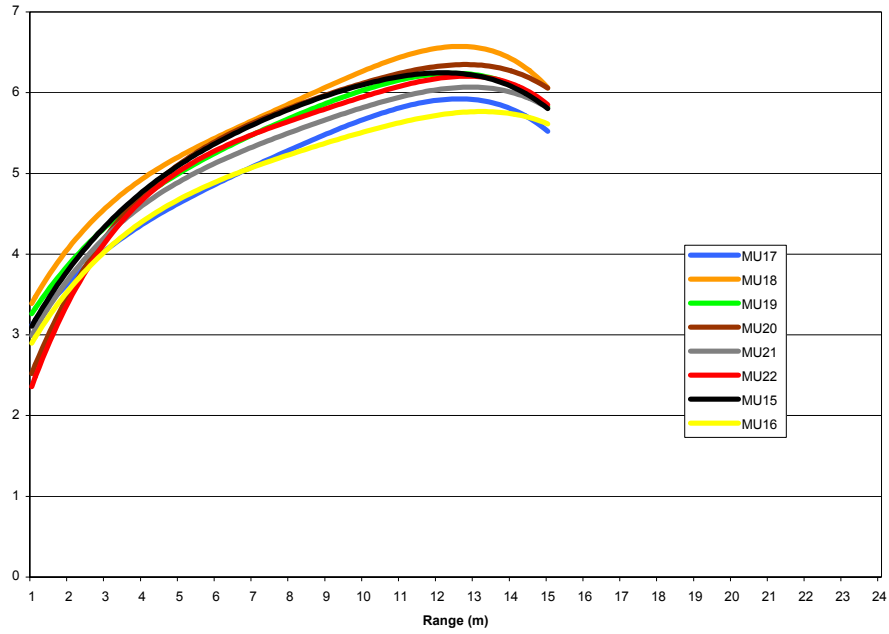
Summer Day Intake Uplooker



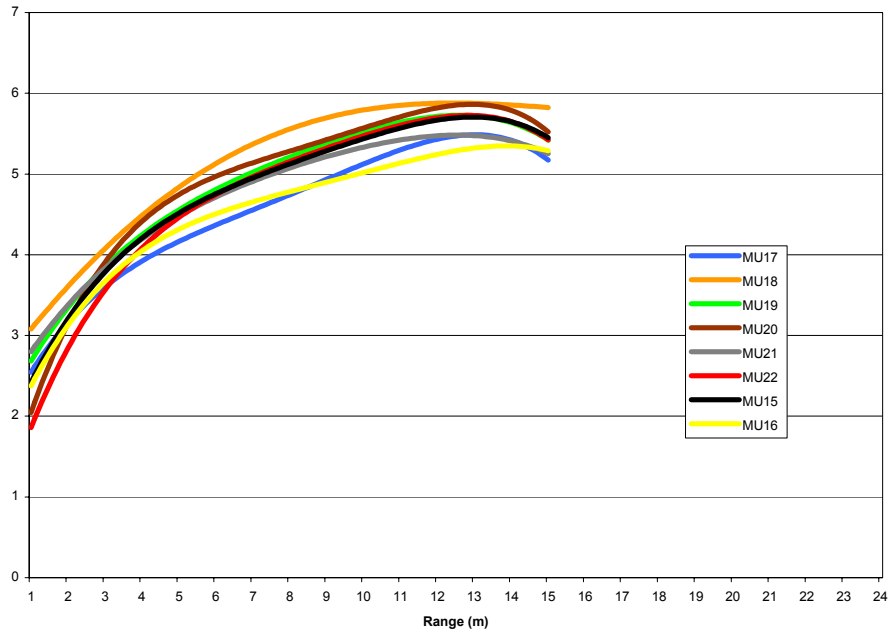
Summer Night Intake Uplooker



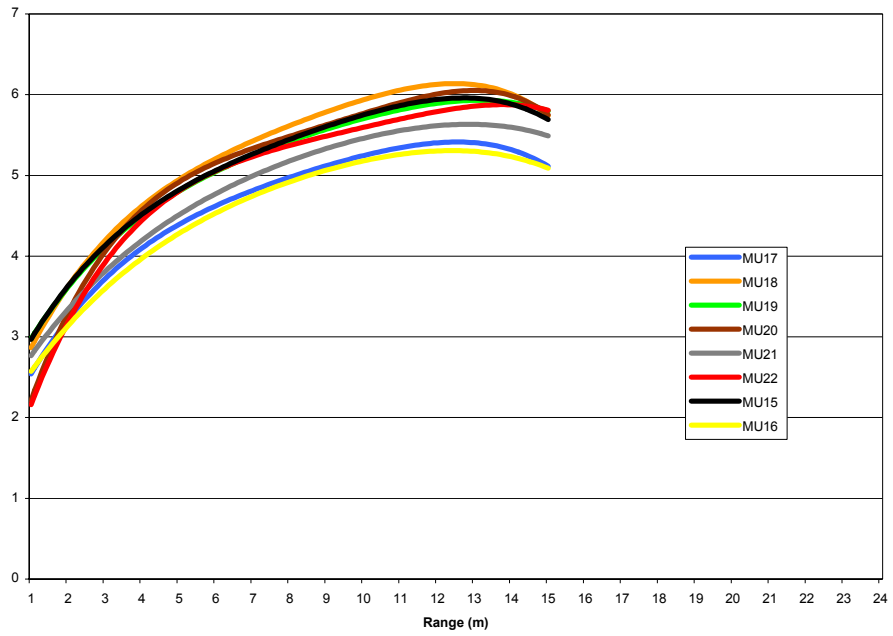
Spring Day Intake Uplooker



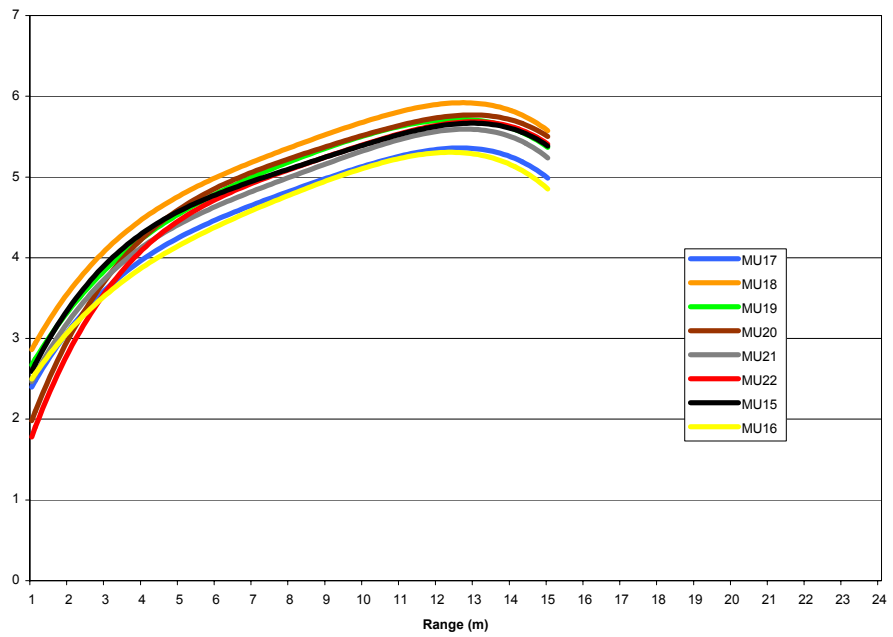
Spring Night Intake Uplooker



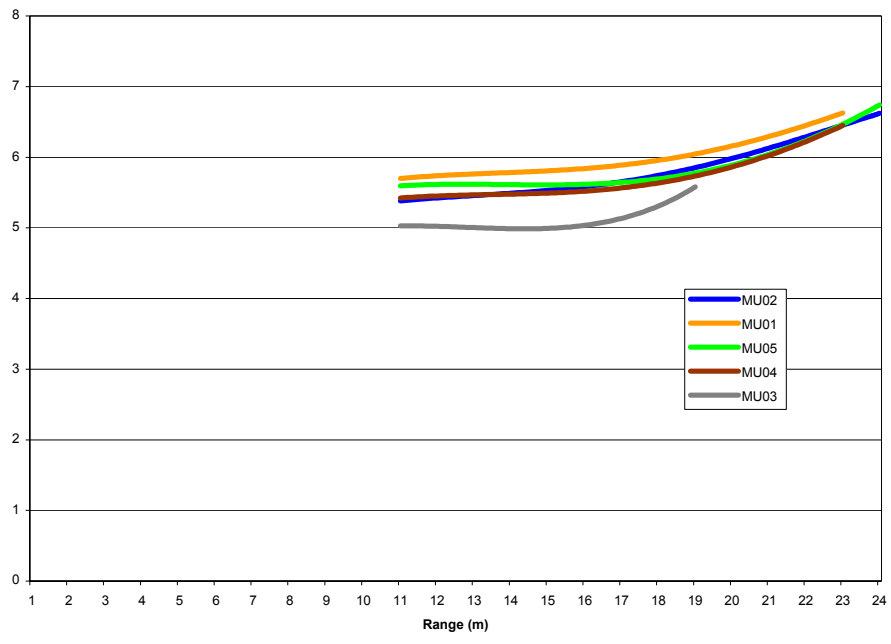
Summer Day Intake Uplooker



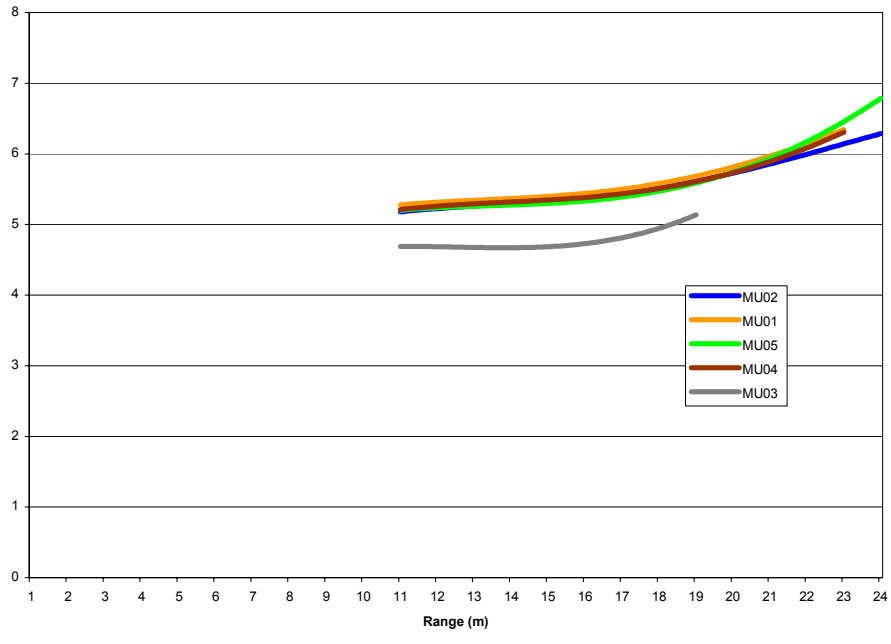
Summer Night Intake Uplooker



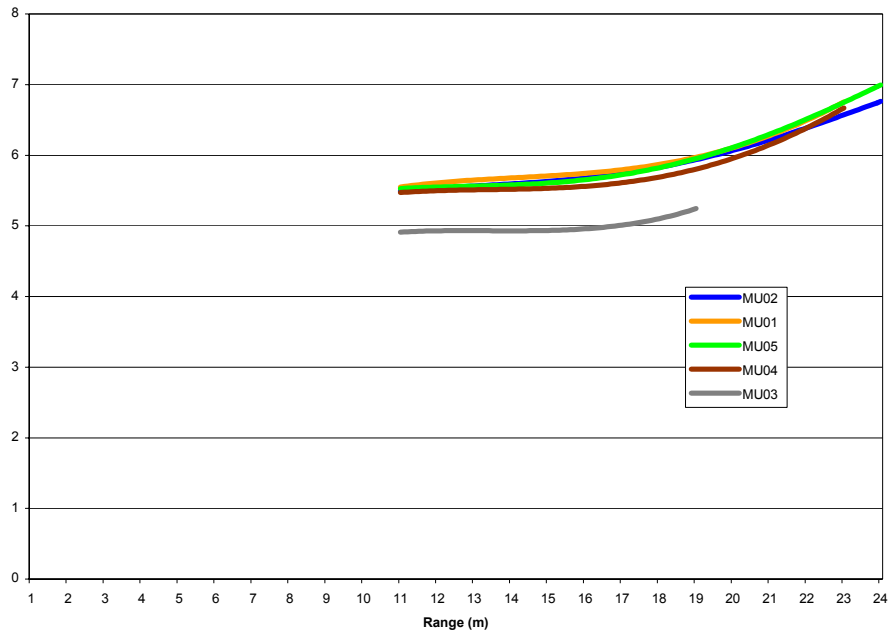
Spring Day Intake Downlooker



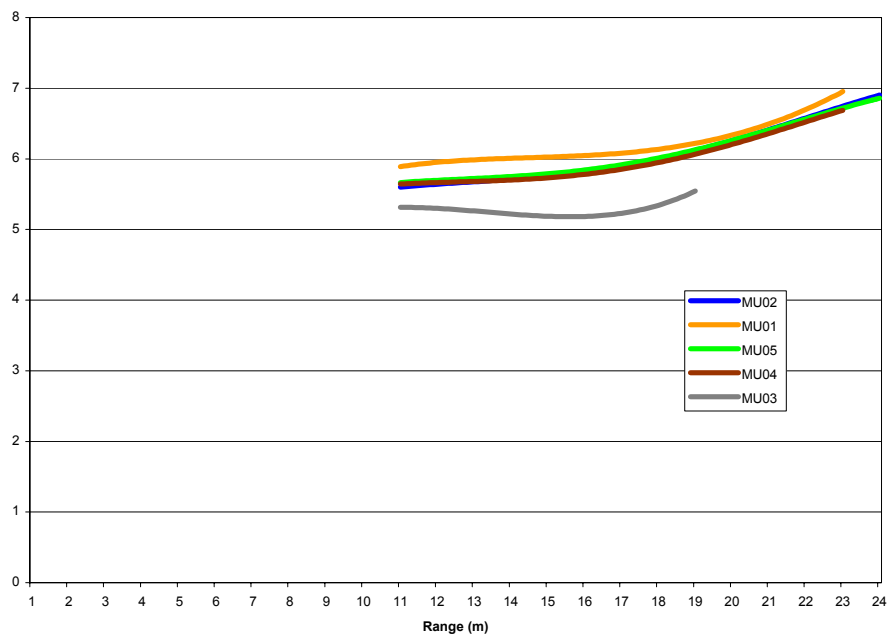
Spring Night Intake Downlooker



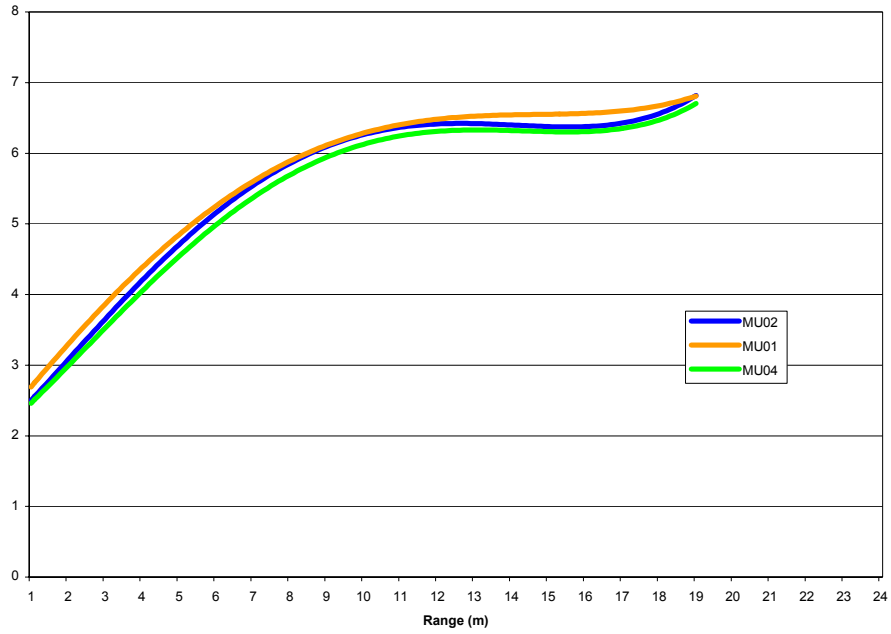
Summer Day Intake Downlooker



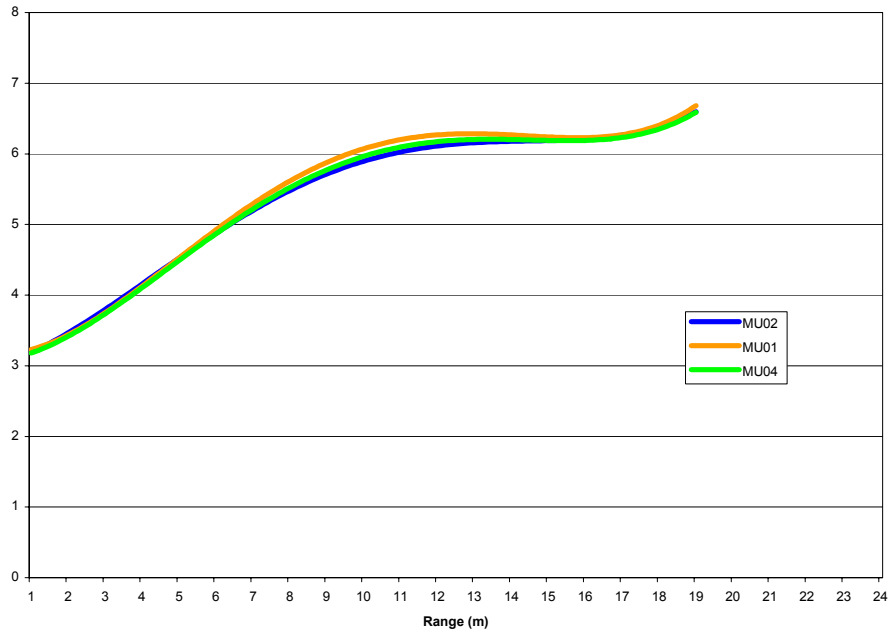
Summer Night Intake Downlooker



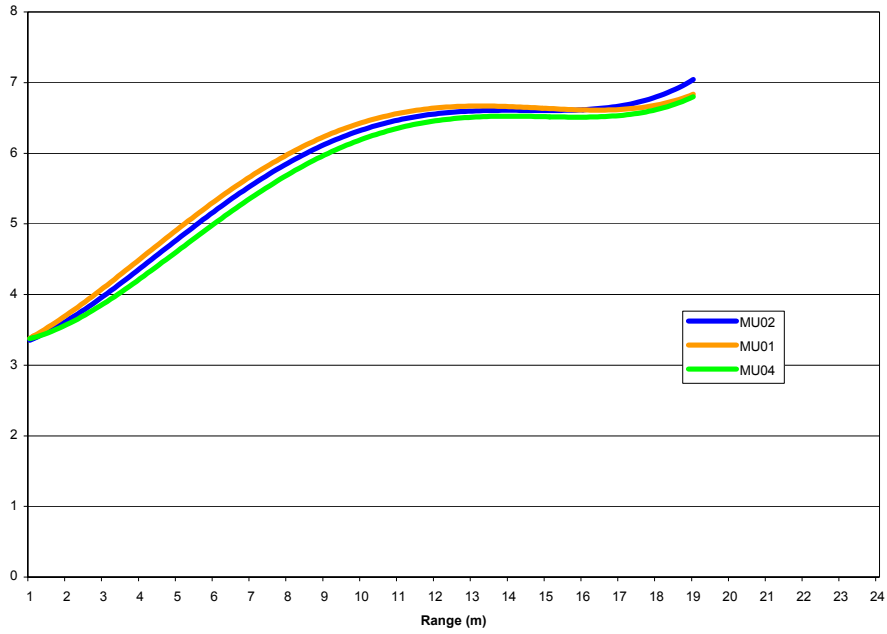
Spring Day
Intake Downlooker Unoccluded



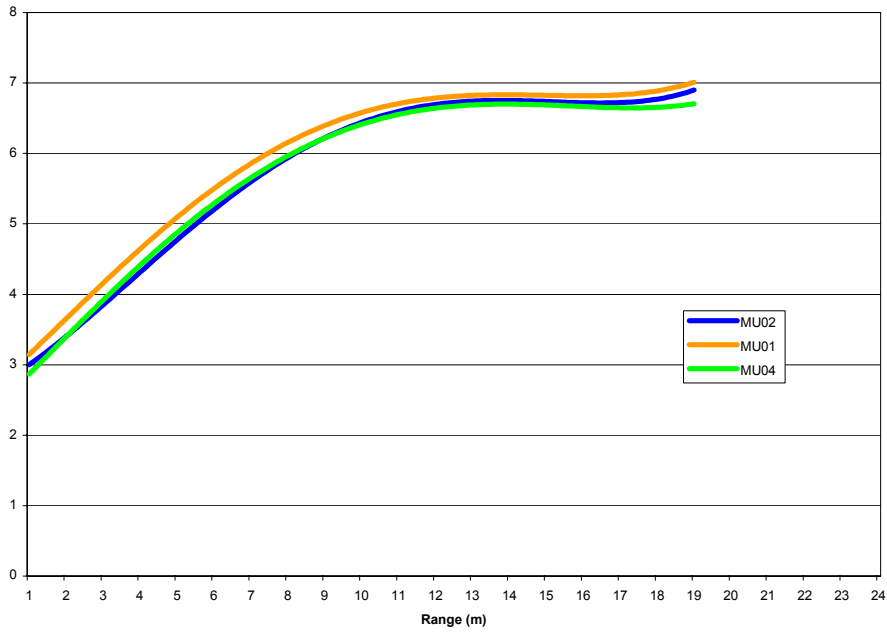
Spring Night
Intake Downlooker Unoccluded



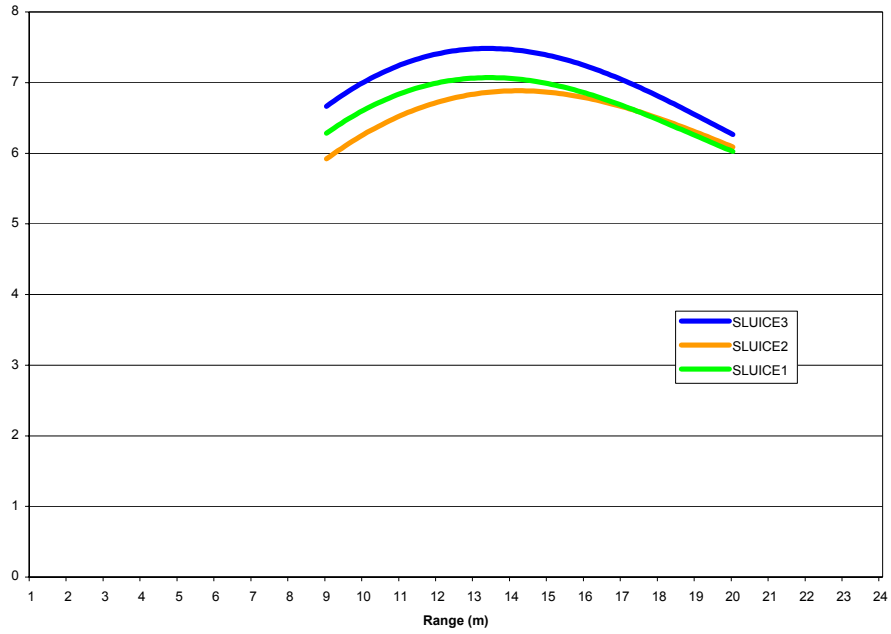
**Summer Day
Intake Downlooker Unoccluded**



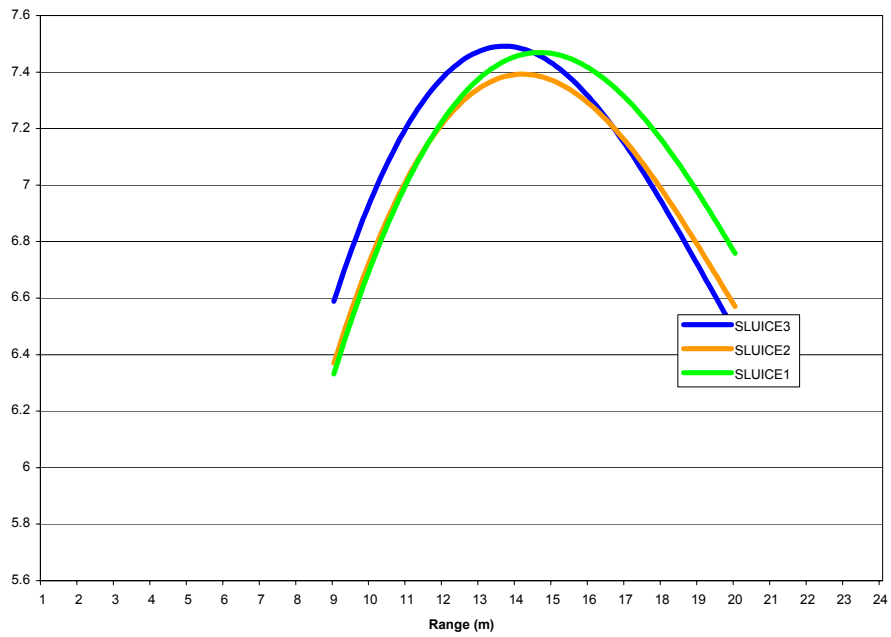
**Summer Night
Intake Downlooker Unoccluded**



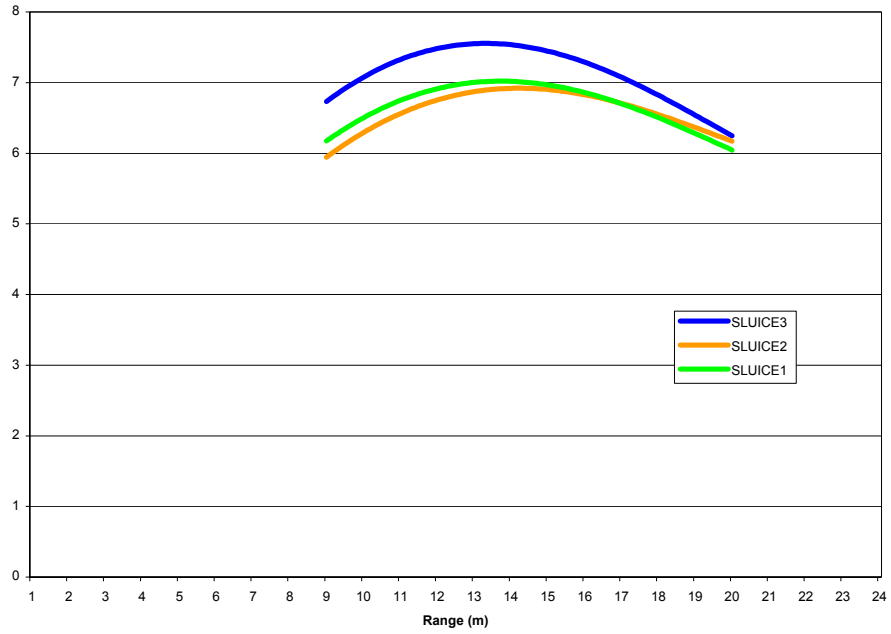
**Spring Day
Sluice Unoccluded**



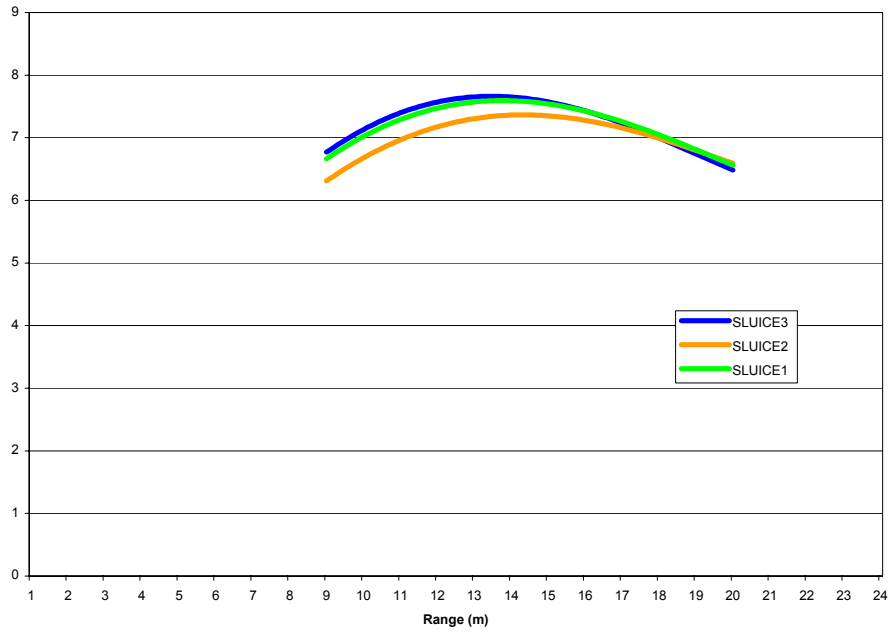
**Spring Night
Sluice Unoccluded**



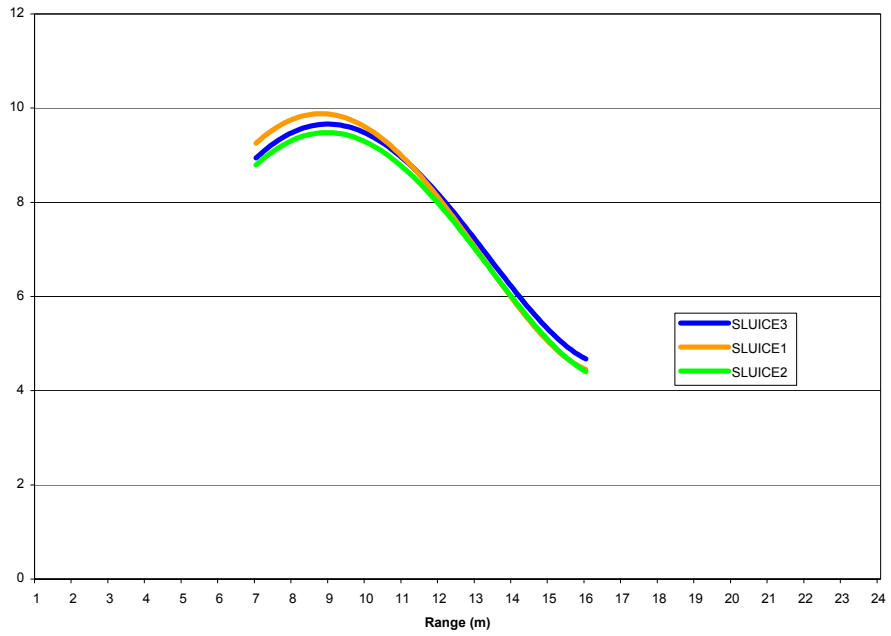
**Summer Day
Sluice Unoccluded**



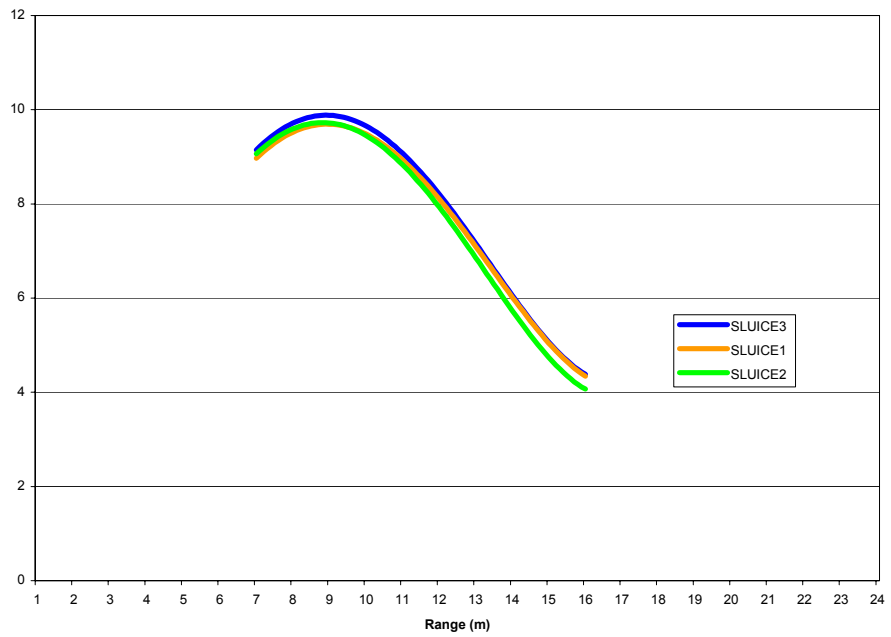
**Summer Night
Sluice Unoccluded**



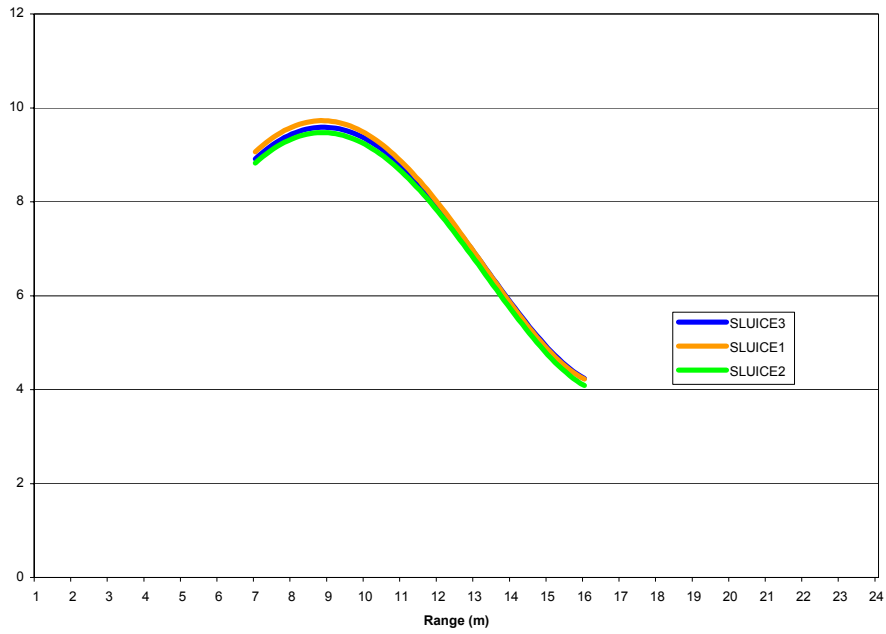
Spring Day
Sluice Occluded



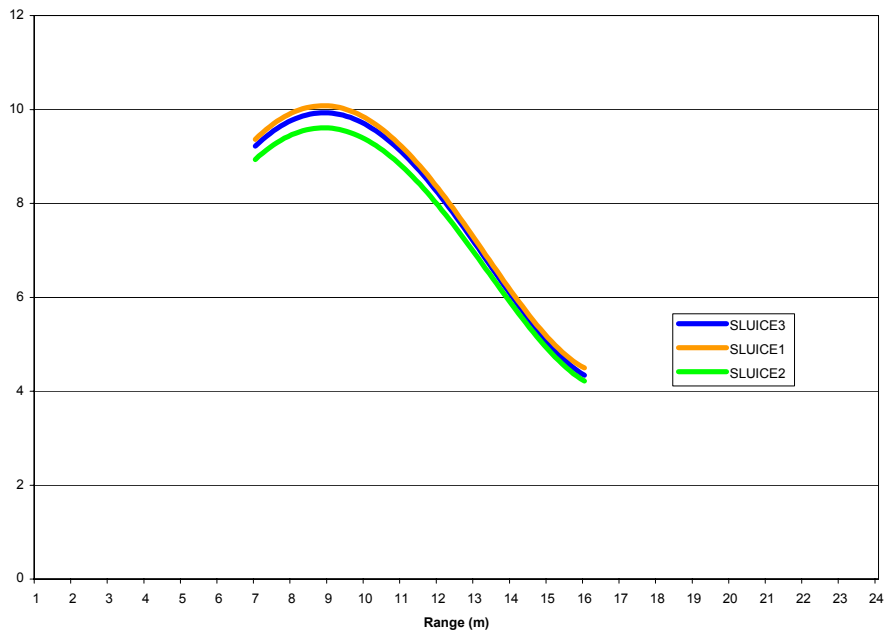
Spring Night
Sluice Occluded



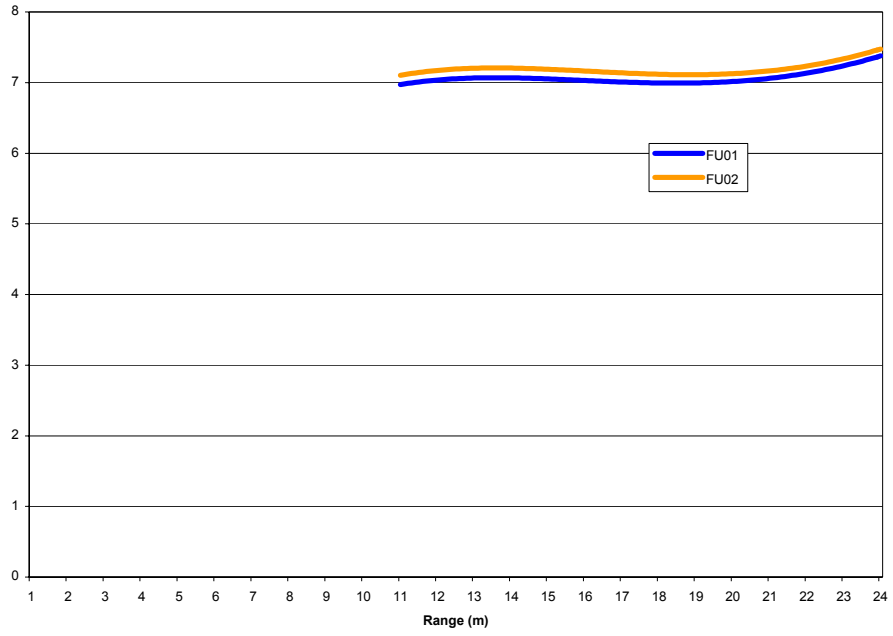
**Summer Day
Sluice Occluded**



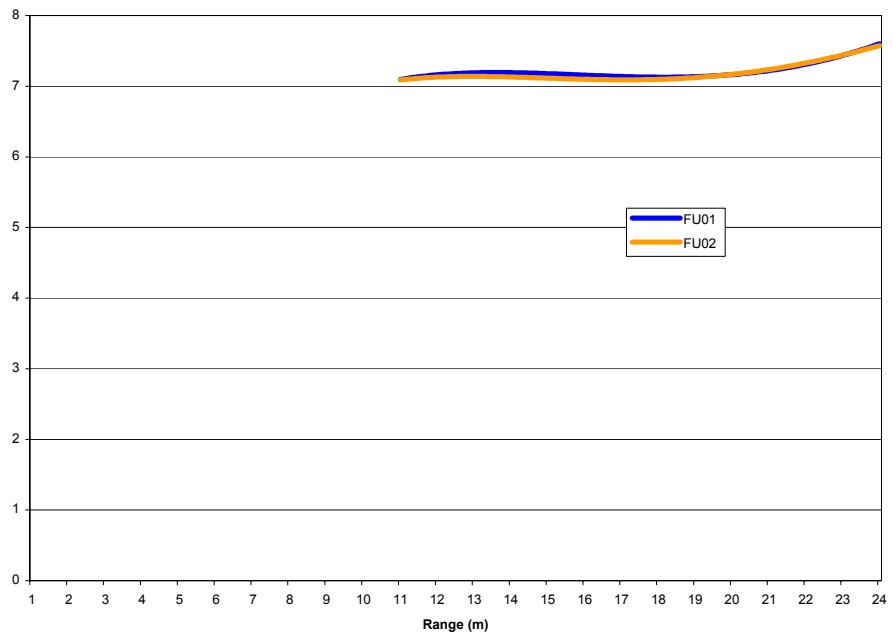
**Summer Night
Sluice Occluded**



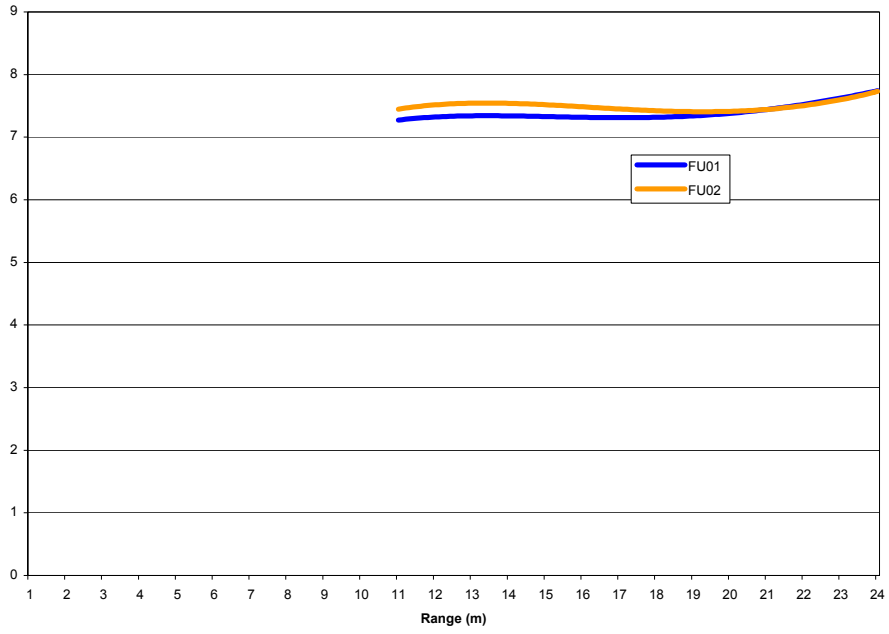
Spring Day Fish Units



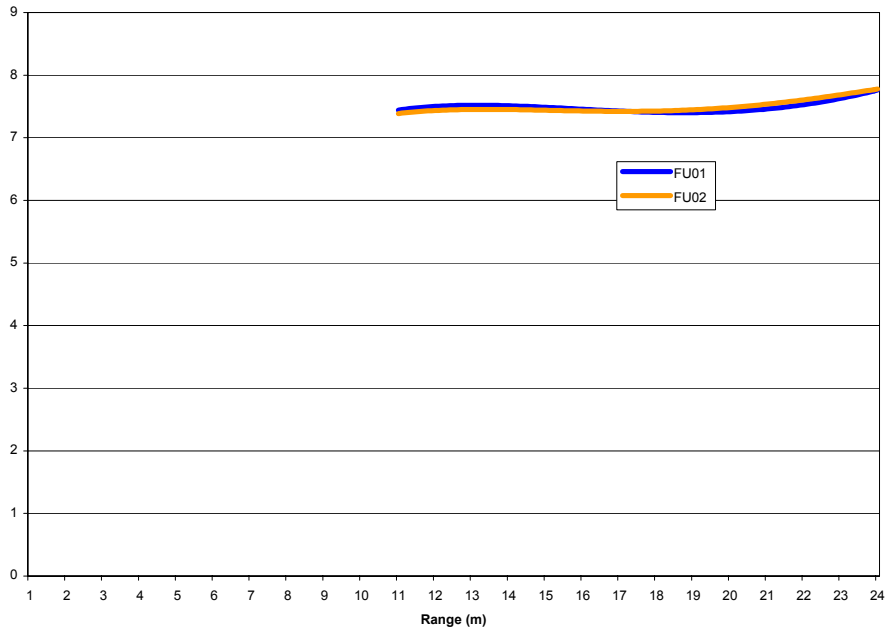
Spring Night Fish Units



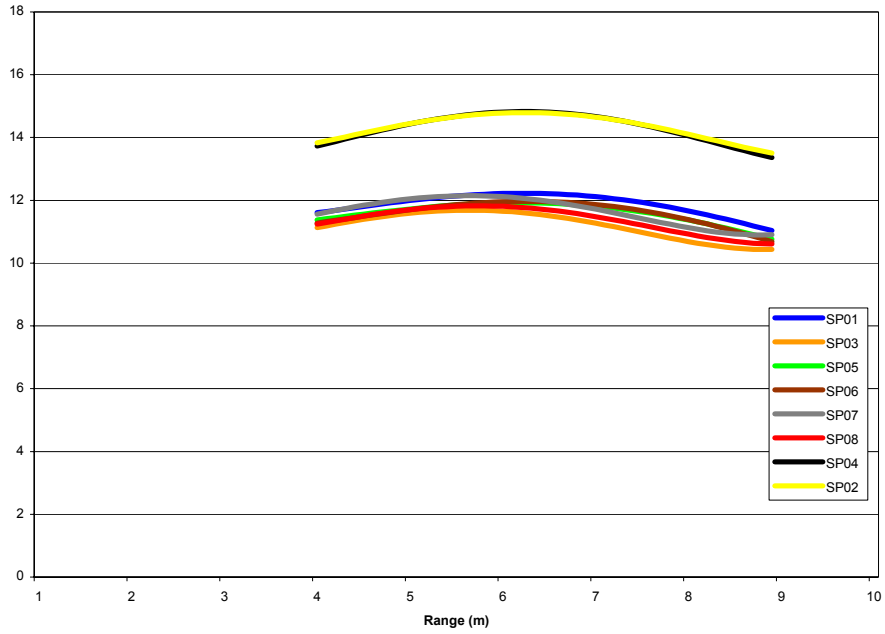
Summer Day Fish Units



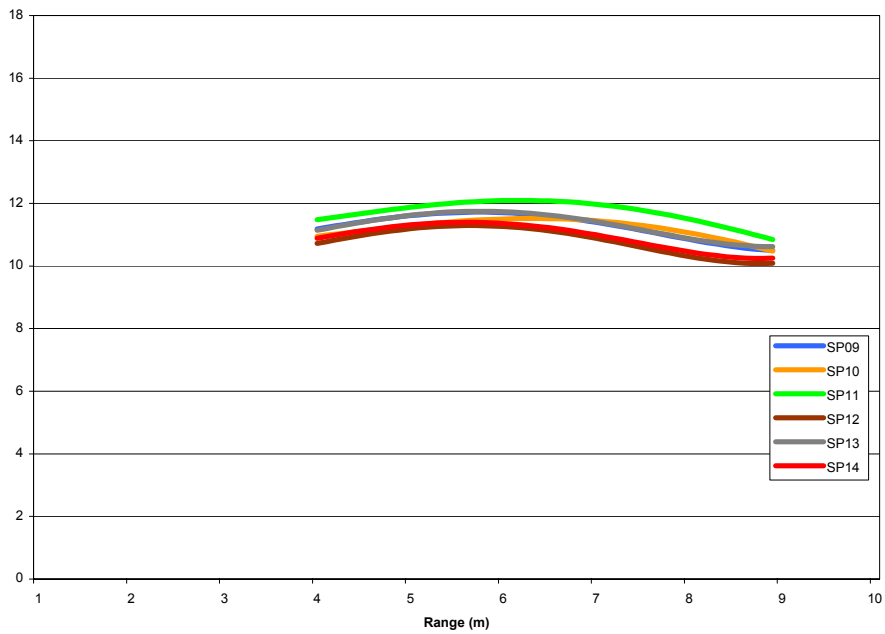
Summer Night Fish Units



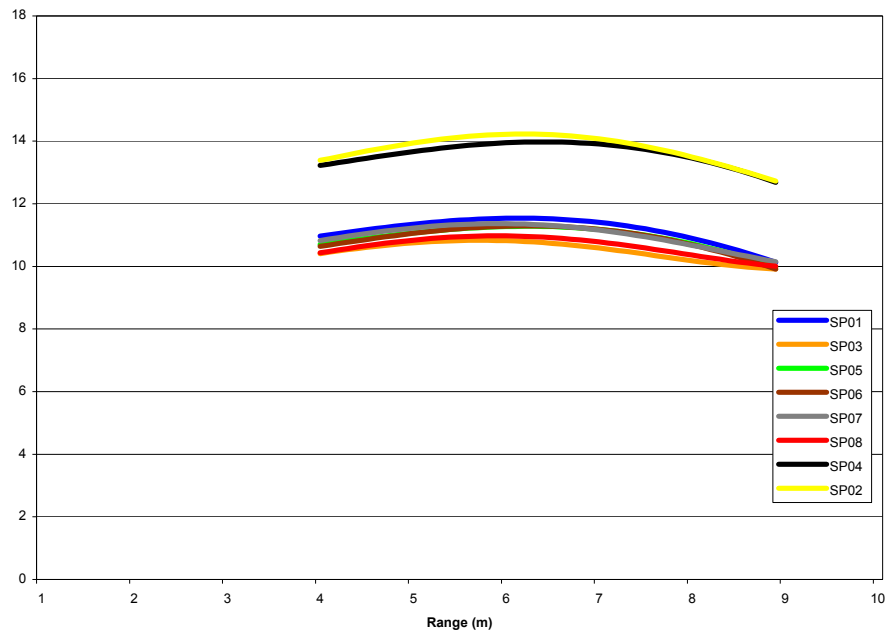
Spring Day
Spillway Gate 1



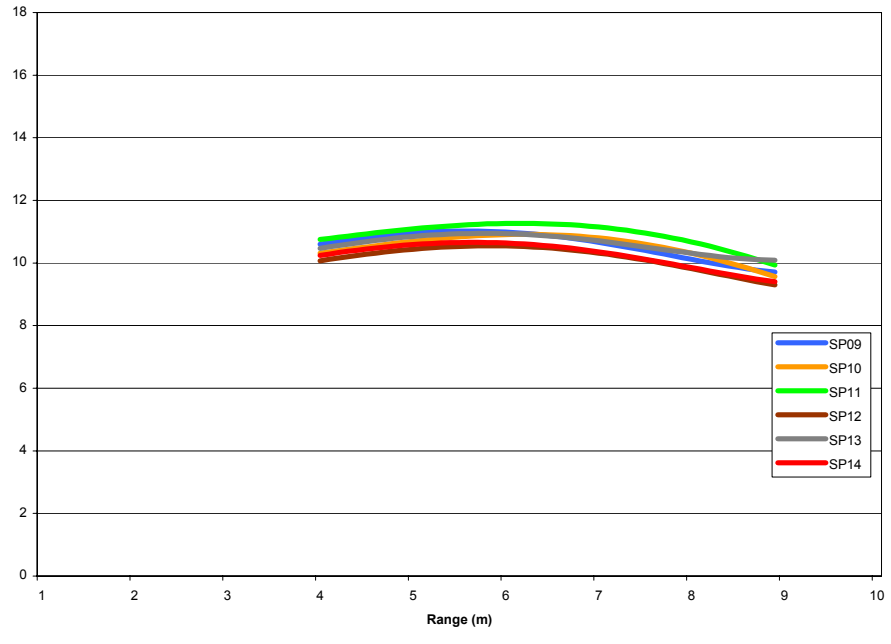
Spring Day
Spillway Gate 1



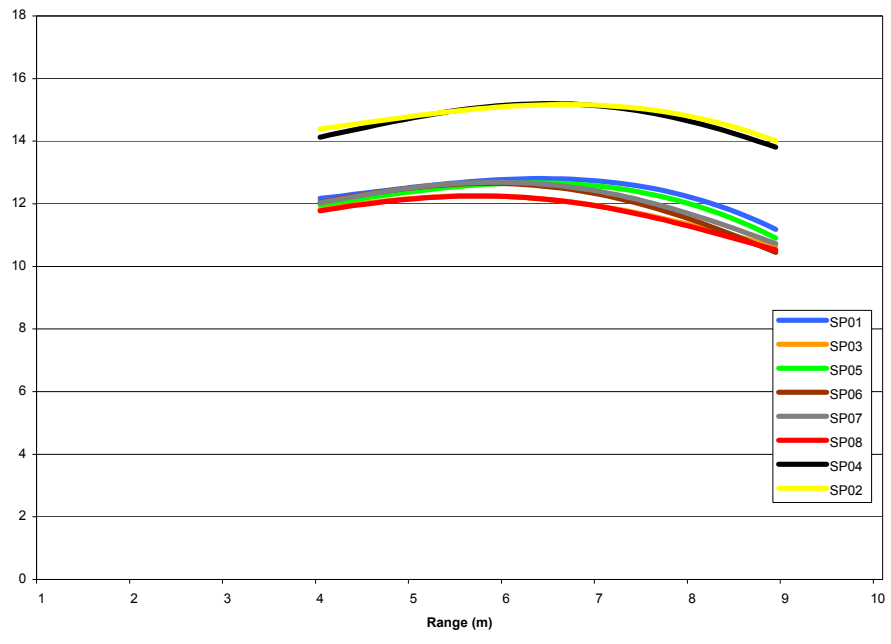
**Spring Day
Spillway Gate 2**



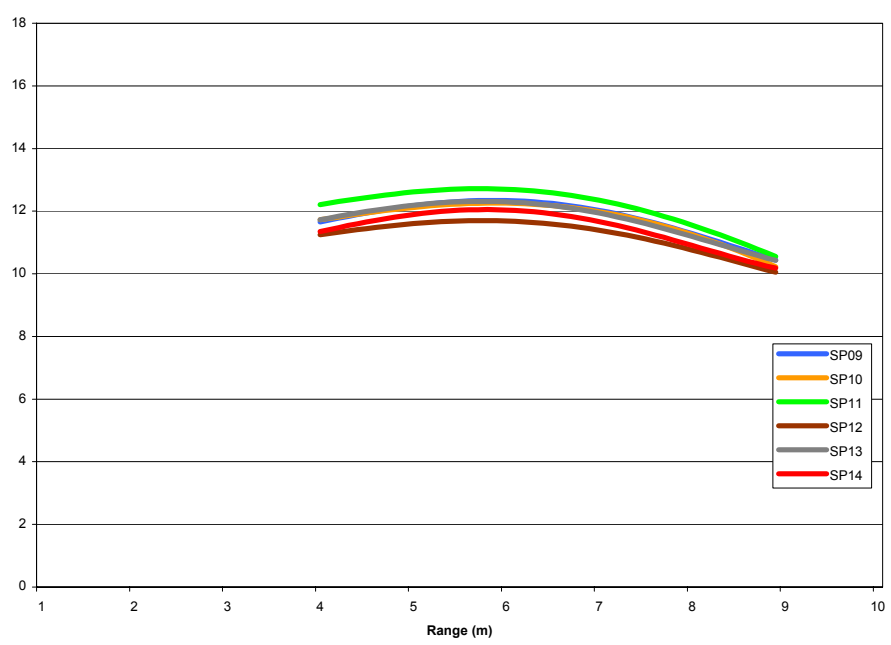
**Spring Day
Spillway Gate 2**



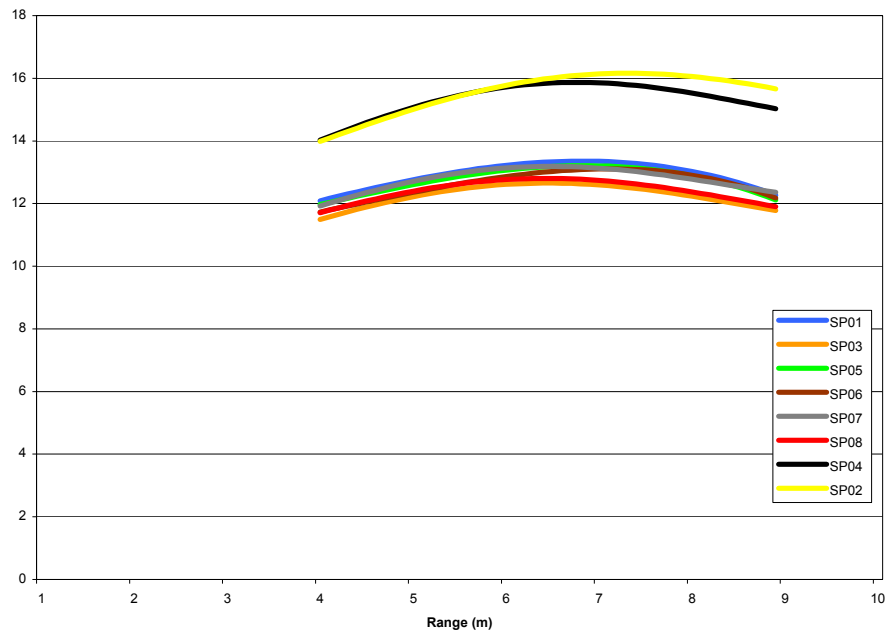
**Spring Day
Spillway Gate 3**



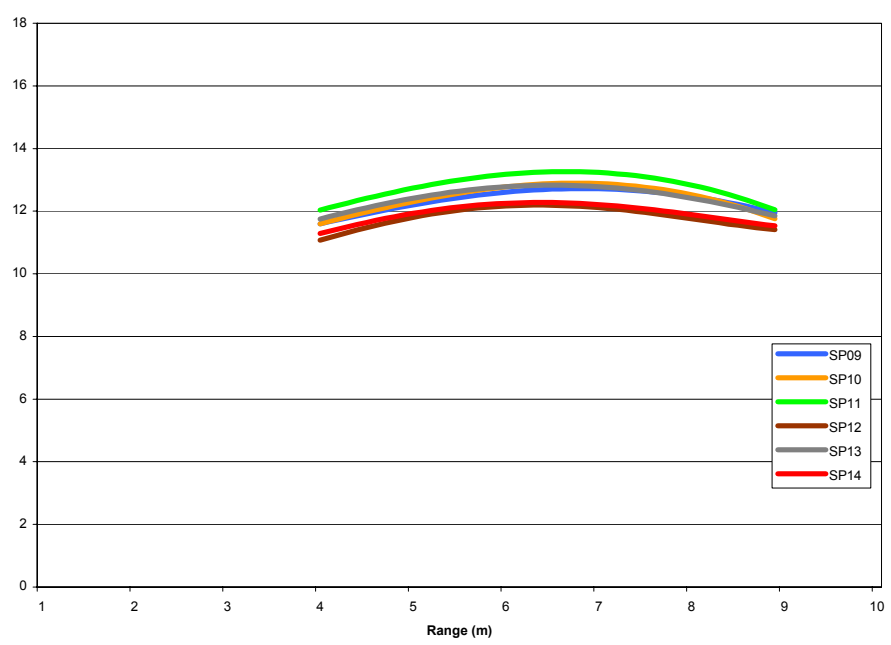
**Spring Day
Spillway Gate 3**



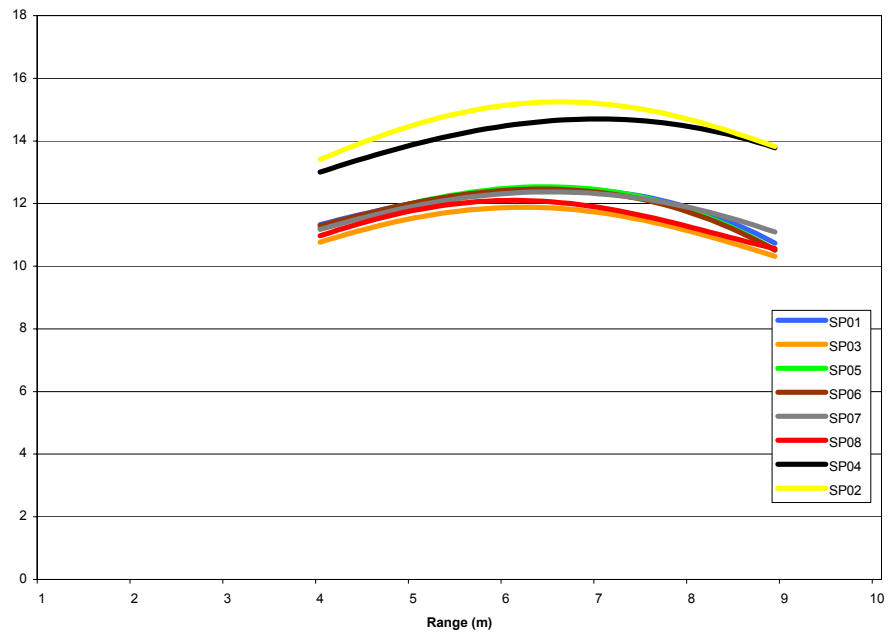
Spring Day
Spillway Gate 4



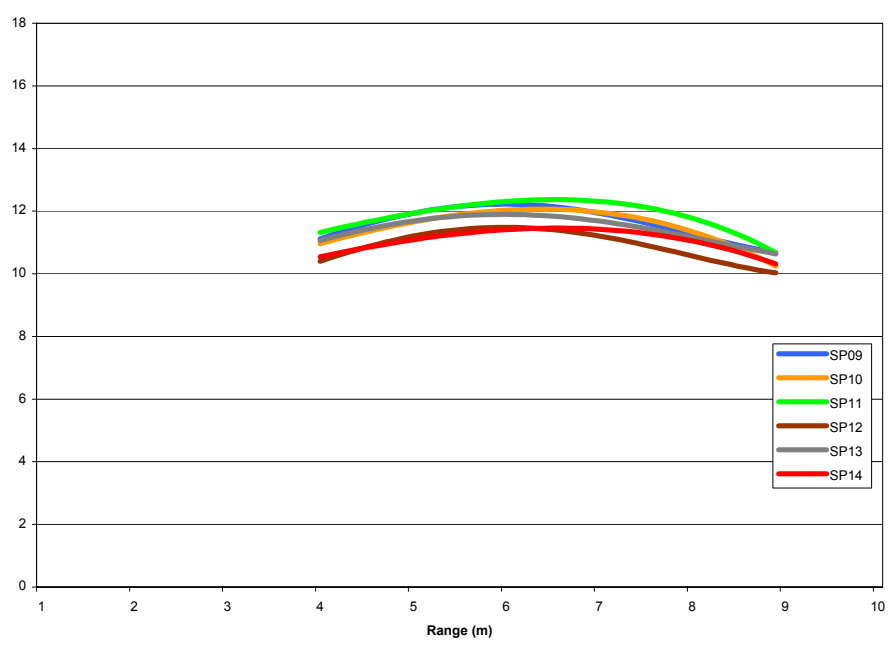
Spring Day
Spillway Gate 4



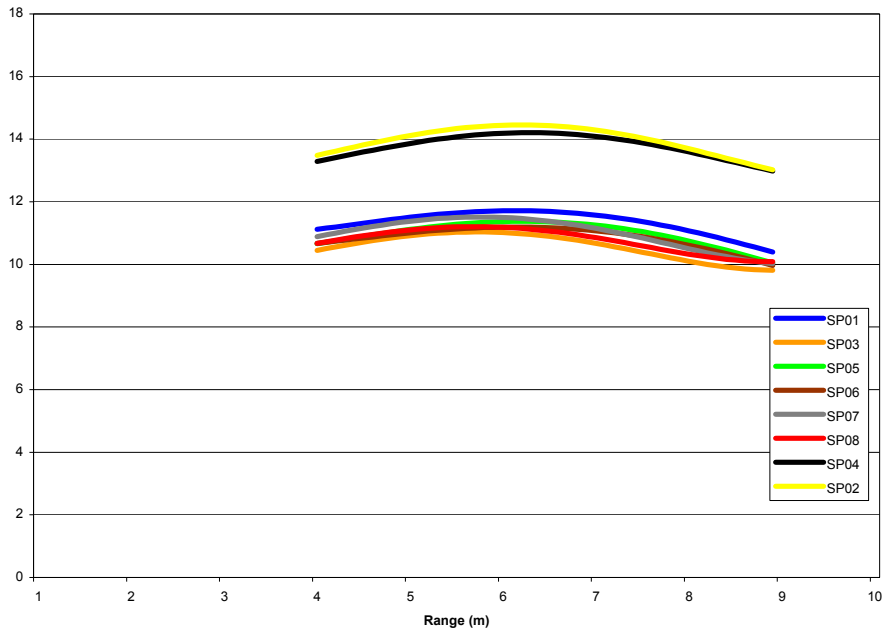
**Spring Day
Spillway Gate 5**



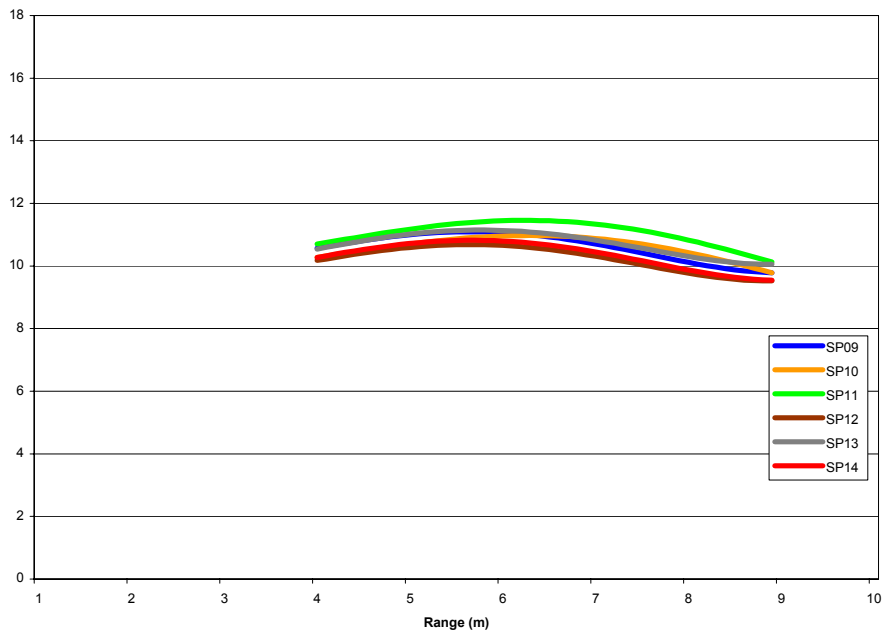
**Spring Day
Spillway Gate 5**



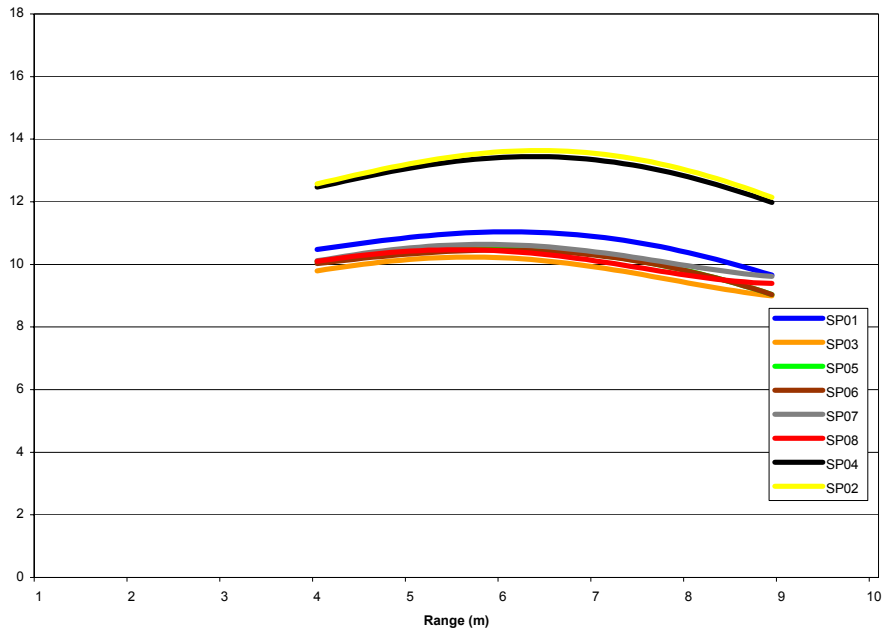
**Spring Night
Spillway Gate 1**



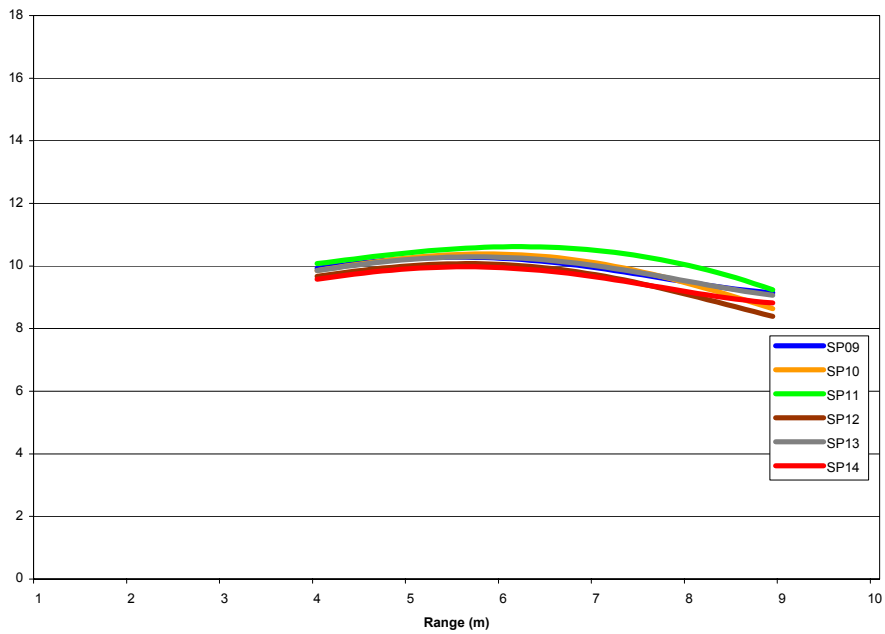
**Spring Night
Spillway Gate 1**



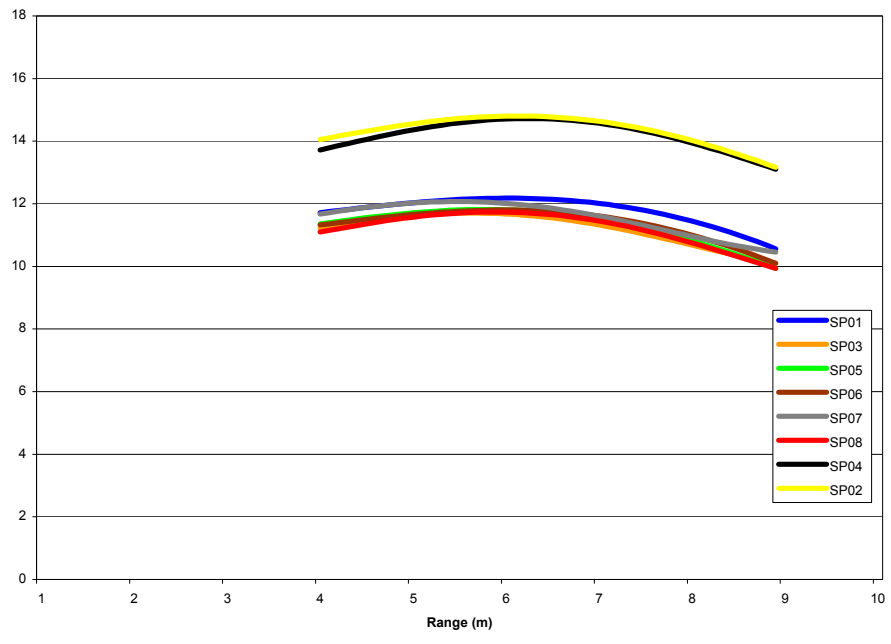
**Spring Night
Spillway Gate 2**



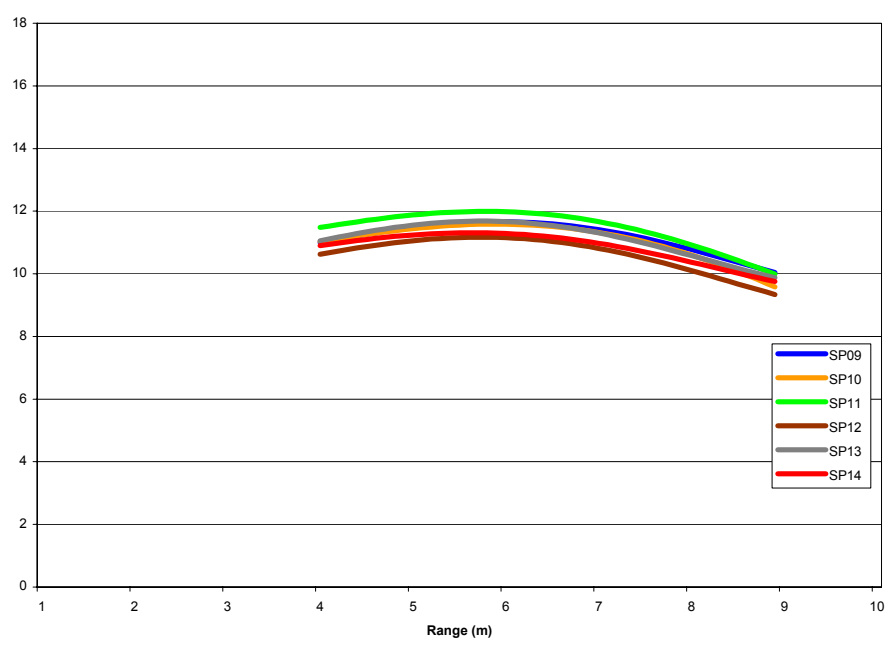
**Spring Night
Spillway Gate 2**



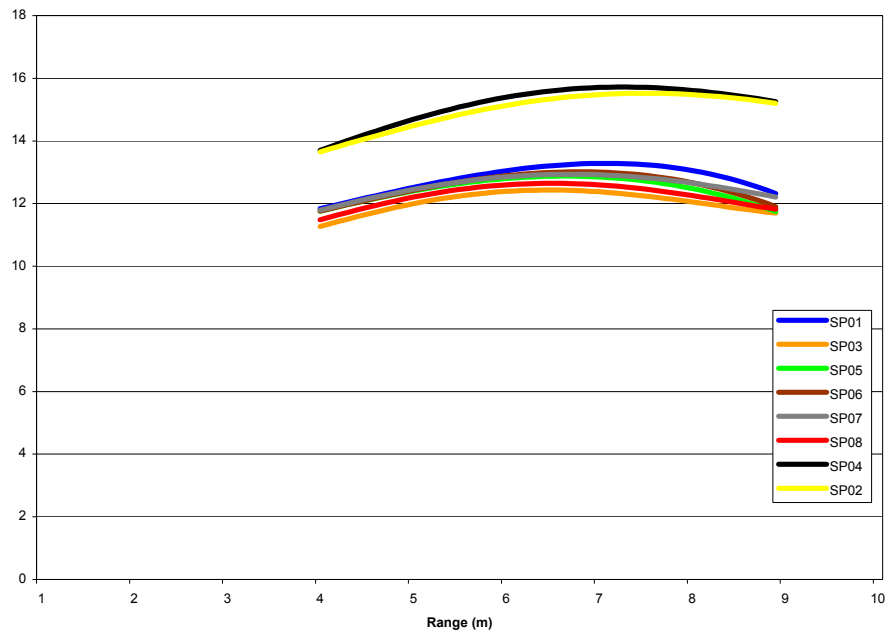
**Spring Night
Spillway Gate 3**



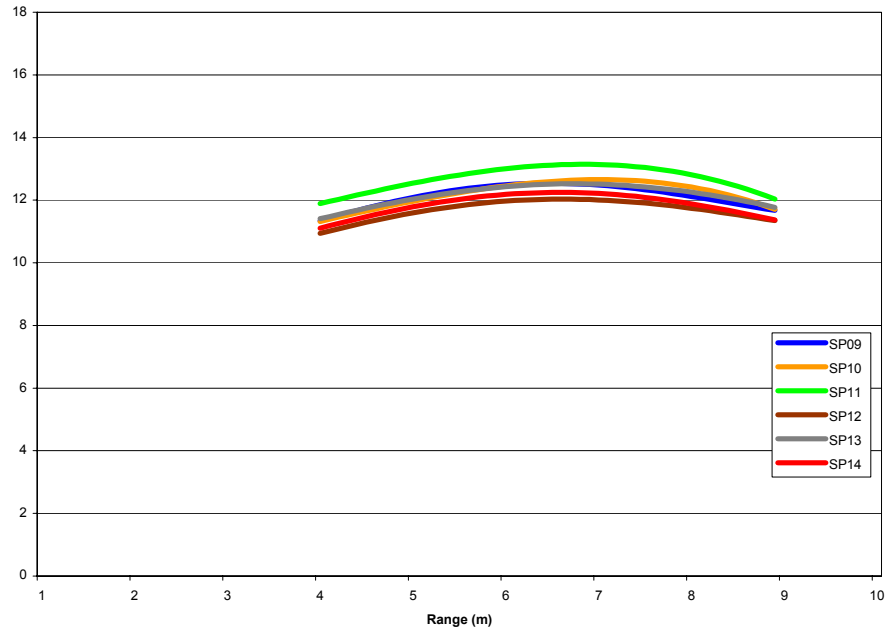
**Spring Night
Spillway Gate 3**



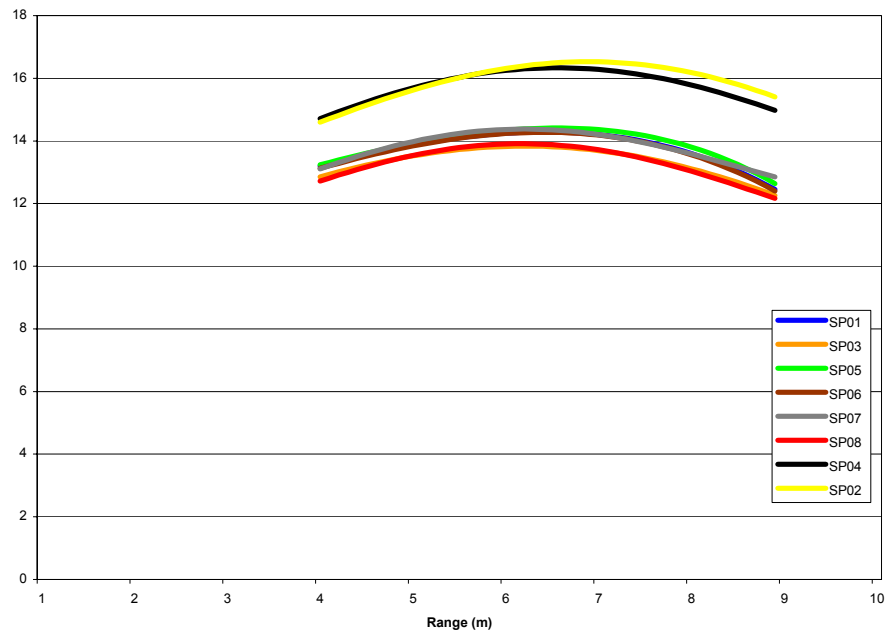
**Spring Night
Spillway Gate 4**



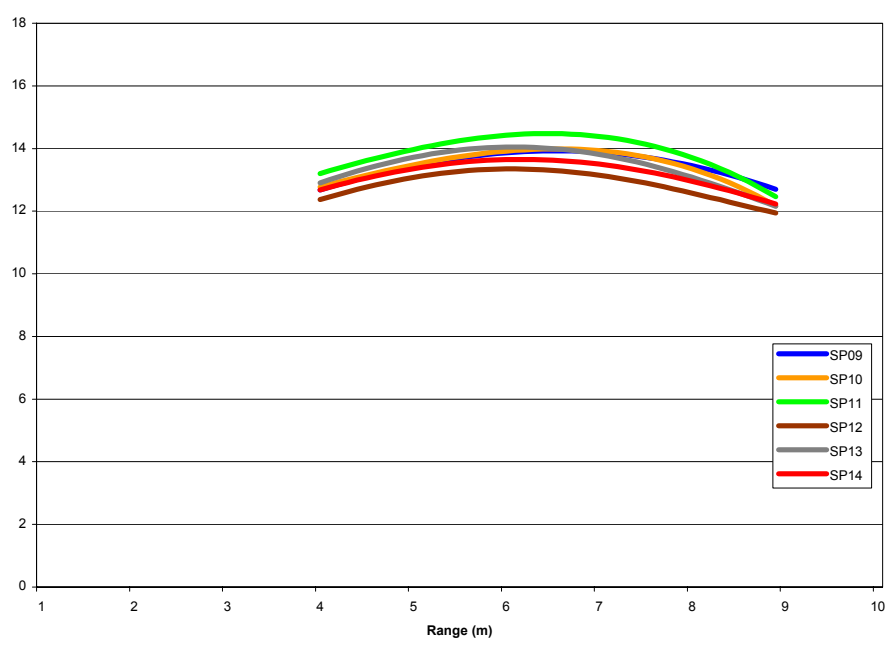
**Spring Night
Spillway Gate 4**



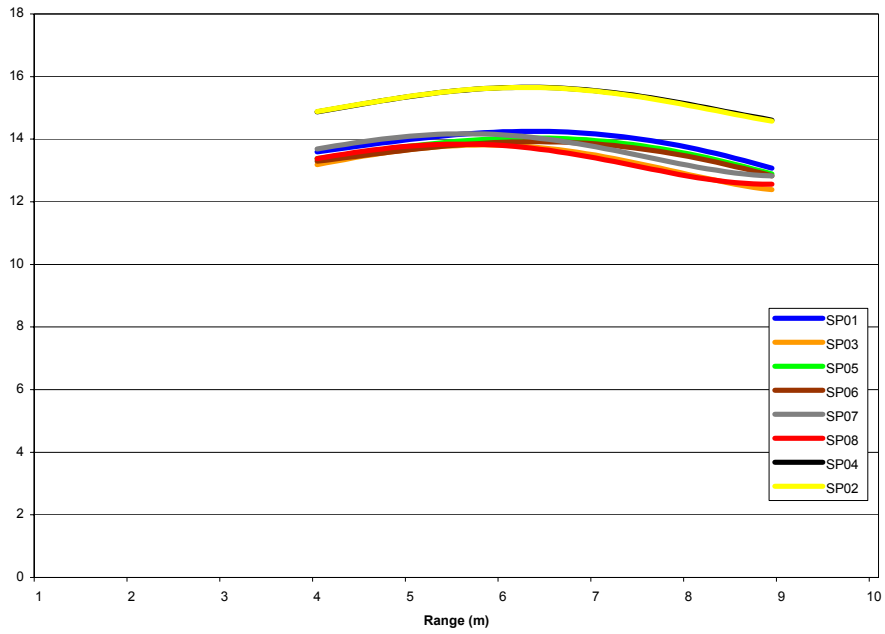
**Spring Night
Spillway Gate 5**



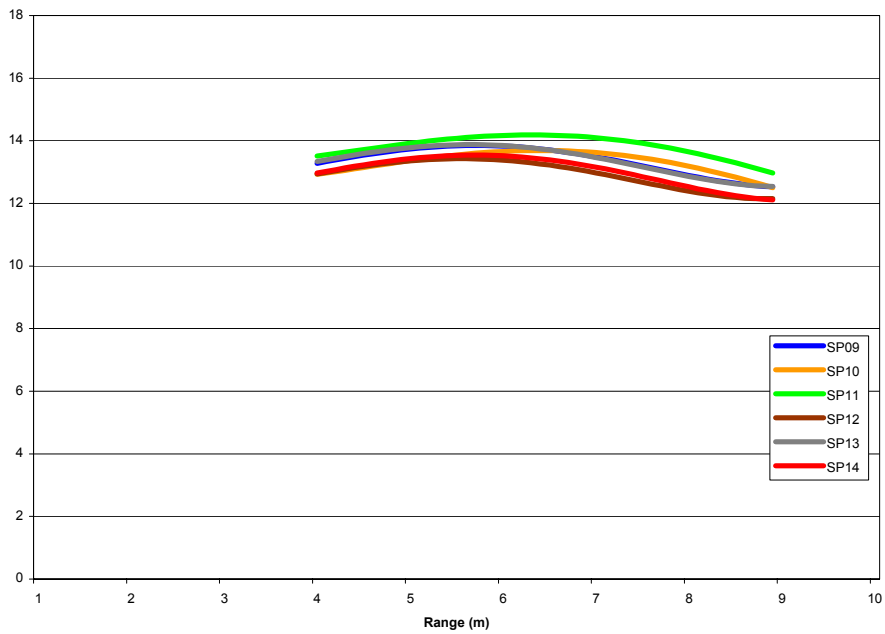
**Spring Night
Spillway Gate 5**



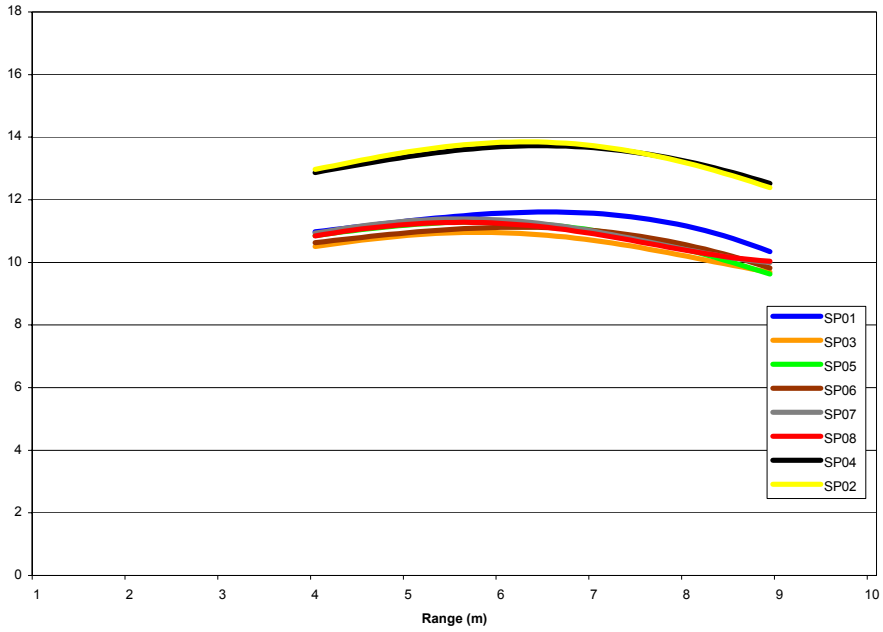
**Summer Day
Spillway Gate 1**



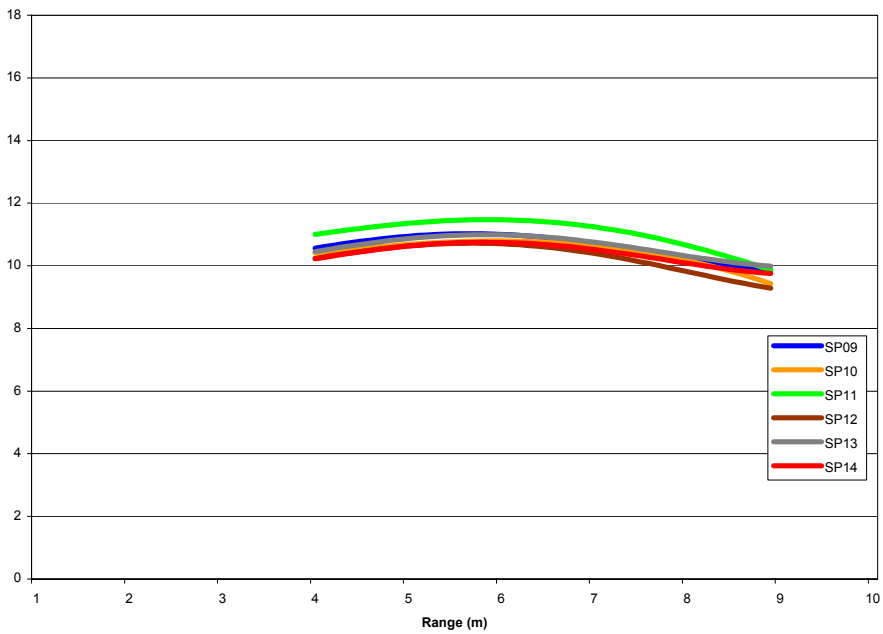
**Summer Day
Spillway Gate 1**



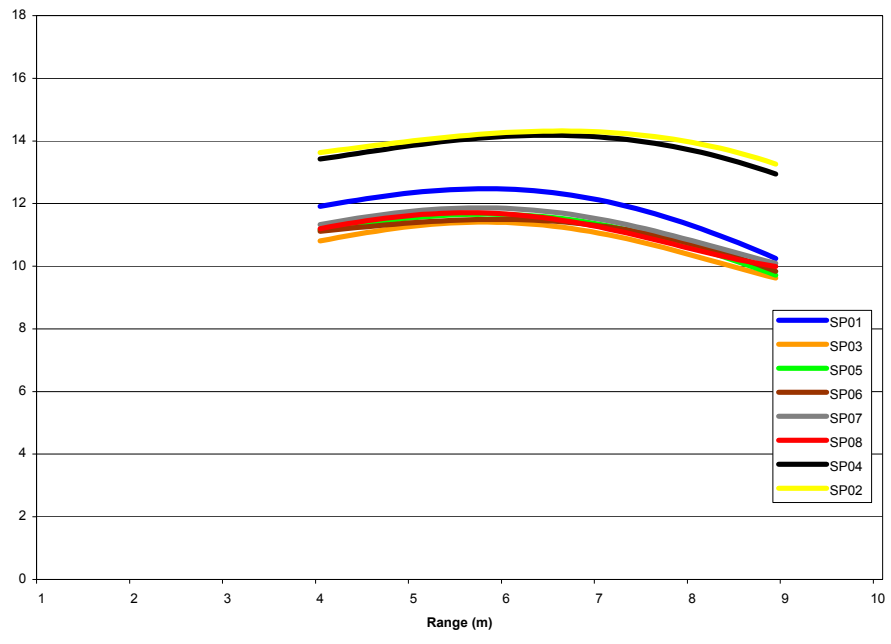
Summer Day
Spillway Gate 2



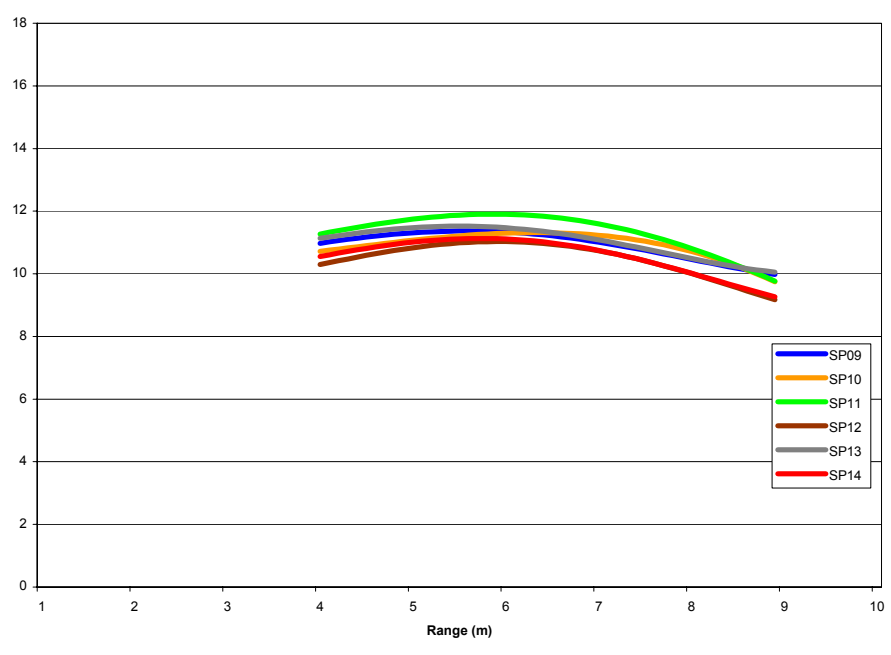
Summer Day
Spillway Gate 2



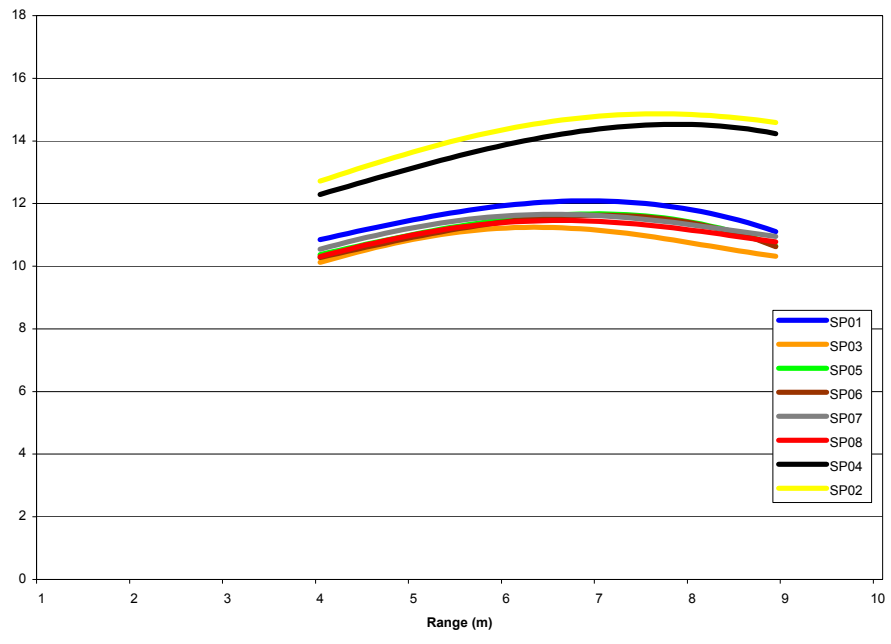
Summer Day
Spillway Gate 3



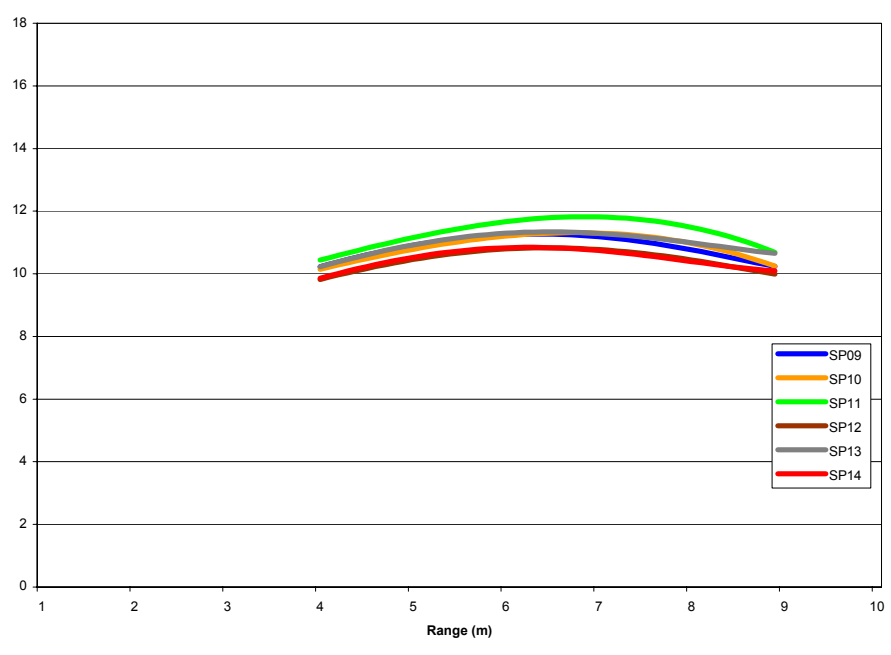
Summer Day
Spillway Gate 3



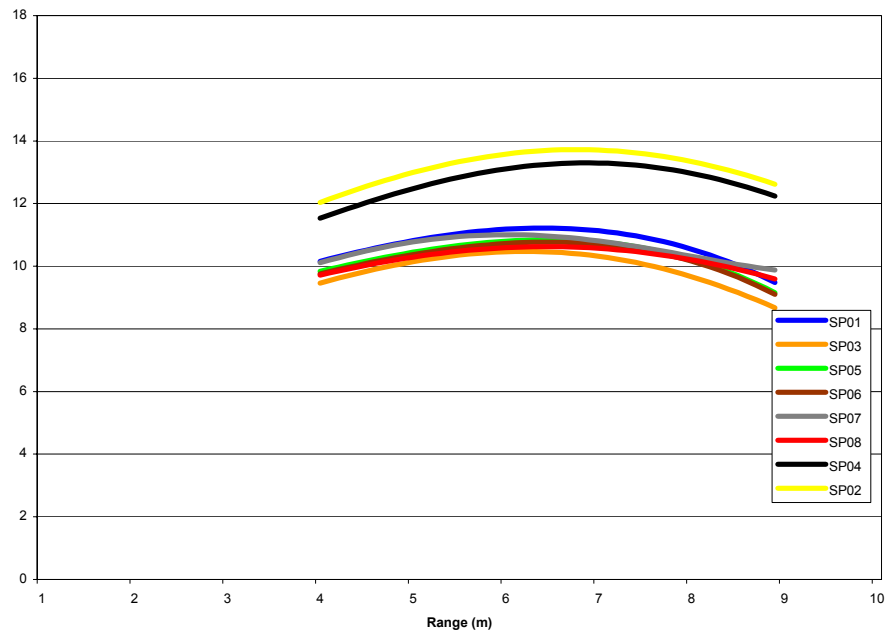
**Summer Day
Spillway Gate 4**



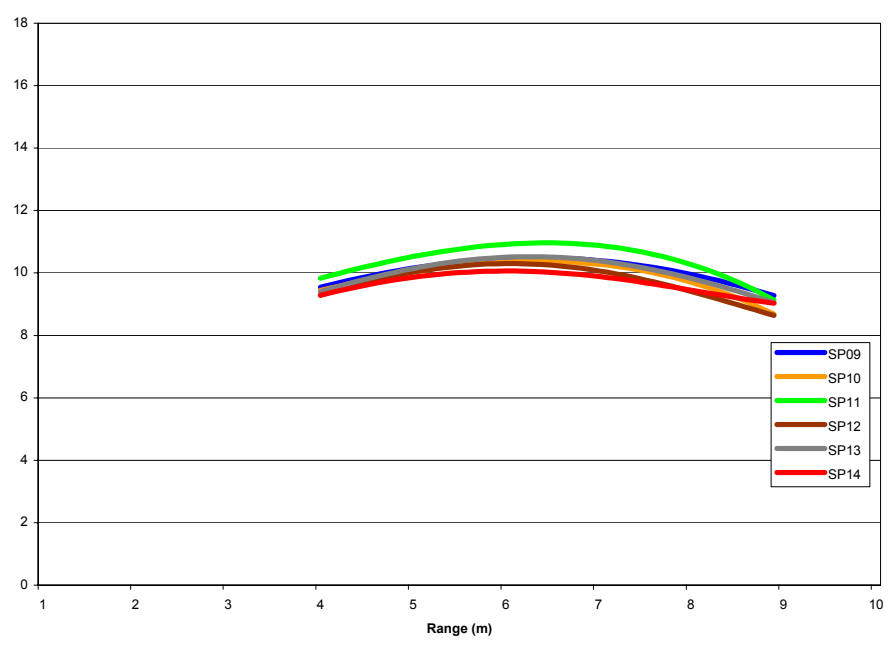
**Summer Day
Spillway Gate 4**



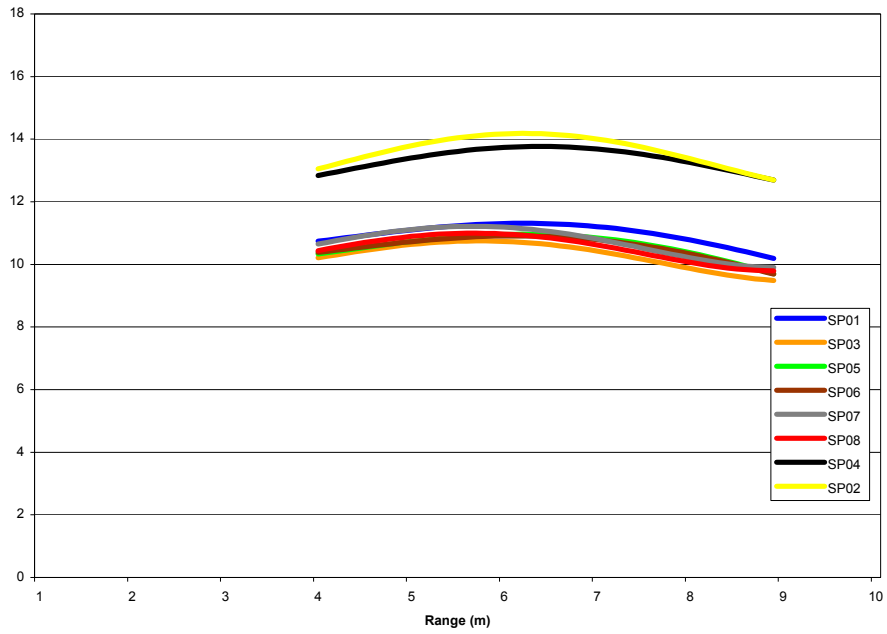
**Summer Day
Spillway Gate 5**



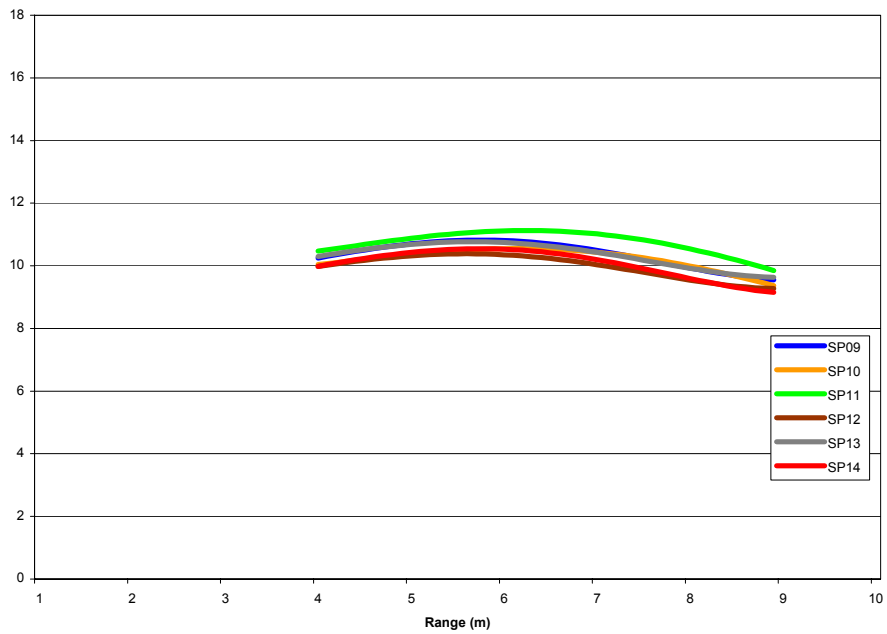
**Summer Day
Spillway Gate 5**



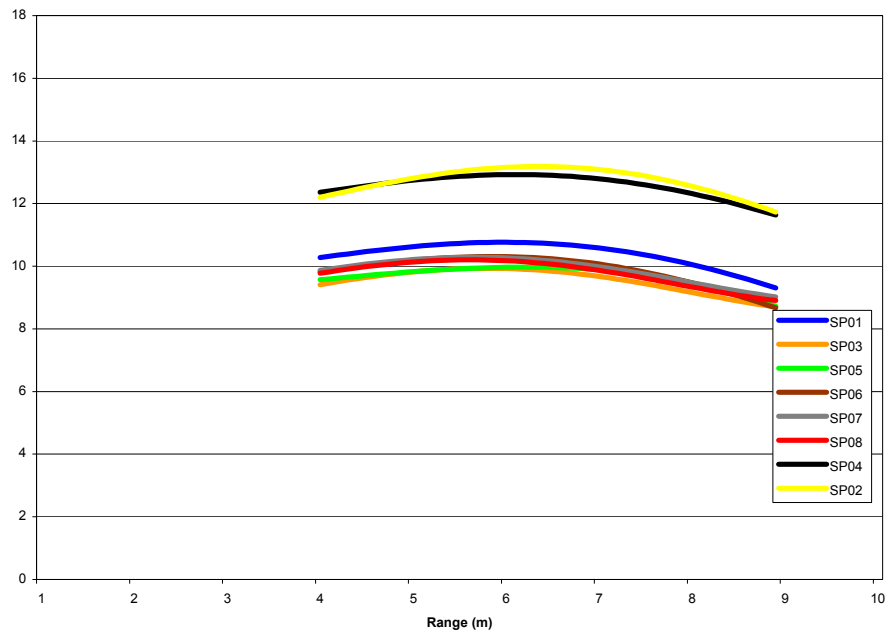
**Summer Night
Spillway Gate 1**



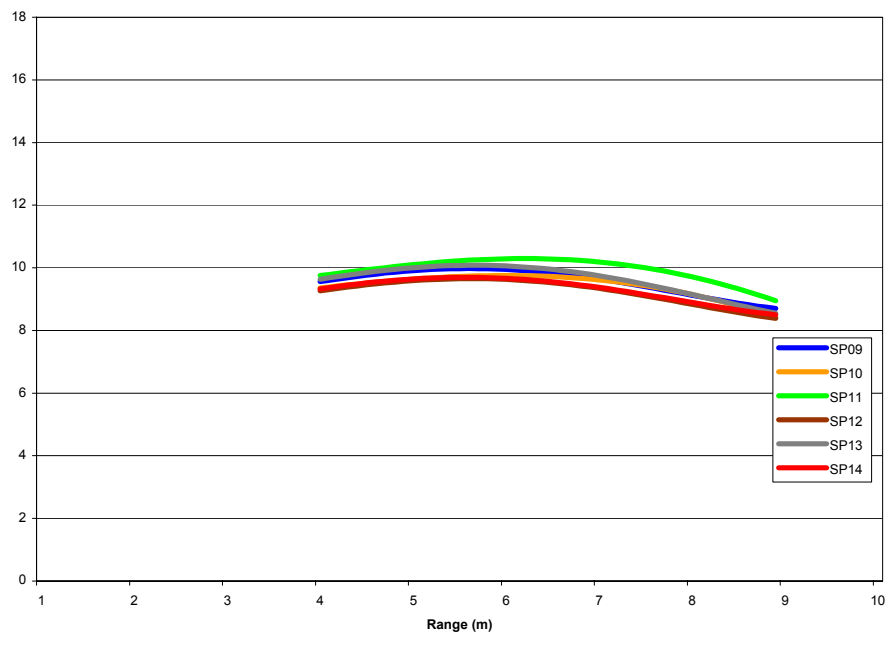
**Summer Night
Spillway Gate 1**



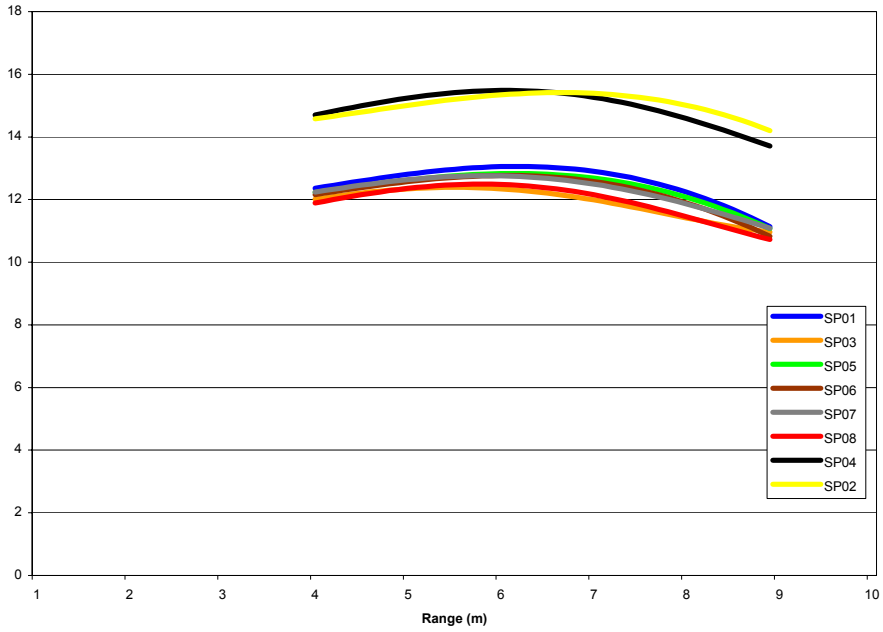
**Summer Night
Spillway Gate 2**



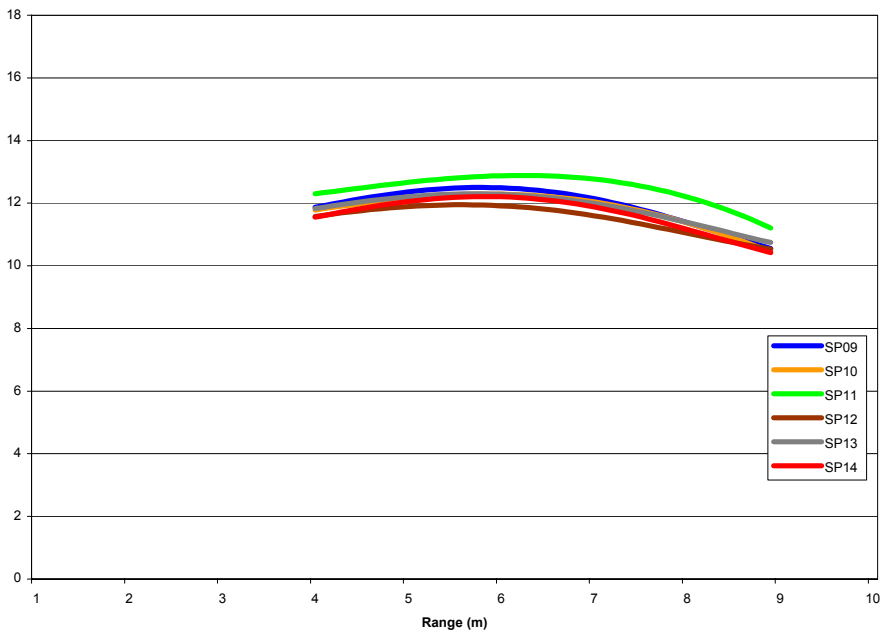
**Summer Night
Spillway Gate 2**



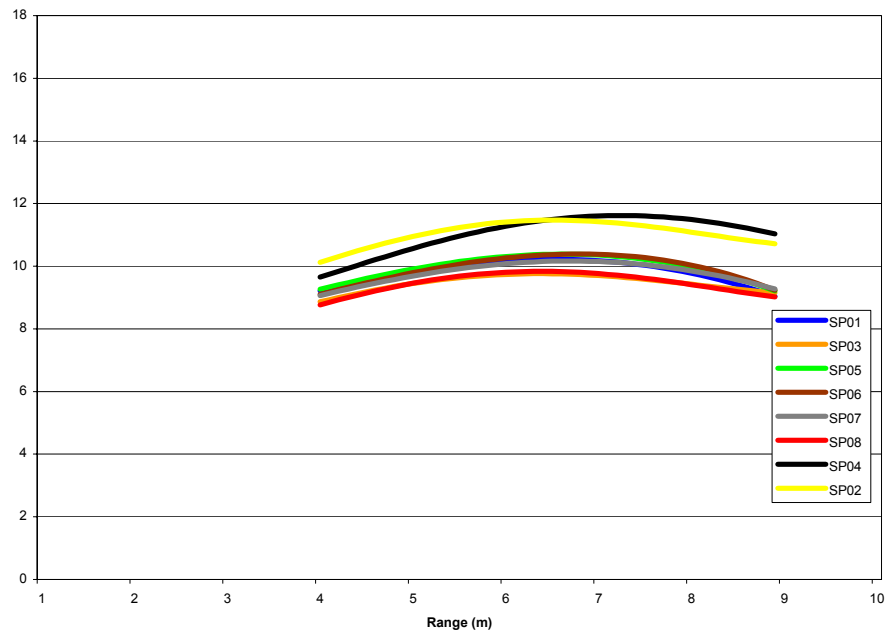
**Summer Night
Spillway Gate 3**



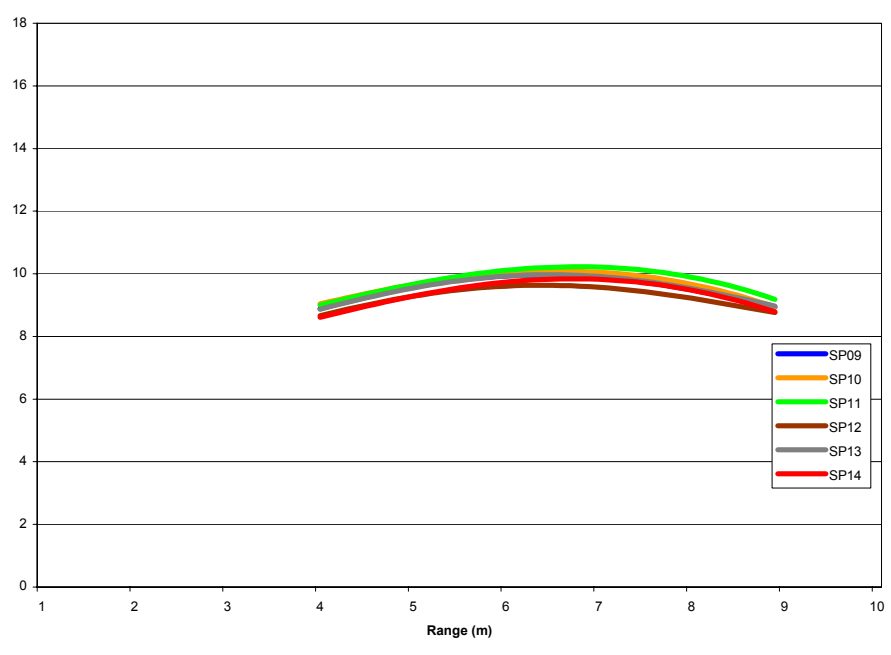
**Summer Night
Spillway Gate 3**



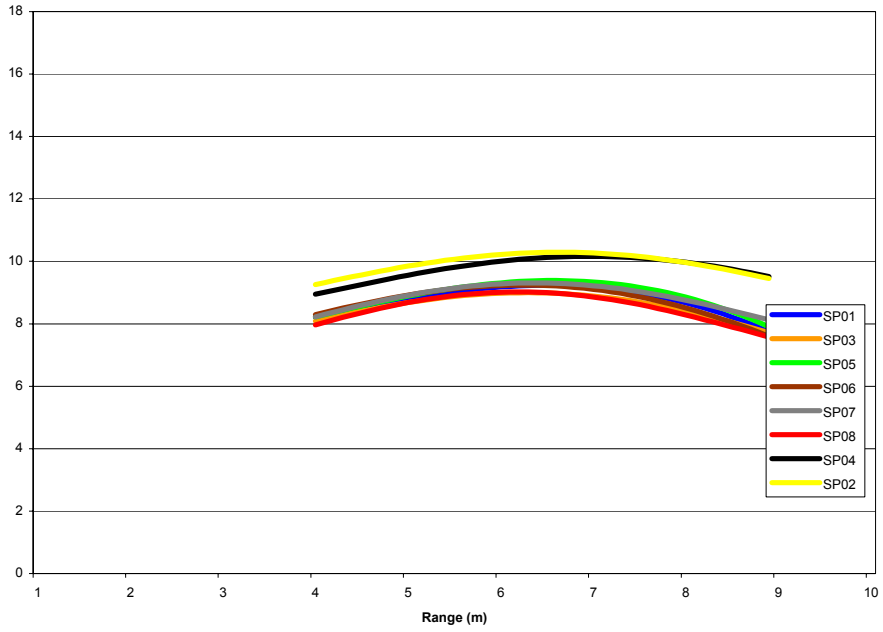
**Summer Night
Spillway Gate 4**



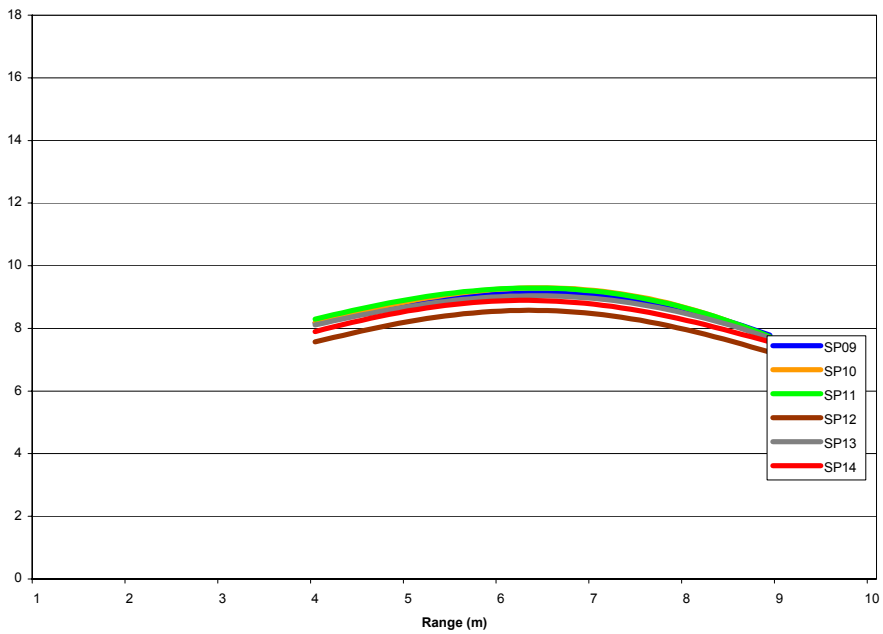
**Summer Night
Spillway Gate 4**



**Summer Night
Spillway Gate 5**



**Summer Night
Spillway Gate 5**



Appendix F

Post Tracking Filters

By Kenneth D. Ham

Filters were developed to eliminate traces having trace statistics inconsistent with a smolt-sized fish committed to passing the dam by the monitored route. Filters were based upon fields contained in the track statistics output by the autotracker. With the exception of the sluice, all filters were based upon fields available in single beam outputs. All transducers deployed on the sluiceway were split-beam, so filters for sluice passage could also include fields available only from split-beam outputs.

Table 1. Fields used in filtering traces.

Field Name	Explanation
ECHO_COUNT	Number of echoes in track
LAST_RANGE	Range in m of last echo
LINEARITY1	Root mean squared error for a straight line fit
MAX_RUN	Maximum number of contiguous echoes
MEAN_ECHO_STRENGTH	Mean echo strength
NOISE_COUNT_AVERAGE	Noise Count / Track echo count
PLUNGE	Angle relative to a tangent of the beam axis in the YZ plane (split beams only)
SLOPE	(last range- first range)/(last relative ping- first relative ping)
SPEED	Speed of the target m per sec (split beams only)
TRACK_TYPE	0 if normal, 1 if flat track near clutter
XANGLE1	X phase angle of first echo
XANGLE2	X phase angle of last echo
YANGLE1	Y phase angle of first echo
YANGLE2	Y phase angle of last echo

Table 2. Operators used in filtering traces

Operator	Function
=	Equal
<>	not equal
>	greater than
<	less than
>=	greater than or equal
<=	less than or equal
Abs(value)	The filter will use absolute value of the variable in parenthesis.

Table 3. Trace filters by deployment type.

Deployment	Filter
All Deployments	TRACK_TYPE = 0 $(\text{NOISE_COUNT_AVERAGE} * \text{ECHO_COUNT}) / ((\text{ECHO_COUNT} + 10) * 5) < 0.35$ MAX_RUN > 3 MEAN_ECHO_STRENGTH < -35.0 MEAN_ECHO_STRENGTH > -54 LINEARITY1/ECHO_COUNT < 0.25
Intake Downlooker	ECHO_COUNT < 30 SLOPE > 0.35 SLOPE < 1 LAST_RANGE >= 13.0 (Occluded only)
Intake Uplooker	ECHO_COUNT < 30 ABS(SLOPE) < 1 SLOPE > 0 LAST_RANGE < 14 OR SLOPE < 0.2
Spill	LAST_RANGE >= 7 SLOPE >= 0.5 SLOPE < 4 ECHO_COUNT < 20 ECHO_COUNT > 5
Sluice	ECHO_COUNT < 60 YANGLE1*YANGLE2 < 0 $(\text{YANGLE1} - \text{YANGLE2}) > \text{ABS}(\text{XANGLE1} - \text{XANGLE2})$ ABS(SLOPE) < 0.5 PLUNGE > -25 PLUNGE < 38 SPEED < 1.4 SPEED > 0.2 LAST_RANGE >= 13 (Occluded only) MUX_CHANNEL <> 2 OR LAST_RANGE >= 16 (Unoccluded Only) MUX_CHANNEL <> 3 OR LAST_RANGE >= 17 (Unoccluded Only) MUX_CHANNEL <> 1 OR LAST_RANGE >= 18 (Unoccluded Only)

Appendix G

Sensitivity Analysis For Fixed-Location Hydroacoustics

DRAFT FINAL REPORT

Prepared by

K. D. Ham

Pacific Northwest National Laboratory, Richland, Washington

March 2002

1.0 Introduction

1.1 Background

The U.S. Army Corps of Engineers (Corps) utilizes fixed-location hydroacoustics for estimating downstream fish passage at many of its projects in the Columbia River Basin. Fish passing through the hydroacoustic beam produce a series of echoes that form a track. The number of target tracks detected is a function of sensor and deployment characteristics as well as the criteria used for track selection. Under the acoustic screen model, the number of tracks within the beam is expanded spatially and temporally to represent total passage through a single route, such as a turbine intake or spillbay.

Johnson (2000) found that detectability modeling was an influential part of the acoustic screen model. The detectability of target tracks must be estimated to convert counts to an estimate of passage. Detectability is a function of target acoustic characteristics and target dynamics. There are two potential sources of information on dynamics within the hydroacoustic beam: flow models and split-beam transducers. Flow models compute flow velocities and trajectories along the beam axis and, if fish behavior is considered negligible, it can be assumed those are similar to mean target dynamics. Split beam sensors can measure the dynamics and certain acoustic characteristics of targets detected within the beam area. The track characteristics can then be summarized in terms of target strengths, velocities and trajectories along the beam axis.

There is a wide range of options on how hydroacoustic sensors are installed and set up. The deployment of each sensor is matched to its location and the assumed target characteristics at that location. Parameters such as ping rate, minimum and maximum target strength thresholds and sampling scheme are set by the user and can affect the apparent acoustic characteristics and dynamics of targets. Detectability can be altered as a result of sensor deployment.

The target characteristics, target dynamics, and track selection criteria are entered into the detectability model to compute effective beam widths. Effective beam widths are used to correct spatial expansion factors involved in estimates of fish passage. Any error in model inputs has the potential to alter passage estimates. By artificially introducing error into the model, it is possible to evaluate the sensitivity of the model to changes in input parameters. Input parameters will be ranked by their relative potential to influence the estimate of fish passage. The ranking of inputs will indicate where greater accuracy in model inputs would be most effective in providing robust estimates of passage.

1.2 Goal and Objectives

The goal of this study was to evaluate which factors have the greatest potential to influence estimates of fish passage. The specific objectives of this study were to:

- Compare the influence of detectability model inputs on passage estimates.

- Rank detectability model inputs by their potential to alter estimates.
- Compare accuracy and precision of human and automated target track selection.

2.0 Methods

2.1 Study Design

The varied deployments at the Dalles Dam in 2001 were selected as representative of the majority of deployment types used to estimate passage at Columbia River hydropower projects operated by the Corps of Engineers. Typical fixed-location hydroacoustic techniques were used to sample passage at the spillway, sluiceway, and turbine intakes. Deployment characteristics were averaged across diel periods and seasons to create a set of 5 typical deployment types for sensitivity analysis. The types were: intake up-looker, intake down-looker, spill, sluice unoccluded, and sluice occluded.

Each deployment type had a set of average input values that were used to model detectability. Introducing realistic ranges of error into the detectability model input parameters and ranking the influence of the inputs evaluated the relative sensitivity of the model to each input.

2.2 Hydroacoustic Systems and Transducer Deployments

A combination of 6° and 12° split-beam transducers were deployed. Split-beam data collection included three PAS split-beam systems, with two systems being multiplexed. All of these systems operated at 420 kHz. The split-beam data collection system required Harp-SB Split-Beam Data Acquisition/Signal Processing Software controlling a PAS-103 Split-Beam Multi-Mode Scientific Sounder. The PAS-103 Sounder then communicated with a PAS-203 Split-Beam Remote 4-Channel Transducer Multiplexer through a PAS-201 Split-Beam Local 3-Channel Multiplexer linked directly to the PAS-103 sounder. Finally, the PAS-203 Remote Transducer Multiplexer multiplexed a maximum of 4 PAS 420 kHz Split-Beam Transducers deployed in a main turbine unit or spillbay. The PAS-201 Split-Beam Local 3-Channel Multiplexer was required only for the system monitoring locations subject to occluded and unoccluded treatment since different transducers were used during each treatment.

2.2.1 Powerhouse

Experiments conducted in 2001 were designed to evaluate the effectiveness of occlusion plates at some of the turbine units in occluded and unoccluded configurations. In main turbine units during unoccluded treatments, passage was sampled with an up-looking transducer attached to the inside of the trash rack at an elevation of 75 feet, aimed downstream at a 31° angle to the plane of the trash rack looking towards the intake ceiling (Figure 1). These deployments are typical of the powerhouse units where occlusion plates are not currently used. During occluded treatments passage was sampled with a down-looking transducer attached to the inside of the trash rack at an elevation of 135 feet, aimed downstream at a 15° angle to the plane of the trash rack looking towards the bottom (Figure 2). Transducers were 6° split-beams sampling at 15 pings per second for 1 minute, 15 times each hour.

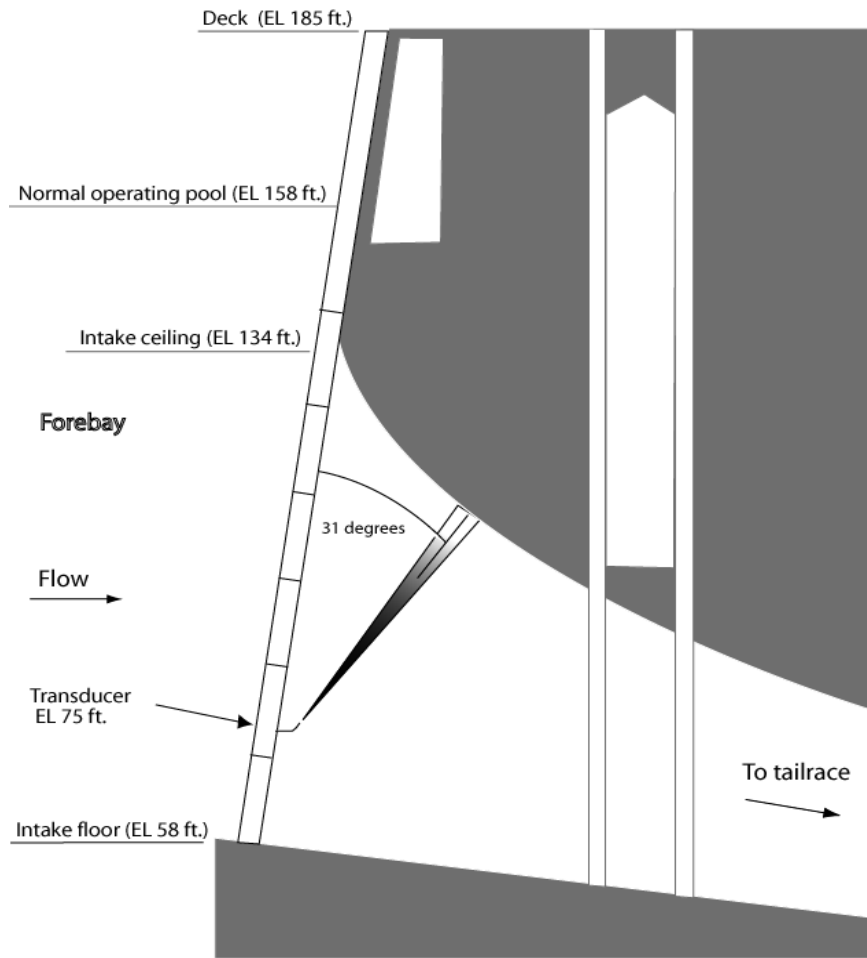


Figure 1. Intake up-looking transducer.

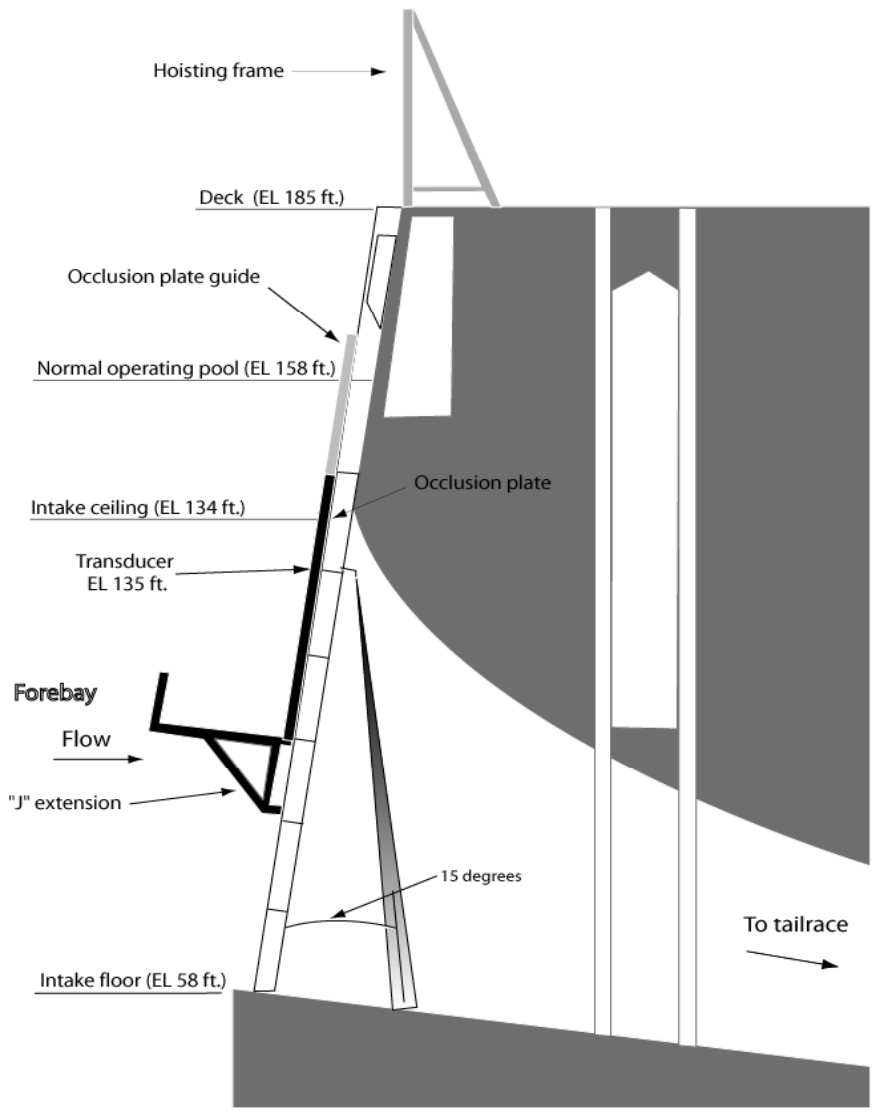


Figure 2. Intake down-looking transducer.

2.2.2 Sluiceway

The sluiceway opening at main unit 1 was monitored at each of three intake slots using 6 split-beam transducers. In order to monitor both occluded and unoccluded treatments, there were 2 transducers in each slot of main unit 1. For the unoccluded treatments, transducers were attached to the outside of the trash rack at an elevation of 95 feet, aimed upstream at a 5° angle to the plane of the trash rack looking up towards the intake ceiling (Figure 3). For the occluded treatments, the corresponding transducer was attached to the upstream side of the occlusion plate at an elevation of 110 feet, aimed upstream at a 5° angle to the plane of the trash rack looking up towards the forebay water surface (Figure 4). Transducers were 6° split beams with 15 pings per second, sampling for 1-minute intervals, 15 times per hour.

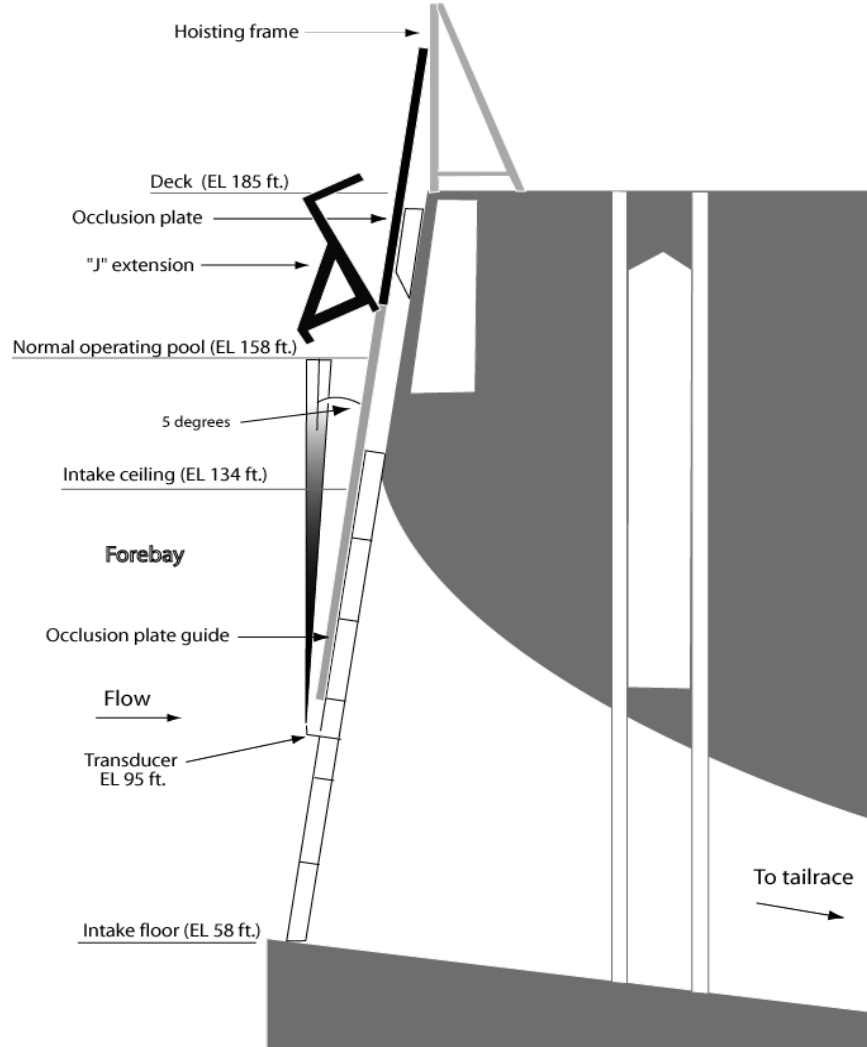


Figure 3. Unoccluded sluiceway transducer.

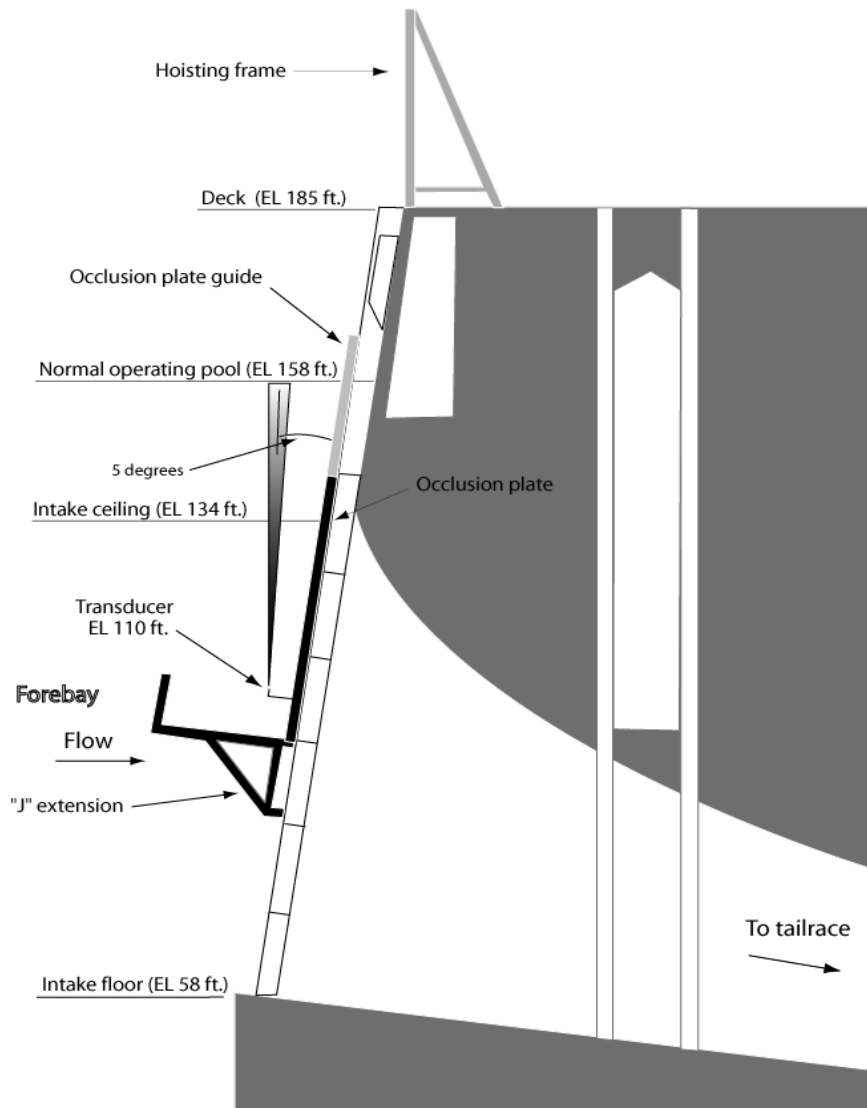


Figure 4. Occluded sluiceway transducer.

2.2.3 Spillway

A pole mount design was used for split-beam deployment. Each transducer was looking down and aimed downstream towards the tainter gate at an 8° angle to a vertical plane. Transducers were 12° split-beams, sampling at a rate of 20 pings per second, for 1-minute time intervals, 15 times per hour.

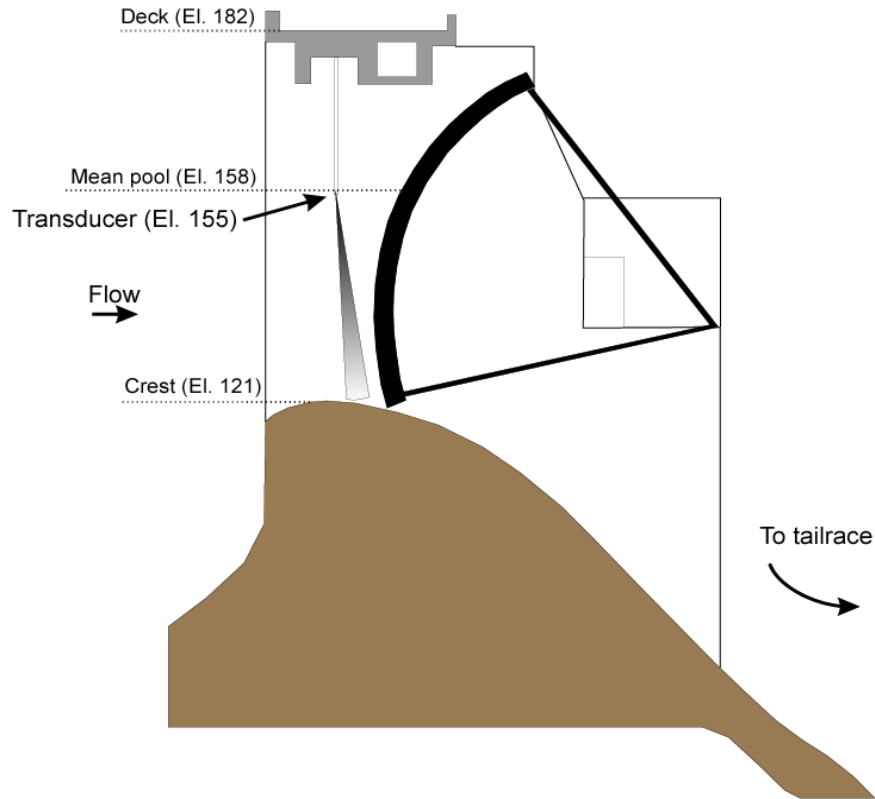


Figure 5. Typical spill bay transducer deployment at The Dalles Dam, 2001.

2.3 Detectability Modeling

Effective beam width was estimated by Monte Carlo simulation of fish passing through the beam as specified by the input parameters. Mean fish velocities, trajectories, and target strengths were computed for each meter range of each deployment type to compute a baseline of detectability as effective beam width versus range. These relationships are the “no error” case for each deployment and are plotted in Figure 6. Ideally, effective beam widths would be near 6 degrees for all deployment types except spill, which would be 12 degrees. It is normal practice to use the differences between the nominal and the effective beam width to adjust the expansion of target tracks. The differences are of concern only where effective beam widths become very small, because that indicates the estimate will be based upon few tracks expanded many times. The low effective beam widths at ranges nearest the transducer for the intake deployments indicates that the ping rates were probably not sufficient for the target velocities in

those regions, given the small tangential width of the beam at that range. Otherwise, the detectability curves do not suggest any problem.

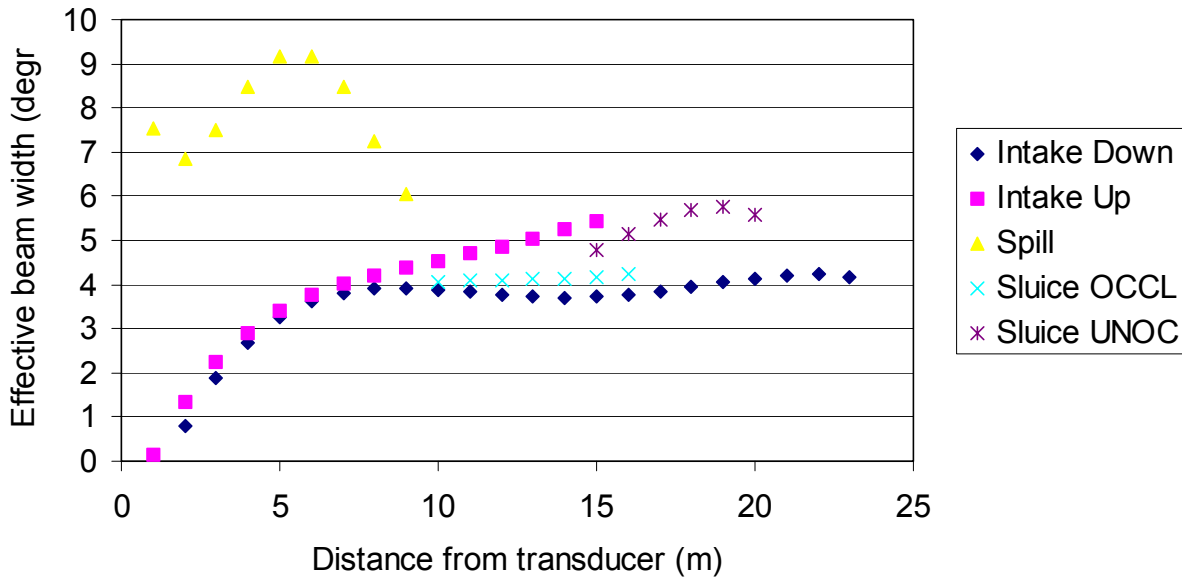


Figure 6. Estimated effective beam widths for each deployment type.

2.4 Sensitivity Analysis

2.4.1 Input Error Ranges

There are many inputs to the detectability model, but a limited set was selected due to their potential error range. The set includes the mean target strength of the species of interest, the standard deviation of target strength, the correlation of target strength among echoes within track, the velocity in YZ plane, the trajectory in YZ plane, the beam pattern, and the mounting angle of the transducer. The YZ plane is a plane that slices through the beam axis perpendicular to the dam. A fish moving in the Y-axis would be moving toward or away from the dam and a fish moving in the Z-axis would be moving toward or away from the transducer.

To evaluate the influence of each input, it is necessary to vary it over a realistic range. The range includes potential measurement errors and other uncertainties that prevent accurate modeling of detectability. Table 1 shows the ranges that were applied relative to the mean. Target strength correlation was varied across its entire potential range, because we have few reliable estimates of the mean value. Ranges were established through discussion with researchers working at Columbia River dams.

Table 1. Range of uncertainty simulated for representative deployments.

Parameter	Low	High
Velocity	-0.2 m/sec	+0.5 m/sec
Beam angle relative to flow	-5 degrees	+5 degrees
Target strength	-95% CI	+95% CI
Target strength variability	-2 dB	+2 dB
Target strength correlation	0	1
Beam pattern	-0.25dB	+0.25dB

2.4.2 Sensitivity Analysis Tools

Sensitivity analysis iterations were conducted using the MEPAS Sensitivity/Uncertainty Module (SUM³), version 1.2 (<http://mepas.pnl.gov:2080/earth/>). SUM³ is a statistical interface allowing users to conduct sensitivity and uncertainty analysis using deterministic models. Sensitivity analysis allows the user to identifying the parameters that impact the results the most. This model uses the Latin Hypercube sampling technique to create an efficient set of iterations encompassing the error range of all parameters for examining correlations of inputs with model output. Partial correlations were computed from SUM³ outputs using Statistica version 6.0 (www.statsoft.com).

2.4.3 Sensitivity Analysis

Input parameters and their respective error ranges were arranged in a Latin hypercube design for efficient simulation. 100 iterations were run for each deployment type with 20,000 fish simulated in each. To summarize the detectability curve, the beam width was integrated across the sample range to form a beam area. Conceptually, an incorrect model input could result in a larger estimated beam area than the true beam area. Such an error could result in a smaller expansion of detected tracks, reducing the passage estimate.

The partial correlations of beam area to input parameters were compared to rank their potential to influence beam area and, by extension, passage estimates. Higher partial correlations indicate a greater range of outputs across the error range for that input.

3.0 Results

The most influential input parameters for all deployment types were target strength correlation and velocity (Table 2). The next most influential input parameter across all deployment types was target strength standard deviation. Fish trajectory angle and beam pattern were significant for spill and intake deployments. Target strength was significant for intake up-looker and sluice deployments. Deployment angle was significant only for intake deployments.

Table 2. Partial Correlations of input parameters with beam area.

	Spill		Intake Downlooker		Intake uplooker		Sluice occluded		Sluice unoccluded	
	Partial Corr.	p	Partial Corr.	p	Partial Corr.	p	Partial Corr.	P	Partial Corr.	p
Target strength	-0.12	0.27	-0.15	0.15	-0.21	0.04	-0.27	<0.01	-0.26	0.01
SD of target strength	-0.47	<0.01	-0.52	<0.01	-0.72	<0.01	-0.43	<0.01	-0.45	<0.01
TS correlation	-0.93	<0.01	-0.92	<0.01	-0.83	<0.01	-0.88	<0.01	-0.94	<0.01
Track speed	-0.86	<0.01	-0.91	<0.01	-0.95	<0.01	-0.75	<0.01	-0.78	<0.01
Track angle	0.53	<0.01	0.43	<0.01	0.45	<0.01	0.18	0.09	0.15	0.16
Beam pattern	0.49	<0.01	0.45	<0.01	0.59	<0.01	0.20	0.06	0.19	0.07
Mounting angle	0.19	0.07	0.21	0.04	0.24	0.02	0.06	0.57	0.00	1.00

4.0 Discussion

The potential error range of detectability model inputs representing both target track dynamics and acoustic characteristics of targets can influence fish passage estimates. Target strength correlation was especially influential in these comparisons, but that is partially a result of uncertainty in the mean value. The uncertainty caused us to expand the error range to include the entire possible range. To mitigate the influence of this input, it is necessary to establish the mean and error range for each deployment.

Velocity was very influential in the detectability model. To lessen the error for this variable, it will be necessary to estimate fish velocities more precisely. There are several ways to accomplish this goal. Velocity estimates would be more precise if ping rates were increased, all else being equal. Velocity could be estimated more precisely if the amount of split-beam sampling was increased. Avoiding tracks in noise could lessen the perturbation of phase information, allowing a more precise estimate of the position of the fish at each ping. Flow model information might also improve velocity estimates where detectability is low. Fish traveling at high velocities might fail to be detected, but flow information could be used to adjust upward the velocity used for detectability modeling. This might result in a more realistic expansion of detected tracks.

Standard deviation of target strength was also influential across all deployment types. The standard deviation of target strengths could be computed more precisely by avoiding tracks in noise. Noise decreases the precision of phase information upon which the computation of target strengths is based. A higher ping rate might also provide a more precise estimate of target strength standard deviation.

Fish trajectory angle was influential for spill and intake deployment types. The methods suggested above for improving velocity estimates could also improve trajectory angle estimates. Both are based upon similar information.

Beam pattern was influential for spill and intake deployment types. Much of the error in beam pattern information is involved in selecting numbers from a plot. If calibration information were digitized while being plotted, very little imprecision would remain.

Mean target strength was influential for intake up-looker and sluice deployments. Target strength could be measured more precisely by increasing the amount of split beam sampling and by avoiding tracks in noise.

Deployment angle was influential only for the intake deployments. Deployment angle is measured very precisely now, but intake deployments are having difficulty detecting fish close to the transducer. A change in deployment angle can improve detectability if tracks cross the beam at a more oblique angle and spend more time in the beam. These effects would be lessened by a higher ping rate.

5.0 Conclusions and Recommendations

The current investigation has indicated several ways to improve the robustness of hydroacoustic fish passage estimates:

- Higher ping rates could reduce uncertainty in parameters that represent track dynamics.
- Increased collection of split beam data could improve mean estimates of all parameters by increasing sample size.
- Avoiding tracks near noise would improve phase angle information, allowing velocities, angles, and target strengths to be measured more precisely.

6.0 References

Johnson GE. 2000. *Assessment of the acoustic screen model to estimate smolt passage rates at dams: case study at The Dalles Dam in 1999*. Prepared for the U.S. Army Corps of Engineers, Waterways Experiment Station, Vicksburg, Mississippi.

Appendix H

Revised Draft
Statistical Synopsis
for the 2001 Hydroacoustic Investigations
at The Dalles Dam

Prepared for:
Russell A. Moursund
Battelle
Pacific Northwest National Lab
P.O. Box 999 / MS K6-85
Richland, WA 99352

Prepared by:
John R. Skalski
Columbia Basin Research
School of Aquatic and Fishery Sciences
University of Washington
1325 Fourth Avenue, Suite 1820
Seattle, Washington 98101

10 October 2001

1.0 Introduction

The purpose of this synopsis is to describe the statistical methods to be used in the analysis of the 2001 hydroacoustic study at The Dalles Dam. The study will estimate fish passage through the powerhouse (i.e., turbines), spillway, fish units, and sluiceway during the spring smolt outmigration. These estimates of fish passage will be used to estimate various measures of spillbay and sluiceway passage performance at The Dalles Dam. The spillway and sluiceway performance measures will be used to test the effect of the J-occlusion plates at turbine units 1-5 on diverting smolts from the turbine intakes at The Dalles Dam.

2.0 Transducer Deployment and Sampling Scheme

This section describes the hydroacoustic sampling schemes that were used to estimate smolt passage at the powerhouse, spillway, sluiceway, and fish units at The Dalles Dam.

2.1 Sampling at Powerhouse

The Dalles powerhouse has 22 turbine units, each with 3 turbine intake slots. At each turbine unit, 1 of 3 intake slots was randomly selected for hydroacoustic monitoring. The selected intake slots were sampled 24 hrs daily throughout the study period. Within an hour at an intake slot, fish passage was systematically sampling over time. The sampling effort within an hour at the various intake slots is summarized below:

Turbine Units	Sampling Effort
1-5	10 1-min samples/hr
6-22	15 1-min samples/hr

2.2 Sampling at Spillway

The Dalles Dam has 23 spillbays within the spillway. During 2001, only spillbays 1-14 were open during all or part of the study period. At each spillbay, a transducer was randomly located across the breadth of the opening (i.e., left, right, or center) to monitor fish passage. Hence, 14 of 14 spillbays were monitored during the study. Hydroacoustic monitoring was conducted 24 hrs daily throughout the study. Within an hour at a spillbay, fish passage was

systematically sampled over time. The within-hour sampling effort was either 10 1-min samples/hr or 15 1-min samples/hr collected systematically over time depending on spillbay location.

2.3 Sampling at Sluiceway

Only the skimmer gates above turbine unit 1 were open during the 2001 study. The sluiceway has 3 intakes; each were sampled with a separate transducer. Hydroacoustic monitoring was conducted 24 hrs daily throughout the study. Within-hour sampling effort was 15 1-min samples/hr collected systematically over time.

2.4 Sampling at Fish Units

There are 2 fish units at The Dalles Dam, each with 2 intakes. During the 2001 study, 1 of 2 intake slots was randomly selected for hydroacoustic monitoring. The selected intakes were sampled 24 hrs daily throughout the study period. Within an hour at an intake slot, fish passage was systematically sampled over time. The sampling effort within an hour at each intake slot was 10 1-min samples/hr.

3.0 Estimating Fish Passage

The following sections describe how the estimates of smolt passage will be calculated at the various locations at The Dalles Dam.

3.1 Powerhouse Passage

The sampling at The Dalles powerhouse turbines can be envisioned as a stratified two-stage sampling program. Constructing spatial strata by combining adjacent turbine units, the first step was the random sampling of turbine intake slots within adjacent turbine units. In practice, 1 of 3 turbine intake slots was actually randomly selected within each turbine unit. Assuming a random selection of a of A intake slots among adjacent turbine units will tend to overestimate the true sampling variance.

One difficulty induced by the low-flow conditions in 2001 was that not all turbine units were operational at any one time. The consequence is that post-stratification will be necessary

to form strata by combining adjacent turbine units actually operating that hour. Hence, the number and size of the individual turbine strata may change from hour to hour.

Another complication of the 2001 season was that there was occasional downtime for some of the turbine slot transducers. Hence, two alternative estimation schemes were needed; one estimator under nominal conditions, another to provide estimates during transducer downtime. Nominally, within a slot-hour, the sampling will be assumed to be a simple random sample, although, in practice, systematic sampling was employed. During downtime, a ratio-estimator will be used to estimate missing values as described below.

The estimator of total turbine passage over the course of D days can be expressed as follows

$$\hat{T} = \sum_{i=1}^D \sum_{j=1}^{24} \sum_{k=1}^{K_{ij}} \left[\frac{A_{ijk}}{a_{ijk}} \left[\sum_{l=1}^{a_{ijk}} \hat{T}_{ijkl} \right] \right] \quad (1)$$

where

\hat{T}_{ijkl} = estimated fish passage in the l th intake slot ($l = 1, \dots, a_{ijk}$) within the k th turbine stratum ($k = 1, \dots, K_{ij}$) during the j th hour ($j = 1, \dots, 24$) on the i th day ($i = 1, \dots, D$);

a_{ijk} = number of intake slots actually sampled in the k th turbine stratum ($k = 1, \dots, K_{ij}$) during the j th hour ($j = 1, \dots, 24$) on the i th day ($i = 1, \dots, D$);

A_{ijk} = total number of intake slots within the k th turbine stratum ($k = 1, \dots, K_{ij}$) during the j th hour ($j = 1, \dots, 24$) on the i th day ($i = 1, \dots, D$);

K_{ij} = number of turbine strata created during the j th hour ($j = 1, \dots, 24$) on the i th day ($i = 1, \dots, D$).

Because of the varying power loads over time, the number of spatial strata (i.e., K_{ij}) formed by post-stratification of adjacent turbine units may vary between hours ($j = 1, \dots, 24$) and days ($i = 1, \dots, D$).

Under nominal conditions, the estimate of \hat{T}_{ijkl} would be based on the assumption of simple random sampling within a slot-hour, in which case

$$\hat{T}_{ijkl} = \frac{B_{ijkl}}{b_{ijkl}} \sum_{g=1}^{b_{ijkl}} w_{ijklg} \quad (2)$$

where

w_{ijklg} = expanded fish passage in the g th sampling unit ($g = 1, \dots, b_{ijkl}$) in the l th intake slot ($l = 1, \dots, a_{ijk}$) within the k th turbine stratum ($k = 1, \dots, K_{ij}$) during the j th hour ($j = 1, \dots, 24$) on the i th day ($i = 1, \dots, D$);

b_{ijkl} = number of sampling units actually observed in the l th intake slot ($l = 1, \dots, a_{ijk}$) within the k th turbine stratum ($k = 1, \dots, K_{ij}$) during the j th hour ($j = 1, \dots, 24$) on the i th day ($i = 1, \dots, D$);

B_{ijkl} = total number of sampling units within the l th intake slot ($l = 1, \dots, a_{ijk}$) within the k th turbine stratum ($k = 1, \dots, K_{ij}$) during the j th hour ($j = 1, \dots, 24$) on the i th day ($i = 1, \dots, D$).

Nominally, $B_{ijkl} = 60 \forall ijkl$ and $b_{ijkl} = 10$ or 15 , depending on location. Based on the assumption of simple random sampling

$$\widehat{Var}(\hat{T}_{ijkl}) = \frac{B_{ijkl}^2 \left(1 - \frac{b_{ijkl}}{B_{ijkl}}\right) s_{ijkl}^2}{b_{ijkl}} \quad (3)$$

where

$$s_{w_{ijkl}}^2 = \frac{\sum_{g=1}^{b_{ijkl}} (w_{ijklg} - \overline{w_{ijkl}})^2}{(b_{ijkl} - 1)}$$

and where

$$\overline{w_{ijkl}} = \frac{1}{b_{ijkl}} \sum_{g=1}^{b_{ijkl}} w_{ijklg} .$$

In circumstances where the uplooking transducer within a turbine intake slot was inoperable, data from the downlooking transducer within the same unit can be used to help estimate smolt passage (Figure 1). Using solely the data from the downlooking transducers is inappropriate, because the acoustic beam will miss most of the smolts that pass in the upper part of the water column. Instead, a ratio estimator will be used to estimate the smolt passage that would likely have been observed if the uplooking transducer had been available. The estimate of smolt passage can then be calculated as follows:

$$\tilde{T}_{ijkl} = \frac{\hat{C}_{ijkl}}{\left(\frac{\hat{D}_{ijkl}}{\hat{D}_{ijkl} + \hat{U}_{ijkl}} \right)} \quad (4)$$

where

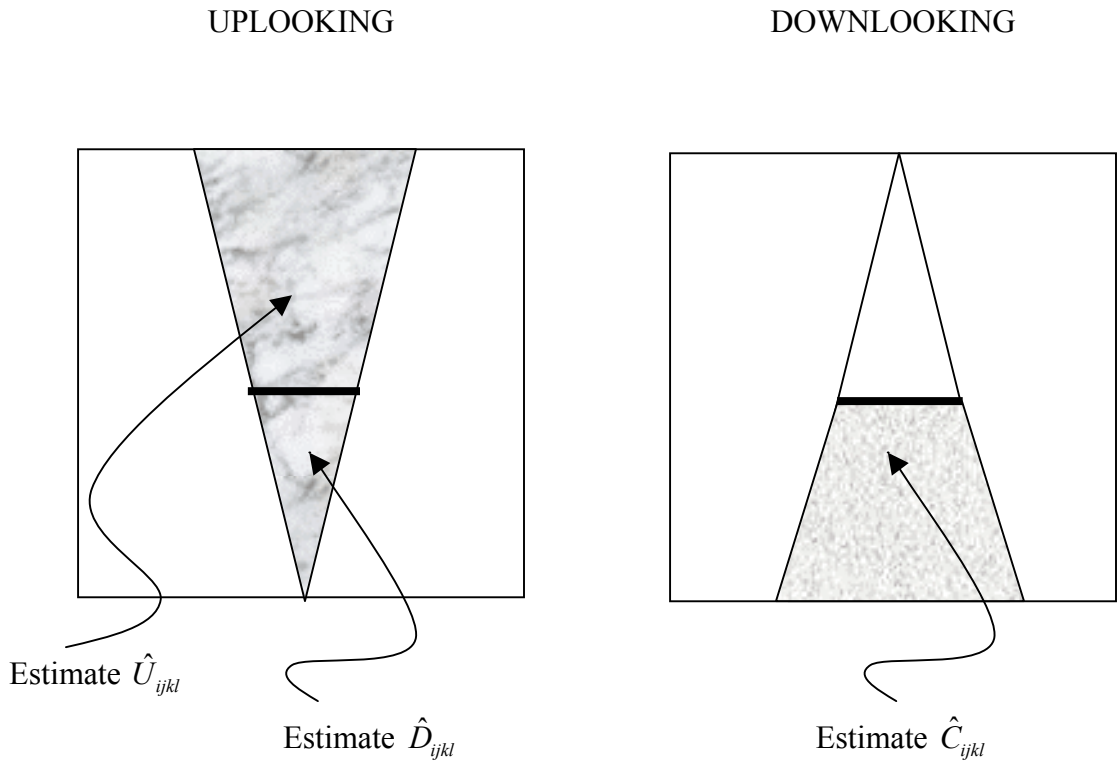
$$\hat{C}_{ijkl} = \frac{B_{ijkl}}{b_{ijkl}} \sum_{g=1}^{b_{ijkl}} c_{ijklg} ,$$

$$\hat{D}_{ijkl} = \sum_{g=1}^{b_{ijkl}} d_{ijklg} ,$$

$$\hat{U}_{ijkl} = \sum_{g=1}^{b_{ijkl}} u_{ijklg} ,$$

and where

Figure 3-1. Schematic of the data used in the ratio estimator for turbine slot passage when missing uplooking transducer data.



\hat{C}_{ijkl} = expanded fish count in the g th sampling unit ($g = 1, \dots, b_{ijkl}$) in the the l th intake slot ($l = 1, \dots, a_{ijk}$) within the k th turbine stratum ($k = 1, \dots, K_{ij}$) during the j th hour ($j = 1, \dots, 24$) on the i th day ($i = 1, \dots, D$) for the downlooking transducer;

d_{ijklg} = expanded fish count in the g th sampling unit ($g = 1, \dots, b_{ijkl}$) in the the l th intake slot ($l = 1, \dots, a_{ijk}$) within the k th turbine stratum ($k = 1, \dots, K_{ij}$) during the j th hour ($j = 1, \dots, 24$) on the i th day ($i = 1, \dots, D$) for the uplooking transducer in the lower portion of the beam during adjacent times;

u_{ijklg} = expanded fish count in the g th sampling unit ($g = 1, \dots, b_{ijkl}$) in the l th intake slot ($l = 1, \dots, a_{ijk}$) within the k th turbine stratum ($k = 1, \dots, K_{ij}$) during the j th hour ($j = 1, \dots, 24$) on the i th day ($i = 1, \dots, D$) for the uplooking transducer in the upper portion of the beam during adjacent times.

Strategic times when the uplooking transducer was operational need to be selected to estimate the proportion of smolts passing through the lower proportion of the acoustic beam.

The variance of \tilde{T}_{ijkl} can be approximated by the delta method as

$$\begin{aligned} \widehat{Var}(\tilde{T}_{ijkl}) = & \widehat{Var}(\hat{C}_{ijkl}) \left(\frac{\hat{D}_{ijkl} + \hat{U}_{ijkl}}{\hat{D}_{ijkl}} \right)^2 + \widehat{Var}(\hat{U}_{ijkl}) \left(\frac{\hat{C}_{ijkl}}{\hat{D}_{ijkl}} \right)^2 \\ & + \widehat{Var}(\hat{D}_{ijkl}) \left(\frac{\hat{U}_{ijkl} \cdot \hat{C}_{ijkl}}{\hat{D}_{ijkl}^2} \right)^2 - 2 \text{Cov}(\hat{D}_{ijkl}, \hat{U}_{ijkl}) \left(\frac{\hat{U}_{ijkl} \cdot \hat{C}_{ijkl}^2}{\hat{D}_{ijkl}^3} \right). \end{aligned} \quad (5)$$

In turn,

$$\widehat{Var}(\hat{C}_{ijkl}) = \frac{B_{ijkl}^2 \left(1 - \frac{b_{ijkl}}{B_{ijkl}} \right) s_{c_{ijkl}}^2}{b_{ijkl}}$$

where

$$s_{c_{ijkl}}^2 = \frac{\sum_{g=1}^{b_{ijkl}} (c_{ijklg} - \bar{c}_{ijkl})^2}{(b_{ijkl} - 1)},$$

$$\bar{c}_{ijkl} = \frac{1}{b_{ijkl}} \sum_{g=1}^{b_{ijkl}} c_{ijklg}.$$

Similarly,

$$\widehat{Var}(\hat{D}_{ijkl}) = \frac{B_{ijkl}^2 \left(1 - \frac{b_{ijkl}}{B_{ijkl}}\right) s_{d_{ijkl}}^2}{b_{ijkl}}$$

where

$$s_{d_{ijkl}}^2 = \frac{\sum_{g=1}^{b_{ijkl}} (d_{ijklg} - \bar{d}_{ijkl})^2}{(b_{ijkl} - 1)},$$

$$\bar{d}_{ijkl} = \frac{1}{b_{ijkl}} \sum_{g=1}^{b_{ijkl}} d_{ijklg}.$$

The $\widehat{Var}(\hat{U}_{ijkl})$ is estimated analogously to the above calculations $\widehat{Var}(\hat{D}_{ijkl})$. The covariance is estimated as follows:

$$\widehat{Cov}(\hat{D}_{ijkl}, \hat{U}_{ijkl}) = \frac{B_{ijkl}^2 \left(1 - \frac{b_{ijkl}}{B_{ijkl}}\right) \widehat{Cov}(d_{ijklg}, u_{ijklg})}{b_{ijkl}}$$

and where

$$\widehat{Cov}(d_{ijklg}, u_{ijklg}) = \frac{\sum_{g=1}^{b_{ijkl}} (d_{ijklg} - \bar{d}_{ijkl})(u_{ijklg} - \bar{u}_{ijkl})}{(b_{ijkl} - 1)}.$$

Returning to the overall estimate of turbine passage (\hat{T}) in Equation (1), the estimate is based on the use of \hat{T}_{ijkl} and \tilde{T}_{ijkl} as appropriate. The variance of \hat{T} can then be estimated by the formula

$$\widehat{Var}(\hat{T}) = \sum_{i=1}^D \sum_{j=1}^{24} \sum_{k=1}^{K_{ij}} \left[\frac{A_{ijk}^2 \left(1 - \frac{a_{ijk}}{A_{ijk}}\right) s_{\hat{T}_{ijk}}^2}{a_{ijk}} + \frac{A_{ijk} \sum_{l=1}^{a_{ijk}} \widehat{Var}(\hat{T}_{ijkl})}{a_{ijk}} \right] \quad (6)$$

where

$$s_{\hat{T}_{ijk}}^2 = \frac{\sum_{l=1}^{a_{ijk}} (\hat{T}_{ijkl} - \hat{T}_{ijk})^2}{(a_{ijk} - 1)},$$

$$\hat{T}_{ijk} = \frac{1}{a_{ijk}} \sum_{l=1}^{a_{ijk}} \hat{T}_{ijkl}.$$

3.2 Spillway Passage

The sampling at The Dalles spillway can be envisioned as stratified random sampling within spillbay-hours. In which case, total spillway passage over D days can be estimated by the formula

$$\widehat{SP} = \sum_{i=1}^D \sum_{j=1}^{24} \sum_{k=1}^{14} \left[\frac{T_{ijk}}{t_{ijk}} \sum_{l=1}^{t_{ijk}} x_{ijkl} \right] \quad (7)$$

where

x_{ijkl} = expanded fish passage in the l th sampling interval ($l = 1, \dots, t_{ijk}$) during the j th hour ($j = 1, \dots, 24$) at the k th spillbay ($k = 1, \dots, 14$) on the i th day ($i = 1, \dots, D$);

T_{ijk} = total number of sampling units within the j th hour ($j = 1, \dots, 24$) at the k th spillbay ($k = 1, \dots, 14$) on the i th day ($i = 1, \dots, D$);

t_{ijk} = actual number of sampling units observed within the j th hour ($j = 1, \dots, 24$) at the k th spillbay ($k = 1, \dots, 14$) on the i th day ($i = 1, \dots, D$).

Nominally, $T_{ijk} = 60 \forall ijk$ and $t_{ijk} = 10$ or 15 .

The variance of \widehat{SP} can be estimated by the quantity

$$\widehat{Var}(\widehat{SP}) = \sum_{i=1}^D \sum_{j=1}^{24} \sum_{k=1}^{14} \left[\frac{T_{ijk}^2 \left(1 - \frac{t_{ijk}}{T_{ijk}}\right) s_{x_{ijk}}^2}{t_{ijk}} \right] \quad (8)$$

where

$$s_{x_{ijk}}^2 = \frac{\sum_{l=1}^{t_{ijk}} (x_{ijkl} - \bar{x}_{ijk})^2}{(t_{ijk} - 1)}$$

and where

$$\bar{x}_{ijk} = \frac{1}{t_{ijk}} \sum_{l=1}^{t_{ijk}} x_{ijkl} .$$

3.3 Sluiceway Passage

The sampling at The Dalles sluiceway can be envisioned as stratified random sampling within sluiceway slots. In which case, total sluiceway passage over D days can be estimated by the formula

$$\widehat{SL} = \sum_{i=1}^D \sum_{j=1}^{24} \sum_{k=1}^3 \left[\frac{H_{ijk}}{h_{ijk}} \sum_{l=1}^{h_{ijk}} y_{ijkl} \right] \quad (9)$$

where

y_{ijkl} = expanded fish passage in the l th sampling interval ($l = 1, \dots, h_{ijk}$) during the j th hour ($j = 1, \dots, 24$) at the k th sluiceway slot ($k = 1, \dots, 3$) on the i th day ($i = 1, \dots, D$);

H_{ijk} = total number of sampling units within the j th hour ($j = 1, \dots, 24$) at the k th sluiceway slot ($k = 1, \dots, 3$) on the i th day ($i = 1, \dots, D$);

h_{ijk} = actual number of sampling units observed within the j th hour ($j = 1, \dots, 24$) at the k th sluiceway slot ($k = 1, \dots, 3$) on the i th day ($i = 1, \dots, D$).

Nominally, $H_{ijk} = 60 \forall ijk$ and $h_{ijk} = 15 \forall ijk$.

The variance of \widehat{SL} can be estimated by the quantity

$$\widehat{Var}(\widehat{SL}) = \sum_{i=1}^D \sum_{j=1}^{24} \sum_{k=1}^3 \left[\frac{H_{ijk}^2 \left(1 - \frac{h_{ijk}}{H_{ijk}} \right) s_{y_{ijk}}^2}{h_{ijk}} \right] \quad (10)$$

were

$$s_{y_{ijk}}^2 = \frac{\sum_{l=1}^{h_{ijk}} (y_{ijkl} - \bar{y}_{ijkl})^2}{(h_{ijk} - 1)}$$

and where

$$\bar{y}_{ijk} = \frac{1}{h_{ijk}} \sum_{l=1}^{h_{ijk}} y_{ijkl}.$$

3.4 Fish Unit Passage

The sampling at The Dalles fish units can be envisioned as a stratified two-stage sampling program. The first stage is the random sampling of 2 of 4 intake slots across the two

fish units. In the second stage, slot-hours are treated as strata, and random sampling within slot-hours performed. In which case, total fish unit passage can be estimated by the formula

$$\hat{F} = \frac{4}{2} \sum_{i=1}^D \sum_{j=1}^{24} \sum_{k=1}^2 \left[\frac{M_{ijk}}{m_{ijk}} \sum_{l=1}^{m_{ijk}} z_{ijkl} \right] \quad (11)$$

where

z_{ijkl} = expanded fish passage in the l th sampling interval ($l = 1, \dots, m_{ijk}$) during the j th hour ($j = 1, \dots, 24$) at the k th fish unit slot ($k = 1, 2$) on the i th day ($i = 1, \dots, D$);

M_{ijk} = total number of sampling units within the j th hour ($j = 1, \dots, 24$) at the k th fish unit slot ($k = 1, 2$) on the i th day ($i = 1, \dots, D$);

m_{ijk} = actual number of sampling units observed within the j th hour ($j = 1, \dots, 24$) at the k th fish unit slot ($k = 1, 2$) on the i th day ($i = 1, \dots, D$).

Nominally, $M_{ijk} = 60 \forall ijk$ and $m_{ijk} = 10 \forall ijk$.

The variance of \hat{F} can be estimated by the quantity

$$\widehat{Var}(\hat{F}) = \frac{\sum_{i=1}^D \sum_{j=1}^{24} \left[\frac{4^2 \left(1 - \frac{2}{4}\right) s_{\hat{F}_{ijk}}^2}{2} \right]}{2} + \frac{4 \sum_{i=1}^D \sum_{j=1}^{24} \sum_{k=1}^2 \left[\frac{M_{ijk}^2 \left(1 - \frac{m_{ijk}}{M_{ijk}}\right) s_{z_{ijk}}^2}{m_{ijk}} \right]}{2} \quad (12)$$

where

$$s_{z_{ijk}}^2 = \frac{\sum_{l=1}^{m_{ijk}} (z_{ijkl} - \bar{z}_{ijk})^2}{(m_{ijk} - 1)}$$

$$\bar{z}_{ijk} = \frac{1}{m_{ijk}} \sum_{l=1}^{m_{ijk}} z_{ijkl} ,$$

and where

$$s_{\hat{F}_{ijk}}^2 = \frac{\sum_{k=1}^2 (\hat{F}_{ijk} - \hat{\bar{F}}_{ij})^2}{(2-1)},$$

$$\hat{\bar{F}}_{ij} = \frac{1}{2} \sum_{k=1}^2 \hat{F}_{ijk},$$

$$\hat{F}_{ijk} = \frac{M_{ijk}}{m_{ijk}} \sum_{l=1}^{m_{ijk}} z_{ijkl}$$

4.0 Estimating Passage Performance

4.1 Fish Passage Efficiency (FPE)

The fish passage efficiency (FPE) at The Dalles Dam will be estimated by the quotient

$$\widehat{FPE} = \frac{\widehat{SP} + \widehat{SL}}{\widehat{SP} + \widehat{SL} + \widehat{T} + \widehat{F}} \quad (13)$$

where

\widehat{SP} = estimated fish passage through the spillway,

\widehat{SL} = estimated fish passage through the sluiceway,

\widehat{T} = estimated fish passage through the turbine units,

\widehat{F} = estimated fish passage through the fish units,

and where the numerator is the estimated spillway and sluiceway passage and the denominator is the total project passage. The estimate of FPE can alternatively be expressed as

$$\widehat{FPE} = \frac{\widehat{G}}{\widehat{G} + \widehat{U}}$$

where

$$\begin{aligned}\widehat{G} &= \widehat{SP} + \widehat{SL}, \\ \widehat{U} &= \widehat{T} + \widehat{F}.\end{aligned}$$

The variance of \widehat{FPE} can then be expressed as

$$\widehat{Var}(\widehat{FPE}) = \widehat{FPE}^2 (1 - \widehat{FPE})^2 \left[\frac{\widehat{Var}(\widehat{G})}{\widehat{G}^2} + \frac{\widehat{Var}(\widehat{U})}{\widehat{U}^2} \right] \quad (14)$$

and where

$$\begin{aligned}\widehat{Var}(\widehat{G}) &= \widehat{Var}(\widehat{SP}) + \widehat{Var}(\widehat{SL}), \\ \widehat{Var}(\widehat{U}) &= \widehat{Var}(\widehat{T}) + \widehat{Var}(\widehat{F}).\end{aligned}$$

4.2 Spill Efficiency (SPY)

Spill efficiency (SPY) at The Dalles Dam will be estimated by the quotient

$$\widehat{SPY} = \frac{\widehat{SP}}{\widehat{SP} + \widehat{SL} + \widehat{T} + \widehat{F}} \quad (15)$$

When the numerator is the estimate of spillway passage and the denominator is the estimate of total project passage. In turn, \widehat{SPY} can be re-expressed as

$$\widehat{SPY} = \frac{\widehat{SP}}{\widehat{SP} + \widehat{U}_1}$$

where

$$\widehat{U}_1 = \widehat{SL} + \widehat{T} + \widehat{F}.$$

The variance of \widehat{SPY} can then be expressed as

$$\widehat{Var}(\widehat{SPY}) = \widehat{SPY}^2 (1 - \widehat{SPY})^2 \left[\frac{\widehat{Var}(\widehat{SP})}{\widehat{SP}^2} + \frac{\widehat{Var}(\widehat{U}_1)}{\widehat{U}_1^2} \right] \quad (16)$$

where

$$\widehat{Var}(\widehat{U}_1) = \widehat{Var}(\widehat{SL}) + \widehat{Var}(\widehat{T}) + \widehat{Var}(\widehat{F}).$$

4.3 Spill Effectiveness (SPE)

Spill effectiveness (SPE) at The Dalles Dam will be estimated by the function

$$\widehat{SPE} = \frac{\left(\frac{\widehat{SP}}{f_{SP}} \right)}{\left[\frac{(\widehat{SP} + \widehat{SL} + \widehat{T} + \widehat{F})}{f} \right]} = \left(\frac{f}{f_{SP}} \right) \cdot \widehat{SPY} \quad (17)$$

where

f = project-wide flow volume,

f_{SP} = spillway flow volume.

The variance of \widehat{SPE} can be estimated by the quantity

$$\widehat{Var}(\widehat{SPE}) = \left(\frac{f}{f_{SP}} \right)^2 \cdot \widehat{Var}(\widehat{SPY}). \quad (18)$$

4.4 Sluiceway Effectiveness (SLE)

Sluiceway Effectiveness (SLE) will be estimated by the function

$$\widehat{SLE} = \frac{\left(\frac{\widehat{SL}}{f_{SL}}\right)}{\left[\frac{\widehat{SL} + \widehat{SP} + \widehat{T} + \widehat{F}}{f}\right]} \quad (19)$$

where

f_{SL} = sluiceway flow volume.

The estimator of SLE can be rewritten as

$$\widehat{SLE} = \left(\frac{f}{f_{SL}}\right) \cdot \left(\frac{\widehat{SL}}{\widehat{SL} + \widehat{U}_2}\right) \quad (20)$$

where

$$\widehat{U}_2 = \widehat{SP} + \widehat{T} + \widehat{F}.$$

In which case, the variance of \widehat{SLE} can be estimated by the quantity

$$\widehat{Var}(\widehat{SLE}) = \left(\frac{f}{f_{SL}}\right)^2 \left[\widehat{SLE}^2 (1 - \widehat{SLE})^2 \left[\frac{\widehat{Var}(\widehat{SL})}{\widehat{SL}^2} + \frac{\widehat{Var}(\widehat{U}_2)}{\widehat{U}_2^2} \right] \right] \quad (21)$$

and where

$$\widehat{Var}(\widehat{U}_2) = \widehat{Var}(\widehat{SP}) + \widehat{Var}(\widehat{T}) + \widehat{Var}(\widehat{F}).$$

4.5 Sluiceway Passage Abundance

As already described, sluiceway passage abundance (\widehat{SL}) and its associated variance estimate [$\widehat{Var}(\widehat{SL})$] will be used as one of the response variables to characterize sluiceway performance.

4.6 Additional Sluiceway Performance Measures

The sluiceway is located directly above turbine unit 1. A localized measure of sluiceway efficiency can be estimated by the quotient

$$\widehat{SLY}_1 = \frac{\widehat{SL}}{\widehat{SL} + \widehat{T}_1} \quad (22)$$

where

\widehat{T}_1 = estimated fish passage through turbine unit 1.

The variance of \widehat{SLY}_1 can be estimated by the quantity

$$\widehat{Var}(\widehat{SLY}_1) = \widehat{SLY}_1^2 (1 - \widehat{SLY}_1)^2 \left[\frac{\widehat{Var}(\widehat{SL})}{\widehat{SL}_1^2} + \frac{\widehat{Var}(\widehat{T}_1)}{\widehat{T}_1^2} \right] \quad (23)$$

Another localized measure of sluiceway efficiency is relative to fish passage through turbine units 1-4 and defined as

$$\widehat{SLY}_{1-4} = \frac{\widehat{SL}}{\widehat{SL} + \widehat{T}_{1-4}} \quad (24)$$

where

\widehat{T}_{1-4} = estimated fish passage through turbine units 1-4.

The variance of \widehat{SLY}_{1-4} can be estimated by the quantity

$$\widehat{Var}(\widehat{SLY}_{1-4}) = \widehat{SLY}_{1-4}^2 (1 - \widehat{SLY}_{1-4})^2 \left[\frac{\widehat{Var}(\widehat{SL})}{\widehat{SL}^2} + \frac{\widehat{Var}(\widehat{T}_{1-4})}{\widehat{T}_{1-4}^2} \right]. \quad (25)$$

A final measure of sluiceway efficiency will be estimated by the quotient

$$\widehat{SLY}_{PH} = \frac{\widehat{SL}}{\widehat{SL} + \widehat{T} + \widehat{F}} \quad (26)$$

where the denominator is the estimate of total smolt passage through The Dalles powerhouse.

The estimator \widehat{SLY}_{PH} can be reexpressed as

$$\widehat{SLY}_{PH} = \frac{\widehat{SL}}{\widehat{SL} + \widehat{U}_3}$$

where

$$\widehat{U}_3 = \widehat{T} + \widehat{F}$$

leading to the variance estimator

$$\widehat{Var}(\widehat{SLY}_{PH}) = \widehat{SLY}_{PH}^2 (1 - \widehat{SLY}_{PH})^2 \left[\frac{\widehat{Var}(\widehat{SL})}{\widehat{SL}^2} + \frac{\widehat{Var}(\widehat{U}_3)}{\widehat{U}_3^2} \right] \quad (27)$$

and where

$$\widehat{Var}(\widehat{U}_3) = \widehat{Var}(\widehat{T}) + \widehat{Var}(\widehat{F}).$$

5.0 Estimating Fish Passage Distributions

If the J-occlusion plates are successful in averting fish away from turbine units, changes in the horizontal and vertical distributions of smolt passage might be anticipated.

5.1 Horizontal Distributions

For the horizontal distributions, the proportion of the smolts using the treatment side of the dam (i.e., turbine units 1-5, fish units and sluiceway) can be computed during control and test periods. Define the estimated proportion of the fish using the treatment side of the dam as

$$\hat{H} = \frac{\hat{T}_{1-5} + \hat{F} + \widehat{SL}}{(\hat{T}_{1-5} + \hat{F} + \widehat{SL}) + \hat{T}_{6-22}}. \quad (28)$$

The estimator \hat{H} can be re-expressed as

$$\hat{H} = \frac{\hat{H}_T}{\hat{H}_T + \hat{H}_C}$$

where

$$\begin{aligned} \hat{H}_T &= \hat{T}_{1-5} + \hat{F} + \widehat{SL}, \\ \hat{H}_C &= \hat{T}_{6-22}, \end{aligned}$$

with associated variance estimator

$$\widehat{Var}(\hat{H}) = \hat{H}^2 (1 - \hat{H})^2 \left[\frac{\widehat{Var}(\hat{H}_T)}{\hat{H}_T^2} + \frac{\widehat{Var}(\hat{H}_C)}{\hat{H}_C^2} \right] \quad (29)$$

and where

$$\begin{aligned} \widehat{Var}(\hat{H}_T) &= \widehat{Var}(\hat{T}_{1-5}) + \widehat{Var}(\hat{F}) + \widehat{Var}(\widehat{SL}), \\ \widehat{Var}(\hat{H}_C) &= \widehat{Var}(\hat{T}_{6-22}). \end{aligned}$$

5.2 Vertical Distributions

To assess the effect of the J-occlusion plates on the vertical distribution of smolts, the proportion of smolt above a demarcation could be calculated at adjacent test units. Define the following:

m_{ijk_g} = expanded fish passage in the g th sampling units ($g = 1, \dots, b_{ijkl}$) in the k th turbine unit ($k = 1, \dots, K_{ij}$) during the j th hour ($j = 1, \dots, 24$) on the i th day ($i = 1, \dots, D$) above the vertical demarcation line;

n_{ijk} = expanded fish passage in the g th sampling units ($g = 1, \dots, b_{ijk}$) in the k th turbine unit ($k = 1, \dots, K_{ij}$) during the j th hour ($j = 1, \dots, 24$) on the i th day ($i = 1, \dots, D$) below the vertical demarcation line;

b_{ijk} = number of sampling units actually observed at the k th turbine unit ($k = 1, \dots, K_{ij}$) during the j th hour ($j = 1, \dots, 24$) on the i th day ($i = 1, \dots, D$);

B_{ijk} = total number of sampling units at the k th turbine unit ($k = 1, \dots, K_{ij}$) during the j th hour ($j = 1, \dots, 24$) on the i th day ($i = 1, \dots, D$).

Then, an estimate of the total passage within a unit-hour above the demarcation can be expressed as

$$\hat{M}_{ijk} = \frac{B_{ijk}}{b_{ijk}} \sum_{g=1}^{b_{ijk}} m_{ijkg}$$

and the estimate of total passage within a unit-hour below the demarcation can be expressed as

$$\hat{N}_{ijk} = \frac{B_{ijk}}{b_{ijk}} \sum_{g=1}^{b_{ijk}} n_{ijkg}.$$

An estimate of the proportion of smolts that passed above the vertical demarcation line is then

$$\hat{V} = \frac{\sum_{i=1}^D \sum_{j=1}^{24} \sum_{k=1}^K \hat{M}_{ijk}}{\sum_{i=1}^D \sum_{j=1}^{24} \sum_{k=1}^K (\hat{M}_{ijk} + \hat{N}_{ijk})} = \frac{\hat{M}}{\hat{M} + \hat{N}}. \quad (30)$$

The variance of \hat{V} can be estimated by the quantity

$$\widehat{Var}(\hat{V}) = \hat{V}^2 (1 - \hat{V})^2 \left[\frac{\widehat{Var}(\hat{M})}{\hat{M}^2} + \frac{\widehat{Var}(\hat{N})}{\hat{N}^2} - \frac{2\widehat{Cov}(\hat{M}, \hat{N})}{\hat{M}\hat{N}} \right] \quad (31)$$

where

$$\widehat{Var}(\hat{M}) = \sum_{i=1}^D \sum_{j=1}^{24} \sum_{k=1}^K \frac{B_{ijk}^2 \left(1 - \frac{b_{ijk}}{B_{ijk}}\right) s_{m_{ijk}}^2}{b_{ijk}} \quad (32)$$

and where

$$s_{m_{ijk}}^2 = \frac{\sum_{g=1}^{b_{ijk}} (m_{ijkg} - \bar{m}_{ijk})^2}{(g-1)},$$

$$\bar{m}_{ijk} = \frac{1}{b_{ijk}} \sum_{g=1}^{b_{ijk}} m_{ijkg}.$$

The estimated variance for \hat{N} is calculated analogously to Equation (32). The covariance between \hat{M} and \hat{N} is calculated as

$$\widehat{Cov}(\hat{M}, \hat{N}) = \sum_{i=1}^D \sum_{j=1}^{24} \sum_{k=1}^K \frac{B_{ijk}^2 \left(1 - \frac{b_{ijk}}{B_{ijk}}\right) \widehat{Cov}(m_{ijkg}, n_{ijkg})}{b_{ijk}}$$

where

$$\widehat{Cov}(m_{ijkg}, n_{ijkg}) = \frac{\sum_{g=1}^{b_{ijk}} (m_{ijkg} - \bar{m}_{ijk})(n_{ijkg} - \bar{n}_{ijk})}{(b_{ijk} - 1)}.$$

The estimates of the vertical distribution can be calculated for varying lengths of time (i.e., D) and varying numbers of adjacent turbine units (i.e., K) in Equation (30).

6.0 Test of J-Occlusion Plates

A completely randomized experiment was performed at The Dalles Dam to test the effect of J-occlusion plates at turbine units 1-5. The goal of the J-occlusion plates is to reduce smolt passage through the turbine units and enhance passage through the spillway and sluiceway. Six test periods each were conducted with J-occlusion plates in and out. Table 6-1

summarizes the dates of the trials of the 2001 study. Each trial was performed for two consecutive days (i.e., 48 hours). Equipment failure at The Dalles Dam precluded completion of the entire experiment planned for 2001.

Table 6-1. Summary of the trial dates (i.e., day of the year) used in the 2001 J-occlusion experiment in The Dalles. Shaded area of the table indicates periods of no spill; unshaded areas, period of spill.

Trials	Occlusion Period	Unoccluded Period
1	114-116	120-122
2	117-119	122-124
3	125-127	137-139
4	128-130	140-142
5	143-145	146-148
6	149-151	152-154

Separate analyses will be performed for the daytime and nighttime periods of the trials. Separate analyses will be performed to assess the following response variables and hypotheses:

1. \widehat{FPE}

$$H_o : \mu_U \geq \mu_O$$

$$H_a : \mu_U < \mu_O$$
2. \widehat{SPY}

$$H_o : \mu_U \geq \mu_O$$

$$H_a : \mu_U < \mu_O$$
3. \widehat{SPE}

$$H_o : \mu_U \geq \mu_O$$

$$H_a : \mu_U < \mu_O$$

- | | | |
|-----|-----------------------|---|
| 4. | \widehat{SLE} | $H_o : \mu_U \geq \mu_O$
$H_a : \mu_U < \mu_O$ |
| 5. | \widehat{SLY}_1 | $H_o : \mu_U \geq \mu_O$
$H_a : \mu_U < \mu_O$ |
| 6. | \widehat{SLY}_{1-4} | $H_o : \mu_U \geq \mu_O$
$H_a : \mu_U < \mu_O$ |
| 7. | \widehat{SLY}_{PH} | $H_o : \mu_U \geq \mu_O$
$H_a : \mu_U < \mu_O$ |
| 8. | \hat{T} | $H_o : \mu_U \leq \mu_O$
$H_a : \mu_U > \mu_O$ |
| 9. | \hat{T}_1 | $H_o : \mu_U \leq \mu_O$
$H_a : \mu_U > \mu_O$ |
| 10. | \hat{T}_{1-4} | $H_o : \mu_U \leq \mu_O$
$H_a : \mu_U > \mu_O$ |
| 11. | \widehat{SL} | $H_o : \mu_U \geq \mu_O$
$H_a : \mu_U < \mu_O$ |
| 12. | \hat{H} | $H_o : \mu_U \geq \mu_O$
$H_a : \mu_U < \mu_O$ |
| 13. | \hat{V} | $H_o : \mu_U \geq \mu_O$
$H_a : \mu_U < \mu_O$ |

where μ_U is the mean under unoccluded conditions and μ_O , the mean under occluded conditions.

During the J-occlusion plate trials, the first half of the experiment was performed under no spill conditions; the second half, under spill conditions (Table 5-1). There is barely

sufficient replication to test for a treatment-by-spill interaction. Furthermore, the spill conditions were not manipulated in a randomized manner but confounded with time. Instead, it is recommended spill/no spill conditions be treated as a discrete covariate and the ANOVA adjusted as indicated in the table below.

Source	df	SS	MS	F
Total	12			
Mean	1			
Total _{Cor}	11	SSTOT		
Covariate (Spill)	1	SSC		
Treatments	1	SST	MST	$F_{1,9} = \frac{MST}{MSE}$
Error	9	SSE	MSE	

The F-test from the ANOVA is a two-tailed test of no treatment effect. The hypotheses of interest are one-tailed. The tests of significance should then be based on

$$t_4 = \sqrt{F_{1,4}}$$

with the appropriate sign assigned to the t-statistic. It is recommended that all response variables be ln-transformed before the ANOVA.

Appendix I

Sonar Tracker Analysis Methods

Data reduction and analysis steps are shown in Figure XX. Hydraulic data were not available; thus, the analysis included only observed fish movement data. Typically, day and night periods (see definitions below) were analyzed separately because of known day/night differences in sluice passage (Ploskey et al. 2001b).

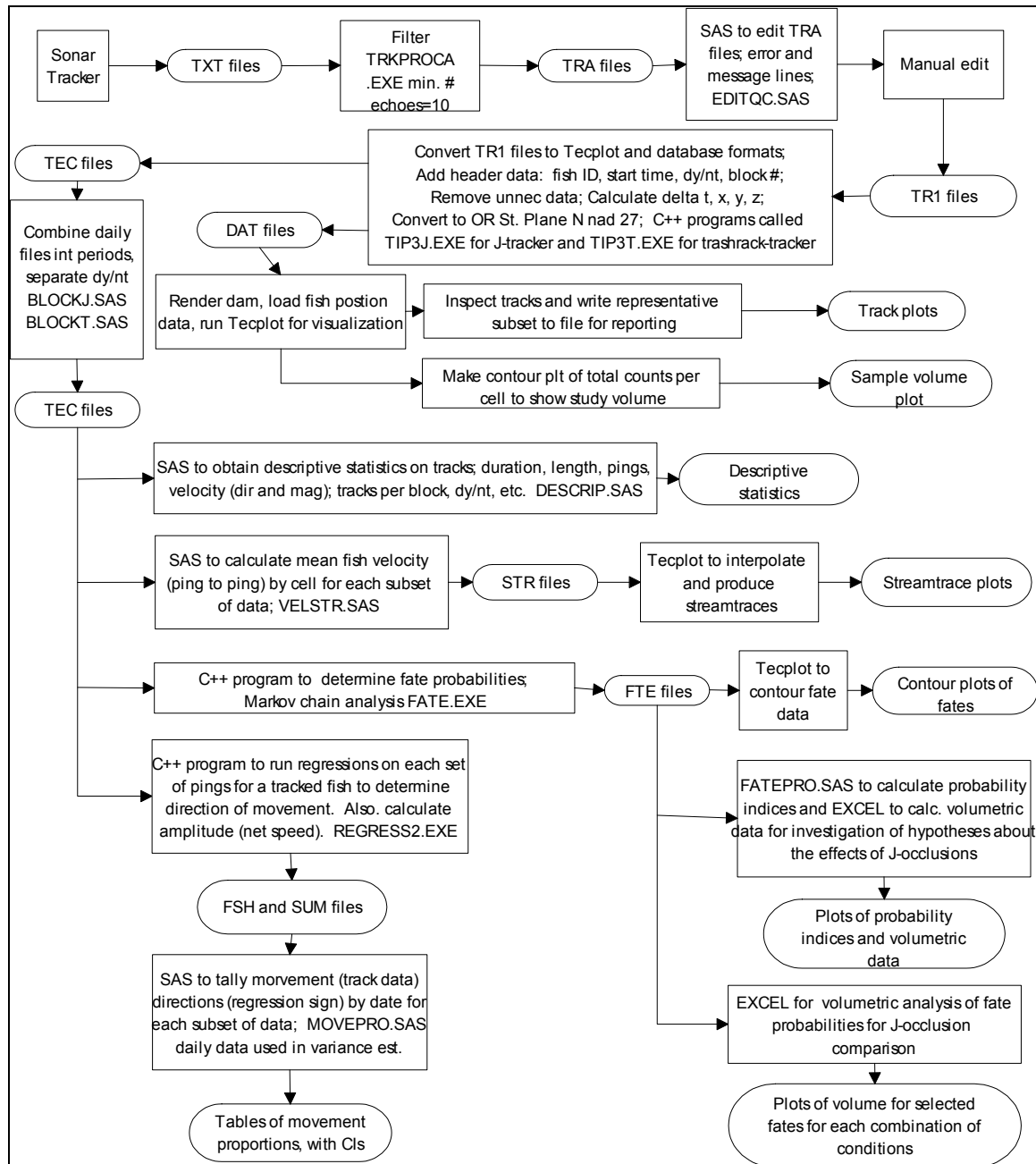


Figure 1. Data flow chart.

The tracking data from AFTS (TXT files) were filtered for minimum number of echoes per track (10) using a C-compiled program called TRKPROCA.EXE. The TRA output files from this program were reduced in a SAS-program called EDITQC.SAS, which removed unnecessary auxiliary information. The TRA files were also manually edited to delete fish track data for the 30 min period before any system crashes because AFTS performed a positioning self-check every 30 min to check for slippage in rotator position during data collection. If there was slippage, AFTS stopped collecting data and waited to be re-started. This occurred seven times during the 73 days data were collected. Thus, data 30 min before these seven events could be erroneous and had to be deleted. The daily output files from the editing process were called TR1 files.

The daily TR1 files were processed using a C-compiled program called TIP3D.EXE. Two daily output files were produced: DAT files formatted to be loaded into Tecplot software (Amtec Engineering, Inc. Bellevue, Washington) and TEC files for further data and statistical analysis. Data processing by TIP3J for the J-tracker and TIP3T for the trashrack tracker included:

- Reassemble tracks – Separate tracks adjacent in time and space were reassembled. This usually occurred when AFTS automatically broke-off tracking when the maximum number of echoes per track was reached (800), or when maximum number of missing pings was reached (20).
- Fish track identification number – The purpose here was to give each track a unique identification number for subsequent data analysis. A fish track identification number was made from the date and an integer starting at 1 and proceeding consecutively.
- Day/night determination – Sunrise and sunset times for each date during the study period were obtained from the U.S. Naval Observatory website (<http://aa.uno.navy.mil/AA/data/>). The time of the start of a given fish track was then compared to the sunrise/sunset times to determine if the track was in day or night. A day/night designator was then written to the output file: day = 0 and night = 1.
- Delta X, Y, Z, T calculations – The difference in three-dimensional fish position (X, Y, Z) and time between consecutive echoes in a track was calculated as follows, using delta X as an example between the i and i+1 echoes of the track:

$$\Delta X = X_{i+1} - X_i$$

- Conversion to dam coordinates – The raw position data are in “tracker” coordinates, i.e., relative to the location of AFTS’s split-beam transducer and rotators (centered at intersection

of axes). This Cartesian coordinate system was converted to “dam” coordinates for the purposes of display and analysis. The origin of the “dam” coordinate system (see Figure 11) was the center of the MU1-1/FU2-2 pier nose at Elevation 48.2 m (158 ft).

- Conversion to Oregon State plane coordinates – Similarly, the raw position data were also converted to Oregon State Plane NAD 27 coordinates. This is the same coordinate system that other researchers and CFD modelers will use.

We used Tecplot software to visualize the fish tracks obtained from AFTS. To do this, we first rendered the dam in Tecplot. Then the specific tracks contained in the DAT files from the TIP3 programs were turned into “zones” in Tecplot. The tracks were superimposed on the dam rendering, both of which were in “dam” coordinates. Tecplot visualization allowed us to manipulate and explore the three-dimensional nature of the tracks relative to the dam.

Descriptive data on the data set were obtained using the SAS-program DESCRIP.SAS. Using the TEC files as input, DESCRIP.SAS produced the following data for each day/night period in each treatment:

- number of observations (distinct fish positions);
- mean, minimum, and maximum number of echoes per track;
- mean, minimum, and maximum positions in the X, Y, and Z dimensions;
- mean, minimum, and maximum velocities in the X, Y, and Z dimensions.

Analysis based on ping-to-ping estimated velocities

Ping-to-ping velocity data averaged within each 0.5 m cell were the basis for the mean velocity analysis. Mean velocities over the entire sample volume were obtained for each study period for each dimension (X, Y, and Z) for day and night separately. All subsequent data analyses were based on fish track data, not ping-to-ping data.

Direction of movement based on identified fish tracks

Fish track directionality relative to the presence of J-occlusions, night versus day and spill condition can be characterized using proportions based on individual track regressions in each of the three dimensions: along the dam, upstream/downstream and up/down. The movement proportions were based on the results of linear regressions applied on each fish track for each dimension separately to estimate three components of movement, as in the following example for the X-dimension:

$$Position_x = a_x + b_x (Time)$$

where, a_x and b_x are the y-intercept and slope coefficients of the linear regression for the X-dimension. Linear regression through all positions comprising a track was more representative of track movement in its entirety than data from just the end points (Figure 13).

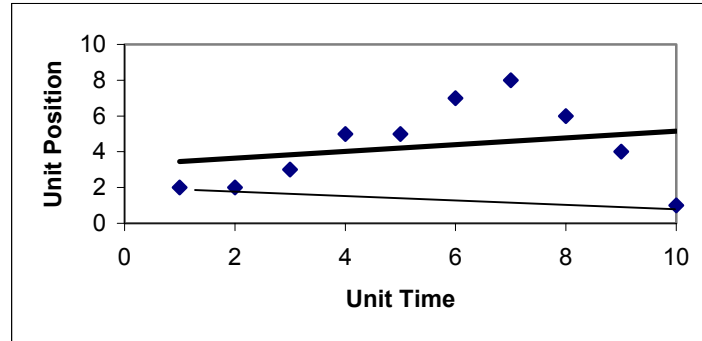


Figure 2. Example fish track data showing linear regression line (thick black) with positive slope and line through end points (thin black) with negative slope.

For this particular analysis, tracked fish in the resulting data set were allocated to 1.0 m cells in the sample volume. Proportions of fish moving in each of three dimensions were calculated for each cell. These movement proportions were then the basis for a comparison of movements with and without J-occlusions in place. A common sample volume was selected across all combinations of J-occlusion plates IN/OUT, day/night, and spill/no spill.

Summary proportions and variances were calculated for direction of movement separately for each dimension (X east/west; Y toward/away; Z up/down) for each condition (J-occlusions IN/OUT, day/night, and spill/no spill) as follows:

$$p_i = \frac{a_i}{m_i}, \text{ the estimated proportion on day } i (i=1, \dots, n),$$

where a_i is the number of tracked fish with a particular sign of regression slope (positive or negative) and m_i is the total number of tracked fish. The overall estimate across n -days of a particular treatment condition is

$$p = \frac{\sum_{i=1}^n a_i}{\sum_{i=1}^n m_i}$$

with associated estimated variance

$$Var(p) = \frac{1-f}{n\bar{m}^2} \left[\frac{\sum_{i=1}^n a_i^2 - 2p \sum_{i=1}^n a_i m_i + p^2 \sum_{i=1}^n m_i^2}{n-1} \right]$$

where $f=0$ (i.e., the fpc is ignored) and where

$$\bar{m} = \frac{\sum_{i=1}^n m_i}{n}.$$

Markov analysis of fates based on identified fish tracks

For the purpose of this study, a fate is specified by where fish tracks exited the sample volume. Fates are expressed as probabilities of passage toward a particular area, e.g., the sluiceway. To determine fate probabilities, we applied a Markov analysis (Taylor and Karlin 1988, pp. 95-266), which described smolt movement as a stochastic process. A couple key ideas from Taylor and Karlin (1998, pp. 95-96) are: (a) a Markov process $\{X_t\}$ is a stochastic process with the property that, given a value X_t , the values of X_s , for $s>t$ are not influenced by the values of X_u for $u<t$, and (b) transition probabilities are functions not only of the initial and final states, but also of the time of transition as well. When the one-step transition probabilities are independent of the time variable, then the Markov chain has stationary probabilities. The Markov-chain analysis for the 2001 TDA sonar tracker study included the following assumptions:

- the movements can be described by a one-step Markov process, i.e., movement decisions are based on the smolt's current position and not upon the prior history getting to that position;
- the transition probabilities are estimated from independent fish observations;
- the transition matrix is stationary.

For the Markov analysis, the three-dimensional sample volume in front of Sluice 1-1 was divided into cells (modified for fate analysis as follows: 0.5 x 0.5 x 0.5 m for X, Y, Z, respectively). The sample volume was decreased to reduce the size of the Markov matrices: X = -3.0 to 3.0 m, Y = 3.0 to 15.0 m, and Z = -6.0 m to -0.5. At the boundaries (sides) of the volume, we defined these passage fates:

- Sluice – cells on side facing the sluiceway, 0.0 to 4.0 m deep;
- Turbine – cells on side facing the sluiceway, 4.0 to 6.0 m deep;

- West – west side cells;
- East – east side cells;
- Bottom – bottom cells of the volume;
- Reservoir – cells of side facing the reservoir upstream;
- Unknown – no movement.

The Markov transition matrix was a square matrix the size of $k \times k$, where k is the number of distinct cells being modeled ($k = 4,080$). The ij th element in the i th row of the j th column of the transition matrix was the estimated probability (p_{ij}) of moving from cell i to cell j in the next time step. These probabilities were estimated by:

$$\hat{p}_{ij} = \frac{x_{ij}}{n_i}$$

where,

n_i = number of observations of smolts in the i th cell;

x_{ij} = number of observations where a smolt in cell i moved to cell j in the next time step.

The cells (0.5 x 0.5 x 0.5 m) that bordered the sides of the volume of interest (sluice, turbine, west, east, bottom, and reservoir) were set to unity to absorb any movement that reached a particular “fate.” Otherwise, C-compiled programs (FATEJ.EXE for the tracker on the J-occlusion and FATET.EXE for the tracker on the trashrack) tallied the transition matrix T using a

time step of 1 sec, and the average position (i.e., $\sum x_i / n$) during each 1 s interval a fish was tracked. This program required that a fish be tracked for at least two seconds before the transition matrix was amended to obtain indices i and j (i from the first interval, j from the second). Non-boundary (including surface) cells were checked to ensure non-zero and non-unity values. If zero or unity was present in an i,i cell after building the matrix T from a set of data, then the closest i,i cell in Cartesian space was found that contained data and was used to augment that particular set of i,j 's. This process created a situation that guaranteed fish movement to one of the absorbing boundaries if there was movement to begin with.

The transition matrix T for one time step was then used to estimate the transition for two or more time steps as:

$$T^t$$

where, t = the number of time steps. For this study, $t = 4,096$ so that the Markov process reached stability, i.e., the transition matrix did not change with additional time steps. The ultimate fate of smolts would be calculated as:

$$T^{4096}$$

After 4,096 time steps (corresponding to 68 min), probabilities for each of the seven fates for each of the 2,970 cells, not including border cells, were extracted from the transition matrix and written to file. The fate data were displayed in Tecplot.

The key assumption in this analysis is that the data exhibit the Markov property (see first assumption above). The one-step model we used in the analysis of day and night fish movement assumed movement to a future cell depended entirely on the fish's current position, not its prior history. However, movement could depend on both the current and past histories. A $R \times C$ table was used to test whether movement from B to C_i is independent of previous position A_i . As many cells as were practical were tested in this manner. Movement and cells were measured using a time step of 1 s and 0.5 m per side cells with x values from 1 to 6.5 m ($i=0 \dots 10$), y values from 1 to 6.5 m ($i=0 \dots 10$), and z value from -3.5 to -0.5 m ($k=0 \dots 5$). Cell codes were formed as $i+j*11+k*121$. A Chi-Square test was not valid due to the sparseness of the contingency tables. Therefore, conclusions about appropriateness of the first order assumption of a one-step Markov process were based on Fisher's exact test (Sokal and Rohlf 1981, p. 740). Cells where the number of fish positions was greater than 10 were tested in this manner. A total of 270 cells during daytime and 226 during nighttime out of the possible 726 were tested from the 2000 data set.

In general, movement was tested to be independent of prior position. P values less than 0.05 showed significance in 24 (8.9 %) of the cases during daytime and 18 (8.0%) of cases at night. That is, the null hypothesis of lack of association was rejected in fewer than 9% of the cases examined. This is a good indication that our use of the Markov-Chain was appropriate for characterizing movement through the volume near Sluice 1-2.

Probability Indices and Volumetric Analysis

In addition to comparing fish movements in general for various conditions, we were interested in assessing specific hypotheses about the effects of the J-occlusions on fish movements in the nearfield of Sluice 1-2. After congruent sample volumes for each combination of conditions were established, we used the fate probabilities from the Markov-chain analysis to

calculate “probability indices.” A probability indices (PI) for a given condition will simply be the average fate probability over all cells in the sample volume, as follows:

$$PI = \frac{\sum_{i=1}^m \sum_{j=1}^n \sum_{k=1}^o F_{ijk}}{m \cdot n \cdot o}$$

where, F_{ijk} is the fate probability for the i th cell along the dam the j th cell away from the dam, and the k th cell deep.

In addition, we calculated the volume ($VTOT_F$) under each condition where the fate probabilities (F) were equal to or greater than 0.7, 0.8, and 0.9:

$$VTOT_F = V_{cell} \sum_{i=1}^p \sum_{j=1}^q \sum_{k=1}^r F_{ijk}$$

where, $F_{ijk} \geq F$ and V_{cell} is the volume per cell.